

Faculty of Engineering – Department of Civil Engineering

ENHANCING THE PERFORMANCE OF COLD BITUMEN EMULSION MIXTURE USING SUPPLEMENTARY CEMENTITIOUS

By

AHMED IZAT MOHAMMED NASSAR

B.Sc (Civil Eng.) and M.Sc (Infrastructure Eng.)

Thesis submitted to the University of Nottingham for the degree of Doctor of Philosophy

September, 2016

بِسْمِ اللَّهِ الرَّحْمَٰنِ الرَّحِيمِ

﴿ يَرْفَعِ اللَّهُ الَّذِينَ آمَنُوا مِنْكُمْ وَالَّذِينَ أُوتُوا الْعِلْمَ دَرَجَاتٍ وَاللَّهُ بِمَا تَعْمَلُونَ خَبِيرٌ﴾

سورة المجادلة (11)

In the Name of Allah, the Most Beneficent, the Most Merciful

﴿ Allah will raise those who have believed among you and those who were given knowledge, by degrees. And Allah is acquainted with what you do ﴾

Sorah Al-Mujadilah (11)

Abstract

Several benefits are gained from using cold mix asphalt (CMA) instead of hot mix asphalt (HMA). The benefits include conservation of materials and reducing energy consumption, preservation of the environment and reduction in cost. One of the common types of CMA is cold bitumen emulsion mixture (CBEM) which is the mixture produced by mixing mineral aggregate with bitumen emulsion. Despite the efforts applied in the last few decades in order to improve and develop CBEM utilization, certain deficiencies remain that make it inferior to HMA, resulting in restricting or minimizing of its use. However, the development of CBEM for road construction, rehabilitation and maintenance is steadily gaining interest in both pavement engineering industrial and research sectors.

The present study was primarily aimed at evaluating the effect of using different cementitious materials on the performance of CBEM. The idea of the research is to provide a sustainable filler from supplementary cementitious materials (SCMs) to be used as fillers to provide enhanced properties of CBEMs. By achieving this aim it is expected that the utilization of CBEM would increase, allowing them to be used as structural pavement materials with some confidence.

Research was first undertaken to optimize the mix design of CBEM using a statistical approach known as response surface methodology (RSM), as an alternative approach to achieve acceptable engineering properties. The optimization of CBEM was investigated, to determine optimum proportions to gain suitable levels of both mechanical and volumetric properties. This optimization focussed on the mix design parameters, namely bitumen emulsion content (BEC), pre-wetting water content (PWC) and curing temperature (CT). This work also aimed to investigate the effect of the interaction between these parameters on the mechanical and volumetric properties of CBEMs. The results indicate that the interaction of BEC, PWC and CT influences the mechanical properties of CBEM. However, PWC tends to influence the volumetric properties more significantly than BEC. The individual effects of BEC and PWC are important, rather than simply the TFC which is used in conventional mix design of CBEM. Furthermore, the experimental results for the optimum mix design corresponded well with model predictions. It was concluded that optimization using RSM is an effective approach for mix design of CBEMs.

The study also investigated in-depth the performance characteristics of CBEMs using different filler treatments. The study was extended to understand the performance enhancement through mineralogical and microstructural investigations. The research was designed to use cement, binary and ternary blended fillers (BBF and TBF). Fly ash (FA) and ground granulated blast-furnace slag (GGBS) were used as BBF while silica fume (SF) was added to the BBF to obtain TBF. A significant improvement was achieved in mechanical and durability properties of CBEMs due to incorporation of both cement and blended fillers. Also, the results indicated that TBF was more suitable than BBF for the production of CBEMs. The microstructural assessment indicated that the effect of BBF on the internal microstructure of CBEMs was slightly negative and more noticeable in CBEMs containing FA. Mineralogical and microstructural assessments also suggested that the presence of bitumen emulsion might not affect the hydration of the silicates in treated CBEMs. The formation of additional CSH was observed due to the replacement of conventional limestone filler by cement, BBF and TBF. However, it seems that this can cause a delay in the formation of other hydration products (Ettringite) resulting from the hydration of aluminates in cement. Furthermore, it is proposed that the addition of SF to BBF mixtures can eliminate the delay in formation of hydration products caused by the bitumen emulsion.

The present work was also aimed at better understanding the curing mechanism of CBEMs and to bridge the gap between laboratory curing and field evolution of these mixtures. This was achieved by evaluating the effect of the curing process on CBEM performance and developing a prediction model to assess in-situ CBEM performance using maturity relationships. Different contributory factors affecting the curing process were investigated such as curing temperature and relative humidity (RH) in addition to the impact of curing time and the presence of cement/active fillers. The results indicated that high curing temperature is responsible for additional stiffness gain by increasing the binder stiffness due to ageing and by increasing the moisture loss by evaporation during the curing process. However, at high curing temperature the moisture loss by evaporation may hinder the hydration of cement/active fillers. Moreover, the results also indicated that the high RH level influences the stiffness modulus of CBEMs negatively. The laboratory results were then used to develop a tool to assess in-situ curing of CBEMs using the maturity approach, which is widely used to estimate in-situ concrete properties. A strong correlation was found between maturity and the stiffness values obtained from the laboratory tests, which resulted in development of maturity-stiffness relationship. The application of this relationship

to assess the in-situ stiffness of CBEMs is presented using three hypothetical pavement sections in the United Kingdom, Italy and Qatar; to simulate different curing regimes.

A pavement analysis and design study was conducted to evaluate the incorporation of treated CBEMs into a pavement structure. CBEMs are suggested to be used in two scenarios: the first is as a surface course and the second is as a base course. The scope of the study is limited here to design based on the fatigue criterion only. Although, the structural design was based on practical hypothetical layer thicknesses, the results provided useful insight into the structural capabilities of CBEMs.

Dedication

To the Messenger Mohammad (Peace and blessing be upon him) for his endless guidance toward the right path….

To the pure soul of my father who had dreamt to witness these moments….

To my kind-hearted mother for her unlimited love, inspiration, sacrifices and prayers….

To my sweetheart and beloved wife for her endless love, patience, encouragement and support….

To my beloved children for their smiles and love that give me energy to work….

To all my brothers and sisters for their help, support and encouragement….

To my parents-in-law for their endless help and continuous support….

To all my friends in Palestine for their friendship and brotherhood….

I dedicate this work hoping that I made all of them proud….

Ahmed Izat Mohammed Nassar,

Acknowledgements

First and foremost, all praise and glory are due to "**ALLAH**" the Almighty, who gave me the opportunity, the health, the patience and the power to accomplish this research.

It is my great pleasure to express my warmest thanks to the people that supported me during my study. I wish to extend my appreciation, gratitude and sincere thanks to **Dr. Nick Thom**, the main supervisor of this study, for his guidance, continuous support, sound advice, kind help and endless encouragement throughout the period of this research. I would like to say something to you "I am very proud to be one of your students". Also, I would like to extend my thanks to my co-supervisor **Dr. Tony Parry**, for his remarkable, continuous support, guidance and essential fingerprint on this research.

I wish to acknowledge with gratitude and appreciation the University of Nottingham which has funded this research through the Dean of Engineering Research Scholarship for International Excellence. Furthermore, the author wishes to express his sincere gratitude to the technicians at the Nottingham Transportation Engineering Centre for their support and assistance. The author also wishes to thank **Dr. Nigel Neate** (University of Nottingham – Faculty of Engineering) for his help in conducting the XRD and SEM tests. The author also wishes to thank **Dr. Majed A. A. Aldahdooh, Dr. Breixo Gómez Meijide, Prof. Ignacio Pérez and Dr. Mohammed J. K. Bashir** for their help and support. The author gratefully acknowledges the valuable support of Nynas, Cemex and Hanson companies for providing the raw materials for this study.

The author would like to give his special thanks to **Dr. Alvaro Garcia Hernandez** as an internal examiner for his continued help, kind advice and suggestions during the PhD project. Also, of course, I would like to thank all PhD researchers at NTEC with whom I shared many enjoyable moments and experiences.

I wish to thank my colleagues **Ahmed Aljubory**, **Dr. Ameer Abdulrahman Hilal** and **Dr. Mahmoud Khashaa Mohammed** for useful conversations, discussions and friendships over the years of the study. Special thanks go to Palestinian friends "**Rami Alfaqawi, Mustafa Abou-foul, Dr. Ahmad AbdAlqader, Rami Alghmri, Rami Salem, Mohammed Habboub, Dr. Osama Dawoud, Dr. Salem Abu Muraheel, Dr. Mahmoud Shatat, Dr. Mohammed Radi and Dr. Ziyad Nada**" for friendship and nice moments shared in the UK.

On a personal note, I would like to thank my beloved wife **Duaa** for her love, patience and support. I would like to say that you deserve a PhD degree in patience and support as compensation for your struggling in the hard moments in the UK. Also, my thanks to my children **Dana** and **Abd Alrahman**, the taxpayers of my success. I promise you all, one day I will be a perfect Dad. I have also to give big thanks to my family and my friends back in Palestine. I could not have pursued this degree without their love and support. Words can never express my affection and gratitude to them. Finally, I would like to thank my big brother **Mohammed Lubbad** and his family for their friendship and moral support which gave my family and me the power to survive in the UK.

Thank you very much for all of you and for all the others who I did not mention……

Ahmed,

September, 2016

Declaration

The research described in this thesis was conducted at the Nottingham Transportation Engineering Centre, Civil Engineering Department, the University of Nottingham between October 2013 and September 2016. I declare that the work is my own and has not been submitted for a degree of another university.

Ahmed Izat Mohammed Nassar,

September, 2016

University of Nottingham

Table of Contents

Abstract ..... **i**

Dedication ..... **iv**

Acknowledgements ..... **v**

Declaration ..... **vii**

Table of Contents ..... **viii**

List of Figures ..... **xvii**

List of Tables ..... **xxv**

List of Abbreviations ..... **xxvii**

Chapter 1: Introduction **1**

1.1 Overview and research motivation 1

1.2 Problem statement 3

1.3 Research aim and objectives 6

1.4 Research significance and contributions 7

1.5 Thesis structure and outline 9

1.6 Publications list 12

Chapter 2: Literature Review **14**

2.1 Introduction 14

2.2 Bitumen emulsion technology 14

2.2.1 Introduction 14

2.2.1 Bitumen emulsion types 15

2.2.2 Bitumen emulsion composition 16

2.2.3 Other bitumen emulsion components 17
2.2.3.1 Stabilizers 17
2.2.3.2 Adhesion promoters 18
2.2.3.3 Solvent 18
2.2.4 Manufacturing process of bitumen emulsion 18
2.2.5 Breaking mechanism of bitumen emulsion 20
2.2.5.1 Breaking mechanism due to adsorption of emulsifiers 21
2.2.5.2 Breaking mechanism due to water evaporation 21
2.2.5.3 Breaking mechanism due to pH change 22
2.2.6 Bitumen emulsion application 24
2.3 Cold mix asphalt (CMA) overview 26
2.3.1 Energy consumptions and emissions of CMA 27
2.3.2 Cold mix asphalt (CMA) challenges 30
2.4 Cold mix asphalt (CMA) practices 31
2.4.1 Cold lay macadam 31
2.4.2 Grave emulsion mixture 32
2.4.3 Foamed bitumen mixture 33
2.4.4 Cold bitumen emulsion mixture (CBEM) 34
2.5 Performance characteristics of CBEMs 36
2.5.1 The effect of compaction effort 36
2.5.2 Treatment of CBEMs using hydraulic binders 40
2.5.3 Treatment of CBEMs using by-products materials 43
2.5.4 Treatment of CBEMs using other materials 45
2.5.5 Evaluation of microstructure of cement treated CBEM 47

2.5.6 The effect of curing of CBEMs 50

2.6 Mix design considerations of CBEMs 57

2.7 Structural design considerations of CBEMs 64

2.8 Critical appraisal of previous studies related to performance characteristics of CBEMs 67

Chapter 3: Methodology and Materials 69

3.1 Introduction 69

3.2 The methodology 69

3.3 Characterization of the materials 73

3.3.1 Virgin limestone aggregate 73

3.3.2 Bitumen emulsion 75

3.3.3 Bitumen 75

3.3.4 Water 76

3.3.5 Fillers 76

3.3.5.1 Introduction 76

3.3.5.2 Limestone filler (LF) 78

3.3.5.3 Ordinary Portland cement (OPC) 78

3.3.5.4 Fly ash (FA) 79

3.3.5.5 Ground granulated blast-furnace slag (GGBS) 80

3.3.5.6 Silica fume (SF) 80

3.3.6 A detailed characterization of fillers 81

3.3.6.1 Morphology of fillers 81

3.3.6.2 Particle size distribution of fillers 82

3.3.6.3 Chemical composition of fillers 83

3.4 Summary 85

Chapter 4: Design and Optimization of CBEM **86**

4.1 Introduction 86

4.2 Methodology 89

4.2.1 Properties of the materials used 90

4.2.2 Compaction characteristic 91

4.2.2.1 Laboratory trial mixes 93

4.2.3 Design of experiment using RSM 95

4.2.4 Multiple responses optimization using RSM 97

4.2.5 Mix proportions of CBEMs 98

4.2.6 Manufacturing procedures of CBEMs 99

4.2.7 Laboratory testing program 101

4.2.7.1 Indirect tensile stiffness modulus (ITSM) 101

4.2.7.2 Indirect tensile strength (ITS) 102

4.2.7.3 Volumetric responses 102

4.3 Results and analysis of performance responses 103

4.3.1 Analysis of mechanical responses 105

4.3.1.1 Indirect tensile stiffness modulus (ITSM) 106

4.3.1.2 Indirect tensile strength (ITS) 109

4.3.2 Analysis of volumetric responses 114

4.3.2.1 Air voids 114

4.3.2.2 Dry density 115

4.3.3 Statistical analysis of responses 117

4.3.4 Optimization of the mix design components 123

4.4 Summary 124

Chapter 5: Performance characterization of CBEMs (Mechanical, Durability and Microstructure) 127

5.1 Introduction 127

5.2 Mixture designation of treated CBEMs 128

5.3 Experimental program 130

5.4 Moisture content evaluation 131

5.4.1 Results and discussion 131

5.5 Indirect tensile stiffness modulus (ITSM) 133

5.5.1 Test configuration 133

5.5.2 Sample preparation 135

5.5.3 Results and discussion 135

5.5.4 The effect of testing temperature on stiffness modulus 139

5.6 Resistance to permanent deformation 142

5.6.1 Test configuration 142

5.6.2 Sample preparation 144

5.6.3 Results and discussion 144

5.6.4 The effect of stress level on permeant deformation of CBEMs 147

5.6.5 The effect of testing temperature 150

5.7 Resistance to crack initiation and crack propagation 151

5.7.1 Indirect tensile strength (ITS) 151

5.7.1.1 Samples preparation 152

5.7.1.2 Results and discussion 152

5.7.2 Indirect tensile fatigue test (ITFT) 154

5.7.2.1 Test configuration 155
5.7.2.2 Samples preparation 157
5.7.2.3 Results and discussion 157
5.7.3 Semi-circular bending (SCB) test 162
5.7.3.1 Test configuration 163
5.7.3.1 Sample preparation 164
5.7.3.2 Results and discussion 165
5.8 Durability evaluation 167
5.8.1 Sample preparation and test procedures 167
5.8.2 Results and discussion of moisture damage evaluation 168
5.8.3 Results and discussion of frost damage evaluation 170
5.9 Mineralogy and microstructure evaluation of CBEMs 173
5.9.1 X-ray diffraction (XRD) evaluation 174
5.9.1.1 Test configuration 174
5.9.1.2 Sample preparation 175
5.9.1.3 Results and discussion 176
5.9.2 Scanning electron microscopy (SEM) evaluation 179
5.9.2.1 Sample preparation 181
5.9.3 Results and discussion 181
5.10 Summary 188
Chapter 6: Parametric Curing Study and Maturity Relationship Application of CBEMs 192
6.1 Introduction 192
6.2 Methodology adopted 194

6.2.1 Sample preperation and curing procedures 196
6.2.2 Experimental programme..... 197
6.2.2.1 Moisture loss monitoring..... 197
6.2.2.2 Indirect tensile stiffness modulus (ITSM) evaluation..... 197
6.2.2.3 Repeated load axial test (RLAT)..... 198
6.2.2.4 Bitumen binder characterization before and after the curing. 198
6.3 Results and discussion of parametric curing study..... 199
6.3.1 Moisture loss monitoring..... 199
6.3.2 Indirect tensile stiffness modulus (ITSM) evaluation..... 201
6.3.2.1 Influence of curing time and temperatures..... 201
6.3.2.2 Influence of active filler content and curing temperatures 201
6.3.2.3 Influence of moisture loss on stiffness modulus 206
6.3.2.4 Influence of moisture loss on the moisture content of CBEMs 211
6.3.2.5 Influence of relative humidity (RH) 212
6.3.3 Resistance to permanent deformation..... 214
6.3.4 Bitumen characterization before and after curing 215
6.4 Laboratory simulation of field curing..... 217
6.4.1 Introduction 217
6.4.2 The maturity approach 217
6.4.2.1 Nurse-Saul method 218
6.4.2.2 Arrhenius method 219
6.4.3 Maturity–strength relationships 221
6.4.3.1 Logarithmic model 222
6.4.3.2 Exponential model 222

6.4.3.3 Hyperbolic model 223
6.4.4 Application of maturity methods to CBEM 223
6.4.4.1 Stiffness–age relationships 225
6.4.4.2 Temperature sensitivity factor 229
6.4.4.3 Age conversion factor and equivalent age 230
6.4.5 Validation of developed maturity models 233
6.4.6 Practical implications 235
6.5 Summary 239
Chapter 7: Pavement Analysis and Design Incorporating CBEMs 241
7.1 Introduction 241
7.2 Pavement arrangements and properties 242
7.2.1 The first scenario: study the effect of incorporating treated CBEMs as a surface course 242
7.2.2 The second scenario: study the effect of incorporating treated CBEMs as a base course 243
7.3 Pavement design methodology 245
7.4 Pavement stress and strain distribution results 246
7.4.1 Vertical stress and strain distributions for the first scenario 246
7.4.2 Horizontal stress and strain distributions for the first scenario 247
7.4.3 Vertical stress and strain distributions for the second scenario 249
7.4.4 Horizontal stress and strain distributions for the second scenario 250
7.5 Pavement design sensitivity analysis 252
7.5.1 Introduction 252
7.5.2 Incorporating CBEMs as surface course 253

7.5.3 Incorporating CBEMs as base course 254

7.6 Summary 255

Chapter 8: Conclusions and Recommendations **257**

8.1 Introduction 257

8.2 Conclusions 258

8.2.1 The main conclusions related to design and optimization of CBEM 258

8.2.2 The main conclusions related to performance characterization of CBEMs 259

8.2.3 The main conclusions related to parametric curing study and maturity relationship application of CBEMs 261

8.2.4 The main conclusions related to pavement analysis and design incorporating CBEMs 262

8.3 Recommendations for further research 263

References **267**

List of Figures

Figure 2.1 Typical particle size distribution diagram of a bitumen emulsion (Miljković, 2014) 15

Figure 2.2 Schematic illustration of charges on bitumen droplets in an emulsion (Read and Whiteoak, 2003) 17

Figure 2.3 Schematic illustration of continuous and batch process plants for producing bitumen emulsion (Read and Whiteoak, 2003) 20

Figure 2.4 Emulsifier ions forming micelle in a stable emulsion(Read and Whiteoak, 2003) 22

Figure 2.5 Schematic illustration of the breaking process (Read and Whiteoak, 2003) 22

Figure 2.6 Classification of mixture technologies by temperature range and fuel usage (D'Angelo et al., 2008) 27

Figure 2.7 Energy consumption for the manufacture and laying of main road technologies (Chappati and Bilal, 2003) 29

Figure 2.8 Greenhouse emissions of the manufacture and laying of main road technologies (Chappati and Bilal, 2003) 29

Figure 2.9 Foaming nozzle examples (EAPA, 2014b) 33

Figure 2.10 The process of in-situ cold recycling using foamed bitumen (Ebels, 2008) 34

Figure 2.11 The process of in-situ recycling using bitumen emulsion (Wirtgen, 2005) 36

Figure 2.12 Influence of compaction degree on stiffness modulus of grave-emulsion (Serfass et al., 2004)..... 37

Figure 2.13 Indirect tensile strength of dry and conditioned CBEMs specimens with different additives (Niazi and Jalili, 2009) 40

Figure 2.14 The effect of different cement contents on CBEM stiffness modulus (Needham, 1996) 41
Figure 2.15 The effect of different cement content on CBEM permanent deformation resistance (Oruc et al., 2007) 42
Figure 2.16 Water sensitivity results of CBEM with different filler treatments (Al-Hdabi et al., 2013b) 44
Figure 2.17 XRD results for cement asphalt mastic and cement paste (Du, 2014) 47
Figure 2.18 Hydration products observed in cement emulsified asphalt mixture (Wang et al., 2014) 48
Figure 2.19 Microtomography detail of an asphalt and cement composite (García et al., 2013) 49
Figure 2.20 Evolution of ITSM as a function of curing temperature and time (Bocci et al., 2011) 50
Figure 2.21 Effect of different curing conditions and compaction on compressive strength of grave emulsion mix (Serfass et al., 2004) 51
Figure 2.22 Schematic representation of the curing process of CBEMs (García et al., 2013) 52
Figure 2.23 General mix design procedure (Jenkins, 2000) 58
Figure 2.24 Compaction characteristics of CBEMs (Oke, 2010) 59
Figure 2.25 The relation between stiffness modulus, tensile strength and moisture susceptibility evaluation with total fluid content (Ojum, 2015) 62
Figure 2.26 Typical mix design procedure for CMA (Jacobson, 2002) 62
Figure 2.27 The effect of mixing time on the stiffness modulus and air voids of CBEMs (Oke, 2010) 64
Figure 2.28 Conceptual behaviour of pavement materials a function of bitumen and active filler content (Asphalt Academy, 2009) 65
Figure 3.1 Flowchart of the research methodology 72
Figure 3.2 Limestone aggregate size fractions 74

Figure 3.3 Aggregate gradation of the nominal sizes of the crushed limestone aggregate 74
Figure 3.4 The candidate fillers 77
Figure 3.5 Morphology of fillers 82
Figure 3.6 Particle size distribution of fillers 83
Figure 4.1 Optimization of CBEM methodology using RSM 90
Figure 4.2 Aggregate gradation for CBEM 91
Figure 4.3 Compaction characteristic of crushed limestone aggregate using modified Proctor compaction 92
Figure 4.4 Volumetric properties of initial CBEM with varying BEC and P 94
Figure 4.5 Mechanical properties of initial CBEM with varying BEC and PWC 94
Figure 4.6 Manufacturing process for CBEMs 100
Figure 4.7 Weight loss over curing period 105
Figure 4.8 The relation between ITSM and total fluid content of CBEMs under different CT after (a) 10 days and (b) 28 days 107
Figure 4.9 Contour plots of $ITSM_{10\ days}$ versus BEC and PWC; (a) CT =10°C, (b) CT =20°C and (c) CT =30°C 108
Figure 4.10 The relation between ITS and total fluid content of CBEMs under different CT (a) dry condition and (b) wet condition 110
Figure 4.11 Contour plots of ITS $dry_{28\ days}$ versus BEC and PWC; (a) CT =10°C, (b) CT =20°C and (c) CT =30°C 112
Figure 4.12 Contour plots of ITS $wet_{28\ days}$ versus BEC and PWC; (a) CT =10°C, (b) CT =20°C and (c) CT =30°C 113
Figure 4.13 The relation between air voids and total fluid content of CBEMs ... 114
Figure 4.14 Contour plot of air voids versus BEC and PWC 115
Figure 4.15 The relation between dry density and total fluid content of CBEMs 116
Figure 4.16 Contour plot of dry density versus BEC and PWC 117
Figure 4.17 3D-surface plots of $ITSM_{10\ days}$, ITS $dry_{28\ days}$, ITS $wet_{28\ days}$, air voids and dry density 122

Figure 5.1 The water content evaluation of CBEMs 132
Figure 5.2 ITSM test configuration..... 134
Figure 5.3 The stiffness modulus of CBEMs treated with cement over the curing period..... 137
Figure 5.4 The stiffness modulus of CBEMs treated with blended fillers over the curing period 137
Figure 5.5 Stiffness modulus of CBEMs treated with cement under different testing temperatures..... 140
Figure 5.6 Stiffness modulus of CBEMs treated with blended fillers under different testing temperatures 140
Figure 5.7 RLAT test configuration..... 143
Figure 5.8 The permanent strain of CBEMs treated with cement under 100kPa stress 145
Figure 5.9 The permanent strain of CBEMs treated with blended fillers under 100kPa stress 146
Figure 5.10 Accumulated permanent strain of cement-treated CBEMs under different stresses 148
Figure 5.11 A damaged LF-CBEM under high-stress level (300kPa) in RLAT 148
Figure 5.12 Accumulated permanent strain of blended filler-treated CBEMs under different stresses 149
Figure 5.13 A comparison of accumulated permanent strain at 40 and 50oC under 300kPa for selected mixes..... 150
Figure 5.14 ITS test configuration 152
Figure 5.15 ITS of CBEMs treated with cement..... 153
Figure 5.16 ITS of CBEMs treated with blended fillers 153
Figure 5.17 ITFT test configuration..... 156
Figure 5.18 Fatigue performance of cement treated CBEMs 160
Figure 5.19 Fatigue performance of blended fillers treated CBEMs 160
Figure 5.20 Relationship between fatigue life and stress ratio for CBEMs 161

Figure 5.21 SCB configuration test 164
Figure 5.22 Effect of treated fillers in CBEM on fracture toughness 166
Figure 5.23 The results of moisture damage for CBEMs treated with cement... 169
Figure 5.24 The results of moisture damage for CBEMs treated with blended fillers 170
Figure 5.25 The results of frost damage for CBEMs treated with cement..... 171
Figure 5.26 The results of frost damage for CBEMs treated with blended fillers 172
Figure 5.27 Fracture surface after moisture conditioning (a) without active filler (b) with active filler 173
Figure 5.28 XRD equipment and schematic of X-ray diffraction, adopted from (Erdem, 2012, Nelson, 2015) 175
Figure 5.29 Methodology to investigate the mineralogy and microstructure of CBEMs 176
Figure 5.30 XRD results of selected CBEMs 178
Figure 5.31 SEM equipment and schematic of SEM process (Fens, 2000) 180
Figure 5.32 Interaction between the beam and the sample, generation of different signals (Fens, 2000) 181
Figure 5.33 Morphology details of the microstructure of LF-CBEM 182
Figure 5.34 Morphology details of the microstructure of 5C-CBEM 183
Figure 5.35 Morphology details of the microstructure of C-G-CBEM (a, b, d and e) and C-G-2S-CBEM (c and f) 184
Figure 5.36 Morphology details of the microstructure of C-F-CBEM (a, b, c, d and e) and C-F-2S-CBEM (f) 185
Figure 6.1 Schematic diagram and photograph of the RH chamber 195
Figure 6.2 Curing CBEM at different curing temperature with lower RH 197
Figure 6.3 Moisture loss by evaporation for CBEMs cured at 40°C..... 199
Figure 6.4 Moisture loss by evaporation for CBEMs cured at 20°C..... 200
Figure 6.5 Moisture loss by evaporation for CBEMs cured at 5°C 200
Figure 6.6 Evolution of ITSM at different curing temperatures for LF-CBEM..... 202

Figure 6.7 Evolution of ITSM at different curing temperatures for 1C-CBEM 203
Figure 6.8 Evolution of ITSM at different curing temperatures for 3C-CBEM 203
Figure 6.9 Evolution of ITSM at different curing temperatures for 5C-CBEM 204
Figure 6.10 Evolution of ITSM at different curing temperatures for C-F-CBEM . 205
Figure 6.11 Evolution of ITSM at different curing temperatures for C-G-CBEM. 205
Figure 6.12 The relationship between moisture loss and stiffness modulus under different curing temperatures for LF-CBEM 208
Figure 6.13 The relationship between moisture loss and stiffness modulus under different curing temperatures for 1C-CBEM..... 208
Figure 6.14 The relationship between moisture loss and stiffness modulus under different curing temperatures for 3C-CBEM..... 209
Figure 6.15 The relationship between moisture loss and stiffness modulus under different curing temperatures for 5C-CBEM..... 209
Figure 6.16 The relationship between moisture loss and stiffness modulus under different curing temperatures for C-F-CBEM..... 210
Figure 6.17 The relationship between moisture loss and stiffness modulus under different curing temperatures for C-G-CBEM 210
Figure 6.18 The effect of RH on the stiffness modulus of CBEM. 213
Figure 6.19 A comparison of accumulated permanent strain for CBEMs cured at 5, 20, 40°C 214
Figure 6.20 The effect of curing temperatures on bitumen properties..... 216
Figure 6.21 Illustrating equivalent age (curing temperature was changed from 5°C to 20°C at 40 days) adopted (Kuna, 2015) 221
Figure 6.22 The methodology adopted to apply a maturity–stiffness relationship 225
Figure 6.23 Stiffness development relationships for LF-CBEM cured at 5°C 227
Figure 6.24 Stiffness development relationships for LF-CBEM cured at 20°C ... 227
Figure 6.25 Stiffness development relationships for LF-CBEM cured at 40°C ... 228

Figure 6.26 Stiffness development relationships for LF-CBEM cured at 5, 20, 40°C with best fit linear-hyperbolic model 228
Figure 6.27 Variation of rate constant with curing temperature for linear-hyperbolic model 229
Figure 6.28 Age conversion factor for reference temperature of 20°C 230
Figure 6.29 Equivalent age referenced to 20°C for LF-CBEM 231
Figure 6.30 Maturity–stiffness relationship for LF-CBEM 232
Figure 6.31 Validation of the maturity–stiffness model for CBEMs cured at 30°C for 28 days..... 234
Figure 6.32 Validation of the maturity–stiffness model for CBEMs cured at 10°C for 21 days + 30°C for 7 days..... 235
Figure 6.33 Mean daily temperatures for month of May, 2015 in locations selected in the study 236
Figure 6.34 Prediction of the stiffness modulus in hypothetical sections using maturity–stiffness relationships for LF-CBEM and 1C-CBEM 237
Figure 6.35 Prediction of the stiffness modulus in hypothetical sections using maturity–stiffness relationships for C-G-CBEM and C-F-CBEM 237
Figure 7.1 Pavement structure considered for analysis of the first scenario..... 243
Figure 7.2 Pavement structure considered for analysis of the second scenario 244
Figure 7.3 Vertical stress distribution through pavement structure for first scenario 246
Figure 7.4 Vertical strain distribution through pavement structure for the first scenario 247
Figure 7.5 Horizontal stress distribution through pavement structure for the first scenario 248
Figure 7.6 Horizontal strain distribution through pavement structure for the first scenario 248
Figure 7.7 Vertical stress distribution through pavement structure for the second scenario 249

Figure 7.8 Vertical strain distribution through pavement structure for the second scenario 250
Figure 7.9 Horizontal stress distribution through pavement structure for the second scenario 251
Figure 7.10 Horizontal strain distribution through pavement structure for the second scenario 252
Figure 7.11 Allowable load applications for variable AC 50 base course thicknesses under 60 mm of treated CBEM as a surface 254
Figure 7.12 Allowable load applications for variable treated CBEM base course thicknesses under 60 mm HRA as a surface 255

List of Tables

Table 2.1 Usage of Bitumen Emulsions (Le Coroller 2002) 25

Table 2.2 Production of CMA in tonnes from 2008 to 2012 26

Table 2.3 Summary of studies performed on the compactability of CBEM 39

Table 2.4 Summary of studies performed to investigate CBEM curing process ... 55

Table 3.1 Physical characteristics of crushed limestone aggregate (BS EN1097-6:2000) 74

Table 3.2 Bitumen emulsion properties 75

Table 3.3 Properties of 40/60 bitumen used in the study 76

Table 3.4 Physical characteristics of fillers 83

Table 3.5 Chemical composition of fillers 84

Table 4.1 Modified Proctor test parameters 92

Table 4.2 Independent parameters and their coded levels for CCD 98

Table 4.3 Matrix of experimental design by CCD 99

Table 4.4 Experimental factors and experimental responses 104

Table 4.5 ANOVA for analysis of variance and adequacy of the quadratic model for responses..... 118

Table 4.6 The optimum BEC and PWC at different CT with their responses 123

Table 5.1 Mixture designations based on filler treatments..... 129

Table 5.2 The experimental program tests..... 130

Table 5.3 ITSM test configuration based on BS EN 12697-26 134

Table 5.4 Stiffness modulus and air voids values for the mixtures studied 136

Table 5.5 Temperature sensitivity of analytical model results..... 141

Table 5.6 RLAT test configuration based on BS EN 12697-25 143

Table 5.7 Summary of RLAT test results for studied mixes 147

Table 5.8 ITFT test configuration based on BS EN 12697-24 156

Table 5.9 Fatigue performance for CBEMs 158
Table 5.10 Regression coefficients for fatigue equations from ITFT tests 158
Table 6.1 Summary of experimental program for the first phase 194
Table 6.2 CBEM curing protocols used in first phase 196
Table 6.3 The relationship between moisture loss and stiffness modulus for CBEMs 207
Table 6.4 Summary of moisture content calculations 212
Table 6.5 Determination coefficient R^2 of curing models 228
Table 6.6 Summary of parameters resulted by regression analysis 229
Table 6.7 Summary of temperature sensitivity factors (B) based on linear-hyperbolic model 230
Table 6.8 Summary of maturity–stiffness model parameters 233
Table 6.9 Comparison the obtained laboratory stiffness modulus of CBEM to in-situ predicted modulus 238
Table 7.1 The properties of the treated CBEMs involved in the pavement analysis 242
Table 7.2 The properties of the other mixes involved the in the pavement analysis 243

List of Abbreviations

AP	Adequate precision
ANOVA	Analysis of variance
AC	Asphalt concrete
BBF	Binary blended filler
BEC	Bitumen emulsion content
BSM	Bitumen stabilized mixture
CCD	Central composite design
CBEM	Cold bituminous emulsion mixture
CMA	Cold mixture asphalt
CT	Curing temperature
DF	Desirability function
EDX	Energy dispersive X-ray fluorescence spectrometer
FA	Fly ash
GGBS	Granulated ground blast-furnace slag
GM	Grouted macadam
HWMA	Half-warm mix asphalt
HMA	Hot mix asphalt
HRA	Hot rolled asphalt
HL	Hydrated lime
ITFT	Indirect tensile fatigue test
ITSM	Indirect tensile stiffness modulus
ITS	Indirect tensile strength
ITSR	indirect tensile strength ratio
LOF	Lack of fit
LF	Limestone filler

MDD	Maximum dry density
MSA	Millions of standard axles
OMC	Optimum moisture content
OPC	Ordinary Portland cement
PWC	Pre-wetting water content
PFA	Pulverized fly ash
RAP	Recycled asphalt pavement
RH	Relative humidity
RLAT	Repeated axial load test
RSM	Response surface methodology
SEM	Scanning electron microscopy
SCB	Semi-circular bending test
SF	Silica fume
SCM	Supplementary cementitious material
TTF	Temperature time factor
TBF	Ternary blended filler
TFC	Total fluid content
WMA	Warm mix asphalt
XRD	X-ray diffraction analysis

Chapter 1

Introduction

1.1 Overview and research motivation

Nowadays, environmental issues related to reducing energy consumption, reducing CO_2 emissions and managing wastes are being increasingly articulated and have been gaining attention worldwide. In pavement materials, hot mix asphalt (HMA) is usually prepared by mixing preheated mineral aggregates (150-250°C), bitumen binder which is usually generated from crude petroleum (160°C), filler and other additives. Since the working temperature is relatively high, large amounts of fuel are required for heating up the aggregates and the bitumen. Recent studies show that about 7.6-9.7 litres of fuel are burned for producing 1 ton of HMA consuming 275 MJ energy (Chappati and Bilal, 2003, D'Angelo et al., 2008, Chehovits and Galehouse, 2010, Sullivan and Moss, 2014) contributing 15% to the total cost of HMA manufacture (Sullivan and Moss, 2014). Furthermore, the health and safety issue due to the use of unsafe high temperatures plus exposure to fumes and dust during production add another dimension to the shortcomings of HMA. All these raise significant discussion on the subject of more economic and sustainable pavement material alternatives. Hence, warm mix asphalt (WMA) technology has attracted many researchers and huge efforts have been expended to develop such a mixture (Hurley and Prowell, 2005, D'Angelo et al., 2008, Prowell et al., 2011). Generally, WMA has slightly reduced CO_2 emissions and energy consumption compared with HMA; however, cost and other issues such as long-term performance need to be proven.

One of the most significant trends towards more eco-friendly asphalt mixes is the use of cold mixture asphalt (CMA). Several research projects have been performed to study and develop the properties of these mixtures incorporating different material such as recycled asphalt pavement, municipal solid waste incineration ash, construction and demolition waste material, cement kiln dust and coal ash (Pasetto and Baldo, 2010, Al-Busaltan et al., 2012, Al-Hdabi et al., 2013a, Pérez et al., 2013, Gómez-Meijide and Pérez, 2014a, Modarres and Ayar, 2014, Gómez-Meijide et al., 2015, Betti et al., 2016).

Moreover, recently, the construction of roads using CMA has gained increasing interest around the world. For example, in 2008 the production of CMA is 2 million tonnes in France and 3.5 million tonnes in Turkey (EAPA, 2014a, Gómez-Meijide and Pérez, 2014a). However, in the UK, the use of CMA is limited to base and sub-base courses of structural layers (Needham, 1996, Khalid and Monney, 2009, Thanaya et al., 2009). Cold bitumen emulsion mixture (CBEM) is the most widely known type of CMA, which comprises bitumen emulsion as a binder. CBEM is preferred over CMA containing cutback binder by road engineers due to its environmental advantages.

The advantages of CBEMs are very attractive regarding environmental, economic and safety issues. But, so far, CBEMs suffer from a lack of essential mechanical properties, making it inferior to HMA, and without addressing this issue CBEMs cannot be a successful alternative to HMA. Previous studies have shown that their performance is inferior compared to HMA; thus it has been used in limited applications such as low/medium trafficked roads, footways and reinstatements (Leech, 1994, Read and Whiteoak, 2003, Thanaya, 2003, Liebenberg and Visser, 2004). Ibrahim (1998) suggested using CBEMs for heavily trafficked roads when overlaid by at least 40 mm of hot bituminous mixture layer. The relatively wet and cold weather in the United Kingdom does not favour the emulsion curing process,

and thus, additionally limits the use of CBEM (Leech, 1994). Consequently, promoting CBEMs has attracted many asphalt researchers, and two general strategies have been adopted to address the above shortcomings, namely incorporating additives into CBEM, and upgrading preparation and construction techniques. For example, different attempts have been used ordinary Portland cement (Terrell and Wang, 1971, Schmidt et al., 1973, Head, 1974, Needham, 1996, Thanaya, 2003, Oruc et al., 2007, Niazi and Jalili, 2009, García et al., 2013, Fang et al., 2016), rapid-hardening cement (Thanaya, 2003, Fang et al., 2016), fibres (Bueno et al., 2003, Ferrotti et al., 2014) and polymers (Chávez-Valencia et al., 2007, Zhang et al., 2011) as additives. However, most of the previous attempts either failed to satisfy the required performance, or achieved a certain improvement but they had extra cost or adverse environmental impact.

There is a significant need to carry out an intensive scientific research in order to develop CMA, more precisely CBEMs, to increase their utilization. This demands novel and sustainable CBEM products. The properties of these novel mixtures should be similar to conventional HMA in order to justify their broader application.

1.2 Problem statement

Despite the efforts applied in the last few decades in order to improve and develop CBEM utilization, there are deficiencies that make it inferior to HMA, resulting in restricting or minimizing their use. Compared with HMA, durability is one of the main concerns if CBEM is to be used as a structural pavement layer. Normally, CBEMs are used as base or subbase courses within a pavement structure (Leech, 1994, Read and Whiteoak, 2003, Liebenberg and Visser, 2004).

The research problem tackled in this thesis was defined as a result of a critical appraisal of the literature. A number of unclear or unresolved issues and knowledge

gaps related to CBEM performance were identified and can be summarized as presented in the following paragraphs.

Most of the background studies have showed that the performance of CBEMs can be improved using cement (Terrell and Wang, 1971, Schmidt et al., 1973, Head, 1974, Needham, 1996, Thanaya, 2003, Oruc et al., 2007, Niazi and Jalili, 2009, García et al., 2013, Fang et al., 2016). However, the use of relatively high cement content for CBEMs increases their cost and would contribute to increasing cement demand worldwide and consequently CO_2 emission. There is a lack of evidence in the literature of comprehensive studies conducted using other alternatives to cement, although limited studies have recently focussed on using rapid-hardening cement to improve the performance (Thanaya, 2003, Fang et al., 2016). However, this is may add extra cost or adverse environmental impact. On the other hand, very few studies have been conducted to investigate the use of by-product materials to enhance CBEM properties as an alternative to cement (Ellis et al., 2004, Al-Busaltan et al., 2012, Al-Hdabi et al., 2013a).

The majority of studies have focussed on evaluating the performance of cement treated CBEMs; studies focussed on internal arrangement and microstructure are rarely found. The assessment of microstructure and internal composition of CBEMs are critical for deeper understanding of the mechanism of performance improvement. However, evaluating the interaction between fillers (cement/active fillers) in the presence of bitumen emulsion and how this affects the hydration and microstructural characteristics of CBEMs is needed as such issues are still unclear. Despite previous studies having discussed this issue from different perspectives, there is no agreement as to whether the presence of bitumen emulsion affects the hydration of cement or not (Giuliani, 2001, Pouliot et al., 2003, Du, 2014, Wang et al., 2014, Fang et al., 2016).

Based on their various findings, different researchers have claimed the that the performance of CBEMs may be at least partially due to the wide variation in available mix design procedures, tests and criteria (Brayton et al., 2000, Liebenberg and Visser, 2004, Sebaaly et al., 2004, Kim et al., 2007, CEDR, 2014). Different authorities and researchers have proposed differing mix design procedures, based on empirical formulae, laboratory tests or past experience (Asphalt Institute, 1989, Nikolaides, 1994, Brayton et al., 2000, Jenkins, 2000, Thanaya, 2003, Lesueur and Potti, 2004, Kim and Lee, 2006). However, unlike HMA, there is no global agreement on mixture design method for CBEMs although the majority of studies have used the Asphalt Institute (1989) method. Thus, it is clear that optimization of mixture parameters has to be made more consistent in order to promote the utilization of CBEMs (Brayton et al., 2000) since variations in material proportions and mix design procedure will generate differences in performance (Sebaaly et al., 2004). It is therefore essential to design and optimize mixture components in order to achieve appropriate properties (Brayton et al., 2000, Kim et al., 2007).

It has been reported in the literature that the performance of CBEM is directly related to the properties and proportions of materials that are used in the mixture and to the curing process (Needham, 1996, Jenkins, 2000, Thanaya, 2003, Oruc et al., 2007, Niazi and Jalili, 2009, Bocci et al., 2011). CBEM requires a certain curing time to build up the required ultimate mechanical properties. Attention should be paid to understand the effect of the curing process on the performance of CBEMs. It was understood that there is a lack of clarity regarding the influence of the curing process under different climatic conditions on the performance of CBEMs particularly when using cement/active fillers. This is because of the complex combination of three phenomena acting together during the curing process: emulsion breaking, moisture loss and hydration of cementitious compounds (Serfass et al., 2004, García et al., 2013, Cardone et al., 2014). A debate has been

reported in the literature about the effect of curing temperature on the hydration process of active filler and the influence of curing temperature on the binder condition (Bocci et al., 2011, Cardone et al., 2014, Godenzoni et al., 2016). No agreement has been achieved on this point due to lack of convincing evidence. Another important point is that a lot of research has been carried out to study the effect of various laboratory curing regimes on CBEM performance. However, unfortunately, very few studies have been performed to evaluate the in-situ performance (Doyle et al., 2013, Kuna, 2015). This raises a very important question about the possibility of using laboratory results to predict the effect of climatic variations on in-situ cured mixture performance.

1.3 Research aim and objectives

The present study is primarily aimed at evaluating the effect of using different cementitious materials on the performance of CBEM. The idea of the research is to provide a sustainable filler from supplementary cementitious materials (SCMs) to be used as a filler which would provide enhanced properties of CBEMs. By achieving this aim it is expected that the utilization of CBEM would increase, allowing them to be used as structural pavement materials with some confidence. Moreover, taking into consideration the shortcomings of CBEM, this study also aimed at developing a novel performance-based mix design approach for CBEM involving a statistical technique.

To be specific the objectives of this study include, but are not limited to, the following:

1. To optimize the mix design of CBEM using a statistical approach called response surface methodology (RSM), as an alternative to achieve acceptable engineering properties.

2. To investigate the performance characteristics of CBEMs using different filler treatments such as cement and SCMs and to understand the performance enhancement through internal composition and microstructure investigation.

3. To understand the effect of the curing process on CBEM performance and develop a prediction model to assess in-situ CBEM performance using maturity relationships.

4. To conduct structural design and analysis of pavement using a mechanistic approach for incorporating CBEMs into the pavement structure as surface and base courses.

1.4 Research significance and contributions

Despite extensive research into different types of CBEM, to date, several problems related to curing time, low early strength, rutting resistance and water sensitivity of CBEMs have not been addressed. Therefore, developing CBEMs with high early strength, resistance to water ingress and with minimal time delay requirements before structural loading would be considered as a breakthrough in CBEM research. Moreover, using a sustainable filler derived from SCMs in combination with cement could provide the enhanced properties of CBEMs and would offer a potential impact on sustainability by reducing the need for cement in CBEMs. Accordingly, it is hoped that wider utilization of CBEMs in the construction of highway and pavement materials (with both environmental and economic impacts) can be derived from the current research. This is because the utilization of such materials will save the environment by reducing CO_2 emissions and energy consumption. Consequently, it could be useful in protecting the environment by minimizing the volume of waste disposed to landfill. Also, among the SCMs, fly ash (FA), granulated ground blast-furnace slag (GGBS) and silica fume (SF) in combination of ordinary Portland cement (OPC) have not been utilized, until now, in producing CBEMs.

Although cement has been extensively used in CBEM treatment, the function of the cement/active filler in the presence of bitumen emulsion is still unclear. Therefore, this work is designed to contribute to a deeper understanding of the microstructure and internal composition of the mixes concerned. Investigation of microstructure is important to explain the improvement in the strength with time due to use of the sustainable fillers.

Furthermore, the current study presents a comprehensive performance evaluation of CBEMs under different testing types and modes. Also, this evaluation was carried out to assess a wide range of engineering properties for pavement materials. All these points can increase the utilization of CBEMs by achieving a proper understanding of their behaviour, which would improve confidence and increase usage level, since, there are still a few countries, e.g. UK, where the current level of CBEM usage leaves considerable room for improvement.

Since, there is no global agreement on mix design method for CBEMs, a consistent optimization of mixture parameters has to be made in order to promote the usage of CBEMs and to ensure a proper performance can be achieved. There is no doubt that CBEM performance depends, to a large extent, on the mix design methods used. At the same time the variations in material proportions will generate differences in performance. An important contribution in the present study will be to develop a performance-based mix design method incorporating a statistical approach using RSM which has not been used before for CBEM optimization. This method has the ability to determine the optimum mix design parameters that yield acceptable mechanical strength and volumetric properties of CBEMs. This approach can, therefore, also be utilized to design, reliably, different pavement materials which do not have a standard mix design procedure.

In order to provide further understanding of the performance of CBEMs, the effect of the curing process will be deeply investigated, focussing on the role of active fillers since curing becomes more complicated in their presence. Also, the study will be extended to propose a reliable tool to estimate in-situ performance of CBEMs using stiffness-maturity relationships, which is an important input parameter for pavement structural design. This tool will be beneficial for road and pavement engineers to evaluate the performance of CBEMs at early age since such assessment using non-destructive testing equipment, such as falling weight and light weight deflectometers, is not practical particularly during construction (early stages of curing).

Also, this study will investigate the incorporation of treated CBEMs as a surface course whereas use as a base course is very common practice in the field. This suggestion will increase the utilization of CBEMs for road construction.

Overall, it is believed that the different subjects related to CBEMs which covered in the current research will provide important information about a sustainable pavement mixture. Besides, this study will enhance the current knowledge and understanding of the behaviour of CBEMs which may lead to increased utilization for road construction, rehabilitation and maintenance.

1.5 Thesis structure and outline

This thesis is organised into eight chapters as follows:

- **Chapter 1** is the introduction, in which the background to the research topic and research motivation are presented. Identification of research problem, objectives, significance and contributions are also included in this chapter.

- **Chapter 2** describes a comprehensive literature review which is related to the background of the current research; several topics are reviewed in this

chapter, including reviews of bitumen emulsion characteristics and applications. An overview of CMA application with more details about CBEM is presented. A critical review of the performance characteristics of CBEMs and several past attempts to improve performance are discussed and highlighted in this chapter. Moreover, this chapter reviews the literature on mix design and structural design considerations of CBEMs.

- **Chapter 3** summarizes the methodology followed to accomplish the objectives of this research project. It also details the characterization of raw materials used in the present study. Alongside the bitumen emulsion, aggregate and water, particular attention is given to filler characterization. This is important as the effect of different filler treatments is considered the core of the present study.

- **Chapter 4** provides the experimental results of mix design optimization using RSM and presents the experimental programme followed during the optimization process. Furthermore, this chapter presents the concept and the application of RSM in different related fields in order to give a simple and reasonable background about this new method.

- **Chapter 5** provides the detailed results of performance characterization of CBEMs treated with different types of filler. Besides cement, binary blended fillers (BBFs) containing a combination of FA or GGBS with OPC, while the ternary blended fillers (TBFs) are a combination of BBFs with SF. This characterization is carried out in terms of mechanical and durability properties. The study also investigates the mineralogy and microstructure of these mixture using specific microanalysis tools. This is followed by summarizing of the test program. A full description of the test configurations used is detailed, then followed by specimen preparation, results and discussion for each performance indicator.

- **Chapter 6** investigates the level of impact of climatic parameters such as curing temperature and relative humidity (RH) in addition to the impact of curing time and the presence of active filler (cement/ blended fillers) on the curing process in CBEMs. The effect of such factors on the curing process has been evaluated in the laboratory in terms of moisture loss monitoring, indirect tensile stiffness modulus and resistance to permanent deformation, and binder characterization before and after curing. The chapter also investigates the application of the maturity method, which is a normalised expression of the degree of curing in a CBEM. The developed maturity model is used to estimate the in-situ stiffness of CBEMs using three hypothetical pavement sections in the United Kingdom, Italy and Qatar; to simulate different curing regimes.

- **Chapter 7** focuses on structural design and analysis of pavement using the mechanistic-empirical approach to investigate the effect of incorporating treated CBEMs on pavement performance. In this chapter, CBEMs are suggested to be used in two scenarios: the first is as a surface course and the second is as a base course. Also, the scope of the study is limited here to design based on the fatigue criterion only and compared with different pavement materials such as hot rolled asphalt, grouted macadam and asphalt concrete.

- **Chapter 8** contains the conclusions and recommendations based on the findings of the study, and directions for future work are also suggested.

1.6 Publications list

The majority of findings obtained in this PhD project have been published or are under review, as follows:

- ***Journal papers:***
  - **NASSAR, A. I.**, THOM, N. & PARRY, T. 2016. Optimizing the mix design of cold bitumen emulsion mixtures using response surface methodology. *Construction and Building Materials,* 104**,** 216-229. (Published)
  - **NASSAR, A. I.**, MOHAMMED, M. K., THOM, N. & PARRY, T. 2016. Mechanical, durability and microstructure properties of Cold Asphalt Emulsion Mixtures with different types of filler. *Construction and Building Materials,* 114**,** 352-363. (Published)
  - **NASSAR, A. I.**, MOHAMMED, M. K., THOM, N. & PARRY, T. 2016. Characterisation of high-performance cold bitumen emulsion mixtures for surface courses. *International Journal of Pavement Engineering***,** 1-10. (Published)
  - **NASSAR, A. I.**, THOM, N. & PARRY, T. 2016. Multi-scale performance response of cold bitumen emulsion mixture under laboratory and in-situ curing conditions. *Materials & Design*. (To be submitted)
- ***Conference papers:***
  - **NASSAR, A. I.**, THOM, N. & PARRY, T. Mix design parameters effects on cold bitumen emulsion mixture using response surface methodology. 6th European Asphalt Technology Association Conference, EATA 2015, 15-17 June 2015 Stockholm, Sweden. (Accepted and presented as poster)

- **NASSAR, A. I.**, THOM, N. & PARRY, T. Examining the effects of contributory factors on curing of cold bitumen emulsion mixtures. 4th Chinese-European Workshop on Functional Pavement Design, CEW 2016, 29 June-1 July 2016 Delft, The Netherlands. Taylor and Francis Group, London, 216-229. (Published)

- **NASSAR, A. I.**, THOM, N. & PARRY, T. Developing a prediction model to assess in-situ cold bitumen emulsion mixture performance. International Conference on advances in Sustainable Construction Materials & Civil Engineering Systems, ASCMCES 18-20 April 2017 Sharjah, United Arab Emirates. (To be submitted)

Chapter 2

Literature Review

2.1 Introduction

This chapter provides a comprehensive literature review which is related to the background of the current research. The most important aspects relating to CBEMs are discussed and presented in seven sections in this chapter. To be specific, the first section (section 2.2) provides a brief introduction to bitumen emulsion technology. The following four sections describe CMA practice, summarizing the previous attempts that have been made to improve CBEM performance. The last two sections review the mix design and structural design considerations of CBEMs. In the end, a critical appraisal of previous studies related to CBEMs was performed in order to define the gaps needing to be filled in this research.

2.2 Bitumen emulsion technology

2.2.1 Introduction

In order to decrease the viscosity of bitumen to enable its behaviour as a liquid, various different methods have been reported in the literature. These methods are heating, dissolving in a solvent, emulsifying and foaming (Read and Whiteoak, 2003). The output of the emulsifying method is bitumen emulsion. Bitumen emulsions are generally two-phase system. This system consists of bitumen, water and some additives. The latter are used to assist in formation and stabilisation or to modify the properties of the emulsion.

In an emulsion, the bitumen is dispersed throughout the water in discrete globules with 0.1 to 50μm globule diameter by the aid of an emulsifier. The emulsifier supplies the bitumen globules with electrostatic charge which then hold the globules stable within the suspension (Read and Whiteoak, 2003). A typical appearance of a bitumen emulsion particle size distribution diagram is shown in Figure 2.1. The particle size distribution of a bitumen emulsion is influenced by its composition and manufacturing process as reported by Gingras et al. (2005).

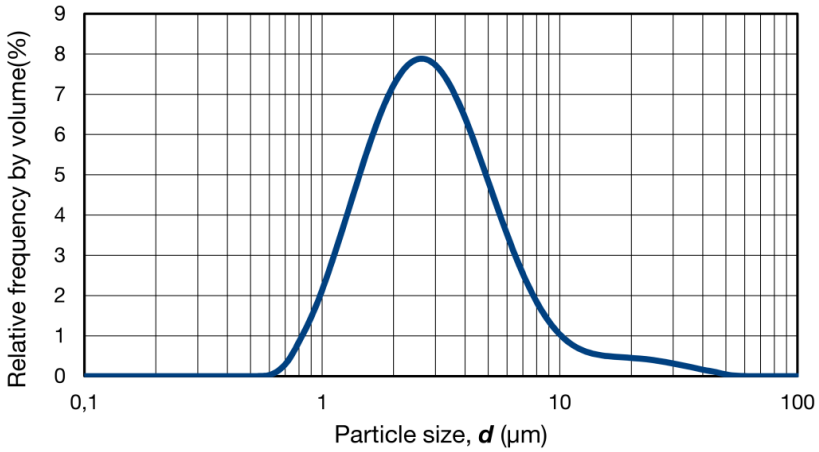


Figure 2.1 Typical particle size distribution diagram of a bitumen emulsion (Miljković, 2014)

2.2.2 Bitumen emulsion types

Bitumen emulsions can be classified into four classes: anionic, cationic, non-ionic, and clay-stabilized emulsions (Read and Whiteoak, 2003). The electrical charges on the bitumen droplets identify the emulsion type. Accordingly, cationic emulsion describes the emulsion system which has positive charges on the bitumen droplets, while anionic is the system of bitumen droplets which have negative charges; both types have been used widely in highway applications. However, the last two types are rarely used in highway works but are commonly used for industrial applications.

2.2.3 Bitumen emulsion composition

Bitumen emulsions are made up of three components that include bitumen, water and an emulsifying agent. Bitumen emulsion is a two-phase system consisting of two immiscible liquids. The ability to stay in suspension is attributed to electrostatic charges provided by the emulsifier. Emulsifiers are surface active agents, so-called surfactants. The role of an emulsifier can be summarized as follows (Gibb, 1996, Read and Whiteoak, 2003):

(1) Reducing the interfacial tension between bitumen and water;

(2) Stabilizing the emulsion and providing stabilizing forces when cooled;

(3) Controlling the performance characteristics of the emulsion such as setting rate and adhesion.

In an anionic emulsifier, the electrovalent and polar head group is negatively charged and conveys a negative charge to the surface of the bitumen droplets. On the other hand, in cationic emulsifier, the electrovalent and polar head group is positively charged and conveys a positive charge to the surface of the bitumen droplets. Figure 2.2 is an illustration of the charges on bitumen droplets in an emulsion.

Cationic emulsifiers are generally acidic with pH < 7, usually 2 to 5. Average cationic emulsifier content by mass in bitumen emulsion ranges from 0.1 to 2% (Salou et al., 1998, Salomon, 2006, Wang et al., 2013). Anionic emulsifiers are usually fatty acids or sulphonate emulsifiers. Fatty acids are insoluble in water and are made soluble by reacting with an alkali (sodium or potassium hydroxide), so that anionic emulsions are alkaline with a pH > 7, usually 9 to 11. Average anionic emulsifier content by mass in a bitumen emulsion ranges from 0.3 to 5% (Salou et al., 1998, Salomon, 2006, Wang et al., 2013).

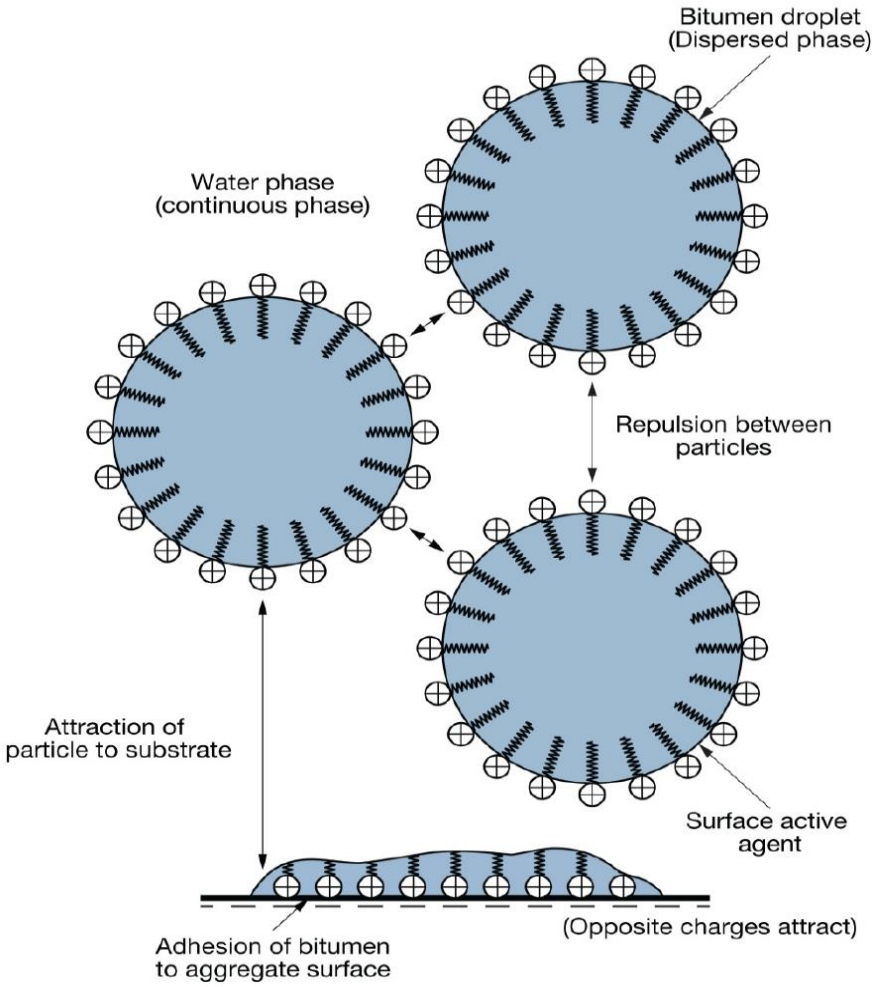


Figure 2.2 Schematic illustration of charges on bitumen droplets in an emulsion (Read and Whiteoak, 2003)

2.2.4 Other bitumen emulsion components

To improve or control some of the bitumen emulsion characteristics during the the manufacturing process, certain components are added. The most important of these additives and their roles are summarized below:

2.2.4.1 Stabilizers

Bitumen contains a small amount of salt, which can lead to an osmotic swelling of the droplets in an emulsion as water is drawn into the droplet, resulting in an increase in emulsion viscosity and later the viscosity decreases as the salt slowly escapes. Calcium and sodium chloride can be added to a level of 0.1 to 0.2% to

assist in the reduction of the osmosis action of water into the bitumen for cationic and anionic, respectively (Salomon, 2006). Also the stabilizers can improve the performance of emulsifiers by reducing the settlement of emulsions through increasing the density of the water phase.

2.2.4.2 Adhesion promoters

Insufficient adhesion of the bitumen film to the aggregate after the breaking, particularly anionic emulsions, but also cationic emulsions, may induce low water resistance in the asphalt mixture itself. Therefore, adhesion promoters are added to improve the adhesion of the cured emulsion film between aggregates. This can be accomplished by addition of surface active amine compounds to either the bitumen phase or the produced emulsion (Salomon, 2006, AkzoNobel, 2009).

2.2.4.3 Solvent

High bitumen density may cause settlement of the base bitumen. Therefore, the addition of solvents can improve emulsification, reduce the settlement phenomenon and regulate curing at lower temperatures. The addition of solvents up to 15% of bitumen content such as Kerosene provides a reasonable level of workability as reported by Salomon (2006).

2.2.5 Manufacturing process of bitumen emulsion

Bitumen emulsions are manufactured by two processes, either a continuous or a batch process. The continuous process is the most widely used. A colloid mill is used with a high-speed rotor (1000-6000 revs/min) in a stator in order to produce the desired bitumen droplet size where the geometrical properties of the mill play a significant role in determining the particle size distribution. Usually, adjustable clearance ranging between 0.25 to 0.5 mm is provided between the stator and the

rotor. Hot bitumen and emulsifier are supplied at the same time into the colloid mill where the bitumen temperature is 120 to 180°C corresponding to a viscosity of 0.2 Pa.s. Miljković (2014) points out that at these values a suitable viscosity of bitumen for emulsification is achieved. However, these temperatures may make the emulsifiers unstable thermally, or at least have a very short lifetime. This means that it may be preferable to mix the emulsifier into the water phase, which is nowadays a very common practice in industry (Miljković, 2014). As a result of mixing the emulsifier into the water phase, the temperature of the water is adjusted to be less than 90°C to satisfy the emulsifier thermal stability requirement (Read and Whiteoak, 2003). However, it is in practice varied between 45 and 60°C as reported by Miljković (2014).

The colloid mill applies shear forces to break up the bitumen and emulsifier mixture into small globules and to help the bitumen globules to become coated with emulsifier, initiating the electrical charges on the bitumen globules. In the case of hard bitumen some consideration should be applied, such as increasing the temperatures of the bitumen, and increasing the input power of the mill to facilitate more bitumen dispersion.

For batch mixing a static mixer may be used as a substitute for the colloid mill, where the globules are initiated from highly turbulent flow. Pumping the bitumen with high speed into a series of baffles generates the necessary shear. The batch process can be used to produce small volumes of the emulsion. Figure 2.3 illustrates the two manufacturing processes for manufacturing cationic emulsion, which is very similar to the anionic emulsion manufacturing process.

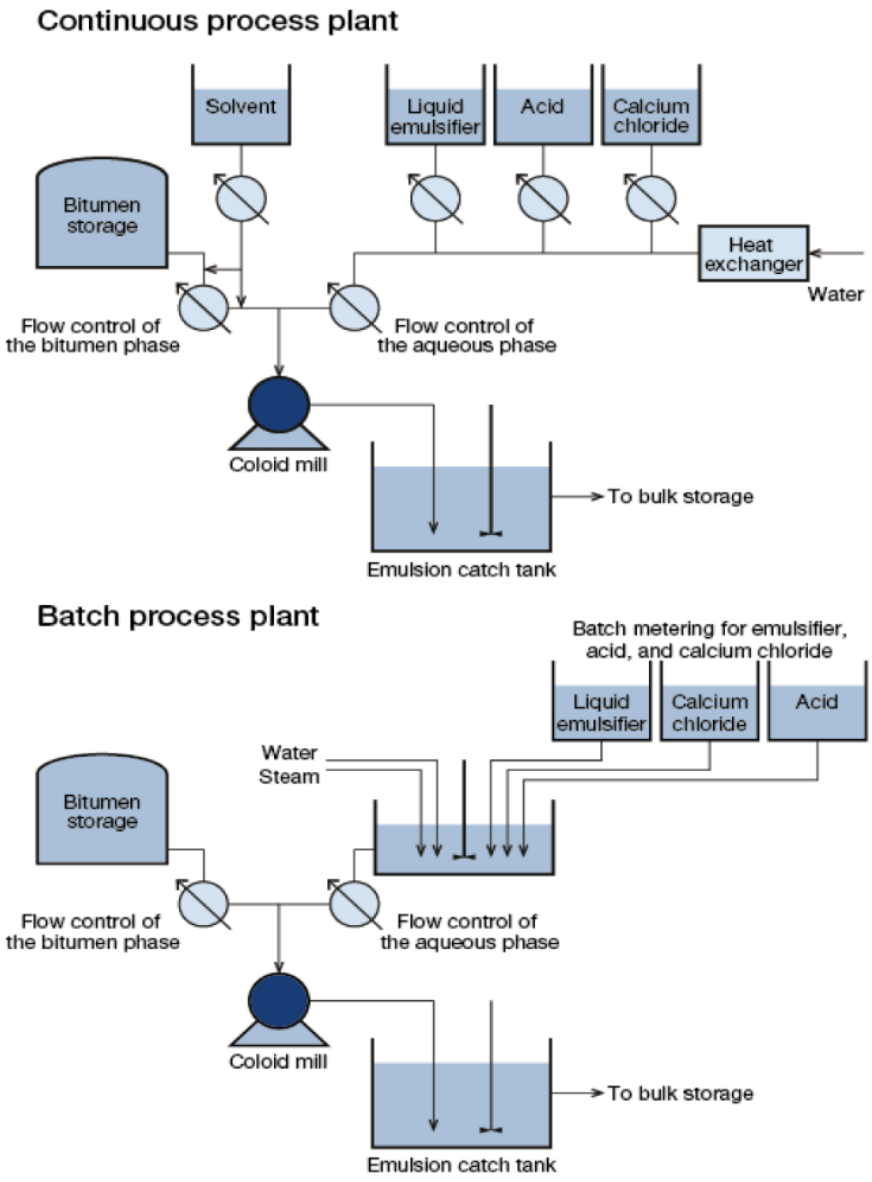


Figure 2.3 Schematic illustration of continuous and batch process plants for producing bitumen emulsion (Read and Whiteoak, 2003)

2.2.6 Breaking mechanism of bitumen emulsion

Basically, there are different approaches to explain the breaking mechanism of the bitumen emulsion as this process has some complications. The exact nature of bitumen emulsion breaking is not completely understood in detail but it fundamentally consists of three essential steps, which are flocculation, coalescence and removal of water (Salomon, 2006). The repulsive force dominates the interaction force between two bitumen droplets. Due to many factors such as

agitation, dilution or addition of more emulsifier, the repulsive force decreases, and the bitumen droplets may come into contact with each other, in a process called flocculation (Miljković, 2014). In this process, water is still the continuous phase. After a period, bitumen droplets are connected by forming cross-links between droplets which leads to coalescence. In coalescence, bitumen becomes the continuous phase. In the third step, water will be removed from the bitumen phase, and bitumen droplets eventually become bitumen (Salomon, 2006). Although bitumen emulsion has been used for decades, the actual breaking mechanism is still not completely understood. In general, different explanations of the breaking mechanism have been found in the literature, as summarized in the following subsections.

2.2.6.1 Breaking mechanism due to adsorption of emulsifiers

The emulsifier molecules are dispersed on bitumen globules and in the water. Some of the emulsifier ions within the water form micelles; however in a stable emulsion system there is equilibrium as in Figure 2.4. This equilibrium will end when these emulsifier ions are adsorbed by oppositely-charged mineral aggregates. Therefore, the breaking rate of the emulsion depends on the rate of adsorption of the emulsifiers onto the mineral aggregate, which is governed by the surface area and the chemical nature of the mineral aggregate (Needham, 1996, Thanaya, 2003). Figure 2.5 shows a schematic diagram of the breaking mechanism.

2.2.6.2 Breaking mechanism due to water evaporation

Breaking of emulsion is significantly influenced by evaporation of water through the emulsion system, and the evaporation is affected by temperature, humidity and wind velocity. It is understandable that water evaporation can lead to emulsion breaking. Specifically, bitumen droplets become concentrated due to water evaporation, resulting in direct contact between droplets. As the bitumen droplets

start merging together, the interfacial area decreases and emulsifiers diffuse from the interfaces to the solution, forming emulsifier micelles. As water can be trapped in closed pores within the bitumen, this evaporation process can take years. This is thought to be the reason that CMA can slowly gain strength even after many years. This initiates the breaking process as shown in Figure 2.5.

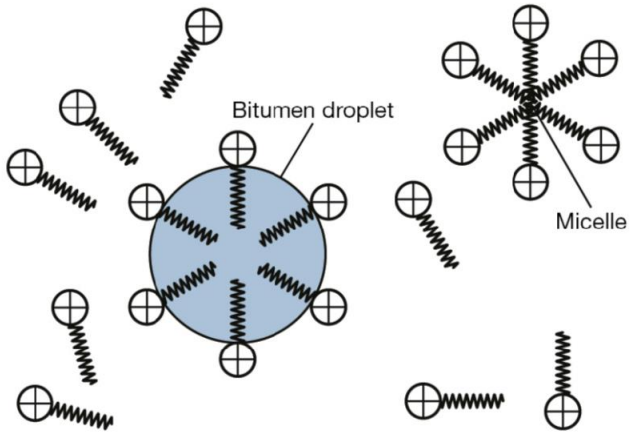


Figure 2.4 Emulsifier ions forming micelle in a stable emulsion(Read and Whiteoak, 2003)

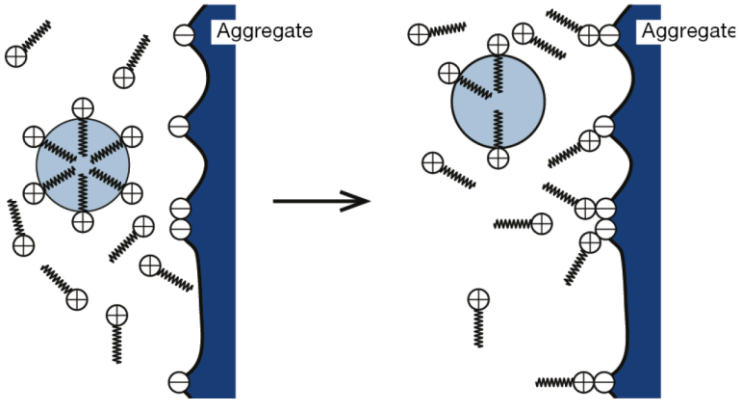


Figure 2.5 Schematic illustration of the breaking process (Read and Whiteoak, 2003)

2.2.6.3 Breaking mechanism due to pH change

Because emulsifier soaps are generated by reacting emulsifiers with acids or alkalis, the surface charge of emulsifiers depends on the pH. Take fatty amines for

example, which are cationic emulsifiers; they are insoluble in water but soluble in acid. HCl is usually used to dissolve fatty amines to obtain water-soluble soap. Water-soluble soap is then blended with hot bitumen in a colloid mill to produce bitumen emulsion. Therefore, when cationic emulsions come into contact with mineral aggregate or cement particles, the emulsifiers may lose their function due to pH rise. In particular, when cement is blended with cationic emulsion, the pH can be reversed immediately. Stability and setting time of bitumen emulsions are usually evaluated using cement. However, it should be noted that some emulsifiers such as Quaternary amines do not lose their function when the pH is changed (Salomon, 2006).

In conclusion, it has been shown that a cationic emulsion breaks chemically when it contacts aggregates with the aid of emulsifiers. Moreover, the cationic emulsifiers work as adhesion and anti-stripping agents; so the breaking mechanism is highly dependent on emulsifier adsorption and pH rise. For anionic emulsions, the breaking mostly depends on evaporation of the volatiles through the emulsion system, where more time and less adhesion can be expected, in comparison to cationic breaking mechanisms. Beside the emulsifier and its content as the major influential factors, the breaking properties of emulsions can be changed by the following additional parameters:

- Bitumen content;
- Aqueous phase composition;
- Particle size distribution;
- Environmental conditions;
- Breaking agents.

At high bitumen contents, the bitumen droplets are more prone to becoming in contact with each other, resulting in an increase in the breaking rate. Also, the breaking rate is increased by reducing the acid content with respect to the content

of the emulsifier. The smaller the size of the bitumen particles, the finer will be the dispersion, resulting in a slower breaking rate of the emulsion (Read and Whiteoak, 2003).

Evaporation of water is influenced by wind velocity, humidity and temperature in that order. Temperature and humidity are related: as the air temperature falls, the relative humidity increases. Working at night with emulsion can, therefore, be difficult with low temperature and relative humidity reaching 100% causing the loss of water to cease entirely. At higher temperatures, the bitumen particles in the emulsion are more mobile and the bitumen is softer. In such circumstances, particles are more likely to come into contact and, therefore, more likely to coalesce (Read and Whiteoak, 2003).

2.2.7 Bitumen emulsion application

The 20th century saw the development of the first emulsions and their use in road construction started around 1920. They were mainly used in spray sealing applications and to prevent dust from ever increasing traffic on roads as stated by Le Coroller (2002). The world emulsion production is estimated to be around 12 million tonnes, of which around 30% are manufactured in USA and 10% in France (Solà, 2013). Table 2.1 shows the main emulsion producers; it is clearly shown that France and the USA topped the listings based on the manufacture and use of bitumen emulsions in road application, which is due largely to secondary and rural networks where the traffic is normally medium to low, and the bitumen emulsion mixtures are proven to be successful (Le Coroller 2002).

Table 2.1 Usage of Bitumen Emulsions (Le Coroller 2002)

Country	Consumption (Tonnes)	Consumption (kg/person)	% of Bitumen used as emulsion (Road Application)
United States	2,300,000	9	5
France	1,010,000	17	25
Mexico	515,000	6	34
Brazil	400,000	3	5
Spain	350,000	9	18
Japan	316,000	3	5
Thailand	300,000	5	24
United Kingdom	160,000	3	5
Germany	130,000	2	3
Italy	100,000	2	3

Worldwide, bitumen emulsions have been used successfully in different applications such as:

- **Cold mix asphalt (CMA)**

Bitumen emulsion can be mixed with graded aggregates to produce CMA suitable for use as base or sub-base courses for medium to low trafficked pavements.

- **Soil stabilization**

Bitumen emulsions have been used in soil stabilization, where the emulsion is spread on the soil surface. This process minimizes erosion, and helps in keeping the water inside agricultural soil.

- **Slip coats**

A slip coat layer is used between two concrete pavement layers to prevent water infiltration, which affects the strength of the concrete and other layers; also it separates the concrete layers so that they can slip over each other.

- **Protective coats**

Bitumen emulsion is used to protect concrete structures, pipes, and other utility facilities from environmental attack.

- **Fog seal**

Diluted bitumen emulsion is applied over weathered surfaces to extend pavement life.

2.3 Cold mix asphalt (CMA) overview

CMA refers to a blend of aggregate and pre-reduced viscosity bitumen binder (Thanaya, 2003). The reason for reducing the viscosity of the bitumen is to facilitate CMA manufacturing at ambient temperature. The pre-reduced bitumen binder generally comprises bitumen emulsion, cut-back bitumen, or foamed bitumen. CMA is currently regaining their importance within the asphalt world market, reaching annual production levels of 2 million tons in France and 3.5 million tons in Turkey in 2008. In 2009, the production of CMA reached around 1 million tonnes in UK and 3.3 million tons in Mexico. Table 2.2 presents the production of CMA in different countries for five consecutive years (EAPA, 2014a).

Table 2.2 Production of CMA in tonnes from 2008 to 2012

Country	2008	2009	2010	2011	2012
Austria	NA	20,000	10,000	20,000	20,000
Belgium	29,500	33,000	30,000	33,000	27,000
Czech Republic	26,400	8,100	11,620	9,907	4,421
France	>2,000,000	>1,500,000	>1,500,000	1,600,000	1,460,000
Switzerland	NA	560,000	630,000	740,000	710,000
Spain	120,000	275,000	185,000	200,000	92,400
Turkey	3,545,845	1,404,000	2,370,000	1,020,000	1,818,000
Mexico	3,000,000	3,300,000	NA	NA	NA
Japan	NA	NA	104,000	95,000	105,000

* NA= No Data.

From the early 1990's, the pursuit of environmentally sustainable and cost-effective technologies for asphalt pavement construction and rehabilitation promoted the use of CMA. CMA reduces energy consumption and greenhouse gas emissions because the aggregates do not need to be heated up and mixing and laying can be carried out at ambient temperature. These advantages can be quantified using life cycle analysis (Santero, 2010). The benefits of CMA including reduced energy consumption and greenhouse gas emissions will be highlighted from a sustainable development perspective in the following subsections.

2.3.1 Energy consumptions and emissions of CMA

Different studies have investigated the energy consumption and emissions of various pavement materials (Zapata and Gambatese, 2005, Chehovits and Galehouse, 2010, Santero, 2010). Generally, it has been demonstrated in the literature that the hot mix asphalt (HMA) is produced at 150-190°C while for hard bitumen in stone matrix asphalt this value might become 180-250°C (Asi, 2006, EAPA, 2014a). For warm mix asphalt (WMA) and half-warm mix asphalt (HWMA) the manufacturing temperatures are 100-140°C and 60-100°C, respectively. No heat is required for CMA, but it is routinely produced at (0-40°C) as reported by Rubio et al. (2012).

D'Angelo et al. (2008) reported that there is 11-35% saving in fuel used during WMA preparation compared to HMA. In her study, Kristjansdottir (2006) indicated that the saving could reach 60 to 80%. But she claimed that the requirements for plant modification for WMA production could compensate this saving. Of course, for CMA it is a 100% saving in burner fuel. To manufacture 1 ton of pavement material, conventional HMA consumes 275 MJ energy while CMA consumes only 14 MJ energy (Chehovits and Galehouse, 2010). Figure 2.6 compares the fuel usage for different pavement materials.

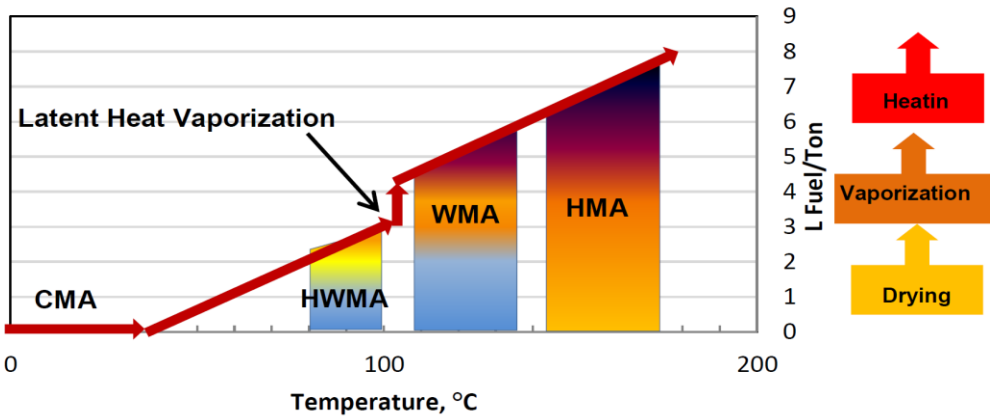


Figure 2.6 Classification of mixture technologies by temperature range and fuel usage (D'Angelo et al., 2008)

Emissions are directly related to production temperature; consequently, the production and laying of 1 ton of HMA and CMA result in 46 and 8 kg of CO_2, respectively (le Bouteiller, 2010). Records indicate that there are no emissions from bitumen at temperatures below 80°C, and even as high as 150°C; considerable emissions are recorded at 180°C (D'Angelo et al., 2008).

Additionally, the asphalt plant emissions limit the position of the plant in rural areas. Therefore, the introduction of new technologies with less CO_2 and fume emissions such as CMA is a real benefit. However, if cement is added, CO_2 emission will be dramatically increased. This is because the production of 1 ton of cement results in approximately 870 kg of CO_2 (Damtoft et al., 2008). The manufacturing process of cement contributes to CO_2 emission through the combustion of fossil fuels alongside the decarbonization of limestone (Damtoft et al., 2008).

To sum up, different values have been observed in the literature regarding the quantity of energy consumption and emissions of pavement materials. The author of this research believes that the above-mentioned values were presented for comparison purposes, not for quantification. A comprehensive study carried out by Chappati and Bilal (2003) compared between a wide range of bituminous materials in terms of energy consumption and greenhouse emissions, as shown in Figure 2.7 and Figure 2.8.

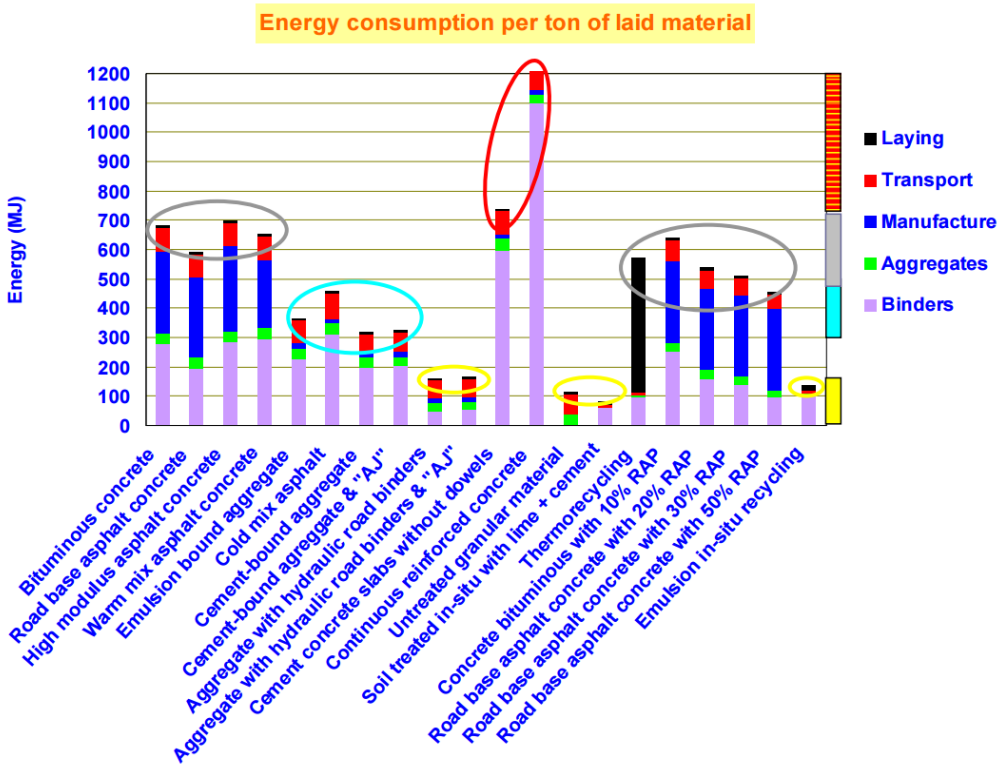


Figure 2.7 Energy consumption for the manufacture and laying of main road technologies (Chappati and Bilal, 2003)

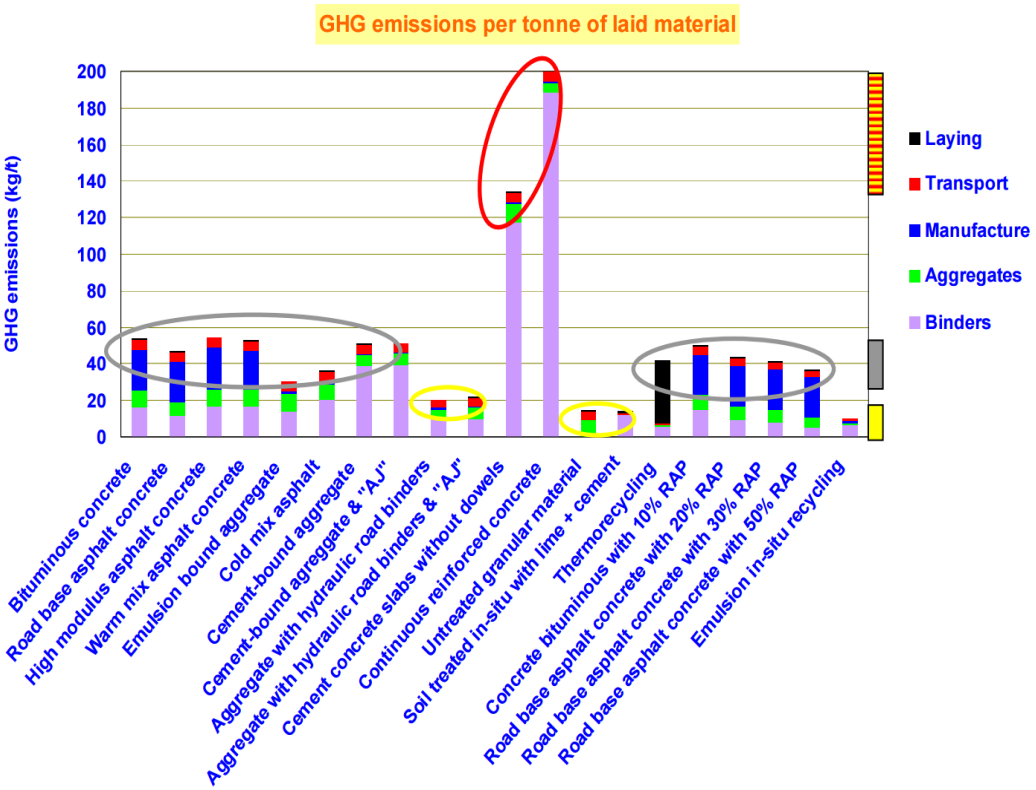


Figure 2.8 Greenhouse emissions of the manufacture and laying of main road technologies (Chappati and Bilal, 2003)

2.3.2 Cold mix asphalt (CMA) challenges

Despite the efforts applied in the last few decades in order to improve and develop CMA utilization, there are some deficiencies that make it inferior to HMA result in restricting or minimizing of its use. These deficiencies are apparent within manufacturing stages and service life performance of such mixtures. Different studies (Leech, 1994, Needham, 1996, Robinson and Thagesen, 2004) have summarized the following as the main shortfalls of CMA:

- Insufficient aggregate coating percentage because of the incompatibility between the aggregates and emulsion.
- Low bituminous film thickness on coarse aggregates, while the emulsion is flocculated on the fines portion.
- High air voids content in the final products after full compaction.
- Low early life strength, this could be attributed to weak adhesion and cohesion characteristics due to the existence of trapped water.
- Long curing time to reach ultimate material strength.
- High sensitivity to water, as shown by low early life resistance to rainfall.

An observation was made by Thanaya (2003) that the binder coating problem is particularly clear in the coarse aggregates. Also, he noticed a binder drainage problem during storage as a result of low binder viscosity. Bocci et al. (2011) reported a problem related to recycled asphalt pavement (RAP) particle size distribution when RAP was involved in CMA. The findings of his study revealed that RAP distribution has a little influence on the compressive strength of CMA. Several studies have limited the use of CMA to form a base or sub-base course layer. This is because CMA is not structurally as strong as HMA and do not have adequate resistance to either abrasion by traffic or moisture induced damage (Epps et al., 1980, Roberts et al., 1984, Staples, 1997).

However, advantages of CMA are very attractive with respect to environmental, economic and safety issues. Furthermore, regular improvements have been made, which have already allowed producers to obtain high-quality CMA, which in many cases are more suitable for certain applications than HMA. It is no wonder then that over recent years the production of CMA has been increasing in many countries as mentioned above.

2.4 Cold mix asphalt (CMA) practices

Over the last century, it has been recognized that CMA has several advantages over conventional HMA in terms of simplicity and energy saving, as it produces almost no emissions to the environment as discussed in the previous section. Therefore, researchers and producers have continued to improve these mixtures in an attempt to increase their competitiveness and utilization (Gómez-Meijide and Pérez, 2014a). Consequently, these efforts have led to several CMA practices around the worldwide as follows:

2.4.1 Cold lay macadam

Production of cut-back bitumen, using flux oil in order to reduce the viscosity of bitumen, allows the production of cold lay macadam. Flux oil contains a non-volatile fraction of petroleum to dilute the bitumen from high to low viscosity. The performance of cold lay macadam markedly relies on factors such as flux oil type, and amount, the evaporation rate of oil due to environmental conditions and usage of the pavement. It has been reported in the literature that different types of flux oil can be used in cold lay macadam production such as white spirit, gas oil, creosotes and kerosene (Nicholls, 1998).

Most of the cold lay macadam applications have been used for surface dressings and base course usages. The use of this mix has started to reduce and be replaced

by HMA due to its inferior performance. This could be attributed to the presence of flux oil as reported by Robinson and Thagesen (2004). Furthermore, the use of cold lay macadam has become restricted due to environment pollution that may occur due to solvent use (Leech, 1994).

2.4.2 Grave emulsion mixture

Grave emulsion mixture has been widely used in France, particularly in the warmer and drier southern regions. This is because the mixture is highly susceptible to moisture damage (Needham, 1996). In grave emulsion mixture, aggregate with dense gradation is mixed with pre-wetting water then mixed usually with a medium setting emulsion as the latter considers the main binder. Different usages have been reported for this mix such as base courses for re-profiling, overlaying and strengthening of deteriorated pavements. Also, it can be used as wearing course for lightly traffic roads (Thanaya, 2003). Typically these mixtures need to be laid directly after mixing which is difficult to implement due the distance between the site and the manufacturing plant. Therefore, a modification to the mixture has been carried out using flux oil, which allows these mixtures to be stockpiled for many days before laying. However, this modification causes a stiffness reduction as a result of softening the bitumen and increases the period of curing.

It is characterized as a low binder content material compared to other types of CMA. Thus the aggregate is not fully coated, and this leads to one of the drawbacks of this mixture (Needham, 1996, Thanaya, 2003). However, grave emulsion mixture is generally protected with a surface dressing some days after laying to seal the surface and prevent ravelling. These materials have rarely been used across most of the world and are mainly limited to France (Needham, 1996).

2.4.3 Foamed bitumen mixture

The development of the foamed bitumen process dates back more than 50 years and was the work of Professor Ladis H. Csanyi at Iowa State University, USA (Csanyi, 1957). The principle of this process depends on injecting water derived steam into hot bitumen to produce foam with thousands of tiny bitumen bubbles. This foaming process is continued for less than one minute and the form then dissipates, whereby the bitumen reverts to its original characteristics. Thus, mixing with aggregates should be achieved while the binder is still in a foamed state. In 1968, Mobil Oil Australia assessed the process as impractical for in-situ conditions, because of the need for specialized equipment such as steam boilers. They then modified the original process by injecting cold water rather than steam into hot bitumen as stated by Button et al. (2007). Thus, foam bitumen technology became much more practical and economical. Figure 2.9 shows a schematic diagram of examples of foaming nozzles.

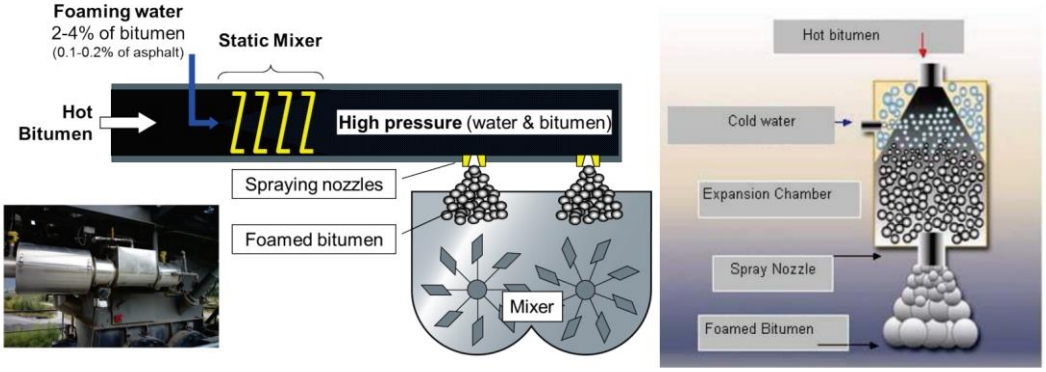


Figure 2.9 Foaming nozzle examples (EAPA, 2014b)

Previous researchers have used a wide range of aggregates to produce foamed bitumen mixtures; these aggregates have varied from virgin crushed stone (Jenkins et al., 1999, Saleh, 2006) to RAP (Akeroyd and Hicks, 1988, Jitareekul, 2009). However, the trend of using RAP has been gaining attention, particularly in the cold recycling field. Recently, a lot of studies have been conducted on

performance investigation of cold recycled mixes using foamed bitumen (Jenkins, 2000, Kim and Lee, 2006, Kim et al., 2007, Sunarjono, 2008, Jitareekul, 2009, Kuna, 2015). Figure 2.10 shows a schematic of the process of in-situ cold recycling using foamed bitumen.

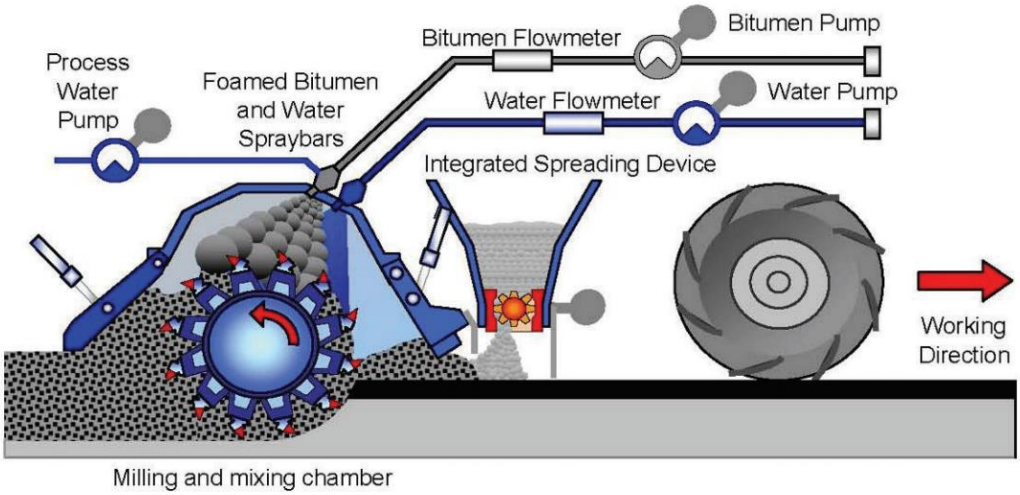


Figure 2.10 The process of in-situ cold recycling using foamed bitumen (Ebels, 2008)

2.4.4 Cold bitumen emulsion mixture (CBEM)

The term cold bitumen emulsion mixture (CBEM), is used to identify a mixture produced by mixing the mineral aggregate with bitumen emulsion. In CBEM, the aggregate could be virgin aggregate or RAP or both to obtain an optimal gradation (Needham, 1996, Thanaya, 2003). However, this mixture comprises a potentially sustainable pavement material as highlighted in section 2.3.1. But CBEMs have several drawbacks, similar to any CMAs. Previous studies showed that their performance is inferior compared to HMA, thus they have been used in limited applications such as low/medium trafficked roads, footways and reinstatements (Leech, 1994, Read and Whiteoak, 2003, Thanaya, 2003, Liebenberg and Visser, 2004). Ibrahim (1998) suggested using CBEMs for heavily trafficked roads when overlaid by at least 40 mm of hot bituminous mixture.

Usually, the aggregate gradation used for CBEM preparation is open or semi-dense to provide suitable aeration within the high air void mixture, facilitating evaporation of the trapped water and shortening the curing time (Nikolaides, 1983). However, recently different gradations have been used; Thanaya (2003) and Al-Busaltan et al. (2012) used dense gradations, Ibrahim (1998) and Al-Hdabi et al. (2013a) used gap gradations. Besides the gradation, the performance of CBEMs is intimately related to bitumen emulsion content and type, pre-wetting water content, curing process, compaction effort and additives used (Thanaya, 2003).

The developments and utilization of CBEMs vary significantly in different countries. France and the USA have the longest experience in using CBEMs in road works (Ojum, 2015). However, the relatively wet and cold weather in the United Kingdom does not favour this kind of mix, and thus, additionally limits the use of CBEM (Leech, 1994). For example, in France, the attempts started with grave emulsion mixture which could be considered as the first generation of CBEM since they used the bitumen emulsion mixture for aggregate stabilization.

In Sweden and Spain, cold recycled mixes using bitumen emulsion are widely used for wearing courses, base courses or road bases, as shown in Figure 2.11. The aggregates are RAP with or without virgin aggregates (Grilli et al., 2012). There is a recent trend to maximize the RAP content to reach 100% of the aggregate content. However, in most cases, about 25-50% virgin aggregates are added (Ojum, 2015).

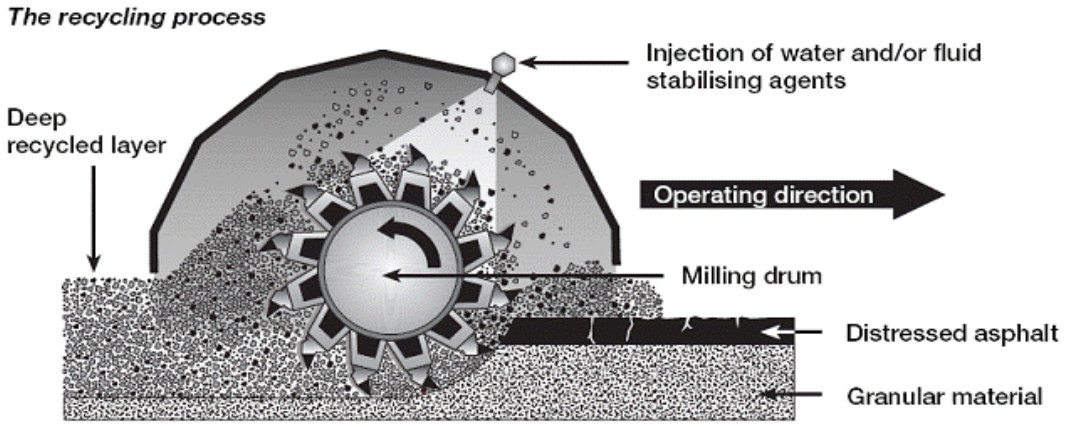


Figure 2.11 The process of in-situ recycling using bitumen emulsion (Wirtgen, 2005)

Cold recycled mixes using bitumen emulsion have been extensively studied over recent decades. Studies have been focused on the gradation, binder content optimization and additives evaluation (Salomon and Newcomb, 2000, Thomas and Kadrmas, 2003, Oke, 2010). More recently, additives such as cement and lime have been used to improve the early strength (Niazi and Jalili, 2009, Ojum, 2015, Modarres and Ayar, 2016). The previous attempts to investigate and improve the performance of CBEMs will be discussed in detail in the following section.

2.5 Performance characteristics of CBEMs

2.5.1 The effect of compaction effort

In HMA, compaction is an important factor that directly affects the performance characteristics. Also, in CBEM a similar role is expected; however, the compaction of CBEM is very different from that of HMA because of the presence of the water and bitumen phase in the mixture. Although various laboratory compaction methods such as Marshall compaction, static compaction, vibratory compaction and gyratory compaction have all been used in previous studies, there is still a debate on the compaction mechanism occurring inside the mixture (Needham, 1996, Thanaya, 2003, Niazi and Jalili, 2009, Oke, 2010, Gómez-Meijide and Pérez, 2014a,

Miljković and Radenberg, 2016). In general, Serfass et al. (2004) proved that increasing compaction effort significantly influences the mechanical properties as shown in Figure 2.12.

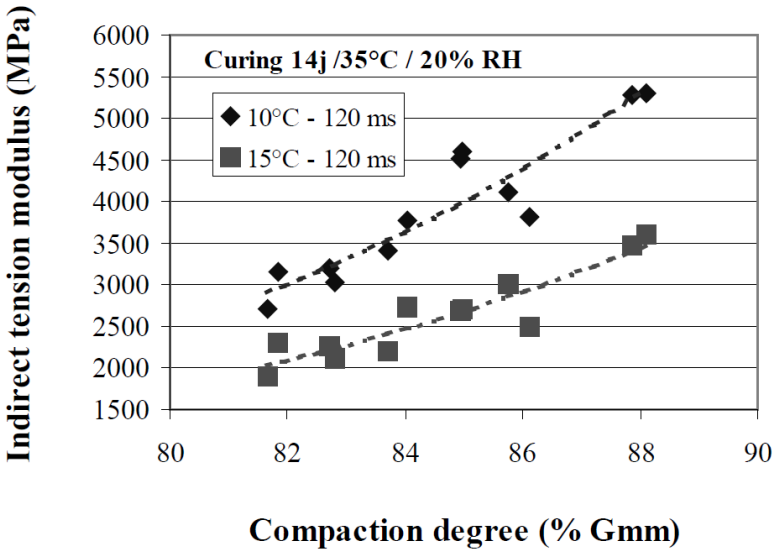


Figure 2.12 Influence of compaction degree on stiffness modulus of grave-emulsion (Serfass et al., 2004)

Different studies have discussed the compaction of CBEMs from the effect of fluid content perspective, as the presence of both water and bitumen phases in the mixes make the process more complicated as mentioned before. The applied stress due to compaction has a role in improving the coalesce of the bitumen droplets by breaking the narrow gap of the aqueous phase between them (Ivanov et al., 1999, Miljković and Radenberg, 2016). So in other words, this enables the interface between the bitumen droplets and the aggregate to develop, thus strongly affecting the entire emulsion breaking process. Needham (1996) indicated that the percentage of emulsion coalescence within CBEM increases with the increase of compaction effort. Moreover, the effect of the compaction on the emulsion breaking is directly recognizable by the water expelled during the compaction (Miljković and Radenberg, 2016, Wendling et al., 2016). This is because the presence of excess water inside the mixture may cause pore water pressure which may prevent the

aggregate from relocating and consolidating properly (Swiertz et al., 2012). In contrast, Grilli et al. (2012) point out that the bitumen emulsion either before breaking or after has no effective contribution to the compaction process. In HMA, Airey et al. (2008) and Hunter et al. (2009) opined that although various compaction methods may produce asphalt specimens with very close volumetric properties, their mechanical properties can be varied. This is mainly affected by differences in aggregate orientation/structure for the different compaction methods (Partl et al., 2007). Most of the studies suggest the application of heavy compaction effort to achieve proper volumetric properties and consequently proper mechanical properties and to ensure the emulsion sets appropriately (Khalid and Eta, 1996, Thanaya, 2003, Serfass et al., 2004). Overall, Table 2.3 summarizes some of the previous studies that have been performed to investigate the compactability of CBEMs.

Table 2.3 Summary of studies performed on the compactability of CBEM

Study	Compaction method	Summary of main findings
(Khalid and Eta, 1996)	Marshall compactor	Dense emulsified bitumen macadams with 100 pen base bitumen emulsion were compacted using a Marshall hammer with 50 blows/per face (medium compaction) and 75 blows/per face (heavy compaction). The porosity values obtained were 18.7% and 16.3% respectively. It was concluded that CBEMs require heavier compaction effort to meet the porosity targets. This is due to the inherent resistance to compaction of the loose mixture. Also, the bitumen emulsion appears to be absorbed by the fine particles quickly causing partial set during the mixing and compaction stage.
(Thanaya, 2003)	Marshall and Gyratory compactors	Thanaya (2003) compared between the effect of Marshall and Gyratory compactors in CBEMs. The results showed that an air void content of between 5-10% was achieved using 240 gyros. He claimed that medium compaction is achieved by 80 gyros which are deemed to be the equivalent of 50 blows/per face, while heavy compaction is achieved by 120 gyros which are deemed to be equivalent to 75 blows/per face. He further stated that the application of a heavy compaction level is essential for CBEMs to ensure that the emulsion sets and the mixes gain stiffness appropriately.
(Serfass et al., 2004)	Gyratory compactor	Serfass et al. (2004) found that the stiffness modulus of CBEMs increases when the degree of compaction increases, as shown in Figure 2.12.
(Grilli et al., 2012)	Gyratory and Proctor compactors	A study has been conducted to the influence of liquid content (emulsion and water) on CBEM compactability using Proctor and Gyratory Compactors. The results indicated that before emulsion breaks, the bitumen did not contribute to the compaction process. It was found that the increase of residual bitumen caused a decrease of dry density and an increase of voids in the aggregate.
(Miljković and Radenberg, 2016)	Static compaction	The research objective was to evaluate the effect of compaction on the performance of bitumen emulsion mortar and to select the most suitable compaction pattern to be adopted as a standard procedure. The finding showed that a suitable static compaction was with a compaction force of 25 kN and a time of 3 mins. Also, the results revealed that the compaction effort did not show any significant effect on the water evaporation process and the residual water content in the mortar.

2.5.2 Treatment of CBEMs using hydraulic binders

In the past, different attempts have been made to investigate and to enhance the performance of CBEMs using hydraulic binder such as cement and lime. The most extensively used hydraulic binders are ordinary Portland cement (OPC) and hydrated lime (HL) as shown in Figure 2.13 (Niazi and Jalili, 2009, Du, 2015).

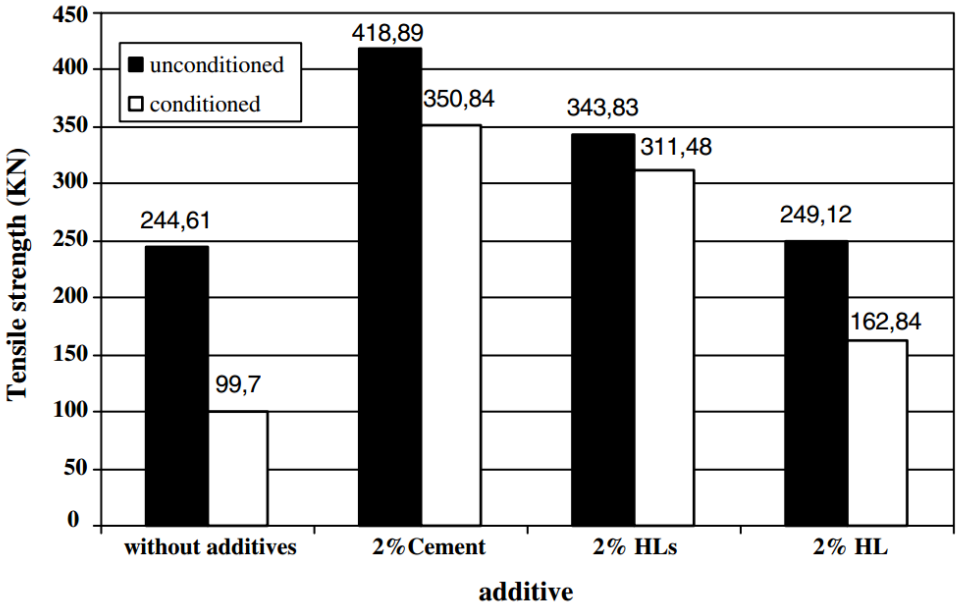


Figure 2.13 Indirect tensile strength of dry and conditioned CBEMs specimens with different additives (Niazi and Jalili, 2009)

The addition of OPC to CBEMs dates back to 1970. A series of three studies were carried out by Terrell and Wang (1971), Schmidt et al. (1973) and Head (1974) to improve the resilient modulus of emulsion treated mixes using cement. The results showed that the rate of development of this property was significantly accelerated by the addition of up to 3% cement in the early stages of curing and the increase in resilient modulus reached up to 200% depending on emulsion type. Needham (1996) claimed that the incorporation of cement into CBEMs could increase: stiffness modulus (see Figure 2.14), resistance to permanent deformation,

resistance to fatigue cracking (at initial strains below 200 microstrain), and improve resistance to moisture damage.

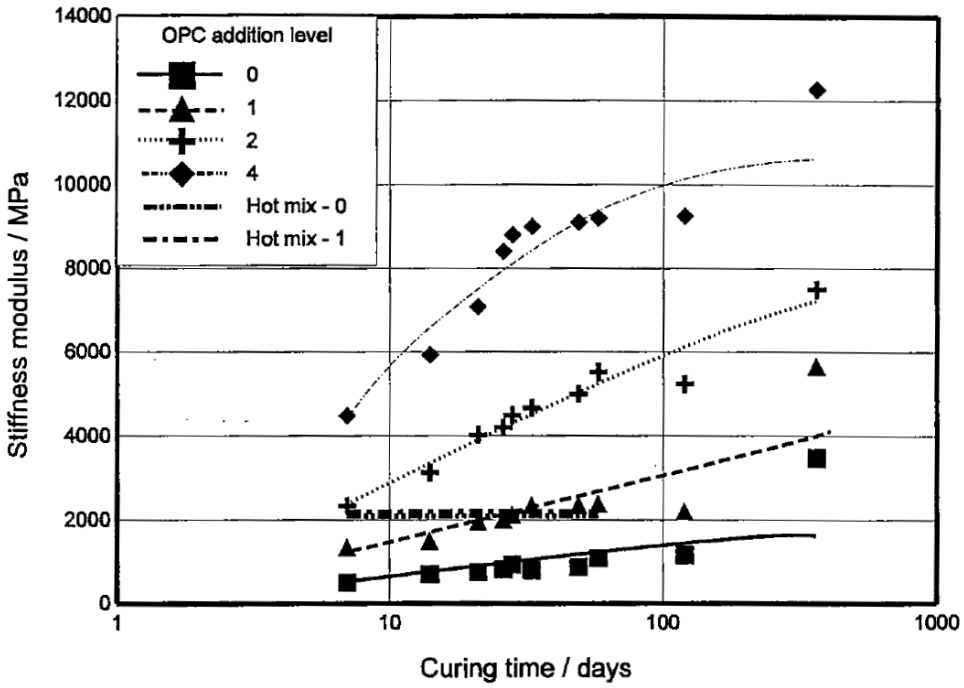


Figure 2.14 The effect of different cement contents on CBEM stiffness modulus (Needham, 1996)

A laboratory study was conducted by Li et al. (1998) to evaluate the mechanical properties of cement-asphalt emulsion composite. This study indicated that combining cement and bitumen emulsion improves material performances by gaining the beneficial properties of both cement concrete and asphalt concrete. The results showed the longer fatigue life and lower temperature susceptibility of cement concrete, and the higher toughness and flexibility of asphalt concrete. Another study was conducted by Oruc et al. (2007) to evaluate the mechanical properties of emulsified asphalt mixtures having 0% to 6% OPC. The results also showed a significant enhancement with high additions of OPC. Figure 2.15 presents the effect of different cement contents on CBEM permanent deformation resistance. Furthermore, the authors of the previous study recommended that CBEMs modified by cement could be used as a pavement surface layer.

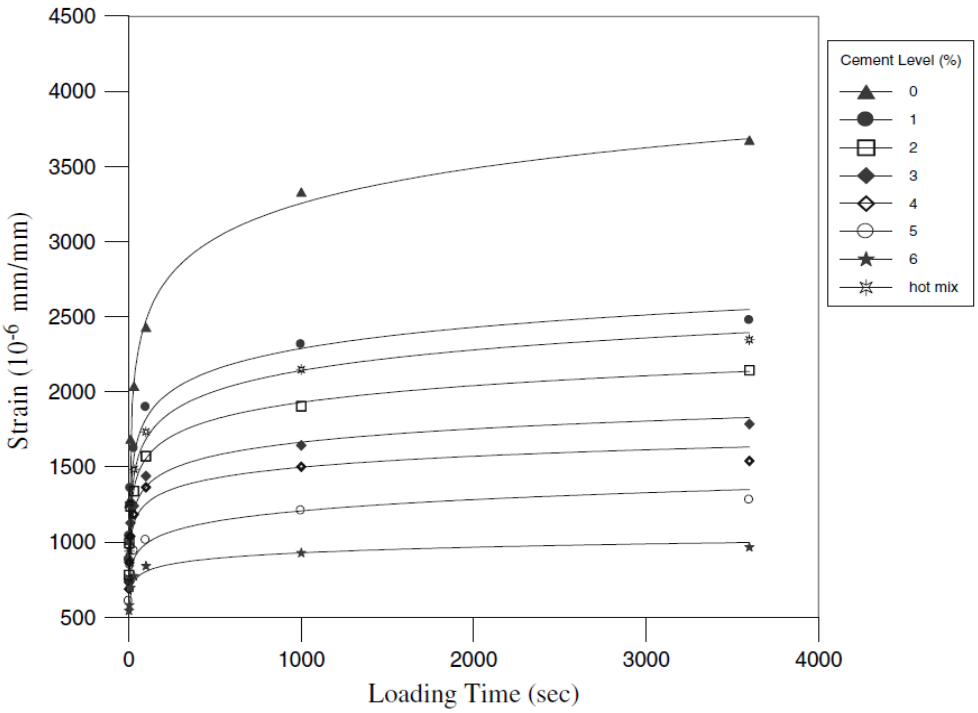


Figure 2.15 The effect of different cement content on CBEM permanent deformation resistance (Oruc et al., 2007)

Thanaya (2003) concluded that the addition of 1% to 2% rapid-hardening cement increases the strength gain significantly and improves the other mechanical properties of CBEMs such as resistance to rutting and fatigue distress at an early age. A study implemented by Wang and Sha (2010) also pointed out that an increase of cement and mineral filler fineness has a positive impact on the micro-hardness of the interface of aggregate and cement emulsion mortar.

Regarding the role of cement in CBEMs, most studies suggest that the cement controls the breaking behaviour of the bitumen emulsion and increases the early mixture strength and stiffness by binding excess water released by the emulsion. Additional cement reduces the negative influence of the released water and improves the adhesion of the binder to the aggregate, which might positively affect the water sensitivity of the mixture in general (Needham, 1996, Lu et al., 2009, Wang and Sha, 2010, Wang et al., 2013, Miljković and Radenberg, 2014).

Furthermore, the presence of cement also increases the pH value of the aqueous phase of the emulsion, and thus, accelerates its breaking (Needham, 1996). However, the use of relatively high cement content for CBEMs increases their cost and would contribute to increasing cement demand worldwide.

Bocci et al. (2011) have studied the influence of temperature on stiffness evolution during the curing stage of CBEM treated with OPC. They concluded that, due to the presence of hydraulic materials, the rate of evaporation increases with the increase in curing temperature. Also, they confirmed that CBEM treated with OPC showed a thermal sensitivity substantially lower than that of HMA; thus they suggested that such mixtures suffer less distortion and rutting during hot seasons.

Limited studies have been performed to evaluate the use of rapid-hardening cement to improve the performance of CBEMs (Thanaya, 2003, Fang et al., 2016). Thanaya (2003) encouraged adding 1-2% rapid-hardening cement to enhance early life strength rather than using OPC. His result showed that CBEM can reach stiffness modulus values of 2000-2500 MPa in just 2 weeks by adding 2%, instead of 16 weeks for CBEM without rapid-hardening cement. Furthermore, Fang et al. (2016) claimed that the improvement in the early strength of CBEMs was achieved not only because of the rapid setting and hardening properties of this kind of cement but also because they bind a higher amount of water than OPC.

2.5.3 Treatment of CBEMs using by-products materials

From a critical inspection of the literature, limited studies have been conducted to investigate the use of by-product materials to enhance CBEM properties. Ellis et al. (2004) studied a range of mixtures of recycled aggregate composed of road base layer, concrete demolition waste and brick sand. These aggregates were stabilized using bitumen emulsion and ground granulated blast-furnace slag (GGBS). They

stated that the addition of GGBS to bitumen emulsion mixtures could provide better mechanical performance than untreated mixtures, especially in the long term under high humidity curing conditions. Thanaya (2003) performed experiments using pulverized fly ash (PFA) as a filler with rapid-hardening cement in CBEM production with a fully cured condition; the stiffness of these mixes was found to be comparable to that of HMA. In their study, Al-Busaltan et al. (2012) confirmed the enhancement of close-graded CBEM to a stage where its mechanical properties are comparable to those of traditional asphalt concrete mixtures. The improvement was due to the replacement of the conventional mineral filler with a domestic FA. They found that an additional binder was produced from the hydration process that took place between the domestic FA and the trapped water involved in the mixtures. Al-Hdabi et al. (2013b) showed a significant improvement in cold rolled asphalt by incorporating a biomass FA with cement; in particular, a considerable improvement in terms of resistance to water damage was reported, as shown in Figure 2.16.

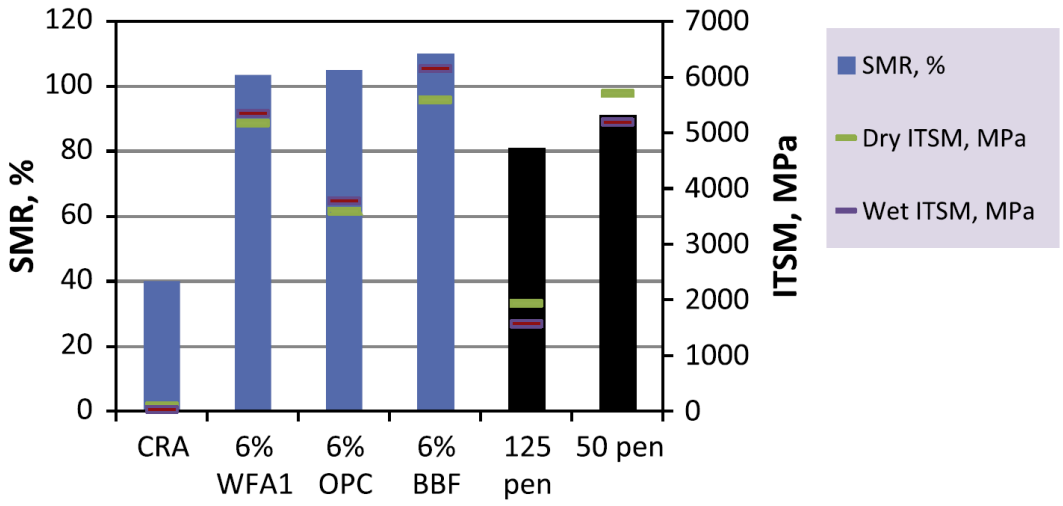


Figure 2.16 Water sensitivity results of CBEM with different filler treatments (Al-Hdabi et al., 2013b)

Moreover, a comparison study between coal ash and OPC in cold recycled mixes was carried out by Modarres and Ayar (2016). The result revealed that the

application of coal waste powder improved the mechanical properties of cold recycled asphalt material, but it could not achieve a positive impact on moisture damage resistance. Based on these comparisons, coal waste powder and its ash were found to have comparable effects to OPC.

2.5.4 Treatment of CBEMs using other materials

This section focuses on using different materials such as fibre, polymers and crumb rubber in CBEMs. Bueno et al. (2003) conducted a laboratory investigation to study the effect of the addition of randomly distributed synthetic fibre on the mechanical properties of CBEMs. The mixture was treated according to weight with 0.1, 0.25, and 0.50% polypropylene staple fibres, 10, 20, and 40 mm long. The result confirmed that the addition of fibre leads to a reduction in the stiffness of the treated mixture in comparison with a non-treated mixture. In general, according to Bueno et al. (2003), the addition of fibre may negatively affect the volumetric and mechanical properties of the mixture. In contrast, Ferrotti et al. (2014) opined that the proper type and content of fibres could improve CBEM performance. A laboratory investigation conducted by Ferrotti et al. (2014) focused on the production of high-performance CBEMs reinforced with three types of fibre (cellulose, glass–cellulose, nylon–polyester–cellulose) treated at two different contents (0.15% and 0.30% by aggregate weight). Results showed that the mixes treated with fibres provided similar or even higher performance than the untreated mixes (without fibres).

The influence of polymer modified emulsion on the performance of CBEM was investigated by Khalid and Eta (1996). A dense graded CBEM with a modified cationic emulsion using ethylene vinyl acetate (EVA) and styrene-butadiene-styrene (SBS) admixtures were evaluated. The results of polymer modified emulsion mixtures showed a significant improvement in mechanical properties

compared with untreated mixtures, i.e. using 4% of SBS and 6% EVA increased the fatigue life of CBEM by 45 and 35 times respectively when compared with untreated mixtures. Chávez-Valencia et al. (2007) performed an experimental study to investigate the effect of Polyvinyl acetate on CBEMs. A polyvinyl acetate emulsion (PVAC-E) was added to a quick cationic set bitumen emulsion to obtain a modified emulsion that was mixed with a local aggregate in order to produce modified CBEMs. The results showed a 31% increase in the compressive strengths of modified mixtures compared to unmodified. Zhang et al. (2011) reported that introducing styrene butadiene rubber to bitumen emulsion lowered temperature susceptibility. This will reflect on both resistance to rutting at high temperature and cracking at low temperature.

From the perspective of maximizing recycled materials, several studies have been carried out regarding the assessment of the effect of incorporating crumb rubber materials in CBEMs. In their study, Dondi et al. (2014) and Pettinari et al. (2014) performed an experimental study to investigate the effect of two different crumb rubbers on the physical and mechanical properties of CBEMs containing 100% RAP and cement. The findings revealed that the replacement of fine RAP with crumb rubbers improved the self-compaction of the mixtures, influencing their volumetric characteristics after compaction. According to tensile strength and stiffness modulus evaluations, the presence of crumb rubbers in mixtures reduced their mechanical characteristics of resistance to failure. More investigation was carried out to study the effect of crumb rubber gradation on the performance of CBEMs (Pettinari and Simone, 2015). The findings revealed that at the same level of rubber treatment, the sample contained finer gradation showed higher values of indirect tensile strength and stiffness modulus.

2.5.5 Evaluation of microstructure of cement treated CBEM

Although cement has been extensively used in CBEM treatment, the function of cement/active fillers in the presence of bitumen emulsion is still imperfectly understood. Acknowledging the role of cement in CBEMs discussed in section 2.5.2, at a molecular level, Giuliani (2001) observed that bitumen emulsion together with cement does not generate a new binder. Cement hydration takes place due to the presence of the water phase of the bitumen emulsion and water added to the mixtures. He also claimed that cement does not act as an inert filler, but it produces strong stringy structures. On the other hand, Pouliot et al. (2003) showed that the presence of a small quantity of bitumen emulsion in cement mortar had a delaying effect on the cement hydration. X-ray diffraction (XRD) analysis has been used to verify the actual production of cement hydration (Du, 2014). The results showed no additional peaks are observed in the cement asphalt composite mastic diffraction pattern compared to cement paste, indicating that no new crystalline substances exist in the cement asphalt mastic, as shown in Figure 2.17.

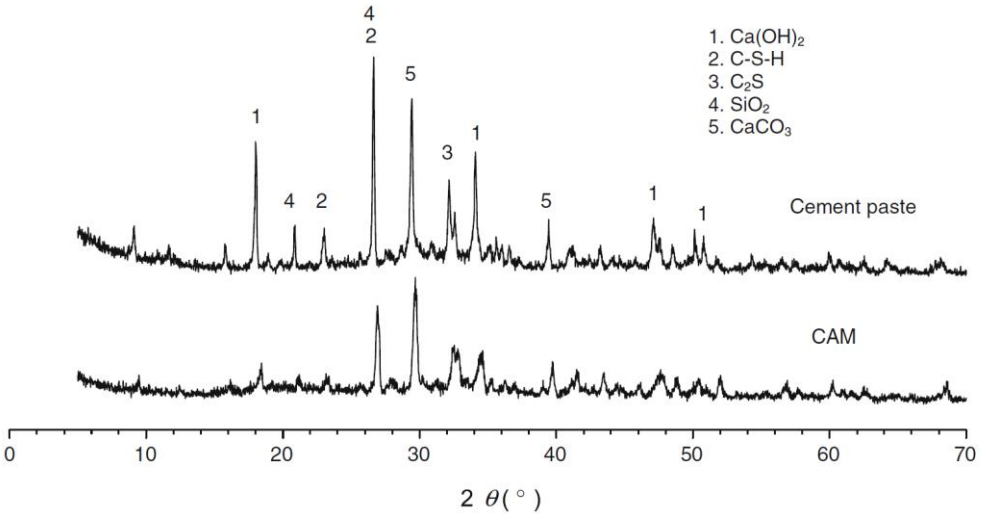


Figure 2.17 XRD results for cement asphalt mastic and cement paste (Du, 2014)

With respect to Figure 2.17, this finding indicates that the hydration reaction that occurs between the cement and water present in the emulsion in a cement asphalt mastic is similar to the reaction between cement and water in a conventional cement paste. Moreover, although the position of the peaks is similar, their magnitude is different. Du (2014) claimed that the lower $Ca(OH)_2$ relative intensity for the cement asphalt mastic curve indicates that the hydration process of cement in the presence of emulsion is delayed, potentially due to secondary reactions with bitumen. It seems that Du (2014) agreed with Pouliot et al. (2003) and proposed a mechanism for the hydration process delay. He suggested that some of the bitumen droplets and cement particles come into contact due to intensive chemical adsorption, and as a result, some of the cement particles are encapsulated by an asphalt film, causing a delay or interruption in the hydration reaction. A study carried out by Wang et al. (2015) showed that the total hydration heat decreased with an increase in bitumen to cement ratio in CBEM. Also, the study revealed that the addition of bitumen emulsion significantly influenced cement hydration behaviour in CBEM. However, his scanning electron microscopy (SEM) observations showed hydration products like these appearing in normal cement mortar, as can be seen in Figure 2.18.

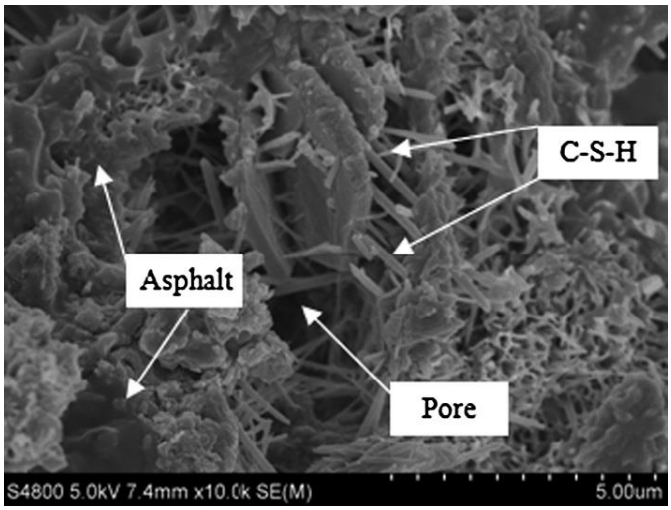


Figure 2.18 Hydration products observed in cement emulsified asphalt mixture (Wang et al., 2014)

In contrast, a recent experimental study carried out by Fang et al. (2014) revealed that the behaviour of bitumen emulsion in the presence of cement and filler is still unclear and may slightly retard or accelerate cement hydration, but has no significant effect on the degree of cement hydration. A detail of the inner microstructure of CBEMs treated with cement was presented using an X-ray technique by García et al. (2013). In Figure 2.19, García et al. (2013) claimed that the bubbles evident possibly appeared due to a suboptimal compaction of the mixture and that there might be scope for improving the compaction method of these mixtures. Another possible cause of these bubbles is air entrainment caused by the emulsifier in the emulsion, a point which was confirmed by Pouliot et al. (2003). Another feature visible in the microstructure shown in Figure 2.19 is some degree of aggregate debonding, which may be improved with a different compaction method and with the use of adhesion promoters (García et al., 2013).

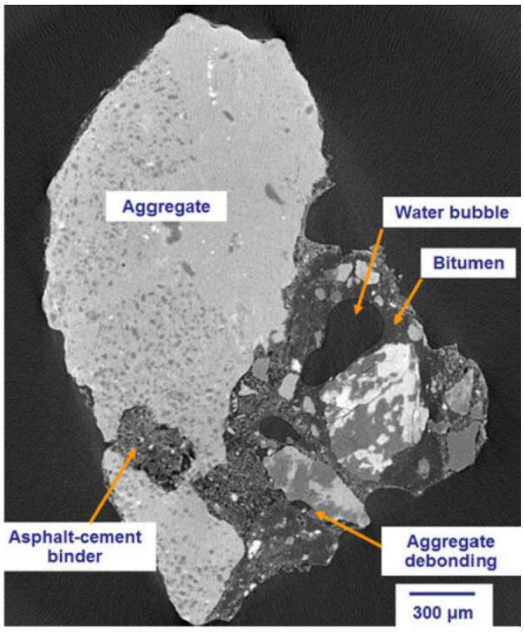


Figure 2.19 Microtomography detail of an asphalt and cement composite (García et al., 2013)

Overall, these research studies have demonstrated developments in the properties of CBEMs by using cement. However, this raises an important question as to how

these fillers (cement/active fillers) interact with bitumen emulsion and affect the hydration and microstructural characteristics of CBEMs. Therefore, a deeper understanding of the microstructure and internal composition of the mixes still needs to be achieved.

2.5.6 The effect of curing of CBEMs

It has been reported in the literature that the performance of CBEM is directly related to the properties and proportions of materials that are used in the mixture and to the curing condition (Needham, 1996, Jenkins, 2000, Thanaya, 2003, Oruc et al., 2007, Niazi and Jalili, 2009, Bocci et al., 2011). The CBEM requires a certain curing time to build up the required ultimate mechanical properties such as strength and stiffness as can be seen in Figure 2.20. This process involves emulsion breaking, moisture loss and/or hydration of cementitious compounds in the case of CBEMs treated with cement/active fillers (Serfass et al., 2004, García et al., 2013, Cardone et al., 2014).

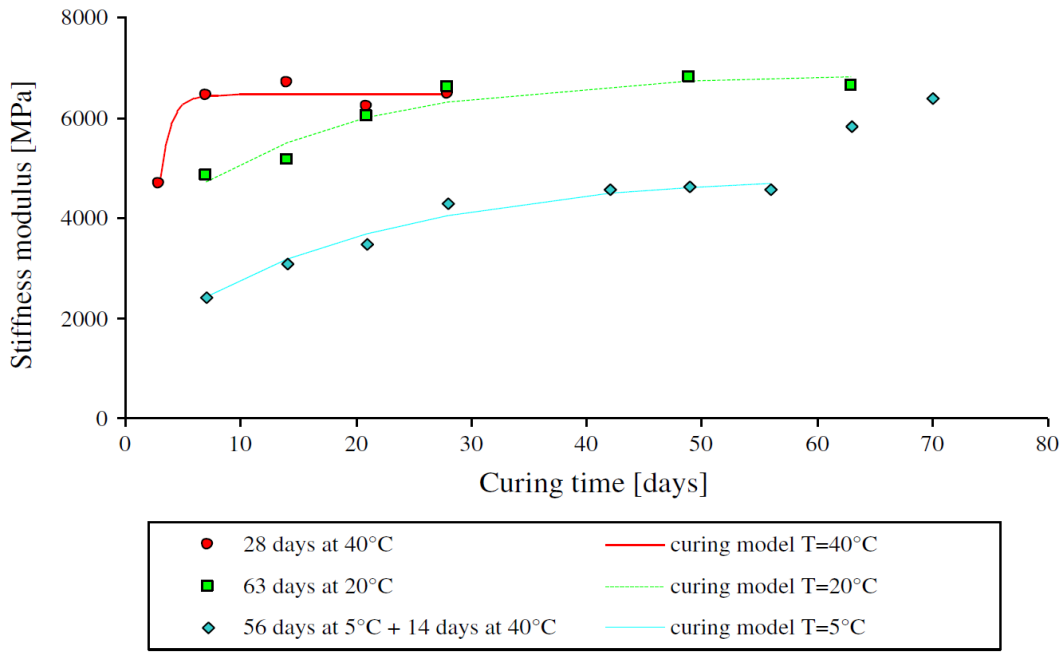


Figure 2.20 Evolution of ITSM as a function of curing temperature and time (Bocci et al., 2011)

Jenkins and Moloto (2008) listed several parameters affecting the curing process, categorized into (1) climatic parameters like temperature, humidity and wind, and (2) other parameters such as aggregate gradation and properties, layer thickness, initial water content, binder content, active filler content, layers applied on top, drainage condition and, finally, traffic load.

Moreover, the curing of CBEMs does not take place immediately after compaction, but is gradual and may require weeks or months. For example, the rate of emulsion breaking depends on the type and content of emulsifier, on the pH value inside the mixture and on the presence of fine particles i.e. filler or cement (Needham, 1996, Miljković and Radenberg, 2016). From their point of view, Serfass et al. (2004) believed that evaluating cured CBEM in the laboratory is clearly necessary, but reproducing exact field curing conditions is too complicated and time consuming. Several studies have found that the rate of moisture loss is strictly related to the conditions applied to the mixture such as compaction effort, temperature and relative humidity as illustrated in Figure 2.12 and Figure 2.21 (Serfass et al., 2004, Cardone et al., 2014, Godenzoni et al., 2016).

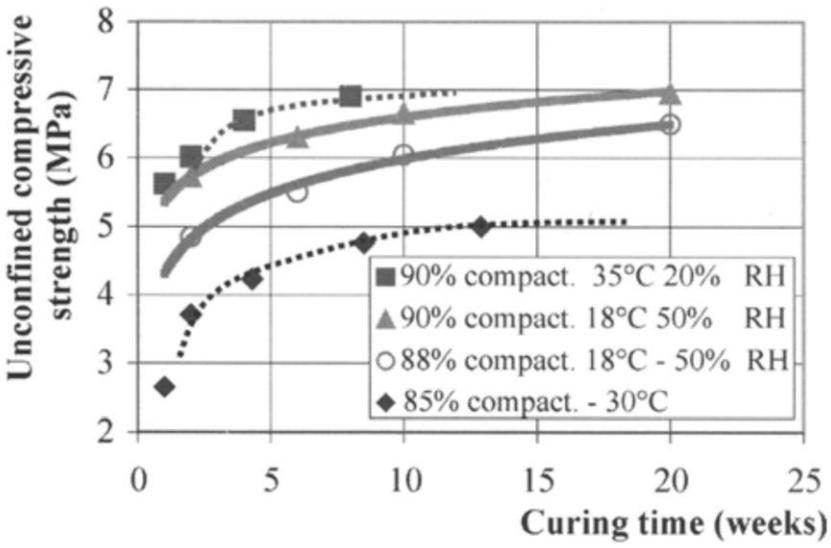


Figure 2.21 Effect of different curing conditions and compaction on compressive strength of grave emulsion mix (Serfass et al., 2004)

Kim et al. (2010) showed that moisture loss is directly proportional to strength gain and this is evident at higher temperatures over the curing time. This is true for CBEM with inert filler such as limestone filler (LF), as increasing the curing temperature leads to facilitating the water removal. In the case of active filler, further to that, a special concerns arises because cement hydration reactions require the presence of water; the use of cement accelerates the emulsion curing process by reducing the amount of free water (Needham, 1996, García et al., 2013). García et al. (2013) proposed a schematic diagram to describe the curing mechanism with CBEM, as shown in Figure 2.22.

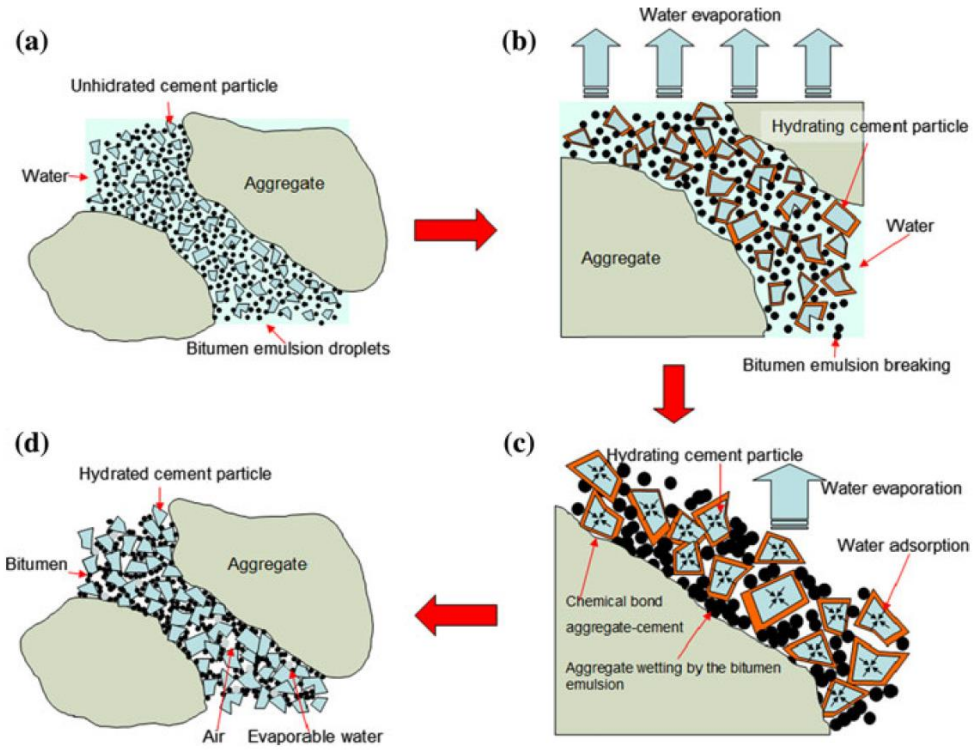


Figure 2.22 Schematic representation of the curing process of CBEMs (García et al., 2013)

In concrete, high early temperature activates the hydration process and plays a significant role in the formation of hydrated phases in addition to the amounts normally produced as reported by Rojas and Cabrera (2002). In their study, Godenzoni et al. (2016) proved that further to the removal of the trapped water,

increasing the curing temperature did not modify the final water content. Also, the results revealed that moisture loss by evaporation did not hinder the hydration process of cement. This contradicts an observation made by Cardone et al. (2014) where their findings showed that excessive evaporation due to high curing temperature can hinder the full potential of the cement hydration process in cement treated CBEMs. This was confirmed by very close observation obtained by Bocci et al. (2011). He found that the specimens subjected to high curing treatment showed lower moisture damage resistance, claiming this behaviour to be related to the density of the hardened cement, becoming less uniform at higher curing temperature. This can lead to weaker spots in the microstructure as reported by Rovnaník (2010).

From reviewing most laboratory curing protocols used in the literature, it could be concluded that the curing temperatures 20 and 40°C have been widely used. Table 2.4 summarizes some studies related to the CBEM curing process. Ruckel et al. (1983) expressed their concern over a curing temperature of 60°C which is above the softening point of many bitumen grades that are commonly used for foaming. This high temperature may cause a change in bitumen properties during curing, which is not desirable. Furthermore, different studies point out that the high curing temperature above the softening point might cause damage to the specimen by its own weight and change the internal microstructure of the specimen (Khalid and Monney, 2009, Fu et al., 2010).

Regarding to humidity effect on curing process, a detailed investigation to study the effect of different relative humidities (RH) on the curing process of CBEMs was carried out by García et al. (2013). A series of mixtures with different amounts of cement cured at a 20°C with different humidity levels (35, 70 and 90% RH) were used. The findings showed a clear relationship between the humidity during curing, the water losses and the rate of curing. At 90% RH, the mixes hardened slower

than those cured at lower level of RH. A similar observation was reported by Fu et al. (2010) that the curing time at any given temperature can be decreased by lowering the relative air humidity. At a temperature of 40°C, the RH of the air is about 2.5 times lower than that at 23°C (Hugener et al., 2014). Recently Tebaldi et al. (2014) proposed sealing of the specimens to provide constant humidity to the specimens during the curing process. However, sealing considerably increases the testing complexity and provides a conservative estimate of curing in the field (Fu et al., 2010). Batista and Antunes (2003) hypothesized that the behaviour in the field would be close to laboratory specimens that are partially sealed. This point was investigated in detail by Ojum et al. (2014). Nevertheless, most of the researchers proposed unsealed specimen curing in order to guarantee free water evaporation (Cardone et al., 2014, Godenzoni et al., 2016, Graziani et al., 2016).

Table 2.4 Summary of studies performed to investigate CBEM curing process

Study	Curing conditions	Summary of main findings
(Serfass et al., 2004)	35 days at the following condition (1) 5°C with 50% RH. (2) 18°C with 50% RH. (3) 35°C with 20% RH. (4) 50°C with 15% RH.	The effects of curing temperature, RH and time on grave emulsion mix were evaluated. The mix moisture content and mechanical behaviour were characterized by compressive strength and stiffness modulus. Different curing procedures were assessed and compared. The authors proposed accelerated curing of 14 days at 35°C to be suitable for road engineers and support the view that the curing at temperatures higher than 50°C dried the specimens too quickly causing premature failure. He stated that the moisture content of small specimens evaporated faster in comparison to larger specimens which take a longer time.
(Khweir et al., 2004)	More than 12 months at 18°C with 80% RH.	This research covers the influence of curing time on the performance of CBEM. The performance parameters included stiffness modulus and fatigue properties. The stiffness modulus for all CBEMs, cured for more than one year, was close to the stiffness modulus of the high compaction HMA. Fatigue properties of the CBEM exhibited continuous performance improvement with increased curing time but fell short of HMA. Nevertheless, the CBEM modified with 1% of cement performed relatively better than all other mixtures including the HMA.
(Bocci et al., 2011)	(1) 28 days at 40°C (summer temperature). (2) 63 days at 20°C (spring and autumn temperature). (3) 56 days 5°C (winter temperature).	In this study the influence of curing conditions, temperature and moisture on the mechanical behaviour of CBEM were investigated. The findings revealed that the higher curing temperatures resulted in higher rates of modulus increase and higher maximum values, while at low temperatures the curing process was slower. Also, the specimens subjected to accelerated curing (40°C) treatment showed lower moisture damage resistance. Bocci et al. (2011) claimed this behaviour to be related to a different microstructure of the hardened cement.
(García et al., 2013)	28 days at 20°C with 30, 50 and 90% RH.	This investigation focused on the effect of cement content and different levels of humidity on the curing mechanisms of CBEMs. The results showed that cement contributes to the hardening of CBEMs both by creating cement paste bridges between the aggregates and by removing water from the mixtures through cement hydration. Also, the results showed a negative effect of high level of humidity (90%) on water loss by evaporation and the strength of CBEMs.

Table 2.4 Continue ……

(Wang et al., 2014)	7 days and 28 days at 20°C with 90% RH.	This study focused on the effects of residual bitumen, cement content and curing ages on properties of cement emulsified asphalt mixture. A ranking for these factors based on the performance of mixes was provided using gray correlation degree analyses.
(Cardone et al., 2014)	100 days at 20±2°C and 40±2°C with 70±5% RH.	The curing process of CBEMs treated with cement was investigated by analysing the influence of cement dosage and curing temperature on moisture loss and evolution of complex modulus. Results showed that moisture loss by evaporation controls the increase in stiffness of the mixtures. However, excessive evaporation can hinder the full potential of the cement hydration process. Results also showed that the increase in stiffness modulus of mixes due to curing was mainly related to moisture loss and higher temperature which accelerated the curing process.
(Ojum et al., 2014)	28 days at 5, 20 and 40°C with the following conditions: (1) Fully wrapped. (2) Unwrapped. (3) Partially wrapped for 7 days + fully wrapped for 14 days.	This research investigated the need for accelerated curing and its effect on mechanical and performance behaviour of cold recycled bituminous mixes using both bitumen emulsion and foamed bitumen with and without cement. The behaviors of emulsion-bound and foamed-bitumen bound materials had very similar trends in terms of the relative effects of curing time and temperature, specimen wrapping and cement addition. However, the emulsion bound materials had consistently better performance. Curing temperature and conditioning played a crucial role. Incomplete evaporation of the water in the fully and partially wrapped specimens resulted in reduced performance of cold recycled bituminous mixes.
(Godenzoni et al., 2016)	100 days at 25±2°C and 40±2°C with 70±5% RH.	The evolution of moisture content and indirect tensile strength (ITS) for cement treated CBEMs were evaluated under these curing condition. The results showed that the curing temperature affected the rate of water evaporation but did not modify the final water content. Also, the results revealed that the moisture loss by evaporation did not hinder the hydration process of cement. The authors of this study confirmed that ITS increased with increasing curing time, regardless of the curing temperature, and approached a constant value after a long curing time i.e. 100 days.

2.6 Mix design considerations of CBEMs

The utilization of CBEMs requires mix design procedures which should be as practical as possible to be readily accepted and used in current quality control and research laboratories. At present, there is no widely accepted method. The subject of mix design of CBEMs has been addressed in the past by various organizations and researchers (Asphalt Institute, 1989, Nikolaides, 1994, Jenkins, 2000, Thanaya, 2003, Lesueur and Potti, 2004, Kim and Lee, 2006). However, in fact, most of the methods used are based on the procedures developed by the Asphalt Institute (Marshall Method for Emulsified Asphalt Aggregate Cold Mixture Design), with slight modifications introduced (Thanaya, 2003, Forth et al., 2006). The corresponding test procedures involved in the mix design process such as compaction methods, curing procedures and testing procedures vary considerably worldwide (CEDR, 2014). In this section, the available literature on different mix design considerations is reviewed together with factors that are affected by these considerations.

The fundamental objective of any mix design method is to produce a mixture able to satisfy the structural and functional requirements. In CBEM, the mix design procedure comprises a determination of fluid content. This means in other words that the relative proportions of emulsion and pre-wetting water should be optimised in order to achieve both acceptable mechanical strength and suitable volumetric properties (Santagata and Chiappinelli, 2004, Ameri et al., 2012, CEDR, 2014). Montepara and Giuliani (2002) confirmed that the essential role of a mix design method is to investigate the best dosage of the bituminous emulsion and pre-wetting water (optimum fluid content). For simplicity, Needham (1996) suggested using empirical formulae to determine the level of fluids content for CBEM design when the laboratory tests are not possible. Unfortunately, the wide variation of

materials and properties of CBEM made the suggestion of Needham (1996) impractical. A general flow chart for a mix design procedure of pavement materials was suggested by Jenkins (2000) as shown in Figure 2.23.

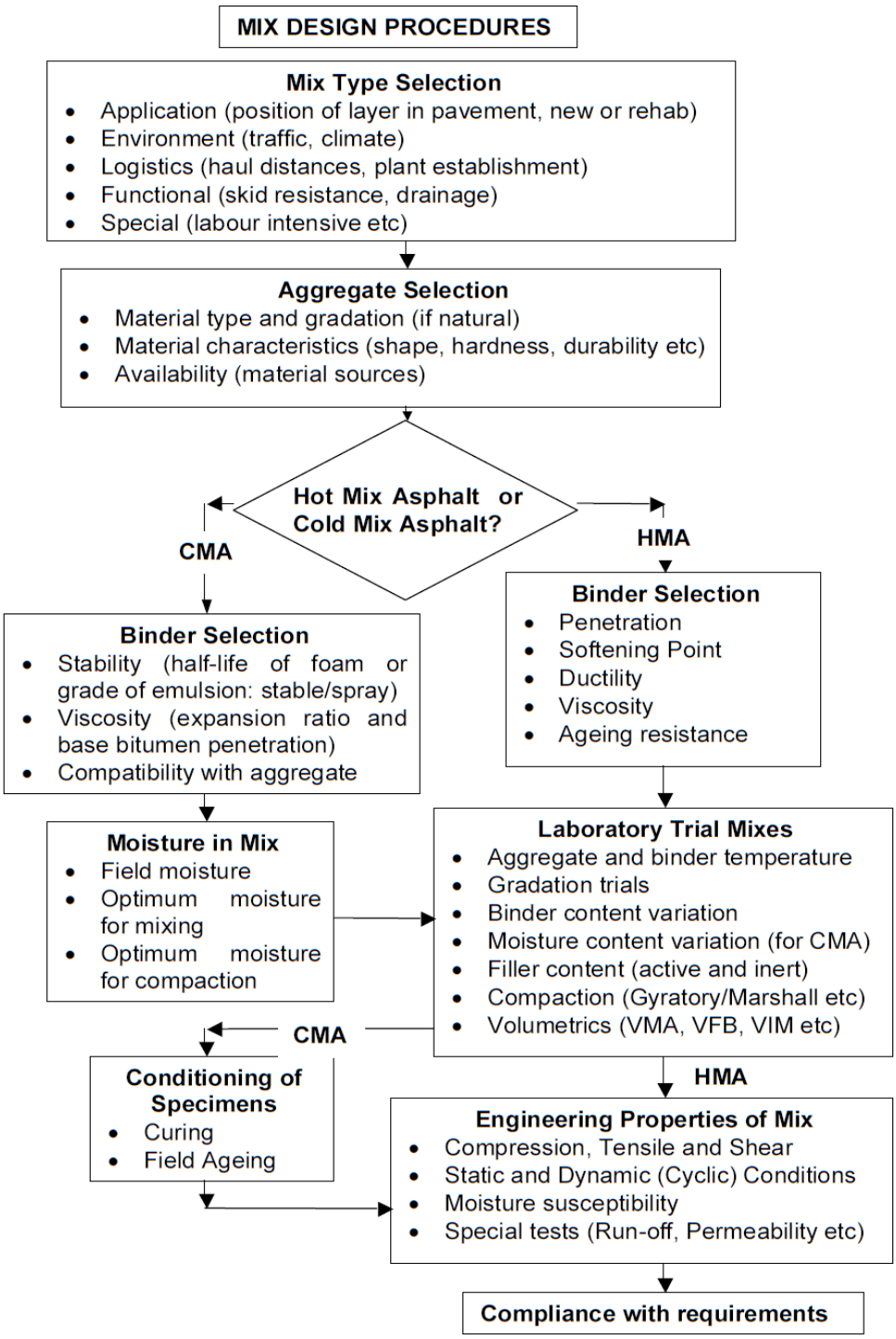


Figure 2.23 General mix design procedure (Jenkins, 2000)

In most mix design procedures, a preliminary study stage is carried out in which the aggregate gradation is defined, the fluid content ranges are determined and a compaction investigation is also performed. The aggregate gradation is determined by referring to an aggregate size gradation envelope or target curve. These may be derived from existing specifications or may be tailored for a specific application as a result of past experience in the laboratory or the field. The aggregate type could be either virgin aggregate or relative proportions of RAP and virgin aggregate (Thanaya, 2003, Oke, 2010, Ojum, 2015). Since the quantities of emulsion and pre-wetting water not only affect the compaction process (workability) but may also influence the mechanical and volumetric properties, they should be defined with care based on experimental investigations (Santagata and Chiappinelli, 2004). However, in the preliminary study phase, the trial dosage of these fluids can be chosen by referring to values which are normally adopted in practice or presented in the literature (Ameri et al., 2012). Following this a compaction study is conducted to determine the optimum total water content for aggregate mixture as can be seen in Figure 2.24.

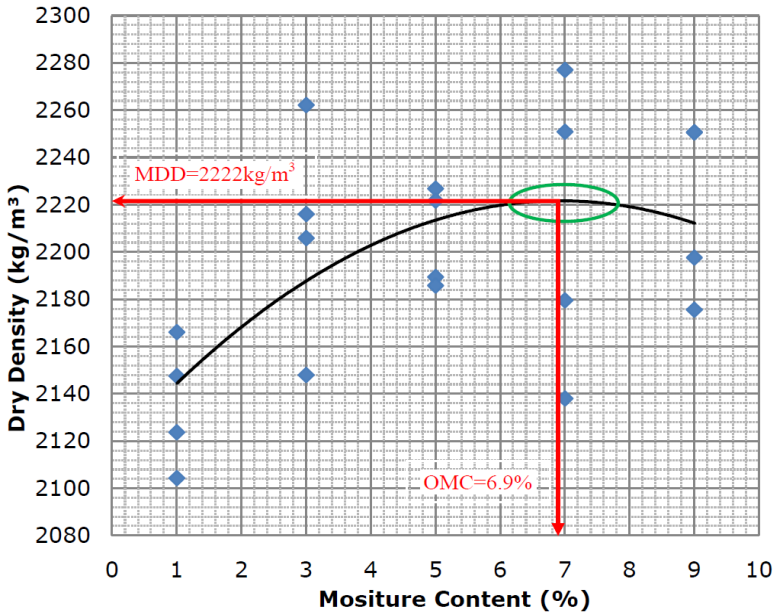


Figure 2.24 Compaction characteristics of CBEMs (Oke, 2010)

This optimization could give an indication of the range of fluids dosage combinations. The compaction study is usually carried out by using Proctor compactor (Kuna, 2015, Ojum, 2015) while a few studies have used a Gyratory compactor (Brayton et al., 2000, Oke, 2010).

After this, the mix design is performed in two stages. The first stage of design starts by assuming a tentative range of the percentage of total fluid content (TFC), composed of bitumen emulsion and pre-wetting water in 0.5-1% increments. Within this range, it is then necessary to detect the value which maximizes the density and strength and minimizes the air voids content. Some studies have used indirect tensile strength (ITS) in both wet and dry conditions to evaluate the performance from a durability perspective (Arimilli et al., 2015). Once the optimum TFC is defined, the second stage repeats a similar procedure to that of the first stage with different variations in the bitumen emulsion and pre-wetting water dosages with total summation equivalent to the optimum TFC.

It appears that the above optimization approach, which is mainly derived from the Asphalt Institute (1989) method, is rather simple for a unique property such as maximum stability/strength or minimum air voids. Moreover, optimization to meet several criteria is also not possible. After reviewing the Asphalt Institute (1989) method, determination of the percentages of emulsion and pre-wetting water from the optimum TFC is carried out subjectively, and it depends on the judgement of the designer. This may cause a variation in the mix design and decrease the quality control.

Generally, the complete set of results deriving from the two stages related to volumetric and mechanical tests have to be carefully analysed in order to choose the mix composition which corresponds to the highest expected performance. As a general rule, selected mixtures should preferably yield a sufficiently high degree of

compaction (i.e. a high-density value) and indirect tensile strength (Santagata and Chiappinelli, 2004). However, selection criteria may also take into account the specific functions which the mixture will have in the pavement. This may require additional performance-related testing which can be linked to the modelling of the behaviour of the pavement in service (Santagata and Chiappinelli, 2004, Ameri et al., 2012, Arimilli et al., 2015). The existing practice of laboratory mechanical test procedures for the determination of mix composition mainly focuses on the effect of moisture damage on the mixture. This evaluation is carried out whether based on tensile strength or stiffness tests, as illustrated in Figure 2.25, (Santagata and Chiappinelli, 2004, Oke, 2010, Miljković, 2014, Ojum, 2015) or Marshall stability (Brayton et al., 2000, Thanaya, 2003, Ameri et al., 2012) . A few studies have used compression strength tests (Zhao, 2007, Gómez-Meijide and Pérez, 2014b). The volumetric properties are mainly evaluated in terms of air voids and dry density. Recently, the trend for mix design has progressed towards performance related and performance based approaches as stated by Ojum (2015). A typical mix design procedure for CMA is shown in Figure 2.26.

During the mix design process, different compaction methods have been used. The gyratory compactor has been employed by several researchers (Brayton et al., 2000, Jenkins, 2000, Thanaya, 2003, Oke, 2010, Ojum, 2015). Also, the Marshall compactor has been used in other studies, for example by Needham (1996) and Al-Busaltan et al. (2012). Other types of compaction such as static compactor were used by Gómez-Meijide and Pérez (2014b) and Miljković and Radenberg (2016). The majority of compaction methods have been adopted with pre-fixed standard parameters, i.e. for Marshall (50 x 2 blows) and for Gyratory (the pressure of 600 kPa, speed of 30 revolutions per minute (rpm), and angle of gyration of 1.25°) (CEDR, 2014, Arimilli et al., 2015). After optimizing the fluids content, the compaction effort may be adjusted in order to improve the properties of the final CBEM production or to achieve target criteria.

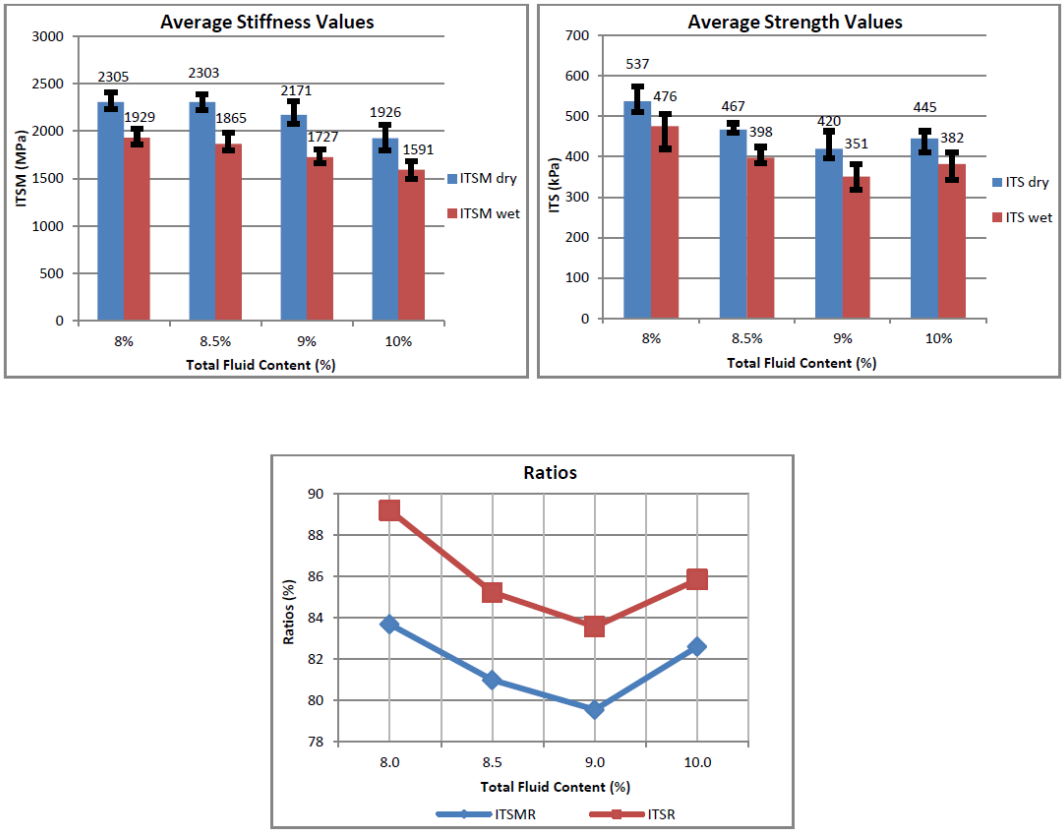


Figure 2.25 The relation between stiffness modulus, tensile strength and moisture susceptibility evaluation with total fluid content (Ojum, 2015)

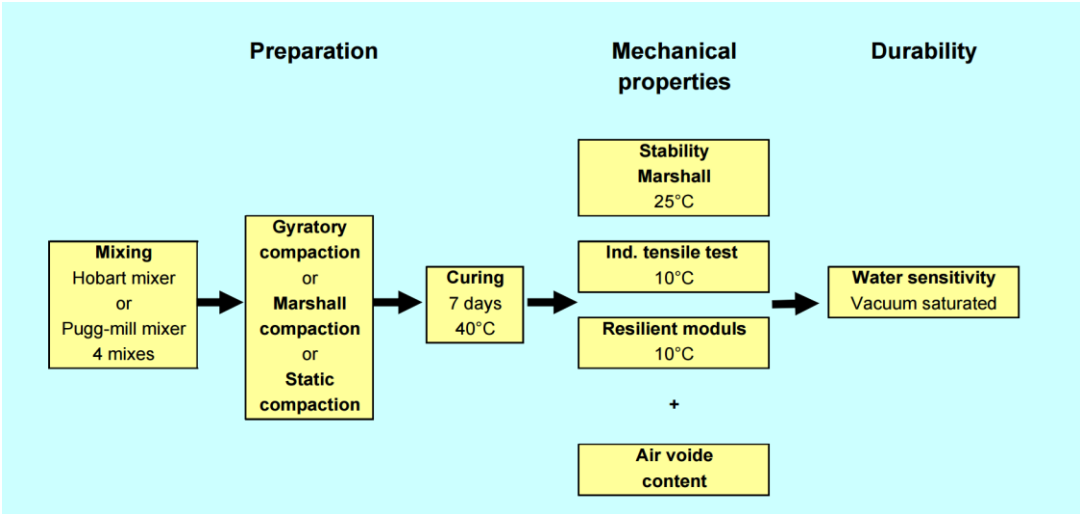


Figure 2.26 Typical mix design procedure for CMA (Jacobson, 2002)

In terms of curing procedure, different protocols have been utilized during the mix design process. This variation is in terms of number of curing days (covering a range between 3 to 28 days). However, 7 days and 28 days have proved most

popular (South African Bitumen Association, 1999). Also, variation is seen in curing temperature (from 18°C to 60°C). But 20°C has been widely used to simulate a usual site condition while avoiding any early ageing of the binder (Serfass et al., 2004). Regarding RH, some studies have not considered it while others have specified values varied from 40% to 95%, or even 100% in the case of sealed specimens as reported by CEDR (2014). For example, Thanaya (2003) used a curing protocol during mix design as follows: 24h @ 24°C in the mould followed by 24h @ 40°C+24h @ 24°C, while 24h @ 20°C in the mould (sealed condition) followed by 72h @ 40°C was applied by other researchers (Oke, 2010, Ojum, 2015).

Another important issue in mix design procedure that should be highlighted is the mixing time. Some studies have demonstrated that care has to be taken in controlling the mixing time which may affect the coating and compactability of the mixture. Several trials have been performed to determine the most suitable mixing time that would provide the best coating, but also such that the bitumen emulsion in the mix had not started breaking (Ibrahim, 1998, Thanaya, 2003, Oke, 2010, Ojum, 2015). Ibrahim (1998) used a mixing time of 120 sec for pre-wetting water while he used times ranging from 90 sec to 120 sec for the mixing bitumen emulsion (depending on the nature of the emulsion). A suggestion of 2-3 minutes for mixing process was recommended by Thanaya (2003). He claimed excessive mixing may cause segregation and possible stripping in the mixture. Recently, Oke (2010) and Ojum (2015) are in agreement that 4 minutes is a proper mixing time, as can be seen in Figure 2.27. They suggest the first 2 minutes are used for the pre-wetting water addition and mixing, while the remaining 2 minutes are used for the bitumen emulsion addition and mixing.

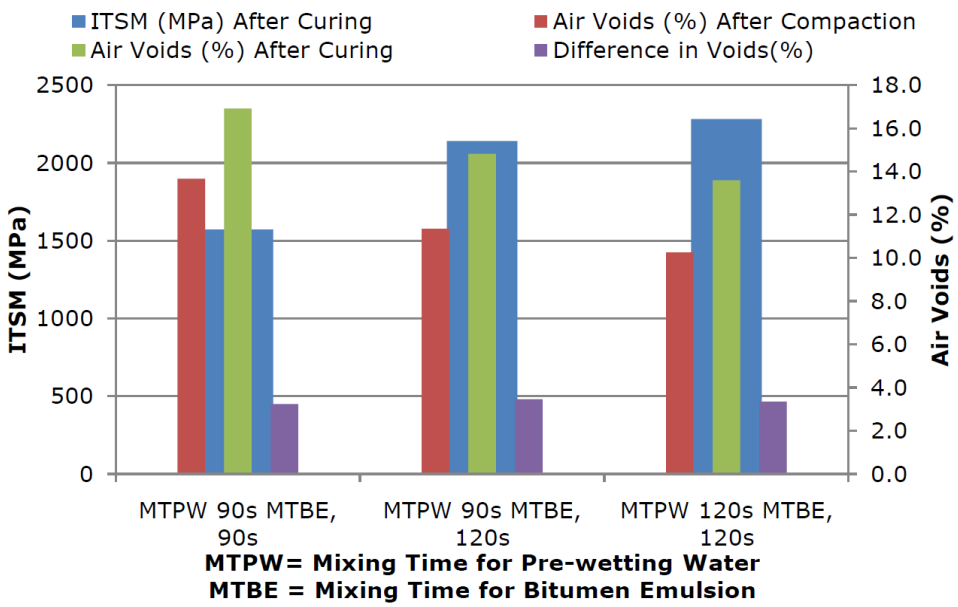


Figure 2.27 The effect of mixing time on the stiffness modulus and air voids of CBEMs (Oke, 2010)

2.7 Structural design considerations of CBEMs

The Asphalt Academy (2009) has published a schematic which describes the general performance of different pavement materials as shown in Figure 2.28. This figure categorizes these materials based on the variation of bitumen and cement content used. As can be seen in Figure 2.28, bitumen stabilized mixture with emulsion (BSM-emulsion), which is CBEM material with a different terminology, sits approximately in the middle compared to unbound/cement bound (left side) and HMA (Asphalt concrete, right side). CBEM properties seem to vary from weak to moderately strong, depending on the aggregate type and active filler content used. Meanwhile, these properties also vary from low to high resistance to permanent deformation. When active filler such as cement is added to this mixture, the strength will increase moderately. In addition, when binder content is increased, the mixture exhibits more flexibility and longer fatigue life. HMA (Asphalt concrete) mixtures appear at the bottom right; this does not mean that these mixtures show low resistance to permanent deformation, but that they normally use high binder content without active filler.

Basically, structural design of a pavement provides an optimization for the layer thicknesses that should give the structural support required for resistance to pavement distress. The two principal modes of failure in asphalt pavements are fatigue cracking of the bound layers and permanent deformation where both of them influence the CBEMs as described in Figure 2.28.

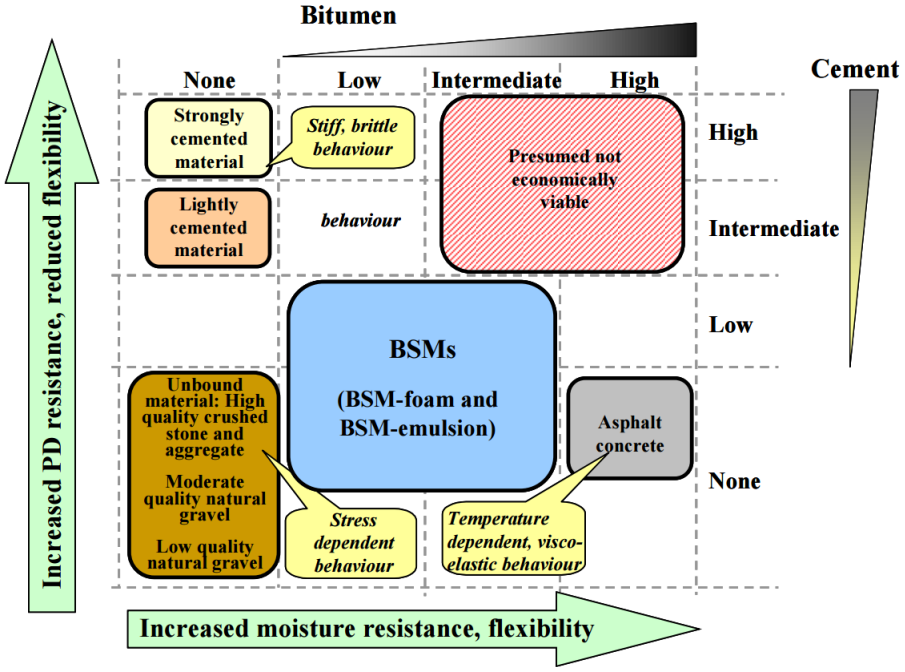


Figure 2.28 Conceptual behaviour of pavement materials a function of bitumen and active filler content (Asphalt Academy, 2009)

In CMA, structural design is not completely new although there is no universally accepted method. Thom (2008) suggested two general approaches for pavements incorporating CMA. The first approach is to treat it as HMA while the second approach is to treat it as a superior granular material. Similarly, empirical approaches have been proposed as reported by Jitareekul (2009) namely, the Catalogue Method, the CBR Design Method, the Asphalt Institute Method, AASHTO Method, and a UK method developed by Milton and Earland (1999).

Recently, the use of modelling tools involving multi-layer linear elastic analysis which are commonly used for optimising layer thicknesses in pavements containing

HMA have also been found useful for pavements which incorporate CMA (Ebels, 2008, Jitareekul, 2009, Oke, 2010, Twagira, 2010, Kuna, 2015, Ojum, 2015). These are implemented based on the results of performance tests conducted on mixtures. BISAR 3.0 and KENLAYER, among other modelling tools, have chiefly been used in this regard. A comparison between using BISAR 3.0 and KENLAYER for structural design of CBEMs was investigated by Oke (2010). Other methods which have been suggested are finite element modelling due to the complex nature of CMA (Ebels, 2008). Although this could be time consuming, the use of finite elements in structural design is gaining attention. This is due to its ability to model the wheel loads correctly under various traffic loadings (Ebels, 2008).

Brown (2013) highlighted the fact that for design purposes, the key locations to ascertain stresses, strains and deflections in the pavement structure due to traffic loadings are the bottom of the asphalt layer and the top of the subgrade, where strains related to cracking and rutting have been considered to be critical for the design of asphalt pavements as stated by Gedafa (2006).

Huang (2004) showed that distress models can be used to predict the life of new pavement structures assuming effective pavement structure configuration. If the reliability for a certain mode of distress is less than the minimum level required, the assumed pavement configuration should be changed. Brown (2013) proposed a structural design procedure which starts by specifying the traffic loading, estimating the components (layers) and sizes (thicknesses), with due consideration of available materials, which is then followed by conducting structural analysis using theoretical principles. The critical stresses, strains and deflections are then compared with allowable values to determine whether the design is satisfactory; adjustments to materials or geometry are made until satisfactory design is achieved followed by conducting an economic feasibility study.

2.8 Critical appraisal of previous studies related to performance characteristics of CBEMs

The purpose of the critical appraisal of the literature review is to determine and identify the gaps in knowledge in this research area. Acknowledging the extensive works that have been performed across different topics related to CBEMs, certain issues and gaps related to CBEM performance arise and can be summarized as follows:

- There is no universally accepted mix design method for CBEM (job mix formula) although the majority of studies have used the Asphalt Institute method. Few studies have been conducted to improve or address the shortcomings in existing mix design practice. One of the candidate approaches is by taking a statistical approach to mix design.
- Despite extensive research into using different types of CBEM, to date, the problems relating to curing time, low early strength, mechanical properties and durability of CBEMs have not been fully addressed. Therefore, enhancing CBEMs by addressing the above-mentioned issues would be a breakthrough in CBEM research.
- Although most of the background studies have showed that the performance of CBEMs can be improved using cement, there is a lack of evidence in the literature of a comprehensive study conducted using alternatives to cement. This would increase the demand for cement and consequently CO_2 emission. Therefore, developing alternative treatments using supplementary cementitious materials derived from industrial process will offer a potential impact on sustainability by eliminating the need for cement in CBEM.
- Evaluating the interaction of fillers (cement/active fillers) with bitumen emulsion and how they affect the hydration and microstructural characteristics

of CBEMs is needed as such issues are still unclear, despite previous studies discussed this issue from different perspectives.

- Different advanced techniques for microstructure assessment have been reported in the literature. SEM and XRD might be helpful tools for the deeper understanding of the microstructure and internal composition of CBEMs.
- There is no widely accepted curing protocol for CBEMs; however, it is believed that to understand the behaviour of CBEMs, there is a need to do more investigation regarding the effect of contributory factors influencing the curing process. This study would be enhanced by developing a prediction model for evaluating the effect of climatic variations on in-situ curing mixture performance.
- In the light of the debate reported in the literature about the effect of curing temperature on the hydration process of active filler and the influences of curing temperature on the binder condition, it will be beneficial to address this point in the current research.
- There is no widely accepted method for structural pavement design using CBEMs. Also, current practice uses modelling tools involving multi-layer linear elastic analysis software such as KENLAYER and BISAR. So it is worth carrying out a structural pavement analysis in order to ascertain the stresses, strains and deflections in pavement structures including CBEMs.

Chapter 3

Methodology and Materials

3.1 Introduction

This chapter is in two main parts. The first part summarizes the methodology followed to accomplish the objectives of this research project while the second one describes the raw materials used in the present study. The methodology describes briefly the work done in each stage of the current research followed by a flowchart which shows the work in more details. The second part provides the essential characteristics of the raw materials which were used with particular attention paid to filler description and characterization as it is related to the central theme in this study.

3.2 The methodology

The methodology utilized in this research comprises the following stages: **Stage I**: This stage includes conducting a comprehensive literature review, materials preparation, characterization and initial laboratory investigation. **Stage II**: comprises optimizing the mix design of CBEMs using response surface methodology to yield acceptable mechanical and volumetric properties and identifying the most suitable test for performance characterization. **Stage III**: extensive evaluations of the mechanical, durability and microstructure of CBEMs after treatment with candidate fillers were carried out. **Stage IV**: includes conducting a parametric curing study to investigate the effect of the curing process on the performance of

CBEM and applying the maturity model as a tool to predict in-situ performance. **Stage V**: evaluates the incorporation of treated CBEMs in the pavement structure as surface and base courses using pavement structural analysis software.

Figure 3.1 illustrates the methodology details followed in conducting the present research.

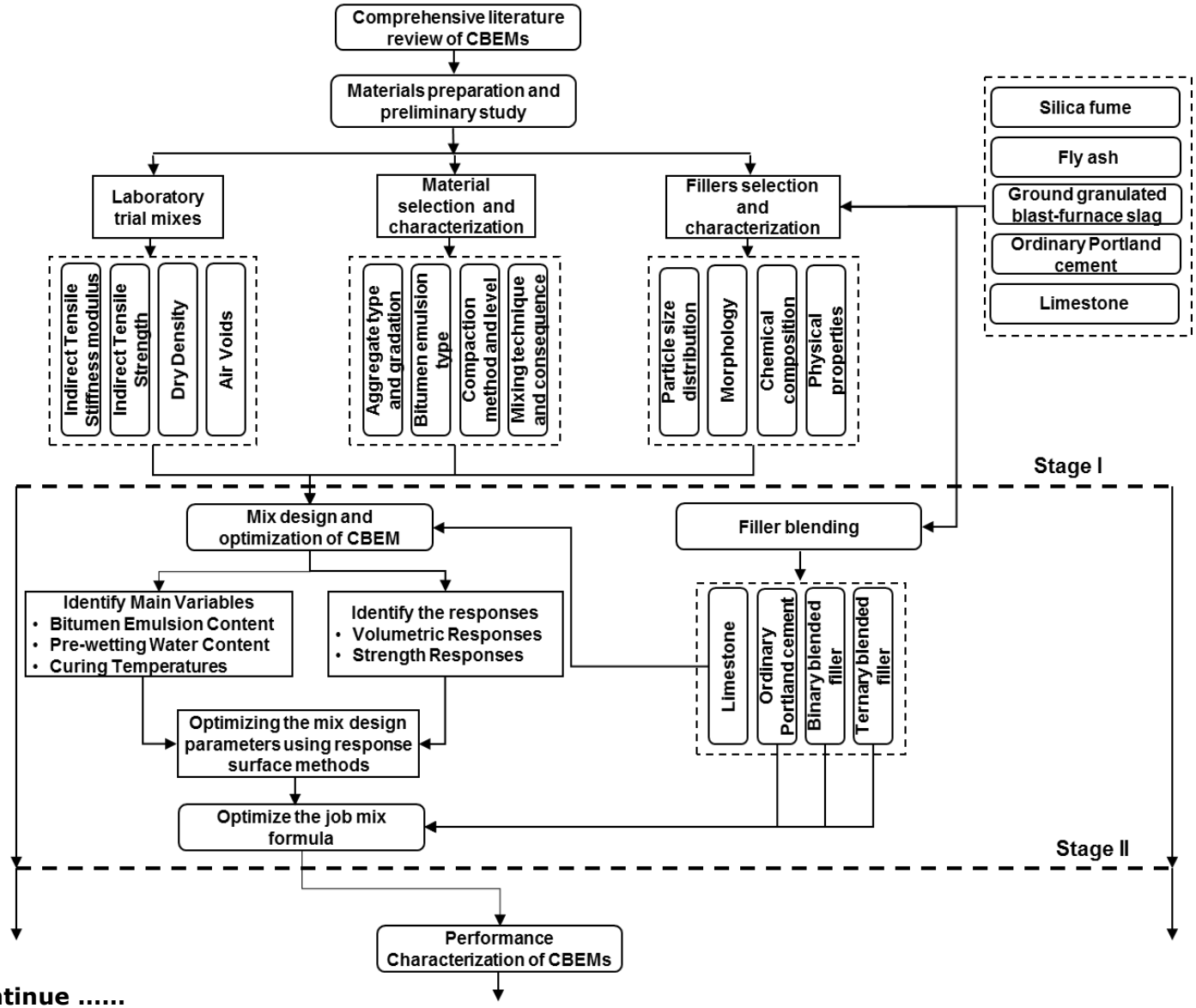


Figure 3.1 Continue ……

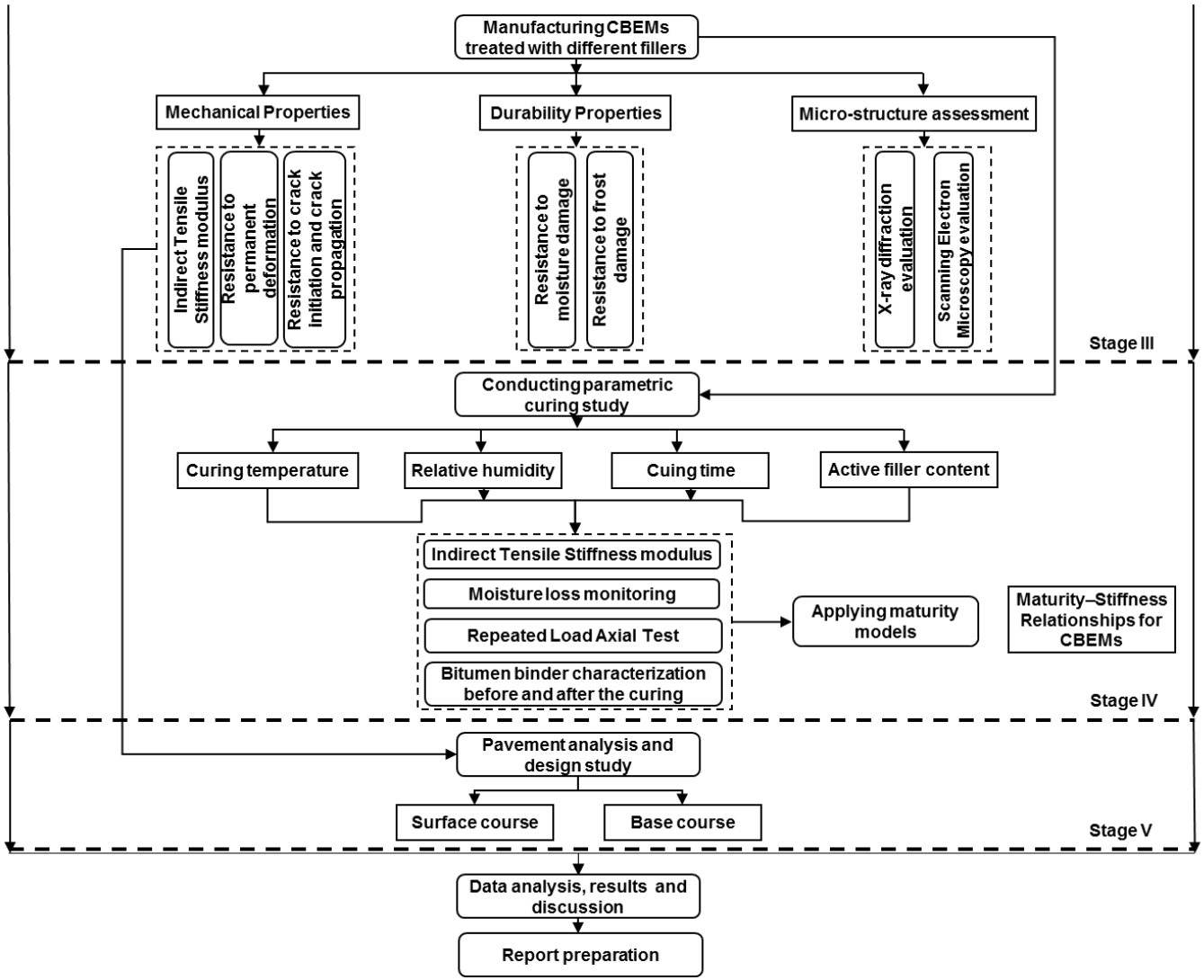


Figure 3.1 Flowchart of the research methodology

3.3 Characterization of the materials

The characterization of the materials used in this study is discussed in the following subsections. Alongside the bitumen emulsion, aggregate and water, particular attention will be given to filler characterization. This is important as the effect of different filler treatments is considered the core of the present study. Thus, this study deals with four types of bituminous mixtures, namely, untreated CBEMs, cement treated CBEMs, blended filler treated CBEMs and conventional HMA.

The materials used for CBEM manufacturing were virgin limestone aggregate, cationic bitumen emulsion, water and limestone filler. Besides these, different fillers were adopted with full or partial replacement using Ordinary Portland cement (OPC) and supplementary cementitious materials (SCMs) such as ground granulated blast-furnace slag (GGBS), fly ash (FA) and silica fume (SF). In this study, binary blended fillers (BBFs) contain a combination of FA or GGBS with OPC, while the ternary blended fillers (TBFs) are a combination of BBFs with SF. More details about the percentages of filler replacement are described in Chapter 5.

3.3.1 Virgin limestone aggregate

The aggregate used in this study was crushed limestone, which was obtained from Tunstead Quarry, Derbyshire, UK. The limestone aggregate material consisted of the following nominal sizes: 14mm, 10mm, 6mm, dust and filler as shown in Figure 3.2. Figure 3.3 and Table 3.1 show the gradation and the physical properties of aggregate materials used.

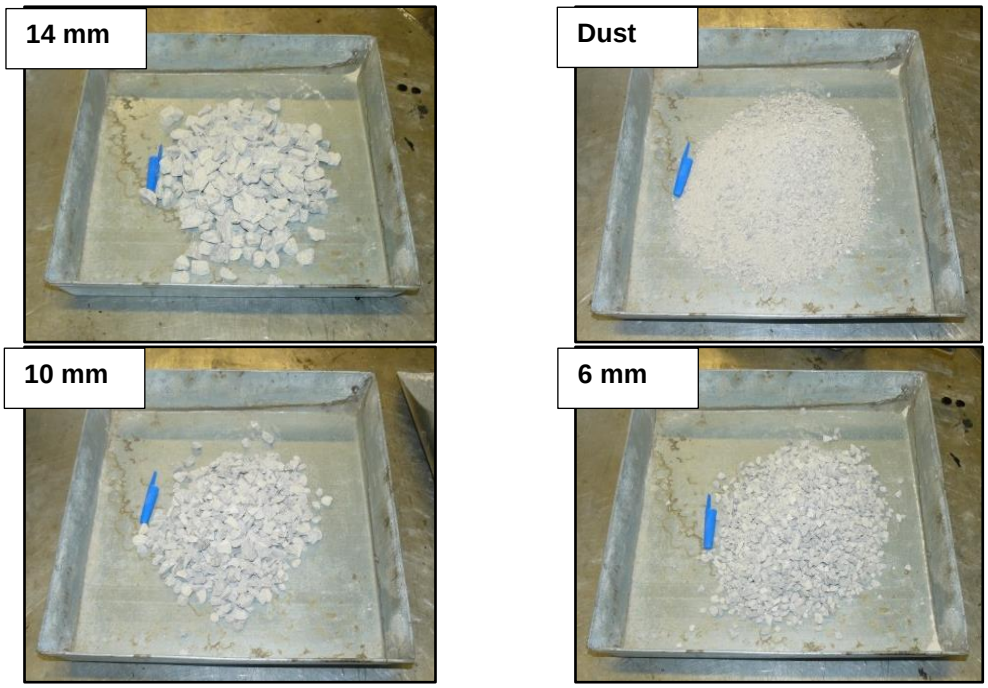


Figure 3.2 Limestone aggregate size fractions

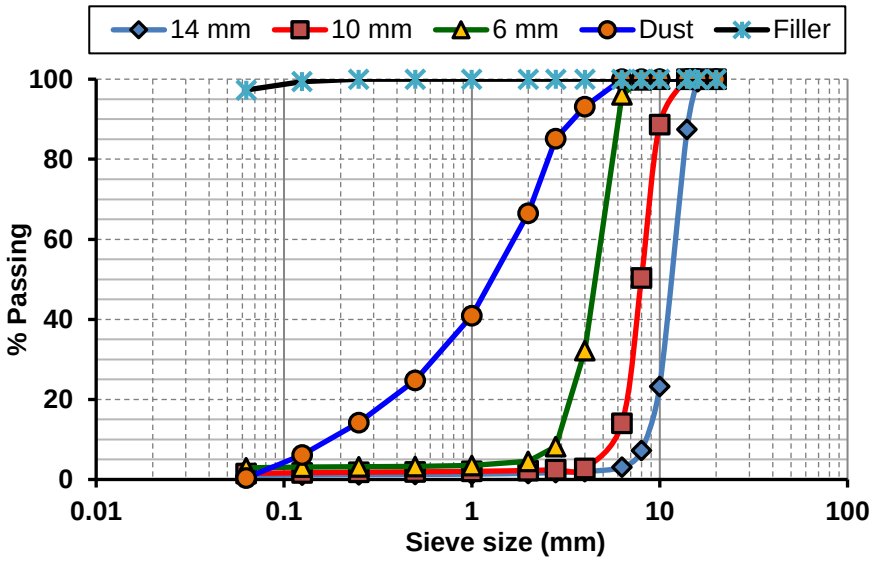


Figure 3.3 Aggregate gradation of the nominal sizes of the crushed limestone aggregate

Table 3.1 Physical characteristics of crushed limestone aggregate (BS EN1097-6:2000)

Size (mm)	14	10	6	Dust	Filler
Density- Oven Dried (Mg/m^3)	2.60	2.61	2.43	2.67	2.7
Density- Saturated Surface Dried (Mg/m^3)	2.63	2.64	2.53	2.67	N/A
Density- Apparent (Mg/m^3)	2.68	2.70	2.70	2.69	N/A
Water Absorption (%)	1.03	1.2	1.97	0.20	N/A

* This information was provided by the aggregate supplier.

3.3.2 Bitumen emulsion

A commercial cationic slow setting bituminous emulsion, C60B5, was used to manufacture the CBEMs. This type of emulsion is called Nymuls CP 50 and is supplied by NYNAS. The high stability and high adhesion of this cationic emulsion were the reason for selection as recommended by Nikolaides (1994) and Thanaya (2003). The relevant properties of the selected bitumen emulsion are shown in Table 3.2 as provide by supplier.

Table 3.2 Bitumen emulsion properties

Property	Value	Standard
Appearance	Black to dark brown	
Breaking Behaviour	> 170	EN 13075-1
Softening Point (°C)	52	EN 1427
Viscosity - Efflux time 2mm - 40°C (sec)	15-70	EN 12846
Adhesiveness	>90	EN13614
Particle surface electric charge	Positive	EN 1430
Bitumen content (%)	60	EN 1428
Penetration (dmm)	47	EN 1426
Density (g/cm³)	1.016	

The bitumen emulsion mixture was kept in air-tight sealed containers stored at room temperature. The bitumen emulsions were stirred into a homogenous state before application in making the CBEMs.

3.3.3 Bitumen

In the present study a 40/60 penetration grade bitumen supplied by Shell was used for HMA manufacture. The reason for selection is that this grade of bitumen is the same base binder grade as used in emulsion manufacturing. The properties of the bitumen used in this study are tabulated in Table 3.3.

Table 3.3 Properties of 40/60 bitumen used in the study

Property	Value	Standard
Specific gravity	1.03	BS 2000-549:2007
Penetration Index at 25°C	43	BS EN 1426:2000
Softening Point (°C)	52.8	BS 2000-58:2007
Viscosity at 135°C (mPa.s)	446.9	BS EN 13302: 2003

3.3.4 Water

Tap water was used in this study for all types of CBEMs. The water was obtained from the domestic water supply pipe in the Nottingham Transportation Engineering Centre at the University of Nottingham, UK.

3.3.5 Fillers

3.3.5.1 Introduction

The use of material such as RAP, municipal solid waste incineration ash, construction and demolition waste material, cement kiln dust and coal ash in pavement materials have been gaining attention worldwide. (Needham, 1996, Thanaya et al., 2009, Pasetto and Baldo, 2010, Al-Busaltan et al., 2012, Al-Hdabi et al., 2013a, Pérez et al., 2013, Gómez-Meijide and Pérez, 2014a, Modarres and Ayar, 2014, Betti et al., 2016). Recently, many significant environmental and economic benefits has been derived from using waste material/ by-product fillers as SCMs in different types of concrete production (Mazloom et al., 2004, Behnood and Ziari, 2008, De Schutter et al., 2011, Aldahdooh et al., 2013, Mohammed et al., 2013). In the current study, the enhancement of the engineering properties of CBEMs using different SCMs as fillers was investigated. It is believed that this may be considered a suitable way to make the CBEMs more economic and sustainable with relatively good performance compared to HMA and to increase the utilization of these mixes around the world.

Fillers can play a major role controlling the engineering properties of asphalt mixtures. It has been demonstrated that filler can significantly influence permanent deformation resistance, stiffness, fracture resistance, and moisture susceptibility of asphalt concrete (Kim et al., 2003, Kim et al., 2008). A recent development aimed at achieving excellent engineering properties of CBEMs is the use of manufactured fillers. This kind of filler is produced as a blend of reactive, semi-reactive and non-reactive natural fillers (Oruc et al., 2007, Bocci et al., 2011, Al-Busaltan et al., 2012, Al-Hdabi et al., 2013a). However, there are still some countries, such as the UK, where the current level of use leaves significant opportunity for development. Research effort is still needed to incorporate these kinds of filler into CBEMs and characterise these materials' properties to achieve a proper understanding of their behaviour, which would improve confidence and increase usage level. Thus, different types of filler were used: LF, OPC, FA, GGBS and SF, as shown in Figure 3.4. The philosophy of incorporating the cement and SCMs was based on partial or full replacement of LF in the optimized LF-CBEM (Chapter 4), assuming the replacement with such fillers will not affect the optimization of the CBEM.

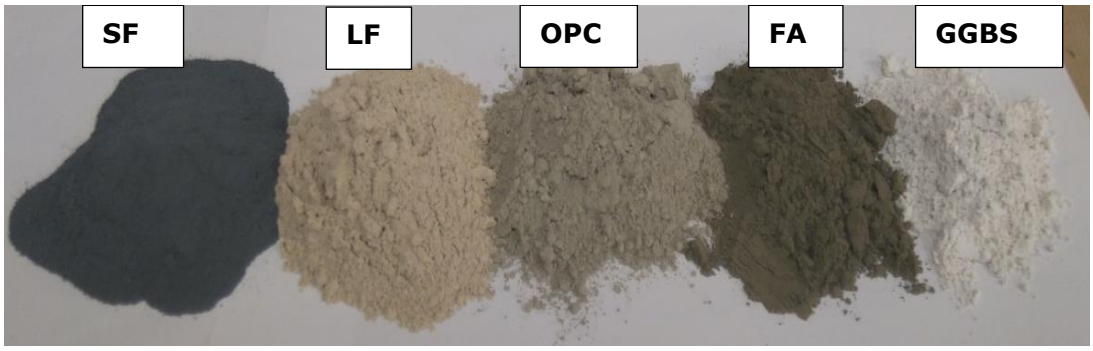


Figure 3.4 The candidate fillers

A brief description of each type is presented then followed by a detailed characterization of the chemical and physical properties of the candidate fillers.

This characterization was performed in terms of morphology, particle size distribution, physical and chemical properties, as presented later in this chapter.

3.3.5.2 Limestone filler (LF)

Conventional LF is a natural filler obtained from Tunsted quarry, Derbyshire, UK. The particle size passes 65 μm. Practically, LF is considered a very common option to be used in cement manufacture particularly in European countries (Mohammed, 2015). Bonavetti et al. (2003) reported the technical, economic, and ecological benefits that could be gained using this type of filler in cement manufacture. Also, they find an increase in the degree of hydration in very low water cement ratio paste when the LF content is increased in cement manufacturing (Bonavetti et al., 2003). To date, there is no clear evidence in the literature that LF can chemically contribute in the hydration process of cement in the concrete. However, LF plays a physical role through filling the pores between cement grains and improving the backing properties (Felekoğlu et al., 2006, Bentz and Peltz, 2008). The latter role of LF depends on different properties of filler such as the morphology, and particle size distribution as reported by De Schutter et al. (2011).

3.3.5.3 Ordinary Portland cement (OPC)

In this study OPC type CEM I 42.5N, obtained from CEMEX Company, was utilized as the main hydraulic binder in this study. Normally, OPC can be categorized as the most extensively hydraulic binder used in different fields. OPC is manufactured using a mixture of limestone and clay, or other materials that contain aluminium, and silicon oxides. This mixture is heated up to approximately 1400 to 1600°C till it melts together to produce a clinker. This is then mixed with gypsum and both materials ground to provide the final cement powder. Chemically, OPC contains four major oxides which mainly control the hydration process of cement. These major oxides are C3S (Alite), C2S (Belite), C3A (Aluminate) and C4AF (Ferrite).

The Alite and Belite form on average 50-70% and 15-30% of the OPC, respectively. Moreover, the hydration of Alite is responsible for the strength gain at early age while the Belite reacts slowly and increases the strength gain after 28 days. The other oxides, Aluminate and Ferrite, constitute on average 5-10% and 5-15% of the OPC, respectively. The Aluminate reacts very quickly for this reason the gypsum is added to control its rapid setting behaviour while the Ferrite reacts very rapidly at early age then releases with time.

3.3.5.4 Fly ash (FA)

Feuerborn (2005) defined FA as a by-product material resulting from the electrostatic or mechanical precipitation of flue ash during the combustion of coal especially in a power station. A large amount of by-products material results from coal combustion at power stations. FA forms 68% of the coal combustion products. In 2005, the annual production of coal FA in the EU exceeded 42 million tonnes (Pedersen et al., 2009). FA has pozzolanic properties, although the final structure and property of FA depends highly on the source of the coal combustion and the furnace firing conditions (van Jaarsveld et al., 2002). In the current investigation, FA type 450-S produced by CEMEX Company was used. This FA contains approximately 50% silica and 26% alumina. This mineral filler could be classified as Class F according to the American Society of Testing Material ASTM C-618, as mentioned in the provided data sheet. It has been reported in the literature that the utilization of FA alongside OPC in the concrete field as a SCM is very common practice to produce a more sustainable and cheaper mix (Mehta, 2004, Feuerborn, 2005, Felekoğlu et al., 2006, Yang et al., 2007). But despite, FA showing a technical, economic, and ecological benefits, 6 million tonnes produced annually in the UK are disposed in landfill as reported by Environmental Agency (2010).

3.3.5.5 Ground granulated blast-furnace slag (GGBS)

GGBS is a by-product of the iron manufacturing industry resulting from the grinding of blast-furnace slag. GGBS used in this work was obtained from Hanson Cement Group. The chemical composition of GGBS varies considerably depending on the composition of the raw materials in the iron production process (Özbay et al., 2016). Normally, silica, calcium, aluminium and magnesium oxides comprise more than 95% of the composition of GGBS, the same oxides that form OPC, but not in the same proportion (Sha and Pereira, 2001). GGBS has cementitious properties, which depend on the chemical composition of the slag; the higher the ratio of calcium over silicon oxide (Ca/Si ratio), the greater its hydraulic activity in the presence of activators (Nkinamubanzi et al., 1998, Pal et al., 2003). GGBS has been widely used for many years as a SCM in Portland cement concrete, either as a mineral admixture or as a component of blended cement, typically replacing 35-65% of OPC (Sarıdemir et al., 2009).

3.3.5.6 Silica fume (SF)

SF is a by-product of the manufacture of Silicon metals from Ferro silicon alloys in an electric arc furnace. SF is classified as a SCM with very reactive pozzolanic properties having 75–95% silica content. However, the silica content of the silica fume is related to the type of alloy being produced (Siddique, 2011). SF has different forms as reported by European Committee for Standardization (2009). It can be considered if collected from the filters as undensified SF while densified SF generated after treatment is applied to increase its bulk density. The last form could be SF slurry when it is mixed with water. In the present study a densified silica fume produced by the Elkem Microsilica Company was used. SF is used widely to produce high performance concrete (Shannag, 2000, Khan and Lynsdale, 2002, Mazloom et al., 2004, Behnood and Ziari, 2008). Siddique (2011) summarizes the

role of silica fume in concrete as follows: (1) mixture densification, (2) improve the hydration process of cement, and (3) increase the interfacial bonding between cement paste and aggregate.

3.3.6 A detailed characterization of fillers

3.3.6.1 Morphology of fillers

For understanding the effect of the filler on the workability and total water absorption, it is essential to characterize the shape and the surface texture of these fillers. For example, Thanaya (2003) reported that sharp and irregular filler particles decrease the workability in contrast to spherical shaped ones. Also, Segui et al. (2012) found that highly porous filler with agglomerated morphology absorbed more water inside its pores. Scanning electron microscopy (SEM) was used in this research to determine the morphology of fillers, as shown in Figure 3.5. SEM analysis was implemented under a resolution of 3-4 nm and an accelerated voltage of 15 kV.

The SEM micrographs at various magnifications revealed that the surface texture of the LF, OPC and GGBS particles is extremely sharp, the particles also being irregular in shape. In contrast, the FA particles are spherically shaped with a very smooth surface texture. The SF showed agglomerated irregular particles. As previously mentioned, the morphology of fillers, particularly those with sharp and irregular shape may affect the workability. Therefore, more caution should be applied during the mixing process leads to compact the fresh mixes directly to avoid any effect on the workability that may occur.

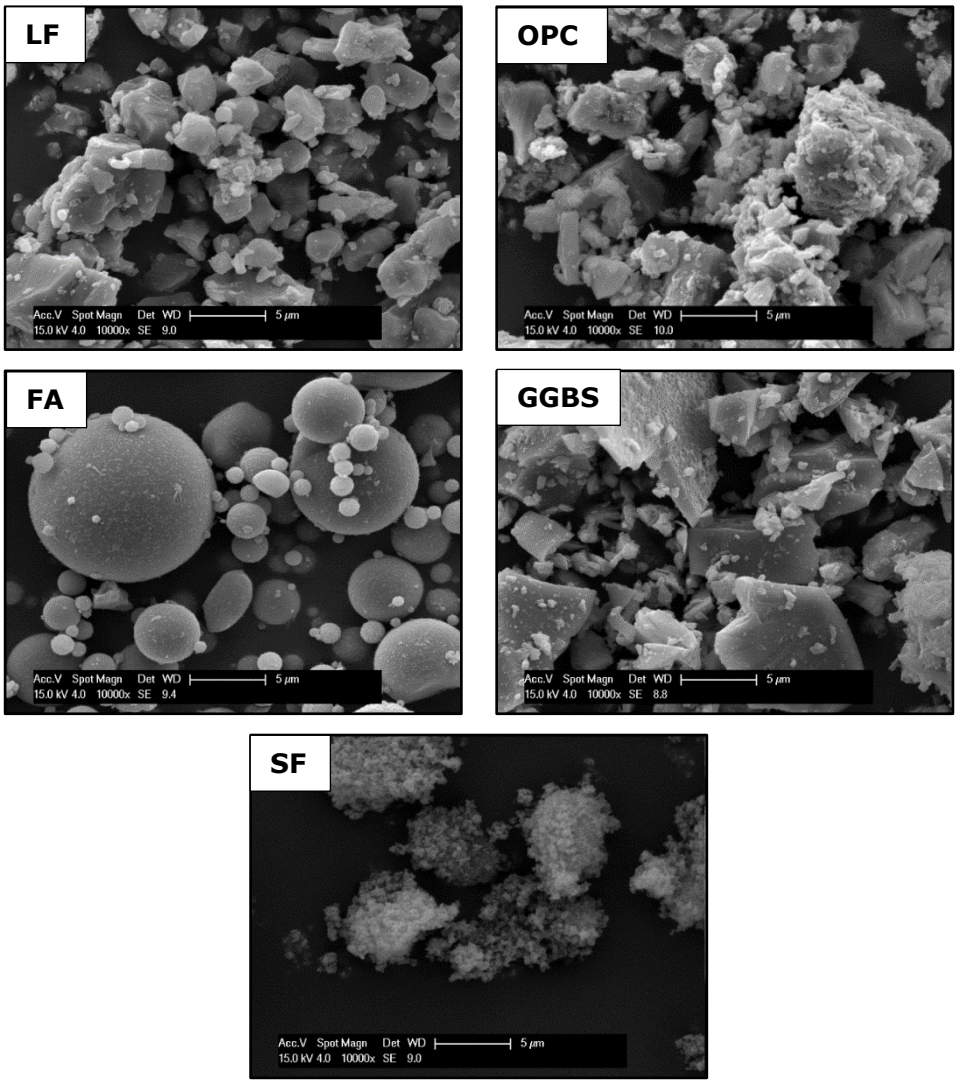


Figure 3.5 Morphology of fillers

3.3.6.2 Particle size distribution of fillers

The particle size distribution was evaluated using a Beckmen Coulter Laser diffraction particle size analyser. In principle, this device utilizes diffraction patterns of a laser beam passed through any object to measure the geometrical dimensions of a particle. Figure 3.6 presents the particle size distribution of fillers. It is recognized in the literature that particle size distribution plays a significant role in improving the packing of pores and producing a dense mixture (Brouwers, 2006). From Figure 3.6, all fillers except SF are fine and well graded which may lead to improving the mix packing properties. However, SF showed a different gradation

due to the agglomeration phenomenon as seen in Figure 3.5. Further details about the physical properties of fillers are summarized in Table 3.4.

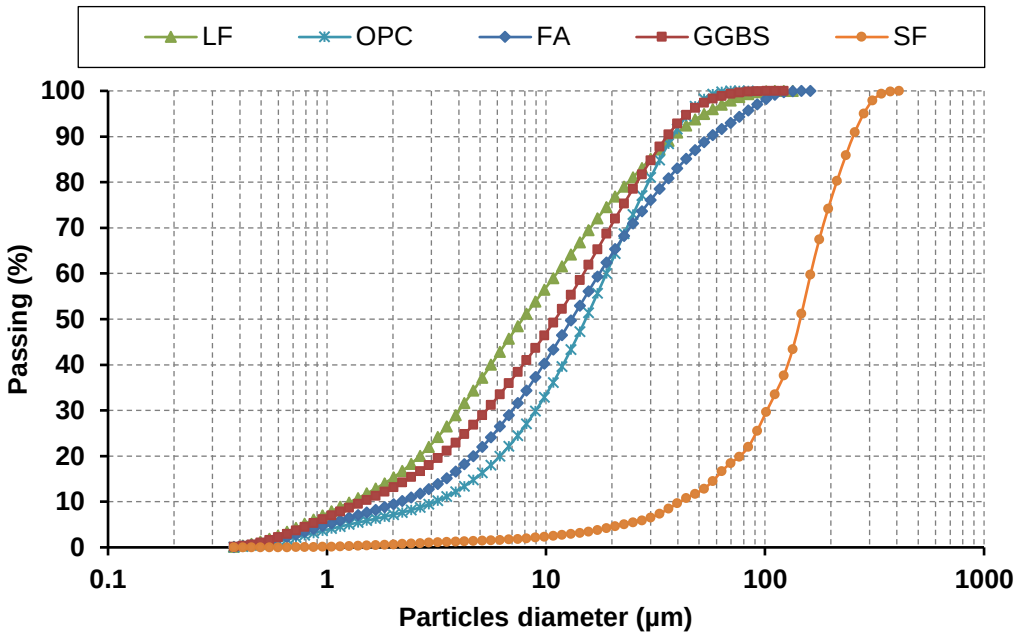


Figure 3.6 Particle size distribution of fillers

Table 3.4 Physical characteristics of fillers

Properties	LF	OPC	FA	GGBS	SF
Specific Gravity*	2.7	2.956	2.21	2.905	2.2
Mean of Particle size (µm)	16.12	19.93	24.34	16.96	160.7
d10 (µm)	1.409	3.433	2.371	1.601	44.96
d50 (µm)	8.596	16.67	14.39	12.13	159.0
d90 (µm)	41.80	41.65	62.33	39.18	277.4
Specific Surface Area* (m^2/kg)	550	395	388.5	505	22400

* provided by supplier.

3.3.6.3 Chemical composition of fillers

The chemical composition of fillers (major oxides) was analysed by EDX, energy dispersive X-ray fluorescence spectrometer. The results are presented in Table 3.5. It is very important to investigate the chemical composition since this could influence the role of the filler in CBEMs particularly their behaviour in the hydration process.

Table 3.5 Chemical composition of fillers

Properties (%)	LF	OPC	FA	GGBS	SF
Na_2O	--	0.56	1.27	0.28	0.17
MgO	--	2.04	1.76	6.89	0.36
Al_2O_3	--	4.11	25.14	11.21	0.39
SiO_2	1.97	19.84	51.32	35.65	97.95
SO_3	--	5.41	1.90	2.43	--
K_2O	--	1.06	4.24	0.64	0.89
CaO	--	64.35	2.57	41.42	0.24
TiO_2	--	0.25	1.29	0.63	--
Fe_2O_3	--	2.39	9.77	0.26	--
P_2O_5	--	--	0.74	--	--
$CaCO_3$	98.03	--	--	--	--
MnO	--	--	--	0.60	--

The major components in OPC responsible for hydration are Calcium oxides (lime) and Silicon dioxide (silica). However, there are other oxides that less significantly affect the process such as Aluminium oxide (alumina) and Iron oxide (iron). Therefore, particular attention has been paid to calcium, silica, aluminium and iron oxides. Table 3.5 shows the contents of these oxides in the fillers. Chemically, the ratio of calcium over silicon oxide (Ca/Si) is considered as an indication on the hydraulic activity of fillers. Therefore, the Ca/Si ratio has been calculated to rank the different fillers relative to OPC. The Ca/Si ratio for OPC is 3.24% while this ratio becomes 0.0, 0.05, 1.16 and 0.0025% for LF, FA, GGBS and SF, respectively. This means the GGBS has the most positive indication that it might contribute to the hydration process compared to the other fillers. Another indication could be the summation of the other main oxides (silica + alumina + iron) which are considered as supportive oxides to CaO in the hydration process. This value is 26.34 for OPC while for other fillers it becomes 1.97, 86.23, 47.12 and 98.34 for LF, FA, GGBS and SF, respectively. This variation in filler oxide content may reflect the differences in expected behaviour in the hydration process in the presence of cement. Furthermore, it is clear that conventional LF contains calcium carbonate ($CaCO_3$) with very little content of silica which explains its role as an inert filler.

3.4 Summary

The methodology utilized in this research comprises five stages and the characterization of the materials used is discussed in this chapter. Since the main emphasis of the present work is examining how the fillers affect the performance of CBEMs, particular attention has been given to filler characterization. A brief description of each type of filler has been presented then followed by a detailed characterization of its chemical and physical properties. The following concluding remarks are made:

- The surface textures of the LF, OPC and GGBS particles are extremely sharp, and of irregular shape.
- The FA particles are spherically shaped with a very smooth surface texture while the SF showed agglomerated irregular particles.
- More caution should be applied during the mixing process leads to compact the fresh mixes directly to avoid any effect on the workability that may occur.
- All fillers except SF are fine and well graded which may lead to improvement in the mix packing properties.
- In terms of hydraulic activity of fillers, GGBS gives a positive indication that it may provide better hydration compared to the other fillers, except OPC.

Chapter 4

Design and Optimization of CBEM

4.1 Introduction

There is currently no mix design method for CBEMs that has received widespread acceptance. This may be at least partially due to the wide variation in available mix design procedures, tests and criteria (Sebaaly et al., 2004). As CBEMs have been gaining attention worldwide, optimizing of CBEM proportions is becoming more desirable. Furthermore, as there is a wide range of materials and parameters involved in CBEM, the problem of identifying optimal mixtures becomes increasingly complicated.

Basically, the objective of any mix design is to produce mixtures that meet their structural and functional requirements. Regarding current practice, some authorities and researchers have proposed mix design guidelines based on empirical formulae, laboratory tests or past experience (Asphalt Institute, 1989, Brayton et al., 2000, Thanaya, 2003, Wirtgen, 2005). However, the trend for mix design is progressing towards performance-based approaches as stated by Ojum (2015).

Thus, it is clear that optimization of mixture parameters has to be made more consistent in order to promote the technology of using CBEM as claimed by Brayton et al. (2000). It is therefore essential to design and optimize mixture components

in order to achieve appropriate properties (Brayton et al., 2000, Kim et al., 2007). Some of the studies reported in the literature on CBEMs have focused on using the method adopted by the Asphalt Institute (1989) (Marshall Method for Emulsified Asphalt Aggregate Cold Mixture Design), with some modifications (Thanaya, 2003, Forth et al., 2006). The general approach of the Asphalt Institute procedures can be described by the following steps (Thanaya, 2003):

(1) Determination of suitable aggregate gradation.

(2) Determination of an initial approximate amount of Bitumen emulsion based on an empirical formula.

(3) Determination of optimum water content at compaction.

(4) Variation of proportions (bitumen emulsion and pre-wetting water content) manually.

(5) Determination of optimum proportions taking into consideration the mechanical and volumetric properties of trial mixtures until finding a trend to the specified criteria.

(6) Establishment of the job mix formula.

There are two kinds of fluid inside CBEM, which are water and bitumen. The water content includes two sources of water: (1) a proportion of the bitumen emulsion content (BEC) and (2) the additional water in the mix, termed the pre-wetting water content (PWC). PWC is defined as the amount of water added to the mixture prior to the addition of bitumen emulsion. This addition is to improve the ability of bitumen emulsion to coat the aggregate and to improve the workability of the mixture.

In Asphalt Institute (1989) method, they keep the BEC constant and specimens are prepared with different PWC to develop a stability/strength curve. Then, indicative tests, such as Marshall stability/ITS, are performed to determine the total fluid content (TFC). Once the TFC has been established, there is the need to optimize

the binder content in the TFC. Hence by keeping the TFC constant, emulsion content was varied. However, it was experienced to the author that these guidelines may not valid for virgin material because most of the work done in this area focused on using RAP. The initial BEC was overestimated, and the determination of PEC was evaluated visibly. Moreover, this is a mix design procedure performed by varying one mix design parameter at a time.

It seems that optimization in the Asphalt Institute (1989) method was rather simple for a unique property such as maximum stability/strength or minimum air voids. The determination of the percentages of BEC and PWC from the optimum TFC is carried out subjectively, and it depends on the judgement of the designer. Moreover, optimization to meet several criteria is also not possible. An additional disadvantage of the existing methods such as the Asphalt Institute (1989) method is that the interaction among the mix design parameters is not considered in the performance evaluation. All these points may cause a variation in the mix design and decrease the quality control.

There would therefore appear to be potential to explore the use of a statistical experimental design method to optimize the mixture design of CBEMs as an alternative approach. In response to the above need, the present study has been undertaken in order to develop a performance-based mix design incorporating a statistical approach using response surface methodology (RSM). RSM is used as the optimization technique to adjust the mixture parameters of CBEM to achieve both acceptable mechanical strength and suitable volumetric properties together. More details about RSM will be presented later in this chapter. Also, the study aimed to investigate the interaction effect of mixture parameters on the mechanical and volumetric properties of CBEM.

4.2 Methodology

An experimental program was undertaken to optimize the CBEM mix design, considering the effects of certain important parameters. The flowchart in Figure 4.1 summarizes the mix design methodology used in this research, which includes the following steps:

- Determine the aggregate type and gradation to suit the recommendations of selected gradation.
- Determine the type and grade of bitumen emulsion required for compatibility with aggregates.
- Check compactability of aggregates using a suitable compactor method to determine optimum moisture content (OMC) and maximum dry density (MDD) by varying moisture content.
- Review the literature in order to determine the main variables of CBEM mix design and the main responses to evaluate the suitability of a mix design.
- Carry out an initial laboratory trial to identify the main variable levels and ranges and characterize the level of compaction.
- Determine the matrix of experimental design (combination of different variable levels) using RSM techniques.
- Carry out laboratory tests based on the performance responses for selected mixes.
- Perform analysis of variances (ANOVA) to select the appropriate type of model and to obtain the interaction among the variables.
- Finally optimize the mixture proportions to fulfill the desirable performance and find the job mix formula. Validate these results of optimization in the laboratory to ensure the accuracy of the model.

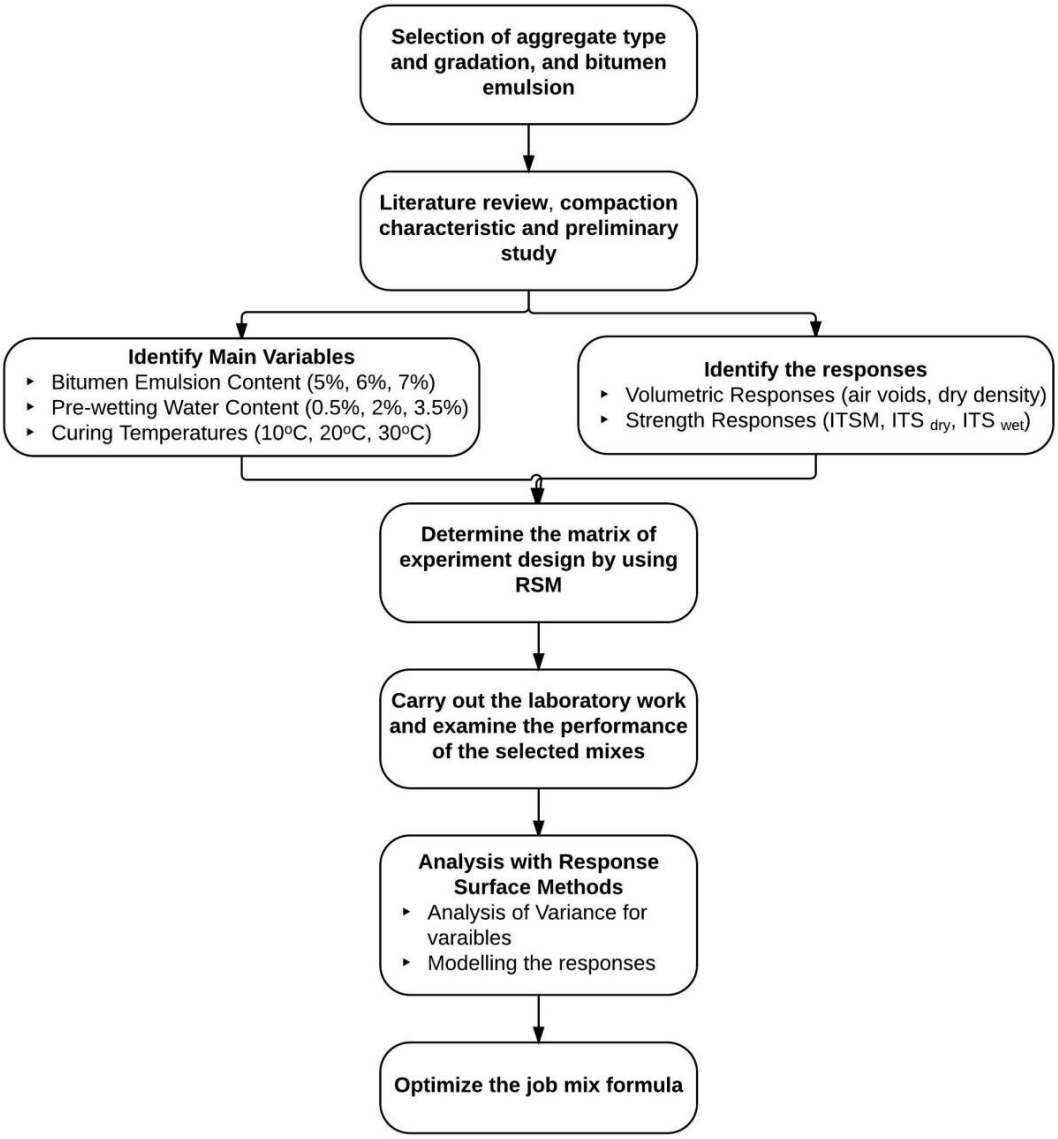


Figure 4.1 Optimization of CBEM methodology using RSM

4.2.1 Properties of the materials used

The aggregate used in this study was crushed limestone, which was obtained from Tunstead Quarry, Derbyshire, UK. The characterization of limestone aggregate are presented in the previous chapter, see Figure 3.2, Figure 3.3 and Table 3.1. The composition of limestone aggregate was designed based on BS EN 13108-1, ensuring that the gradation of the aggregate fell into the recommended grading envelope for 0/14 mm size (close graded surface course). This selection was made in order to ensure an appropriate interlock between the aggregate particles in the mixtures as recommended by the European Committee for Standardization (2006).

The composition of the aggregate used in this study was 25%, 25%, 15%, 30% and 5% for 14mm, 10mm, 6mm, dust and limestone filler (LF), respectively. The gradation of the aggregate is shown in Figure 4.2.

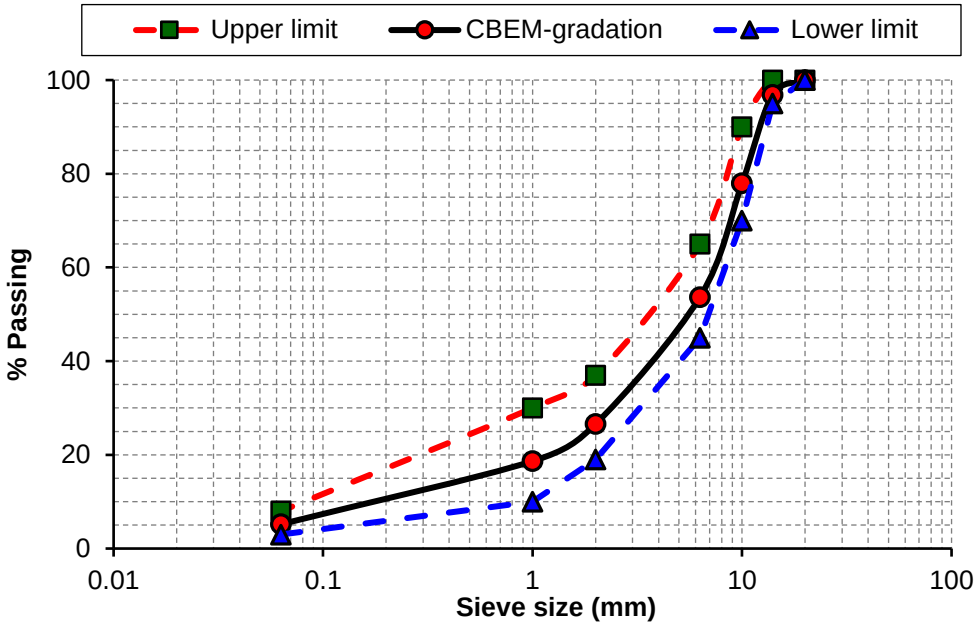


Figure 4.2 Aggregate gradation for CBEM

A commercial cationic slow setting bituminous emulsion, C60B5, was used to manufacture the CBEMs. This type of emulsion is called Nymuls CP 50 and is supplied by Nynas Bitumen. The high stability and high adhesion of this cationic emulsion were the reason for selection as recommended by Nikolaides (1994) and Thanaya (2003). The relevant properties of the selected bituminous emulsion are presented in previous chapter, see Table 3.2 .

4.2.2 Compaction characteristic

The modified Proctor test in accordance with BS EN 13286-2:2004 was performed to obtain the OMC and MDD. Table 4.1 states details of the parameters used for the modified Proctor test. This gives an indication of the water content at which the mixtures can be compacted in order to achieve MDD.

Table 4.1 Modified Proctor test parameters

Characteristics of test	Values
Diameter of mould	150mm
Mass of Rammer	4.5kg
Diameter of Rammer	50mm
Height of Fall	457mm
Number of Layers	5
Number of blows per face	56

Analogously, the OMC gives an indication of the TFC for the CBEM. However, it should be noted that the mechanism of compaction involving water and bitumen emulsion is slightly different in CBEMs. As the mixture cures, moisture evaporates and the residual bitumen from emulsion starts performing its dual role of binding the matrix together and also enhancing the density of mix (Ibrahim, 1998, Thanaya, 2003, Oke, 2010, Arimilli et al., 2015). The water content of the materials was increased in 1% increments ranging between 2-10% of dry weight of aggregate. As shown in Figure 4.3 the value of MDD is expected to be reached between 6-10% water content with an average values of 2235 kg/m^3.

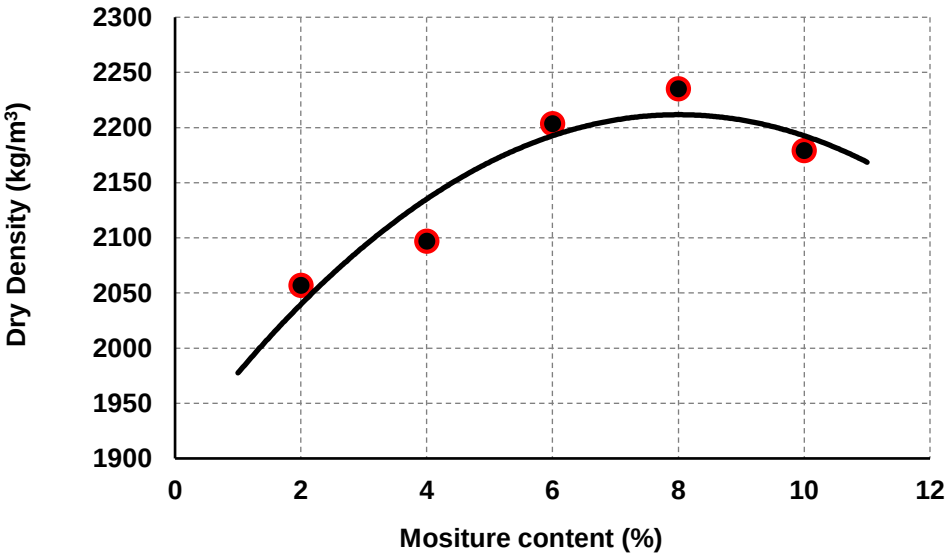


Figure 4.3 Compaction characteristic of crushed limestone aggregate using modified Proctor compaction

Therefore, an initial laboratory evaluation was carried out with different combinations of PWC and BEC in order to validate this range and determine the compaction effort accordingly.

4.2.2.1 Laboratory trial mixes

Different mixing combinations of PWC and BEC were carried out with varying water content (1.5%, 2.5% and 3.5%) and varying emulsion content (6%, 5% and 4%), ensuring the same TFC in each mix. In Figure 4.4 and Figure 4.5, (Mix 5, 2.5) refers to a mixture with 5% of BEC and 2.5% of PWC. These mixtures were compacted using Marshall Hammer compaction at 50 and 75 blows each face since 100 blows was found to damage the top surface of the sample. Airey et al. (2008) reported 100 blows of Marshall compaction caused a slight increase in the percentage of fine materials and a decrease in coarse materials compared to specimens subjected to 50 blows each face. Therefore, the comparison was limited to between 50 and 75 blows each face. After compaction specimens were kept at room temperature for 24 hours and then extracted. The extracted specimens were cured at 40°C for 3 days. Volumetric and mechanical tests were carried out on the cured specimens. The effect of mixing fluid combinations on the volumetric and mechanical properties can be seen in the plots in Figure 4.4 and Figure 4.5, respectively.

With respect to Figure 4.4, it was observed that mix performance was improved at 75 blows of compaction. For example Mix 5, 2.5 shows 10.5% of air voids at 75 blows while the value became 11.9% at 50 blows. Similar behaviour was observed with respect to dry density.

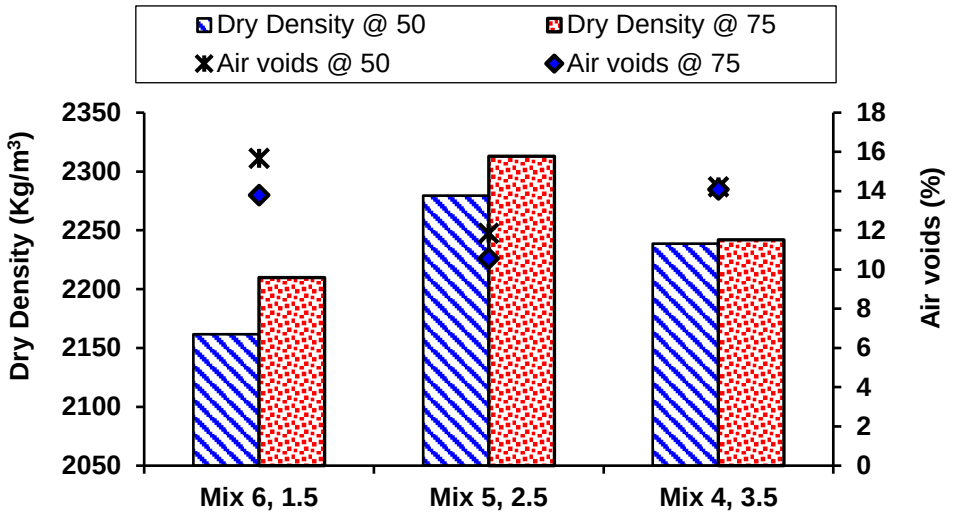


Figure 4.4 Volumetric properties of initial CBEM with varying BEC and P

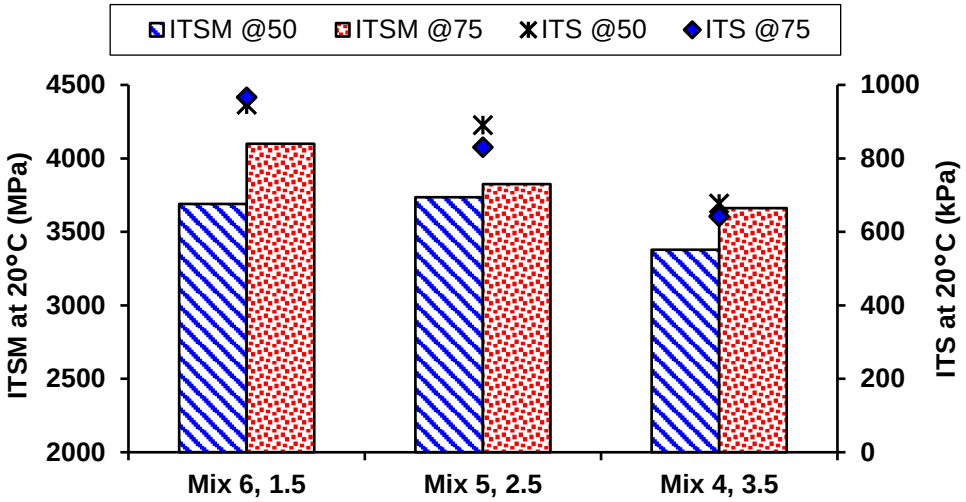


Figure 4.5 Mechanical properties of initial CBEM with varying BEC and PWC

Furthermore, as can be seen from Figure 4.5 the performance of mixes under 75 blows presents better performance relative to 50 blows. A higher stiffness and strength was noticed at 75 blows. Hence, 75 blows of compaction were applied in subsequent studies to produce Marshall compacted mixes. This level of compaction is consistent with previous studies on CBEM which used 75 blows Marshall compaction (Khalid and Eta, 1996, Thanaya, 2003, PEREZ et al., 2004, Kim and Lee, 2006, Yan et al., 2010, Du, 2014). However, Khalid and Eta (1996) is in

agreement with Thanaya (2003) that the application of heavier compaction level tended to be required for CBEM, allowing the bitumen droplets of the emulsion to coalesce.

4.2.3 Design of experiment using RSM

Montgomery (2008) defined RSM as a mathematical and statistical technique used for designing experiments in order to establish relationships between multiple factors and to optimize the relevant conditions of parameters to predict the best responses.

RSM and a three-level factorial experimental design have been applied to satisfy these conditions. The central composite design (CCD) method has been used. CCD is a fractional factorial experimental design able to provide the relationship between responses and factors over a range of factor levels (Khuri and Cornell, 1996, Montgomery, 2008).

RSM is regularly applied in disciplines such as concrete (Bayramov et al., 2004, Aldahdooh et al., 2013, Bektas and Bektas, 2014), material and mechanical engineering technologies (Nekahi and Dehghani, 2010, Younesi and Bahrololoom, 2010, Faseeulla Khan et al., 2012). Recently, there has been growing attention to the application of RSM in asphalt research (Chávez-Valencia et al., 2005, Khodaii et al., 2012, Haghshenas et al., 2013, Hamzah et al., 2013, Kavussi et al., 2014, Hamzah et al., 2015, Khodaii et al., 2015, Moghaddam et al., 2015). Chávez-Valencia et al. (2005) also implemented RSM to evaluate the ageing phenomenon of bituminous binder in HMA. Haghshenas et al. (2013) studied the effects of frequency, temperature and their interaction, on rutting of HMA using RSM. Hamzah et al. (2013) used RSM to optimize the binder content of warm mix asphalt incorporating Rediset by evaluating the volumetric and strength properties of

mixes. Kavussi et al. (2014) investigated the effect of aggregate gradation, hydrated lime content and Sasobit content on moisture damage of warm mix asphalt. An experimental study (Khodaii et al., 2012) used RSM to assess the effects of aggregate gradation and lime content on stripping of HMA in terms of the strength and stiffness. Also, Khodaii et al. (2015) evaluated the effects of aggregate gradation, lime content, Sasobit content and binder content on stripping potential of warm mix asphalt. RSM was used to investigate the effects of short-term aging on asphalt binder rheological properties (Hamzah et al., 2015). A laboratory study (Moghaddam et al., 2015) assessed the properties of stone mastic asphalt mixtures incorporating waste polyethylene terephthalate using RSM.

A fractional factorial design such as CCD is usually used in RSM (Khuri and Cornell, 1996). It has been reported as a potentially useful approach which is able to provide a suitable functional relationship between the responses and the factors (i.e. input parameters) (Khodaii et al., 2012). Design Expert 9.0.6.2 software (Stat-Ease Inc., Minneapolis, USA) was used for the design, mathematical modelling, statistical analysis, and optimization of the process parameters. ANOVA was conducted in order to obtain the interaction among the different parameters and the influence of each individual parameter. The appropriate regression model, recommended by Khuri and Cornell (1996) and Montgomery (2008) , was applied, as shown in the Equation 4.1:

$$Y = \beta_0 + \sum_{j=1}^{k} \beta_j X_j + \sum_{j=1}^{k} \beta_{jj} X_j^2 + \sum_{i} \sum_{<j=2}^{k} \beta_{ij} X_i X_j + e_i \qquad \text{Equation 4.1}$$

where:

Y: Response; X_i and X_j: Parameters; β: Regression coefficient; k: Number of parameters included in the experiment; e: Random error.

4.2.4 Multiple responses optimization using RSM

The optimization process in RSM deals for a combination of factor levels that simultaneously satisfy the requirements placed (i.e. optimization criteria) on each of the responses. Desirability function (DF) is a common and established technique to concurrently determine of input parameters that can give the optimum performance levels for one or more responses.

The desirability procedure involves three steps: (1) predicting responses on the dependent parameter by fitting the observed responses using an equation, based on the levels of the independent parameters, (2) finding the levels of the independent parameters that simultaneously produce the most desirable predicted responses on the dependent variables and (3) maximize the overall desirability with respect to the controllable parameters. With the individual desirabilities, it is then possible to obtain the overall desirability. The overall DF is defined as the weighted geometric average of the individual desirability (d_i) according to Equation 4.2:

$$\mathrm{DF} = \sqrt[m]{d_1 d_2 \dots\dots\dots\dots\dots\dots\dots d_m} \qquad \text{Equation 4.2}$$

Where

m is number of responses studied in the optimization process.

The scale of the individual desirability function ranges between 0 to 1, where if the response is at its goal or target, then $d_i=1$, and if the response is outside an acceptable region, $d_i=0$. In multi-response optimization, the design variables are chosen to maximize the overall desirability. More details about DF functions as discussed and presented in Costa et al. (2011).

4.2.5 Mix proportions of CBEMs

An experimental program was undertaken in order to consider the effects of certain important parameters on CBEM mix design. The parameters (independent variables) considered were BEC, PWC and curing temperature (CT). BEC and PWC are presented as a percentage of total mass of dry aggregate. These three parameters together with their respective ranges were selected based on a preliminary study (section 4.2.2.1) and extant literature (Brayton et al., 2000, Ameri et al., 2012, Gómez-Meijide and Pérez, 2014a). It is well known that the curing process significantly affects the properties of the CBEM (Konrad and Walter, 2001, Loizos, 2007, Jenkins and Moloto, 2008, Ojum et al., 2014). Therefore, the CT was considered as a parameter in mix design, 10°C, 20°C and 30°C being taken to represent cold, moderate and warm climatic conditions, respectively. The ranges and the levels of all the parameters investigated are given in Table 4.2.

Table 4.2 Independent parameters and their coded levels for CCD

Parameters	Code	Unit	Coded parameter levels		
			-1	0	+1
BEC	X_1	%	5.0	6.0	7.0
PWC	X_2	%	0.5	2.0	3.5
CT	X_3	°C	10	20	30

(-1) refers low level; (0) refers to mean level; (+1) refers to high level

The total number of experiments carried out was 20 (= 2^k +2k +6), where k is the number of parameters (k= 3). Fourteen different combinations were supplemented with six replicates of the mean case. The set of 14 mixes considered three levels of each studied parameter; all factors were varied in this way. The set of six replicate mixes considered the mid-level of each studied parameter; this point is often replicated in order to improve the precision of the experiment and minimize any possible sources of bias. The CCD matrix employed is presented in Table 4.3.

Table 4.3 Matrix of experimental design by CCD

Run No.	Mix design parameters			TFC (%)
	BEC (%)	PWC (%)	CT (°C)	
Mix 01	5.0	3.5	10	8.50
Mix 02	7.0	0.5	10	7.50
Mix 03	7.0	3.5	10	10.5
Mix 04	5.0	0.5	10	5.50
Mix 05	6.0	2.0	10	8.00
Mix 06	6.0	3.5	20	9.50
Mix 07	6.0	0.5	20	6.50
Mix 08	7.0	2.0	20	9.00
Mix 09	6.0	2.0	20	8.00
Mix 10	6.0	2.0	20	8.00
Mix 11	6.0	2.0	20	8.00
Mix 12	6.0	2.0	20	8.00
Mix 13	5.0	2.0	20	7.00
Mix 14	6.0	2.0	20	8.00
Mix 15	6.0	2.0	20	8.00
Mix 16	6.0	2.0	30	8.00
Mix 17	7.0	3.5	30	10.50
Mix 18	7.0	0.5	30	7.50
Mix 19	5.0	3.5	30	8.50
Mix 20	5.0	0.5	30	5.50

4.2.6 Manufacturing procedures of CBEMs

The mix proportions presented in Table 4.3 were used to prepare Marshall specimens. Figure 4.6 summarizes the manufacturing process for CBEM, considering some recommendation related to manufacturing and mixing procedures concluded form previous studies as discussed in section 2.6.

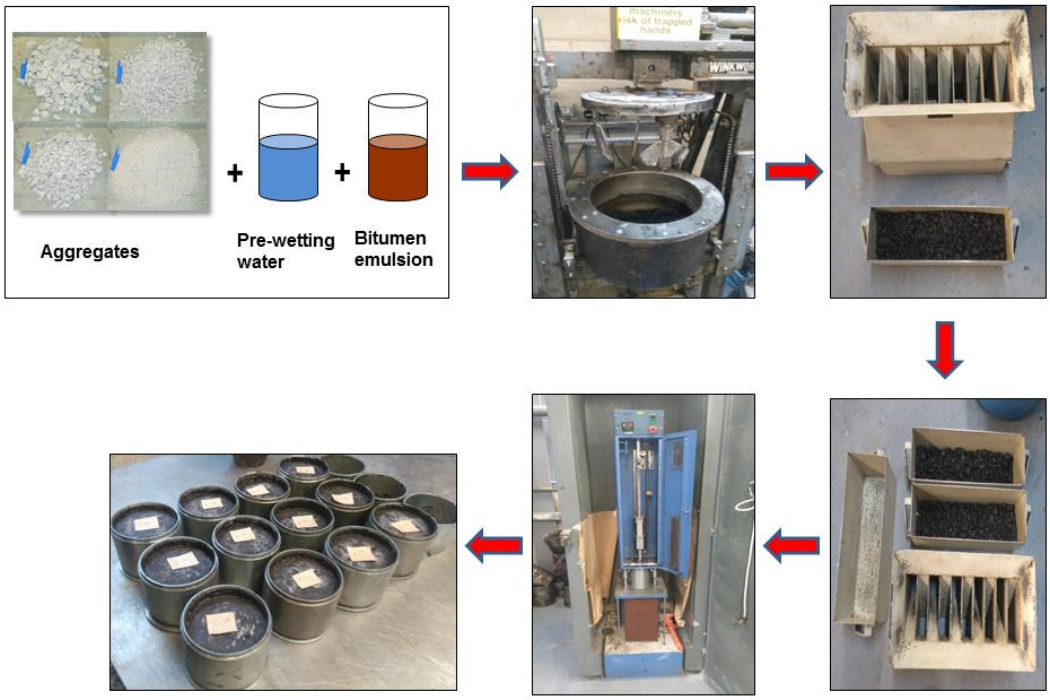


Figure 4.6 Manufacturing process for CBEMs

The procedure followed for preparing the specimens was such that the PWC was first added to the dry batched mixture and mixed using a Sun and Planet mixer for 60s. This was followed by mixing using a spatula for 60s ensuring that the aggregate materials were thoroughly blended and wetted ready for the addition of the bitumen emulsion. The required emulsion was subsequently added and the mixture mixed for another 60s. To ensure homogeneity and consistency in the mix, the materials were then mixed by hand using a spatula for a further 60s. These timings were found to be suitable for such mixes in previous related works (Sunarjono, 2008, Oke, 2010, Ojum, 2015). Then, a Marshall hammer was used to compact the specimens; 75 blows applied to each face. After compaction, the curing protocol followed was such that the specimens were left in the moulds for 24hrs (in a sealed condition) at the same ambient temperature before they were carefully extruded. After that, specimens were conditioned for 28 days in a thermostatically controlled air chamber at temperatures of 10°C, 20°C, and 30°C as stated in Table 4.3.

4.2.7 Laboratory testing program

The mix design considered here relies on the information obtained from fundamental tests, which are used to evaluate the mixes proposed using CCD, as shown in Table 4.3. The literature shows that CBEM design methods are similar to those of HMA, but with no universally accepted method or procedure (Oke, 2010). There are two sets of tests commonly conducted when assessing HMA, mechanical tests and volumetric tests respectively. In the current study, the responses considered represented the mechanical and the volumetric properties of CBEMs. Indirect tensile stiffness modulus (ITSM) and indirect tensile strength in both dry and wet conditions (ITS dry and ITS wet) were performed in order to evaluate the mechanical properties. Air voids and dry density were measured to assess the volumetric properties, calculated according to Asphalt Institute (1989) recommendations.

4.2.7.1 Indirect tensile stiffness modulus (ITSM)

The ITSM is a non-destructive test used mainly to evaluate the stiffness modulus of bituminous mixes. Stiffness modulus is considered as an indicator of the structural behaviour of mixtures because it is related to the capacity of the material to distribute traffic loads. The test was carried out according to BS EN 12697-26 (European Committee for Standardization, 2012). Following BS EN 12697-26, an impulsive load was applied with a rise-time of 124 ms, to achieve a target horizontal deformation of 5 ± 2 μm. Ten conditioning pulses were applied to the specimens followed by five test pulses. The measurements were repeated along two diameters and the average stiffness values were calculated. More details about this test procedures and configuration are presented in next chapter, section 5.5. Four specimens per mix were tested under the same conditions.

4.2.7.2 Indirect tensile strength (ITS)

The ITS test involved applying diametric compression with a constant deformation rate of (50 ± 2) mm/min to the samples between two loading strips, which creates tensile stresses along the vertical diametral plane causing a splitting failure. The test was conducted at 20°C using an INSTRON test equipment in accordance with BS EN 12697-23 (European Committee for Standardization, 2003). More details about this test procedures and configuration are presented in next chapter, section 5.55.7.1.

4.2.7.3 Volumetric responses

It was demonstrated by Thanaya (2003) that satisfactory volumetric properties are essential to the design of CBEMs. The volumetric properties of mixes were evaluated using the methodology proposed by Asphalt Institute (1989) as shown in Equation 4.3 to Equation 4.8.

$$G = \frac{D}{F - E} \quad \text{Equation 4.3}$$

$$G_d = G \times \frac{(100 + A)}{(100 + A + K)} \quad \text{Equation 4.4}$$

$$K_{(\text{water content at testing})}\% = \frac{\text{mass of water, (g)}}{\text{mass of dry mixture, (g)}} \quad \text{Equation 4.5}$$

$$V_{(\text{total voids})}\% = \left[\left(\frac{100 + A + K}{G} - \frac{100}{C} - \frac{A}{B}\right) \div \left(\frac{100 + A + K}{G}\right)\right] \times 100 \quad \text{Equation 4.6}$$

$$\text{Air Voids } \% = V - \left[\left(\frac{K \times 100}{L}\right) \div \left(\frac{100 + A + K}{G}\right)\right] \quad \text{Equation 4.7}$$

$$\text{Dry Density} = G_d \times 1000 \ (\text{Kg/cm}^3) \quad \text{Equation 4.8}$$

where

D: Mass of specimen in air; E: Mass of specimen in water; F: Mass of specimen in saturated surface-dry (SSD) condition; G: Bulk specific gravity; G_d: Dry specific gravity; A: Bitumen residue as a percentage of dry aggregate mass; B: Specific gravity of bitumen; C: Apparent specific gravity of aggregate; L: Specific gravity of water.

4.3 Results and analysis of performance responses

A total of 80 Marshall specimens were produced for the 20 mixes proposed using CCD, four for each mix. The results are presented in Table 4.4 and discussed in the following sections.

Table 4.4 Experimental factors and experimental responses

Run No.	Performance responses									
	Mechanical Responses						Volumetric Responses			
	$ITSM_{10\ days}$ (MPa)	Standard Deviation	$ITS\ dry_{28\ days}$ (kPa)	Standard Deviation	$ITS\ wet_{28\ days}$ (kPa)	Standard Deviation	Dry density (kg/m^3)	Standard Deviation	Air voids (%)	Standard Deviation
Mix 01	2141	(113.77)	639	(31.24)	444	(27.28)	2232	(0.063)	13.70	(0.072)
Mix 02	2142	(265.68)	688	(54.41)	543	(4.56)	2212	(14.45)	13.85	(0.787)
Mix 03	2551	(259.80)	662	(29.22)	477	(31.52)	2203	(3.532)	13.11	(0.156)
Mix 04	1149	(244.79)	401	(47.77)	307	(11.86)	2129	(11.08)	18.01	(0.433)
Mix 05	2859	(194.05)	858	(26.49)	502	(41.46)	2280	(0.645)	11.09	(0.031)
Mix 06	2928	(152.39)	697	(33.05)	597	(30.92)	2229	(15.07)	12.85	(0.569)
Mix 07	1735	(230.94)	614	(74.77)	524	(29.98)	2167	(7.11)	15.44	(0.341)
Mix 08	2999	(234.07)	1015	(40.87)	865	(41.29)	2257	(12.67)	11.27	(0.536)
Mix 09	2953	(161.68)	924	(42.38)	798	(36.21)	2243	(8.16)	10.82	(0.296)
Mix 10	2957	(203.94)	918	(15.09)	783	(20.82)	2253	(7.04)	10.85	(0.341)
Mix 11	3055	(245.03)	941	(31.25)	788	(40.25)	2286	(9.28)	11.36	(0.325)
Mix 12	2953	(161.68)	909	(28.15)	773	(35.01)	2273	(8.14)	10.92	(0.301)
Mix 13	2576	(181.15)	910	(33.95)	790	(30.33)	2294	(1.81)	11.075	(0.065)
Mix 14	2988	(161.68)	928	(42.38)	793	(33.58)	2279	(9.28)	11.36	(0.325)
Mix 15	2955	(203.94)	934	(15.09)	778	(24.28)	2248	(7.04)	10.85	(0.341)
Mix 16	4313	(260.56)	997	(51.74)	837	(35.07)	2276	(3.79)	11.24	(0.148)
Mix 17	3306	(213.82)	817	(22.97)	736	(3.74)	2218	(13.55)	12.65	(0.708)
Mix 18	3354	(299.96)	985	(65.47)	861	(24.98)	2215	(13.05)	13.14	(0.475)
Mix 19	3750	(230.55)	705	(69.08)	601	(38.91)	2235	(8.16)	13.59	(0.128)
Mix 20	2192	(109)	503	(74.77)	343	(30.81)	2118	(8.12)	18.34	(0.348)

4.3.1 Analysis of mechanical responses

The performance of CBEM is influenced by the time and temperature of the curing process (Needham, 1996, Doyle et al., 2013, García et al., 2013). Doyle et al. (Doyle et al., 2013) found that it was necessary to vary both time and temperature of curing in order to represent the material achieved in the field. Logically, measurement of evaporated water will enable a better understanding of the performance of these mixtures. Therefore, periodically, specimen weights were recorded over 28 days. The results of average loss of water for all 15 individual mixes are shown in Figure 4.7, in which for example (10°C Mix 5, 3.5) refers to curing at 10°C with 5% BEC and 3.5% PWC.

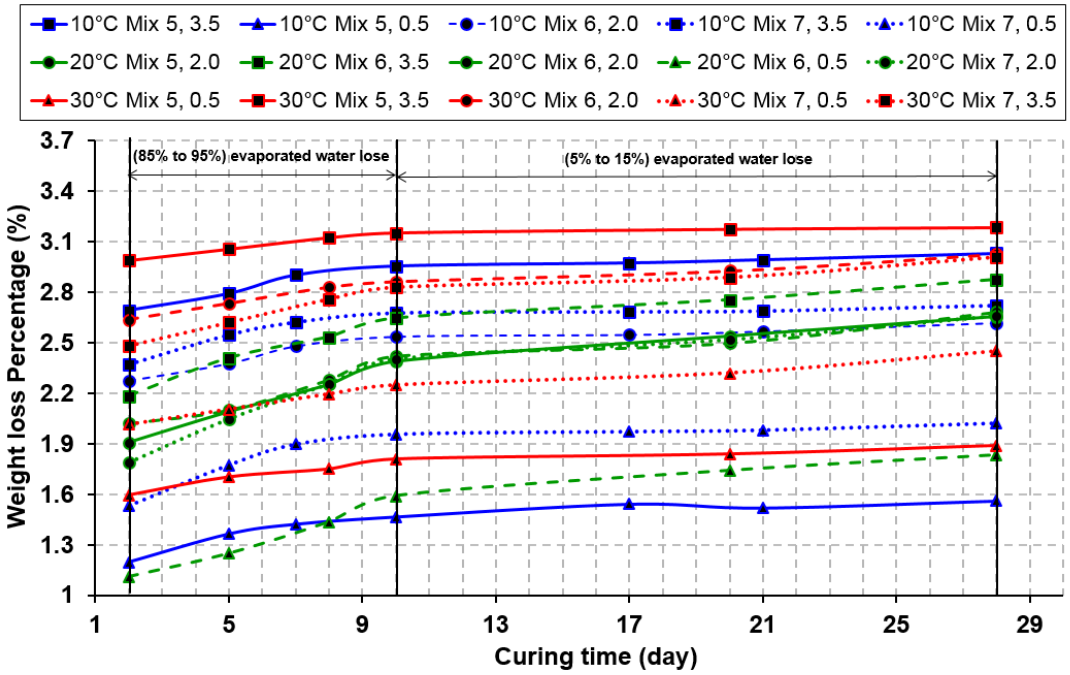


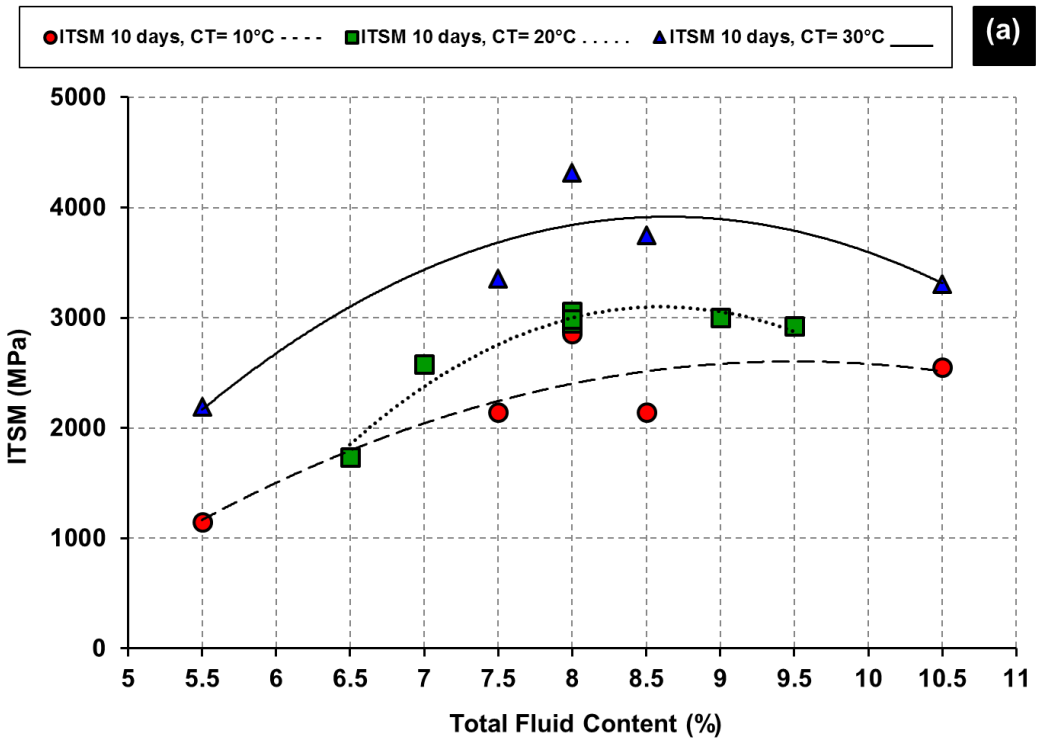
Figure 4.7 Weight loss over curing period

The percentage of water loss was calculated based on the weight of specimens after demoulding directly. It can be observed that around 85% to 95% of the total evaporation occurs during the first 10 days and 5% to 15% through the remainder of the period.

The evaluation of stiffness was performed at 10 days and 28 days. This is broadly consistent with the South African Bitumen Association (1999) recommendation to evaluate CBEMs at room temperature at 7 days and 28 days.

4.3.1.1 Indirect tensile stiffness modulus (ITSM)

This test has often been used as an indicative test for ranking CBEMs during mix design (Thanaya, 2003, Oke, 2010). Following a conventional mix design method (Asphalt Institute, 1989), the performance of CBEM was initially evaluated based on the relationship between TFC, which is the sum of BEC and PWC, and mechanical properties. The $ITSM_{10\ days}$ and $ITSM_{28\ days}$ are plotted against TFC in Figure 4.8 in order to give a better understanding of the performance of the CBEM.



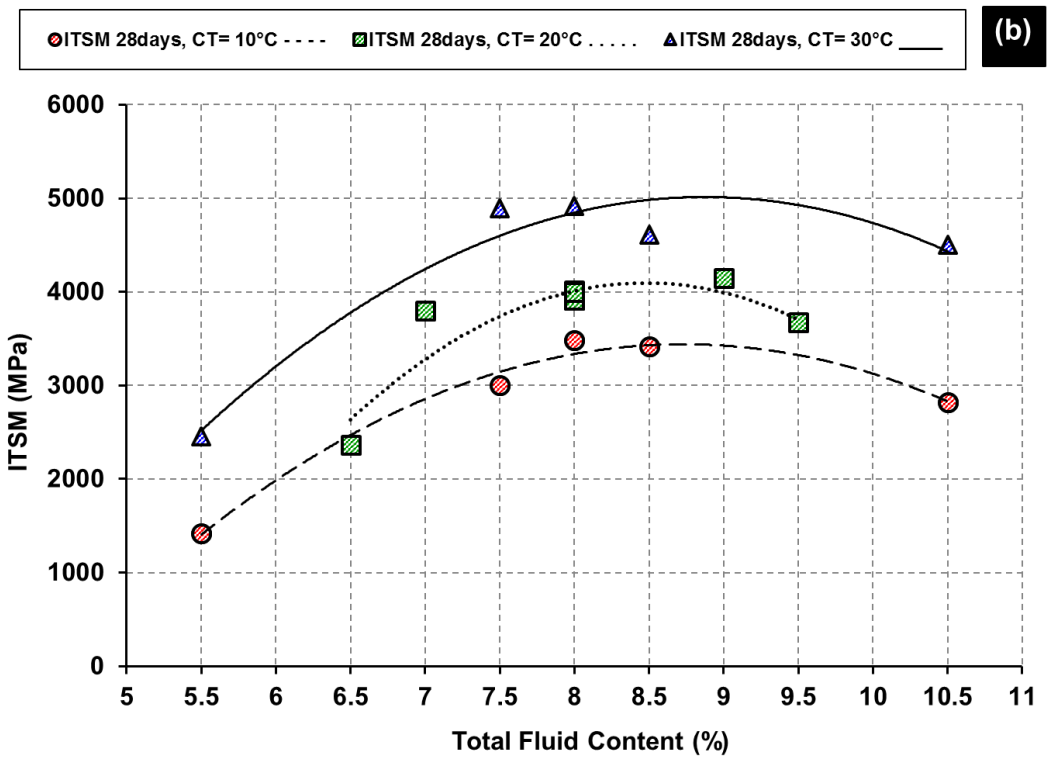


Figure 4.8 The relation between ITSM and total fluid content of CBEMs under different CT after (a) 10 days and (b) 28 days

As can be seen from Figure 4.8, the stiffness values show the same trend at 10 and 28 days. Peak ITSM values occurred at between 8.5% to 9.5% total fluid content at both 10 and 28 days. Therefore, it is reasonable to propose that evaluation at 10 days will probably give the designer appropriate information to optimize the mix design of CBEM, although, a wide range of curing times has been used by different researchers (South African Bitumen Association, 1999, Brayton et al., 2000, CEDR, 2014). Also, as expected, ITSM increases with CT at both 10 and 28 days. This is consistent with results obtained in previous studies (Thanaya, 2003, Sebaaly et al., 2004, Al-Busaltan et al., 2012) and can at least partly be attributed to rapid water loss at higher temperature, which yields higher stiffness values with time. The results in Figure 4.8 show that the lowest stiffness values were obtained from mixtures with the least TFC. This may be due to insufficient TFC in these mixes restricting the degree of compaction and increasing the air voids content in the mixture. It is worth noting the sensitivity of CBEMs' stiffness to the

variation of individual mix components. Consequently, to assess the interactive relationship between the mix design parameters and the properties of CBEMs, a RSM model has been used to generate a contour plot for $ITSM_{10\ days}$ shown in Figure 4.9.

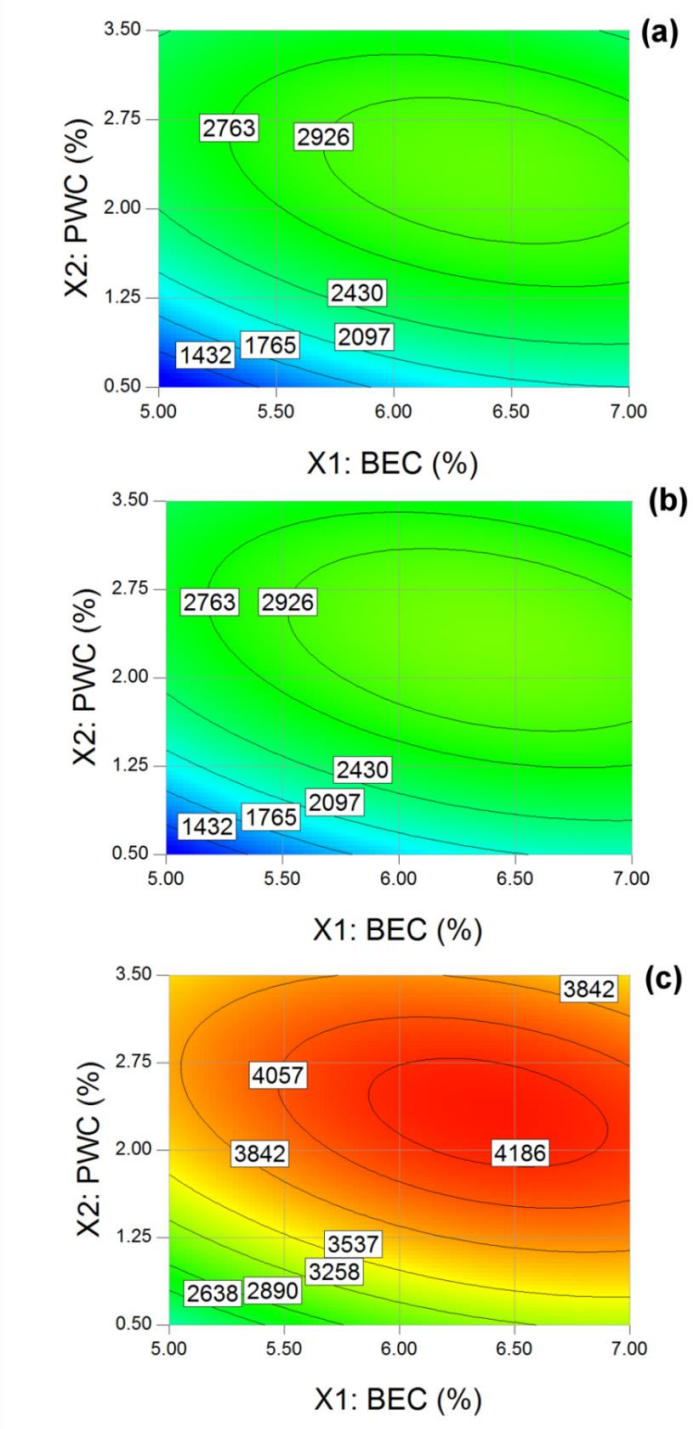


Figure 4.9 Contour plots of $ITSM_{10\ days}$ versus BEC and PWC; (a) CT =10°C, (b) CT =20°C and (c) CT =30°C

The results in Figure 4.9 show the effect of BEC and PWC versus $ITSM_{10\ days}$ at different CT. From these contour plots $ITSM_{10\ days}$ values tend to increase markedly with increasing PWC from 0.50% to 2.75% and with increasing BEC from 5.0% to 6.5%. However, $ITSM_{10\ days}$ markedly decreases when increasing PWC from 2.75% to 3.5% and increases slightly when increasing BEC from 6.5% to 7.0%. Moreover, the results in Figure 4.9 show that in reality the individual effects of BEC and PWC are important, rather than simply TFC. The response surface presented in Figure 4.9 shows elliptical contours which is the pattern obtained when there are perfect interactions between independent variables (Muralidhar et al., 2001, Wang et al., 2011). Accordingly, there is a region of optimum performance at around 6.0 to 6.5% BEC and 2.0 to 2.5% PWC, whereas ITSM is lower with other BEC/ PWC proportions, even at the same TFC. The effect of increasing CT is to increase ITSM (by approximately 1.25-1.60 times as the CT increases from 10°C to 30°C) but optimum BEC and PWC are not significantly affected.

4.3.1.2 Indirect tensile strength (ITS)

The ITS test was conducted on two sets of specimens: the first set (dry) was tested at 28 days immediately after curing; the second set (wet) was cured and then subjected to a vacuum (with 6.7 kPa pressure) for 30±5 minutes and immersed in a water bath for 3 days at 40°C before being tested as recommended by European Committee for Standardization (2005b). The reason for performing the ITS test on conditioned specimens is to take into consideration water damage as a criterion in mix design as recommended by several researchers (Thanaya, 2003, Al-Busaltan et al., 2012). A similar picture to that for ITSM is presented in Figure 4.10; the results show the relation between TFC and ITS for dry and wet specimens.

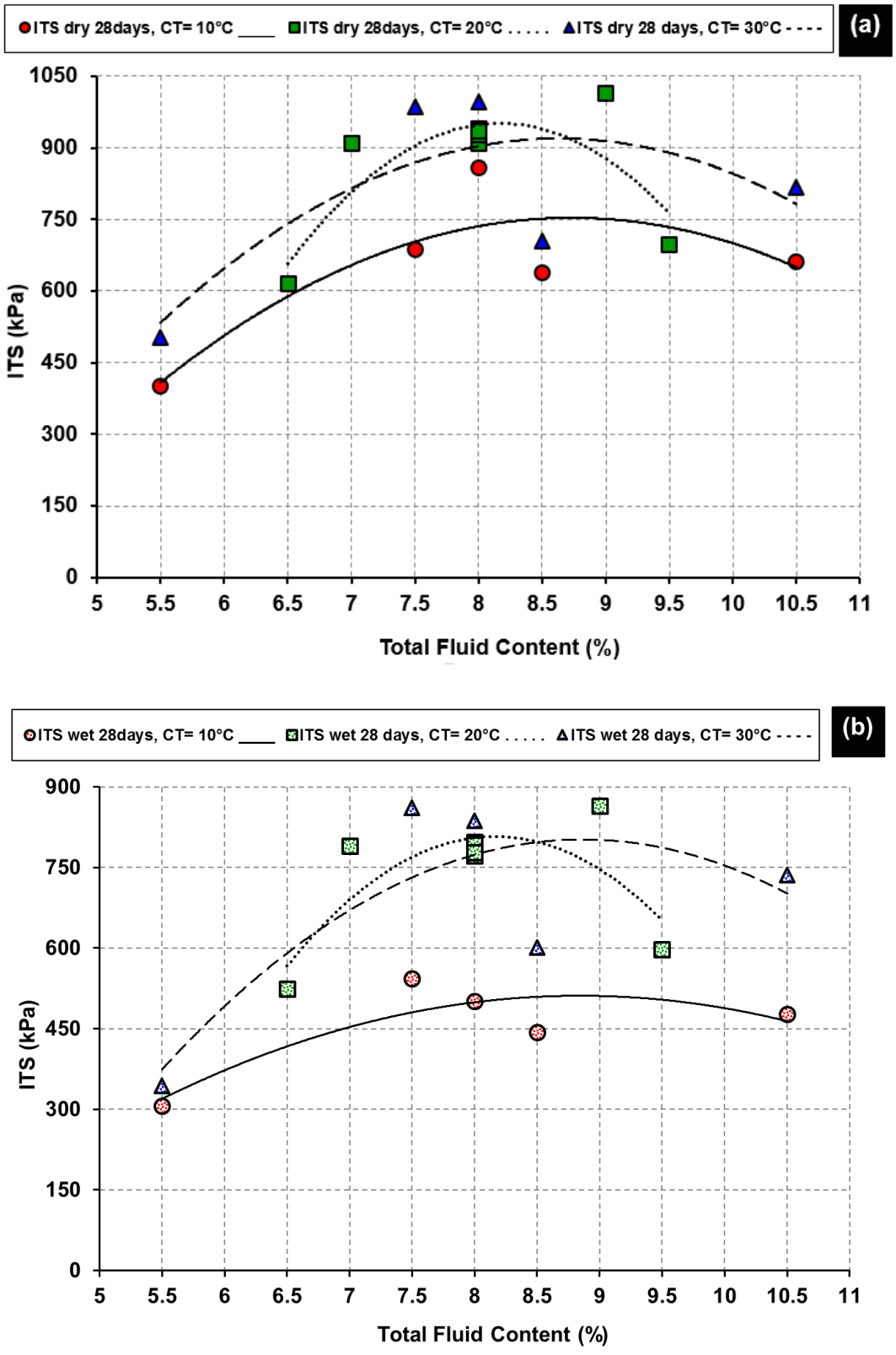


Figure 4.10 The relation between ITS and total fluid content of CBEMs under different CT (a) dry condition and (b) wet condition

The strength values for both sets display similar behaviour to that seen for ITSM. The peak ITS values for all mixtures were consistently found to lie between 8% and 9% of TFC which is a similar range to that for ITSM. The effect of increasing CT is generally to increase ITS, although the difference in peak ITS between CTs of 20°C and 30°C is slight.

Based on the developed model, Figure 4.11 and Figure 4.12 present the interaction effect of BEC and PWC on ITS values under different CT for dry and wet specimens, respectively. From Figure 4.11 and Figure 4.12, at a given CT, the results again indicate that ITS values significantly increase by increasing PWC from 0.50% to 2.375% and always increase with BEC while they markedly decrease by increasing the PWC from 2.375 to 3.5%. Overall, increasing ITS was observed by increasing BEC and CT. The response surface presented in Figure 4.11 and Figure 4.12 shows distorted parabolic contours which are obtained in cases with fewer interactions between independent variables (Muralidhar et al., 2001, Wang et al., 2011). This means that the optimum region is less clear than was the case for ITSM. Optimum PWC is between 1.5 to 2.5%, but optimum BEC may be around 6.5 to 7.0% or higher. The effect of CT on these optima is again slight and both dry and wet data sets present a similar picture. A more general conclusion from both ITSM and ITS, is that the interaction of BEC and PWC (and to a lesser extent CT) is complex and that CBEMs must be carefully and accurately designed. This conclusion is consistent with the findings of Gómez-Meijide and Pérez (2014b).

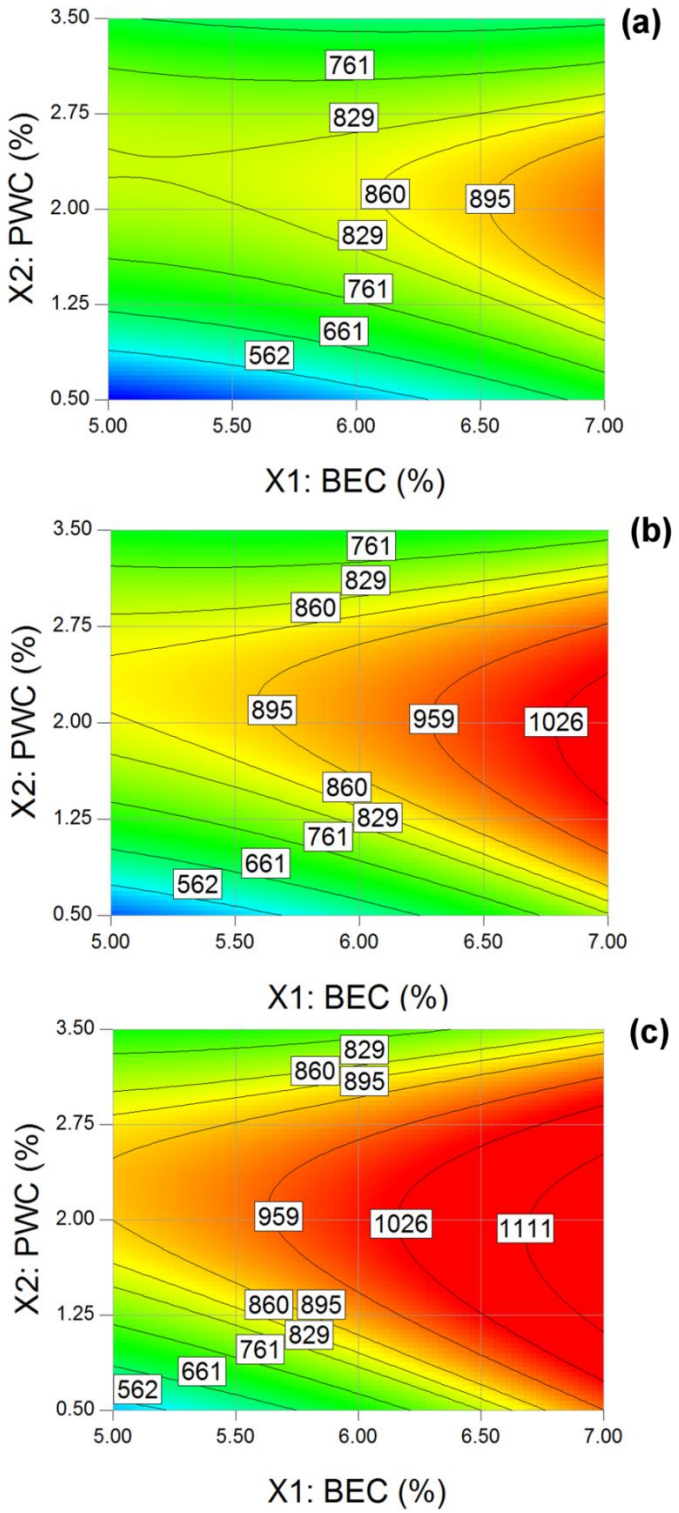


Figure 4.11 Contour plots of ITS dry$_{28\ days}$ versus BEC and PWC; (a) CT =10°C, (b) CT =20°C and (c) CT =30°C

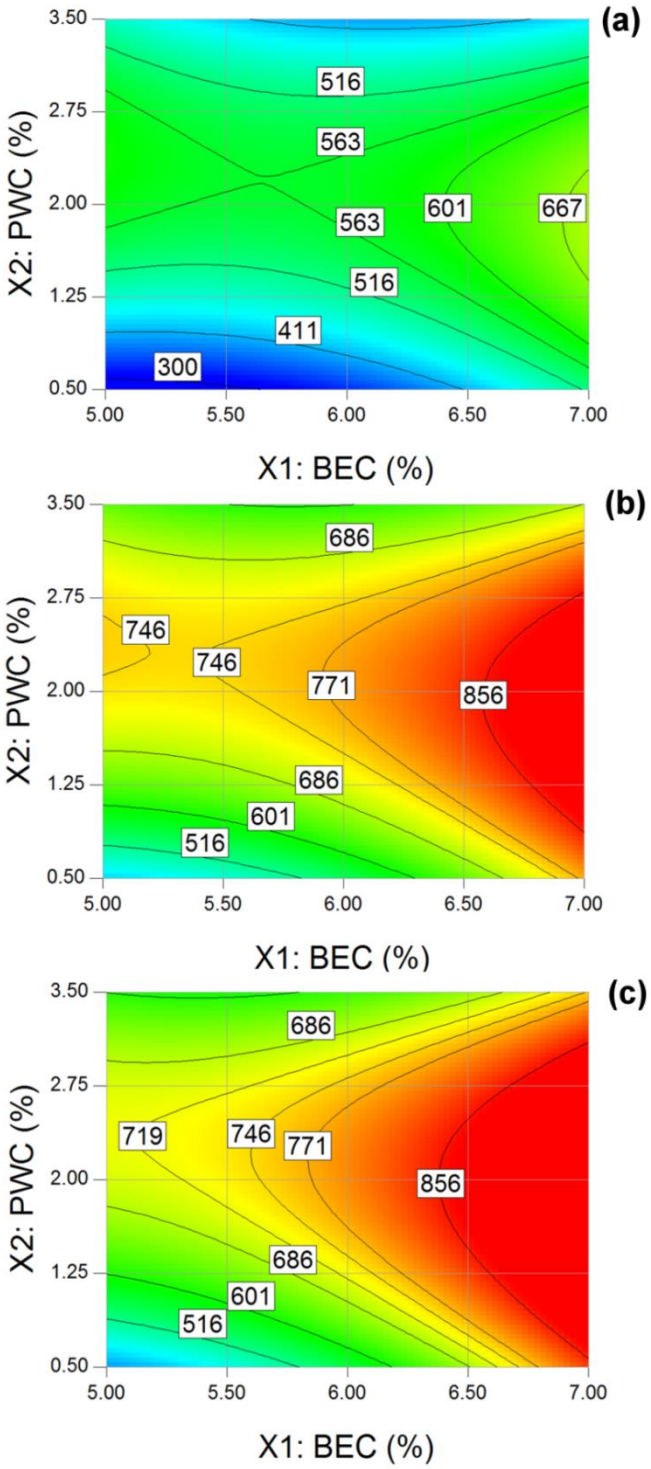


Figure 4.12 Contour plots of ITS wet$_{28\ days}$ versus BEC and PWC; (a) CT =10°C, (b) CT =20°C and (c) CT =30°C

4.3.2 Analysis of volumetric responses

A volumetric analysis was carried out to determine the air void content and dry density present in each mix.

4.3.2.1 Air voids

The results are presented in Table 4.4. The air voids ranged from 10.82% to 18.34%, higher than 9 to 14% suggested by others (Asphalt Institute, 1989, Brayton et al., 2000, Ameri et al., 2012). Figure 4.13 shows the relation between the TFC and resulting air voids content. The highest values of air voids were observed at the lowest TFC, whereas the lowest air voids values were found at 8% to 9% of TFC. The results demonstrate the role of fluid inside the CBEM to determine the degree of compactibility of mixes.

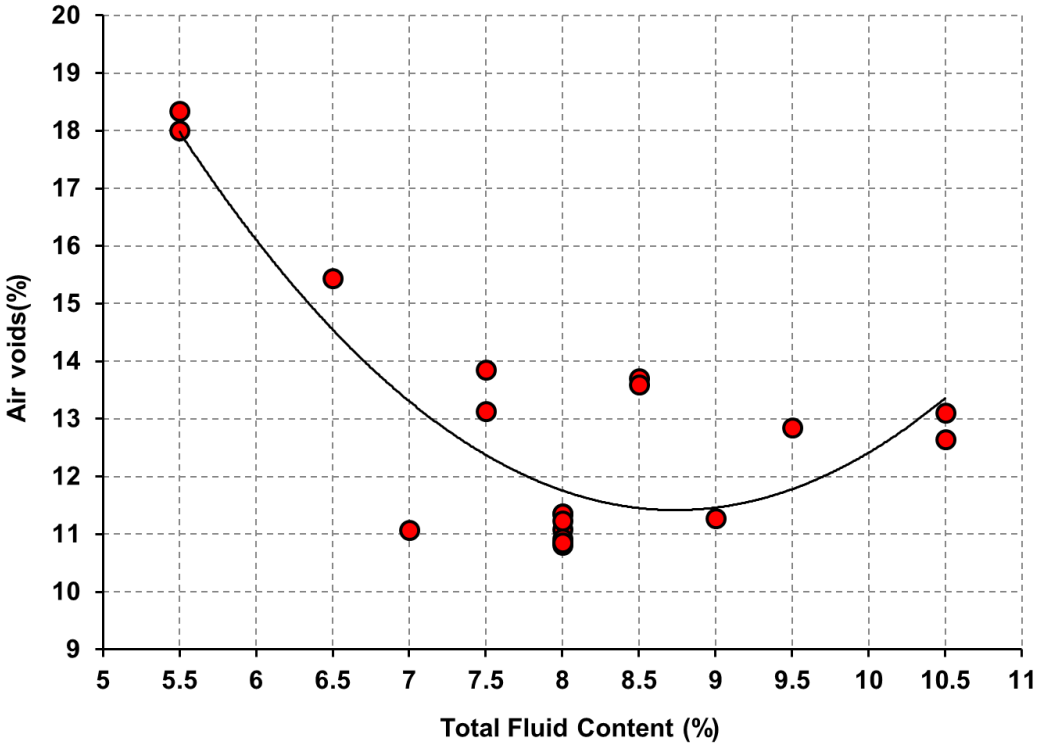


Figure 4.13 The relation between air voids and total fluid content of CBEMs

Based on RSM modelling, Figure 4.14 presents a contour plot for the air voids measurement in which it is clear that the individual effects of BEC and PWC are both important. Air voids values decreased when increasing the BEC from 5.0% to 7.0% and markedly decreased when increasing the PWC from 0.50% to 2.0% then significantly increased when increasing PWC from 2.0% to 3.5%. As for ITS there is a clear optimum region for PWC, about 1.5 to 2.5%, but optimum BEC would appear to be at 7% or more and is therefore less clear on the plot. However, it is evident that PWC plays a key role in determining air voids in CBEM.

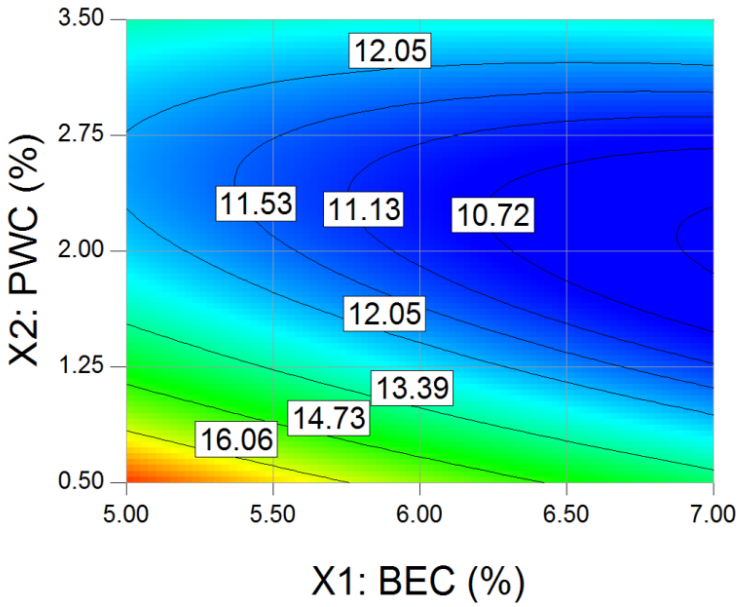


Figure 4.14 Contour plot of air voids versus BEC and PWC

4.3.2.2 Dry density

The dry density results are shown in Table 4.4. Figure 4.15 presents the relation between dry density and total fluid content. Dry density values peak at around 8% to 9% of TFC. Based on the RSM model, Figure 4.16 presents a contour plot for dry density in terms of BEC and PWC.

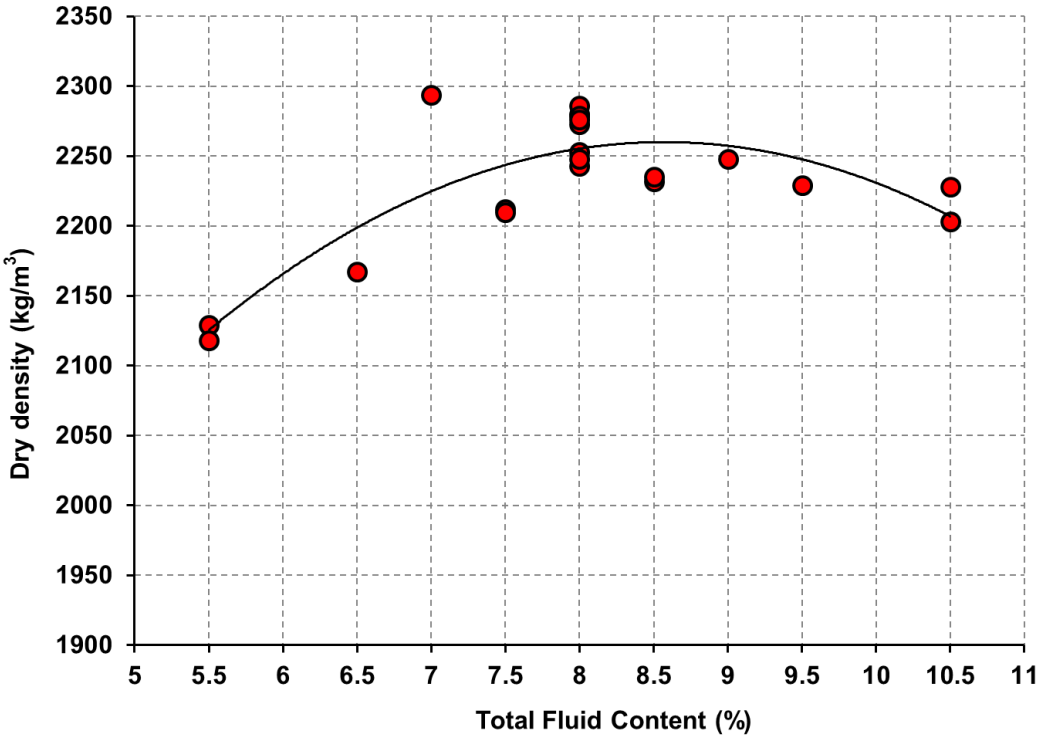


Figure 4.15 The relation between dry density and total fluid content of CBEMs

Figure 4.16 indicates that the dry density of CBEMs increased dramatically with an increase of PWC from 0.50% to 2.375% then decreased with an increase of PWC from 2.375% to 3.5%. The dry density slightly increased when BEC increased from 5.0% to 7.0%. The optimum PWC is in a narrow band either side of 2%, while optimum BEC is less definite but appears to be close to 7%. Low dry density corresponds to high air voids and poor mechanical performance, while the optimum for each measure approximately coincides.

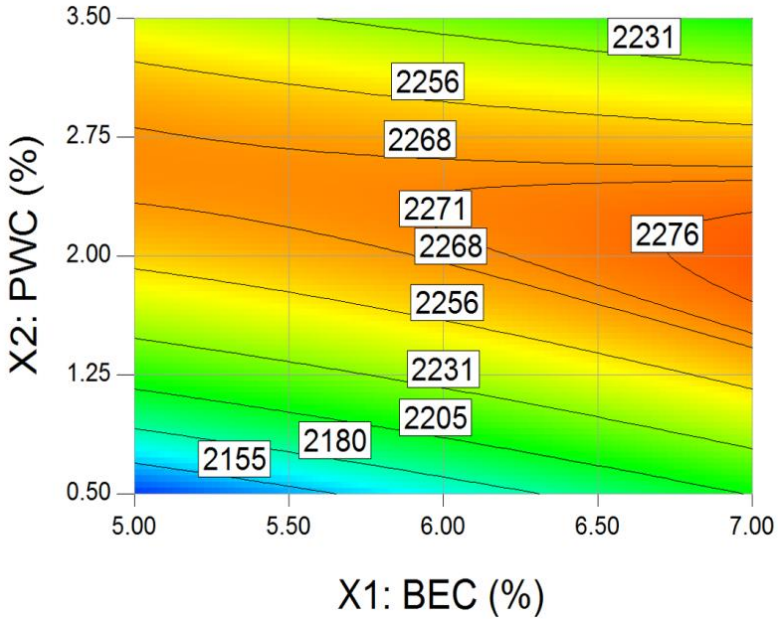


Figure 4.16 Contour plot of dry density versus BEC and PWC

4.3.3 Statistical analysis of responses

A statistical analysis was conducted to evaluate mix performance in terms of the above-mentioned tests. A quadratic model was developed for prediction purposes. The quality of the developed model was evaluated based on the coefficient of determination, R^2 and also the standard deviation values. Determination coefficients were obtained as 0.96, 0.98, 0.95, 0.95 and 0.90 for $ITSM_{10\ days}$, ITS $dry_{28\ days}$, ITS $wet_{28\ days}$, air voids and dry density, respectively. For a good model fit, the coefficient of determination should be a minimum of 0.80. A high R^2 value close to 1.00 demonstrates a desirable and reasonable agreement between the calculated and observed results (Noordin et al., 2004). An additional tool used to evaluate the developed model was ‘‘adequate precision’’ (AP). AP compares the range of the predicted values at the design points to the average prediction error. In this particular case, the AP values of the models were 29.3, 35.3, 21.1, 28.5 and 17.6 for, respectively. They are greater than 4 and therefore confirm that the model can be used to navigate the space defined by the CCD (Aldahdooh et al., 2013).

The results of ANOVA analysis presented in Table 4.5. show that the models' F-values of 44.76, 94.77, 32.64, 77.77 and 36.82 and P-values are low, which mean that the models are statistically significant for $ITSM_{10\ days}$, ITS $dry_{28\ days}$, ITS $wet_{28\ days}$, air voids and dry density, respectively. Only a 0.01% chance exists that a model F-value of this magnitude can occur because of noise.

Table 4.5 ANOVA for analysis of variance and adequacy of the quadratic model for responses

SoD	SoS	DoF	MS	F-value	P-value>F	Comment
$ITSM_{10\ days}$						
Model	8.88E+06	7	1.27E+06	44.76	< 0.0001	SD= 168.34 Mean= 2792.8 R^2 = 0.96 Adj. R^2 = 0.94 AP =29.2
X_1	6.47E+05	1	6.47E+05	22.84	0.0004	
X_2	1.68E+06	1	1.68E+06	59.44	< 0.0001	
X_3	3.69E+06	1	3.69E+06	130.15	< 0.0001	
X_1^2	1.78E+05	1	1.78E+05	6.27	0.0277	
X_2^2	1.39E+06	1	1.39E+06	48.94	< 0.0001	
X_3^2	8.15E+05	1	8.15E+05	28.76	0.0002	
X_1 X_2	5.99E+05	1	5.99E+05	21.14	0.0006	
Residual	3.40E+05	12	28338.13			
Lack of Fit	3.318E+05	7	47402.40	28.76	0.0010	
Pure Error	8240.83	5	1648.17			
ITS $dry_{28\ days}$						
Model	5.81E+05	8	72628.92	94.77	< 0.0001	SD= 27.68 Mean= 802.25 R^2 = 0.98 Adj. R^2 = 0.97 AP =35.3
X_1	1.02E+05	1	1.02E+05	132.84	< 0.0001	
X_2	10824.1	1	10824.1	14.12	0.0032	
X_3	57608.1	1	57608.1	75.17	< 0.0001	
X_1^2	2497.61	1	2497.61	3.26	0.0985	
X_2^2	2.49E+05	1	2.49E+05	325.16	< 0.0001	
X_1 X_2	50244.5	1	50244.5	65.56	< 0.0001	
X_1 X_3	10082	1	10082	13.16	0.004	
X_2 X_3	3960.5	1	3960.5	5.17	0.0441	
Residual	8430.39	11	766.4			
Lack of Fit	7781.05	6	1296.84	9.99	0.0116	
Pure Error	649.33	5	129.87			
ITS $wet_{28\ days}$						
Model	5.767E+005	8	72081.68	32.64	< 0.0001	SD= 46.99 Mean= 656.95
X_1	99496.64	1	99496.64	45.06	< 0.0001	

SoD	SoS	DoF	MS	F-value	P-value>F	Comment
X_2	7623.12	1	7623.12	3.45	0.0901	R^2 = 0.95 Adj. R^2 = 0.93 AP =21.1
X_3	1.223E+005	1	1.223E+005	55.38	< 0.0001	
X_1^2	10170.78	1	10170.78	4.61	0.0550	
X_2^2	1.163E+005	1	1.16E+005	52.66	< 0.0001	
X_3^2	25776.15	1	25776.15	11.67	0.0058	
X_1 X_2	43087.27	1	43087.27	19.51	0.0010	
X_1 X_3	18294.98	1	18294.98	8.29	0.0150	
Residual	24289.82	11	2208.17			
Lack of Fit	23837.05	6	3972.84	43.87	0.0004	
Pure Error	452.77	5	90.55			
Air voids						
Model	92.97	4	23.24	77.77	< 0.0001	SD= 0.55 Mean= 12.78 R^2 = 0.95 Adj. R^2 = 0.94 AP = 28.5
X_1	11.44	1	11.44	38.28	< 0.0001	
X_2	16.59	1	16.59	55.51	< 0.0001	
X_2^2	57.27	1	57.27	191.66	< 0.0001	
X_1 X_2	7.66	1	7.66	25.65	< 0.0001	
Residual	4.48	15	0.30			
Lack of Fit	4.14	10	0.41	6.12	0.0295	
Pure Error	0.31	5	0.062			
Dry density						
Model	41661.05	4	10415.26	36.82	< 0.0001	SD= 16.82 Mean= 2232.35 R^2 = 0.90 Adj. R^2 = 0.88 AP = 17.6
X_1	940.90	1	940.90	3.33	0.0882	
X_2	7617.60	1	7617.60	26.93	0.0001	
X_2^2	26718.05	1	26718.05	94.44	< 0.0001	
X_1 X_2	6384.50	1	6384.50	22.57	0.0003	
Residual	4243.50	15	282.90			
Lack of Fit	2636.17	10	263.62	0.82	0.6321	
Pure Error	1607.33	5	321.47			

SoD: source of data; SoS: sum of squares; DoF: degree of freedom; MS: mean square.

X1 = BEC, X2 = PWC and X3 = CT.

ANOVA results confirm that all the main parameters in the mix design of CBEMs (BEC (X_1), PWC (X_2) and CT (X_3)) have significant effects on mechanical response according to the t-test at a 5% significance level ($P < 0.05$). Both BEC and PWC have a significant effect on volumetric response, as shown in Table 4.5. Insignificant terms, which have limited influence ($P > 0.1$), were excluded from the

study to improve the models. The lack of fit (LOF) F-test was also used to evaluate the adequacy of the model. LOF depicts the variation of the data around the fitted model. For this investigation, the small p values for LOF ($p < 0.05$), as presented in Table 4.5, show that except the dry density, which was insignificant, other responses including $ITSM_{10\ days}$, $ITS\ dry_{28\ days}$, $ITS\ wet_{28\ days}$ and air voids were significant. It is worth noting that while LOF values were significant, reasonable agreement between the predicted and adjusted R^2 were found for all responses such that it can be concluded that the suggested models for all responses can be used to navigate satisfactorily into design space to find optimum mix design parameters. Similar observations were reported in (Younis et al., 2014, Hamzah et al., 2015, Moghaddam et al., 2015).

The final regression models, in terms of the significant influencing factors, are expressed by second-order polynomial equations as shown in Equation 4.9 to Equation 4.13:

$$\mathrm{ITSM}_{10\,\mathrm{days}} = -10708.36 + 3668.86X_1 + 2630.56X_2 - 157.01X_3 - 254.13X_1^2 - 315.61X_2^2 + 5.44X_3^2 - 182.41X_1X_2 \quad \text{Equation 4.9}$$

$$\mathrm{ITS\ dry}_{28\,\mathrm{day}} = 369.05 - 199.68X_1 + 864.71X_2 - 10.74X_3 + 27.93X_1^2 - 124.02X_2^2 - 52.83X_1X_2 + 3.55X_1X_3 - 1.48X_2X_3 \quad \text{Equation 4.10}$$

$$\mathrm{ITS\ wet}_{28\,\mathrm{day}} = 1344.55 - 627.82X_1 + 677.51X_2 + 21.09X_3 + 60.81X_1^2 + 60.81X_2^2 - 0.96X_3^2 - 48.92X_1X_2 + 4.78X_1X_3 \quad \text{Equation 4.11}$$

$$\text{Air voids} = 33.06 - 2.37X_1 - 10.79X_2 + 1.50X_2^2 + 0.65X_1X_2 \quad \text{Equation 4.12}$$

$$\text{Dry Density} = 2268.90 + 9.70X_1 + 27.60\,X_2 - 73.10X_2^2 - 28.25X_1X_2 \quad \text{Equation 4.13}$$

The significant interactions between variables are presented by 3D-surface plots, as shown in Figure 4.17. These plots give more information on the interaction between mix design parameters affecting the mechanical and volumetric responses. Where the interactive term in Table 4.5 was not statistically significant, their surface plots were not represented in Figure 4.17.

The curvature of the surface plot in Figure 4.17 (a) indicates that both BEC and PWC have interaction effect on $ITSM_{10\ days}$. Also, Figure 4.17 (b-f) depicts the effects of mix design parameters, BEC, PWC and CT, on ITS values in both conditions (dry and wet). Based on the curvature of the surface plots, it is clear that BEC and PWC have the more powerful effect. However, the other interactions of parameters BEC and CT and PWC and CT are clearly observed on the ITS results, which means that ITS is influenced more strongly than ITSM in terms of mix design parameters. This is further confirmed by the result presented in section 4.3.1.2. Figure 4.17 (g and h) presents the interaction effects of BEC and PWC on the volumetric properties of CBEMs. The curvature of the surface plot in Figure 4.17 (g and h) shows that PWC tended to influence the volumetric responses more markedly than BEC.

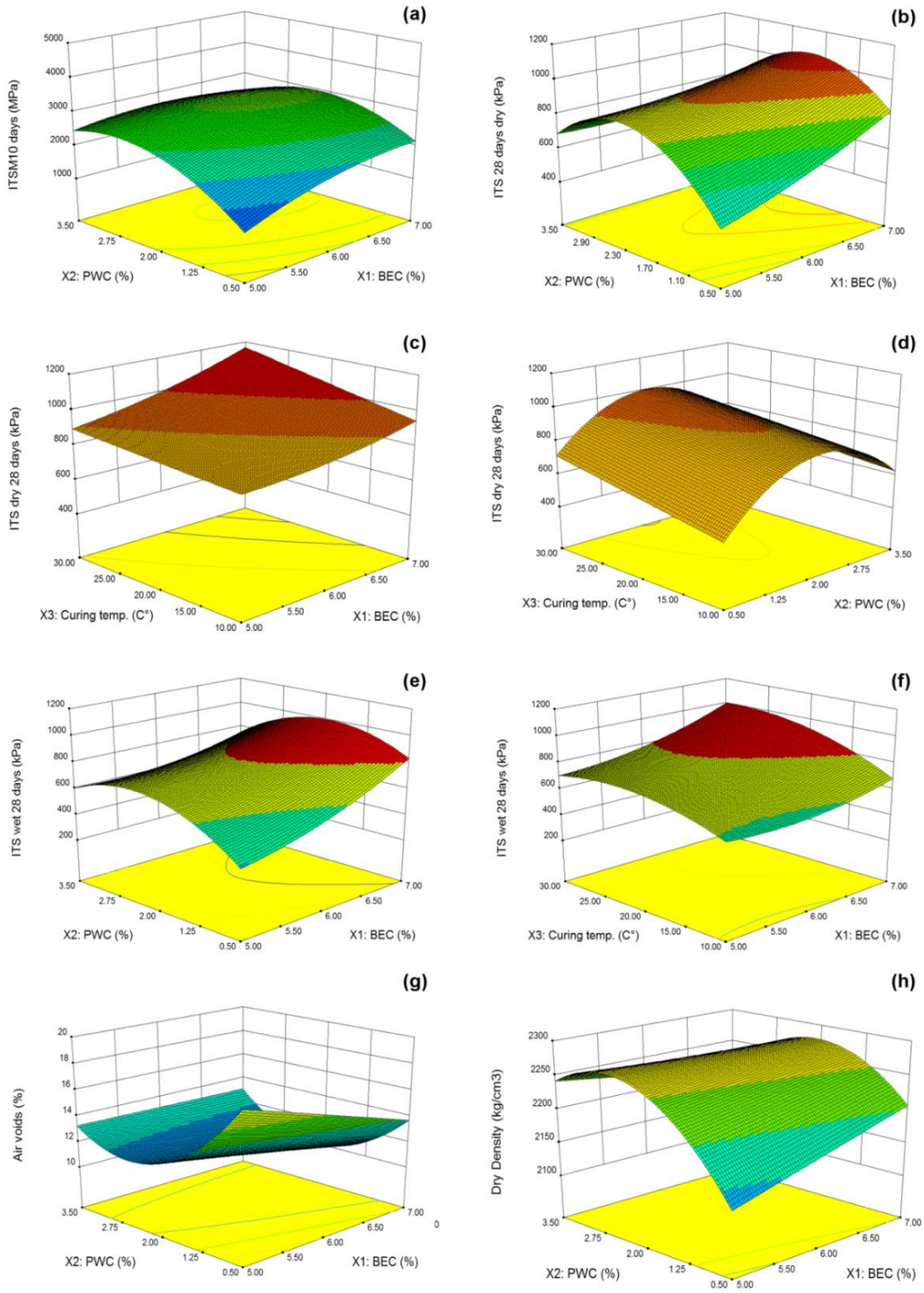


Figure 4.17 3D-surface plots of $ITSM_{10\ days}$, ITS $dry_{28\ days}$, ITS $wet_{28\ days}$, air voids and dry density

(a) $ITSM_{10\ days}$ versus BEC and PWC (b) ITS $dry_{28\ days}$ versus BEC and PWC (c) ITS $dry_{28\ days}$ versus BEC and CT (d) ITS $dry_{28\ days}$ versus PWC and CT (e) ITS $wet_{28\ days}$ versus BEC and PWC (f) ITS $wet_{28\ days}$ versus BEC and CT (g) Air voids versus BEC and PWC (h) Dry density versus BEC and PWC

4.3.4 Optimization of the mix design components

An optimization process was carried out to determine the optimum value of BEC, and PWC under different CTs, using the Design Expert 9.0.6.2 software (Stat-Ease Inc., Minneapolis, USA). According to the software optimization step, the desired goal for each mix design parameter (BEC and PWC) was chosen within the range shown in Table 4.2. The desirable mechanical responses ($ITSM_{10\ days}$, $ITS\ dry_{28\ days}$ and $ITS\ wet_{28\ days}$) were defined as being a maximum to achieve the highest performance, the desirable air voids was defined as a minimum and desirable dry density was defined as a maximum in order to achieve a dense mixture with the lowest value of air voids. The derived second-order polynomial models were used to interpolate the mix design parameters within the range and based on the desired responses. The results are presented in Table 4.6.

Table 4.6 The optimum BEC and PWC at different CT with their responses

Items	RSM model prediction			Laboratory experiment
CT (°C)	T= 10°C	T= 20°C	T= 30°C	T= 20°C
BEC (%)	7.00	6.75	6.58	6.75
PWC (%)	1.96	2.12	2.16	2.12
$ITSM_{10\ days}$ (MPa)	2936	3063	4235	3049
ITS dry $_{28\ days}$ (kPa)	946	1015	1086	1000
ITS wet $_{28\ days}$ (kPa)	684	883	894	889
Air voids (%)	10.02	10.26	10.42	10.34
Dry density (kg/m^3)	2279	2276	2275	2278

The DF value was found to be 0.887 for these optimum conditions. The relatively high DF value shows that the RSM model may represent the experimental model and desired conditions in a satisfactory manner. Therefore, an additional laboratory experiment was carried out to validate the optimum mix design proportions obtained by the RSM model. The experimental work was performed at CT equal to

20°C. The results in Table 4.6 demonstrate that the experimental results are close to the results predicted by the developed model at CT of 20°C.

The results in Table 4.6 show a limited variation of optimum mix design proportions (BEC and PWC) over the range of CT from 10°C to 30°C. The maximum variation of BEC is 0.42% and 0.20% for PWC. The TFC (BEC + PWC) for the optimized mixes lies within the range from 8.74% to 8.96%. Therefore, it can be concluded that the optimum proportions (BEC and PWC) tend to be only slightly influenced by CT. Overall, the results are comparable with those published by other authors on the subject of mix design of CBEM (Thanaya, 2003, Oke, 2010, Gómez-Meijide and Pérez, 2014a).

In the end, the decision for the optimum value was subsequently based on the optimization result. This decision implies that the BEC and PWC adopted and which were subsequently used in this work were 6.75% and 2.12% at CT 20°C, respectively.

4.4 Summary

The primary objective of this work was to optimize the CBEM with the main focus being on the use of a statistical approach, as an alternative tool of optimization. To attain this objective, the optimization of CBEM has been investigated, to determine optimum proportions to gain suitable levels of both mechanical and volumetric properties. A central composite design (CCD) with response surface methodology (RSM) was applied to optimize the mix design parameters, namely bitumen emulsion content (BEC), pre-wetting water content (PWC) and curing temperature (CT). One of the objectives during mix design optimisation is to investigate the interaction effect between these parameters on the mechanical and volumetric properties of CBEMs. The indirect tensile stiffness modulus (ITSM) and indirect

tensile strength (ITS dry and ITS wet) tests were performed to obtain the mechanical response while air voids and dry density were measured to obtain volumetric responses.

Overall, the current research introduces a novel performance-based mix design approach for CBEM involving mechanical and volumetric properties. Based on the laboratory experiments and analyses, the following conclusions can be drawn:

- An alternative mix design approach for CBEMs was investigated using RSM. This approach involves the mechanical and volumetric properties. It was statistically demonstrated that the alternative approach output results were consistent with the laboratory tests.
- The RSM approach offers a more comprehensive view of the effect of the variation of each mix design parameter on the mechanical and volumetric responses of CBEMs than would otherwise be the case. It has the advantage that all parameters are investigated at one time.
- After the responses have been characterized by an equation (model), several analyses are possible. For instance, a user could determine the mixture proportions that would yield one or more desired properties.
- The individual effects of BEC and PWC are important, rather than simply the total fluid content (TFC) which is used in conventional mix design methods. The results show a lower strength/ stiffness of CBEM at the same TFC and with different BEC/ PWC proportions.
- The results indicate that the interaction of BEC, PWC and CT influences the mechanical properties of CBEM. However, the PWC tended to influence the volumetric properties more significantly than BEC.
- The evaluation of stiffness modulus of CBEMs after 10 days is likely to give the designer appropriate information to optimize the mix design of CBEMs in a relatively short time.

- Based on the optimization by RSM, it can be concluded that the optimum mix design proportions (BEC and PWC) tend to be only slightly influenced by CT. The results show only limited variation in optimum mix design proportions (BEC and PWC) over a range of CT from 10°C to 30°C. The variation range for optimum BEC was 0.42% and 0.20% for PWC.
- The optimum BEC and PWC were designed as 6.75% and 2.12% at a CT 20°C, respectively.

Chapter 5

Performance characterization of CBEMs (Mechanical, Durability and Microstructure)

5.1 Introduction

This chapter discusses and analyses the performance characterization of CBEMs from mechanical, durability and microstructure perspectives. The investigation includes results of the properties of CBEMs produced using different filler treatments. In the past, various attempts have been made to investigate and to enhance the performance of CBEMs using a hydraulic binder such as ordinary Portland cement (OPC) or hydrated lime (HL) (Needham, 1996, Thanaya, 2003, Oruc et al., 2007, Niazi and Jalili, 2009). The findings have shown the promising performance potential of CBEM with notable environmental advantages. However, there are still some countries, such as the UK, where the current level of use leaves significant opportunity for development. Research effort is still needed to characterise these materials' properties to achieve a proper understanding of their behaviour, which would improve confidence and increase usage level. Thus, the first treatment involved in this chapter is the use of cement, as a traditional treatment. The addition of cement is made as different levels of replacement of conventional limestone filler (LF) using OPC. Although previous studies have highlighted the benefits of using OPC and HL, it is nevertheless desirable to develop

more sustainable CBEMs using supplementary cementitious materials (SCMs) such as ground granulated blast-furnace slag (GGBS), fly ash (FA) and silica fume (SF) in combination with OPC. The purpose is to reduce production and environmental costs inherent in the manufacturing process of both cement and lime. Therefore, this study has adopted the incorporation of a low cement content (1%) together with relatively sustainable SCMs. In fact, the addition of 1% cement is common practice for CMA (Wirtgen, 2005), and the trend to keep the cement content low in CBEM has been gaining increasing attention. For instance, Miljković and Radenberg (2016) suggest 1.5% OPC could be an acceptably low cement content in CBEM. The methodology adopted here is the replacement of conventional LF with binary blended fillers (BBFs) and ternary blended fillers (TBFs). The BBFs contain a combination of FA or GGBS with OPC, while the TBFs are a combination of BBFs with SF. These fillers are used for many reasons. The abundance and availability of FA, GGBS and SF worldwide create opportunity to utilize these SCMs, which are some of the most used supplementary cementitious material alternatives. Additional reference hot mix asphalt (HMA) has been tested for comparison purposes as recommended by European Committee for Standardization (2006).

The chapter starts by presenting the mixture designation of treated CBEMs using different filler treatments. This is followed by summarizing the test program used in this study. A full description of the tests configurations used is detailed, then followed by specimen preparation, results and discussion for each performance indicator.

5.2 Mixture designation of treated CBEMs

In this study, incorporation of active filler treatments, i.e. cement, BBFs and TBFs, was achieved through partial replacement of the conventional LF in an untreated reference mix (LF-CBEM). The full list of mixture tested is presented in Table 5.1.

It was assumed that the presence of active filler does not affect the optimum binder or water content of CBEM (Oruc et al., 2007, Al-Busaltan et al., 2012, Al-Hdabi et al., 2013a, García et al., 2013). Thus, the same mixture proportions as LF-CBEM were used to prepare the other CBEMs. Based on the previous chapter, the optimum bitumen emulsion content was 6.75% and the optimum pre-wetting water content was 2.12% of the total mass of dry aggregate for the reference mix (LF-CBEM) cured at 20°C.

Table 5.1 Mixture designations based on filler treatments

Treatment type	Mixture type	Filler content as percentage of total aggregate weight			
		LF	OPC	FA/GGBS	SF
Reference mixes	HMA 40/60	5%	-	-	-
	LF-CBEM	5%	-	-	-
Cement-treated mixes	1C-CBEM	4%	1%	-	-
	2C-CBEM	3%	2%	-	-
	3C-CBEM	2%	3%	-	-
	4C-CBEM	1%	4%	-	-
	5C-CBEM	-	5%	-	-
BBF-treated mixes	C-G-CBEM	-	1%	4%	-
	C-F-CBEM	-	1%	4%	-
TBF-treated mixes	C-G-1S-CBEM	-	1%	4%	1%
	C-G-2S-CBEM	-	1%	4%	2%
	C-F-1S-CBEM	-	1%	4%	1%
	C-F-2S-CBEM	-	1%	4%	2%

Cement treatment was made by replacing LF with 1%, 2%, 3%, 4% and 5% of OPC. BBF treatment was prepared using full replacement of LF with a combination of FA or GGBS with OPC. Meanwhile, TBF treatment used a combination of BBF with the addition of SF as recommended in the literature (Al-Busaltan et al., 2012, Al-Hdabi et al., 2013a). For instance, 3C-CBEM, is a CBEM mix with 3% of OPC and 2% of LF by mass of dry aggregate; C-F-CBEM, is a CBEM mix with 1% of OPC and 4% of FA.

5.3 Experimental program

The experimental programme mainly involved assessment of CBEMs in two areas, namely: mechanical properties and durability. It was also extended to cover the microstructure of CBEM. Table 5.2 summarizes the experimental program for CBEM performance evaluation.

Table 5.2 The experimental program tests

Test	Standards	Curing process
Mechanical properties		
Indirect tensile stiffness modulus (ITSM)	BS EN 12697-26	Curing at 20°C for 365 days.
Repeated axial load test (RLAT)	BS EN 12697-25	Curing at 20°C for 28 days + Curing at 40°C for 7 days.
Indirect tensile strength (ITS)	BS EN 12697-23	Curing at 20°C for 365 days.
Indirect tensile fatigue test (ITFT)	BS EN 12697-24	Curing at 20°C for 28 days + Curing at 40°C for 7 days.
Semi-circular bending test (SCB)	BS EN 12697-44	Curing at 20°C for 28 days + Curing at 40°C for 7 days.
Durability evaluation		
Moisture damage	BS EN 12697-12	Curing at 20°C for 7 days.
Frost damage	AASHTO T283	Curing at 20°C for 7 days.
Microstructure evaluation		
X-ray diffraction analysis (XRD)	-	Curing at 20°C for 28 days
Scanning electron microscopy (SEM)	-	Curing at 20°C for 28 days

At present, there are no standard methods to characterize the performance of CBEMs. Therefore, researchers in CMA usually use HMA testing methods (Needham, 1996, Thanaya, 2003). However, these methods need special consideration if they are to be applicable for CBEMs, particularly with respect to the curing process.

5.4 Moisture content evaluation

It has been already established that the stiffness of CBEM is highly reliant on the removal of moisture from the mixture as well as the breaking of bitumen emulsion (Needham, 1996). This implies that it is necessary to track the moisture loss from CBEM during the curing period. The moisture in the CBEM comprises water added during mixing and water in the bitumen emulsion. In order to evaluate the moisture content in CBEM, it was divided into two parts, namely, evaporated and trapped water. The evaporated water has been quantified by: (1) tracking the mass loss of CBEM specimens over the curing period at 20°C and (2) further drying the CBEM specimens for 7days at 40°C to measure any residual evaporated water inside the mixture. Trapped water inside the mixture is defined as: (1) the water physically adsorbed onto the surface of aggregate/filler, (2) the water trapped in closed pores within the bitumen and (3) the water used to hydrate the cement paste or cement paste plus active filler. The main feature of this water is that it cannot easily evaporate.

Selected mixtures were prepared as mentioned previously in section 5.2. After three months of curing the moisture loss by evaporation was evaluated. Moisture loss by evaporation is defined as the difference between the initial weight of the specimen and the weight after three months. The trapped water was calculated by subtracting the evaporated water from the initial water content present in the CBEMs specimens.

5.4.1 Results and discussion

It is clear from Figure 5.1 that the trapped water content, as percentage of total weight of mixture, increases with the presence of cement/blended fillers. For instance, in 1C-CBEM the trapped water was 0.30% while this value became 2.27%

in 5C-CBEM. A similar observation is noticed in CBEMs treated with blended fillers; the trapped water in C-F-CBEM, C-F-2S-CBEM and C-G-CBEM is about 0.54%, 1.95% and 1.83%, respectively. The trapped water in C-G-2S-CBEM reaches a maximum value of 2.63% which is slightly higher than those of 5C-CBEM. However, LF-CBEM shows only 0.21% of trapped water.

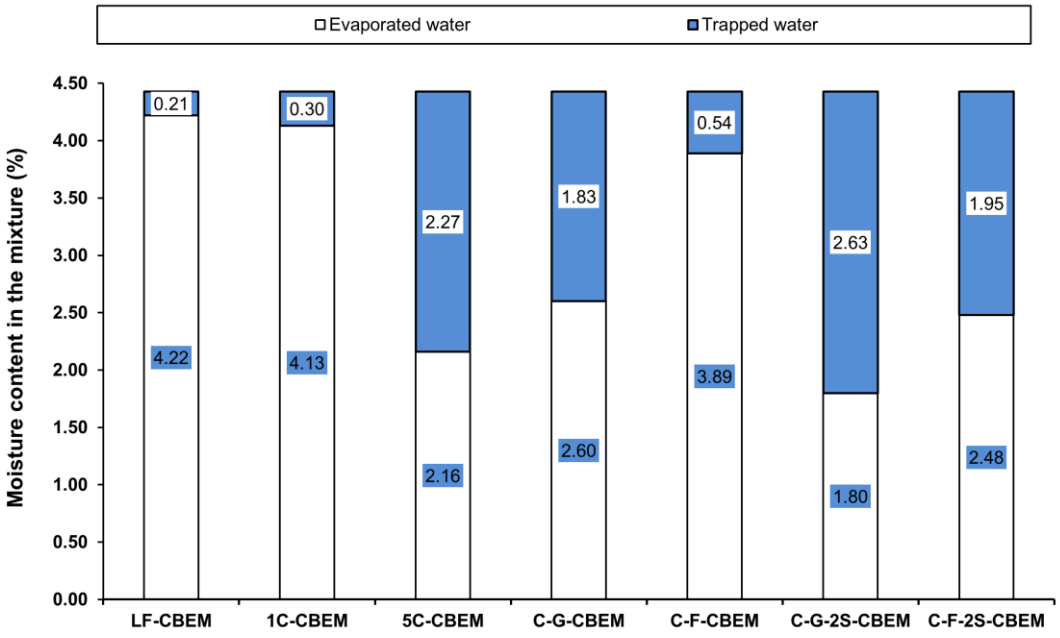


Figure 5.1 The water content evaluation of CBEMs

It is clearly deduced that the amount of trapped water in mixes treated with blended filler is quite as high as in 5C-CBEM. This indicates the role of the FA, GGBS and SF in maintaining trapped water inside the mixture, enhancing the hydration process with time and producing new hydration products due to filler reactivity. It is known that the use of GGBS and FA has a positive effect on reducing the amount of the $Ca(OH)_2$ (undesirable cement hydration products) in the concrete mix (Oner and Akyuz, 2007). Moreover, GGBS and OPC exhibit very similar chemical oxides, particularly the main oxides CaO and SiO_2, as discussed in Chapter 3. Therefore, this might significantly increase the efficiency of GGBS in enhancing the hydration process. However, it has to be mentioned that it is not expected that all the trapped water would be used for hydration. The first reason is the amount of trapped water

is more sufficient for the hydration process, particularly at this curing temperature (20°C). A second reason is that some of the moisture could be trapped within the voids at the bitumen-aggregate interface rather than being consumed by the hydration products as stated by García et al. (2013) and Miljković and Radenberg (2016). Additionally, a fraction of potentially evaporable water was found after drying the mixture at 40°C for 7 days; and in fact this point supports the validity of the second reason. This observation suggests the usefulness of a study into the hydration process in CBEM in different curing environments. This point will be addressed in the next chapter.

5.5 Indirect tensile stiffness modulus (ITSM)

Stiffness modulus is considered as an indicator of the structural behaviour of mixtures because it is related to the capacity of the material to distribute traffic loads. Therefore knowledge of stiffness modulus of any layer in such road pavements is required for adequate structural design. Stiffness modulus of bituminous mixtures is strongly reliant on the temperature and frequency of loading (Read and Whiteoak, 2003). The ITSM test was used since it is inexpensive, simple and can be quickly conducted compared to other traditional means of testing the stiffness modulus of bituminous mixtures (Oke, 2010). In addition, ITSM was performed in order to allow repeat tests on the same specimens at different ages to nullify variability in the mixtures and to derive reliable results for stiffness evolution.

5.5.1 Test configuration

The non-destructive stiffness test, ITSM, as shown in Figure 5.2, was selected for assessing the stiffness modulus of CBEMs. It was carried out according to BS EN 12697-26 (European Committee for Standardization, 2012). Table 5.3 summarizes the test configuration.

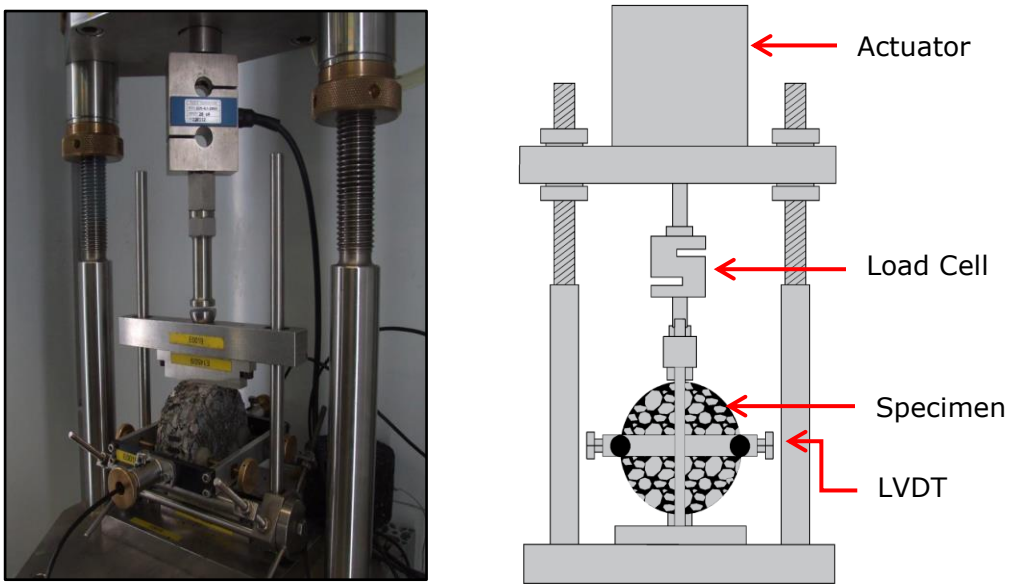


Figure 5.2 ITSM test configuration

Following BS EN 12697-26, an impulsive load was applied with a rise-time of 124±4 ms, to achieve a target horizontal deformation of 5±2 μm. Ten conditioning pulses were applied to the specimens followed by five test pulses.

Table 5.3 ITSM test configuration based on BS EN 12697-26

Item	Range
Specimen diameter	100±2 mm
Transient peak horizontal deformation	5±2 μm
Rise time	124±4 ms
Poisson's ratio (assumed)	0.35
Test temperature	20°C
Specimen thickness	40-80 mm

Automatically, the test data load and horizontal strain were measured and stored, and the stiffness modulus was calculated by Equation 5.1. The measurements were repeated along two diameters, and the average stiffness values were calculated.

$$ITSM = \frac{F}{(z \times t)} \times (v + 0.27) \qquad \text{Equation 5.1}$$

where

ITSM: Stiffness modulus (MPa); F: Vertical load (N); z: Horizontal deformation (mm); t: Thickness of specimen (mm); v: Poisson's ratio (0.35 assumed)

5.5.2 Sample preparation

The same mixture proportions of the control mix (LF-CBEM) were used to prepare other CBEMs treated with cement, BBFs and TBFs, as stated in Table 5.1. Marshall specimens with thickness (55 to 60) mm were prepared for all CBEMs. Mixing and preparation were carried out as described in section 4.2.6. Thereafter, impact compaction (Marshall Hammer) was utilized to compact the specimens; 75 blows were applied to each face. After compaction, the curing protocol followed was such that the specimens were left in the moulds (in a sealed condition) after compaction for 24h after which they were extruded. Specimens were conditioned in a thermostatically controlled air chamber at 20°C. An additional standard HMA was tested for comparison purposes. This mix contained the same aggregate type, gradation and base binder (40/60) as used in the CBEMs; the bitumen content in the HMA was 4.9% as recommended by the European Committee for Standardization (2006). The HMA 40/60 was mixed and compacted at 165°C using 75 blows applied to each face.

5.5.3 Results and discussion

It is known that monitoring of CBEM properties over the curing period is essential in order to understand the performance properly. The ITSM was performed at 3, 5, 7, 14, 28, 45, 84 and 365 days on the same specimens. Three specimens per mix were tested under the same conditions. Table 5.4 presents stiffness modulus and air voids of CBEMs after 7 and 28 days. Figure 5.3 shows the stiffness gain over the curing period for CBEMs treated with cement, while Figure 5.4 presents the stiffness improvement for CBEMs treated with BBFs and TBFs.

Table 5.4 Stiffness modulus and air voids values for the mixtures studied

Treatment type	Mixture type	ITSM after 7 days (MPa)	ITSM after 28 days (MPa)	Air voids (%)
Reference mixes	HMA 40/60	5420	5420	3.15
	LF-CBEM	1940	3580	10.34
Cement-treated mixes	1C-CBEM	5000	7675	9.83
	2C-CBEM	11305	14805	9.39
	3C-CBEM	16980	19735	9.20
	4C-CBEM	20680	23700	8.66
	5C-CBEM	24160	27000	8.50
BBF-treated mixes	C-G-CBEM	16960	20180	8.62
	C-F-CBEM	5500	8270	10.04
TBF-treated mixes	C-G-1S-CBEM	18690	21810	8.90
	C-G-2S-CBEM	19335	22300	8.88
	C-F-1S-CBEM	7990	11400	9.96
	C-F-2S-CBEM	9030	12670	10.56

The maximum and minimum coefficients of variation for all the mixes were 7.65% and 0.94%, respectively. These low coefficient of variation values from three replicates show a satisfactory repeatability from the test. With respect to Figure 5.3, a considerable increase in modulus was found when all or part of the conventional LF in LF-CBEM was replaced with cement. The stiffness modulus increases significantly with increasing cement content. At the same time, an improvement in the air voids was noticed. The air voids decreased from 10.34% to 8.50% by increasing the cement content in the mixture from 0% to 5%. This improvement might be due to improved workability of the mixtures. The presence of cement accelerates the breaking of the bitumen emulsion which may lead to free water in the mix before compacting and the compactability of the mix is increased accordingly. Another reason might be an improvement in the microstructure of these mixtures. This enhancement will be discussed later in section 5.9.

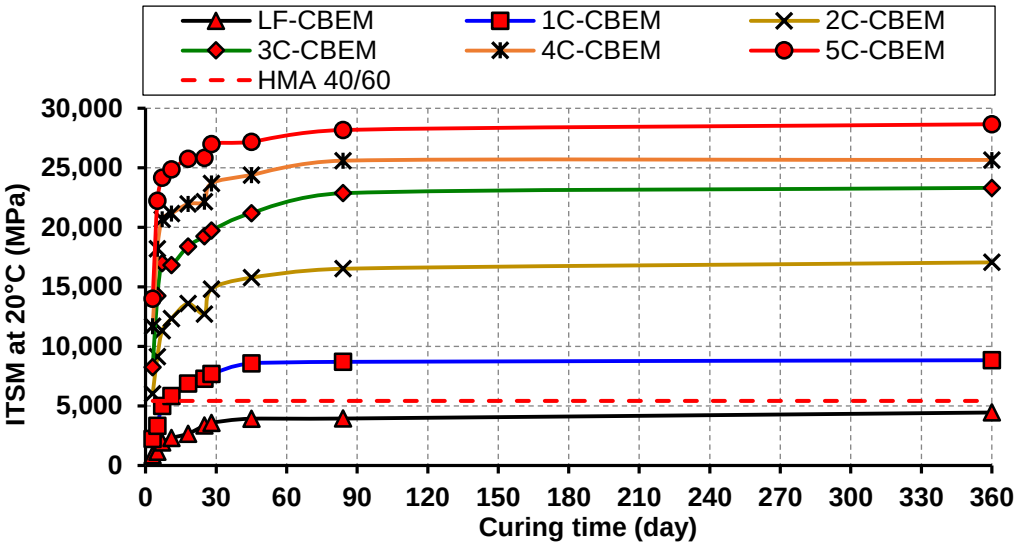


Figure 5.3 The stiffness modulus of CBEMs treated with cement over the curing period

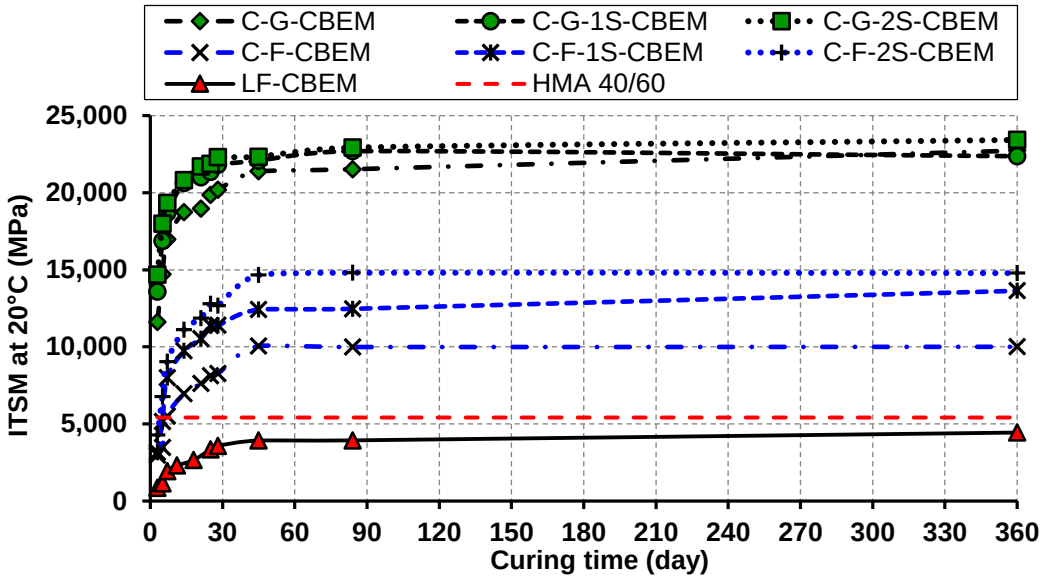


Figure 5.4 The stiffness modulus of CBEMs treated with blended fillers over the curing period

In CBEMs containing blended fillers, as seen in Figure 5.4 , a significant increase was observed when both BBFs and TBFs totally replaced the conventional LF. TBF-treated mixes show generally higher stiffness modulus than BBF-treated mixes, indicating a positive effect from adding SF. However, SF addition improved the stiffness of the mixes containing FA much more than those containing GGBS. The values of stiffness modulus for TBF-treated CBEMs containing GGBS are only

slightly lower than those for the 5C-CBEM, indicating the positive effect of this kind of cement replacement, while the TBF-treated mix containing (FA+SF) shows a stiffness modulus close to 2% of OPC replacement. In relative terms, these findings are consistent with those obtained by Al-Busaltan et al. (2012) and Al-Hdabi et al. (2013a). However, the stiffness values were much higher than those found by Al-Busaltan et al. (2012) and Al-Hdabi et al. (2013a). This might be related to factors such as the aggregate type, bitumen emulsion content and compaction method.

Moreover, the volumetric properties of BBF and TBF-treated mixes indicate an improvement in air voids content which may reflect the same reasons mentioned in regard to cement-treated mixes. Another point that should be more fully discussed is the early stiffness of CBEM. Low early stiffness is one of the main drawbacks of CMA containing conventional LF, as is clear in the reference mix (LF-CBEM). However, a remarkable stiffness increase was achieved within only one week of curing using cement or blended fillers. The obtained stiffness for these mixes can contribute effectively to minimizing the curing time in the field. For example, the early stiffnesses of C-F-CBEM, C-F-1S-CBEM and C-F-2S-CBEM are approximately 3 to 5 times higher than those of the reference mix (LF-CBEM), and these become 13 to 17 times in C-G-CBEM, C-G-1S-CBEM and C-G-2S-CBEM mixes during the first week. The results also demonstrate that the HMA 40/60 mix did not show any stiffness development during the curing period. In comparison, the stiffness modulus of HMA 40/60 (5400 MPa) was surpassed by the CBEM treated with 2% or more of OPC and all the CBEMs including GGBS within the first three days. Meanwhile the C-F-CBEM, C-F-1S-CBEM and C-F-2S-CBEM mixes achieved this value after 5-7 days whereas the LF-CBEM never reached this stiffness value during the curing period.

The improvement of stiffness modulus in CBEMs treated with cement and blended fillers may be referring to a complex mechanism occurring inside the treated CBEMs. This mechanism could be described as follows:

- The cement and active filler create another binder in the mixture through the hydration process of cement and SCMs.
- The presence of this kind of filler would increase the breaking of bitumen emulsion as reported in the literature.
- Cement and SCMs fillers could absorb the trapped water and enhance the hydration process.
- The presence of cement and SCMs may lead to an improvement in the volumetric properties.

More details about this mechanism will be presented and discussed in this chapter and chapter 6.

5.5.4 The effect of testing temperature on stiffness modulus

Stiffness modulus of CBEMs after 28 days of curing at 20°C was evaluated at different testing temperatures, namely 5, 10, 20, 30 and 40°C, as shown in Figure 5.5 and Figure 5.6 for CBEMs treated with cement and blended fillers, respectively.

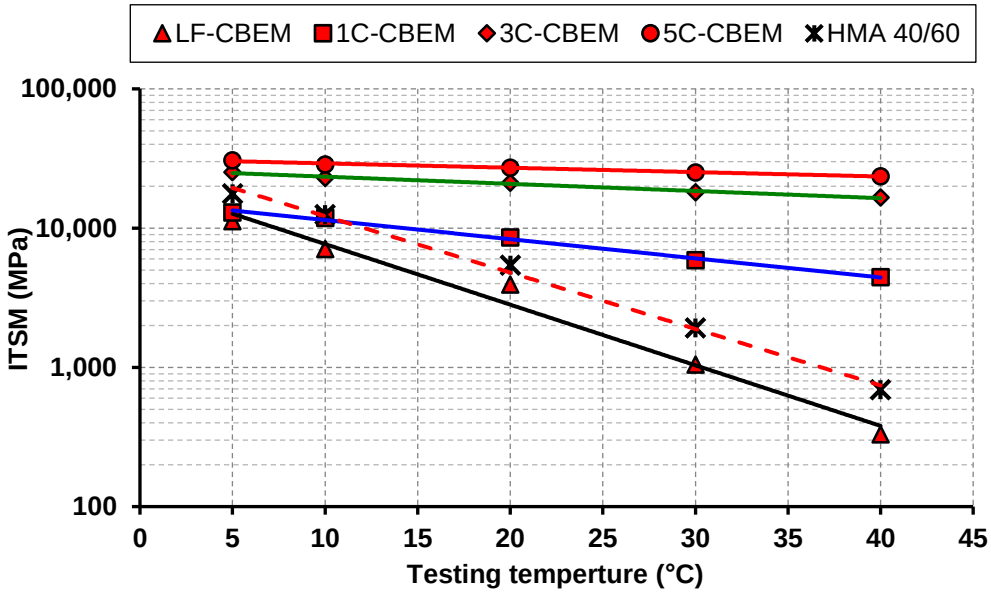


Figure 5.5 Stiffness modulus of CBEMs treated with cement under different testing temperatures

The stiffness modulus decreased with the increase of temperature. This trend is evident in both HMA 40/60 and LF-CBEM. However, in treated CBEMs, the reduction in the stiffness depends on the type of fillers. In Figure 5.5, the variation of stiffness significantly decreased with the increasing presence of OPC in the mixtures, especially at more than 3% of OPC.

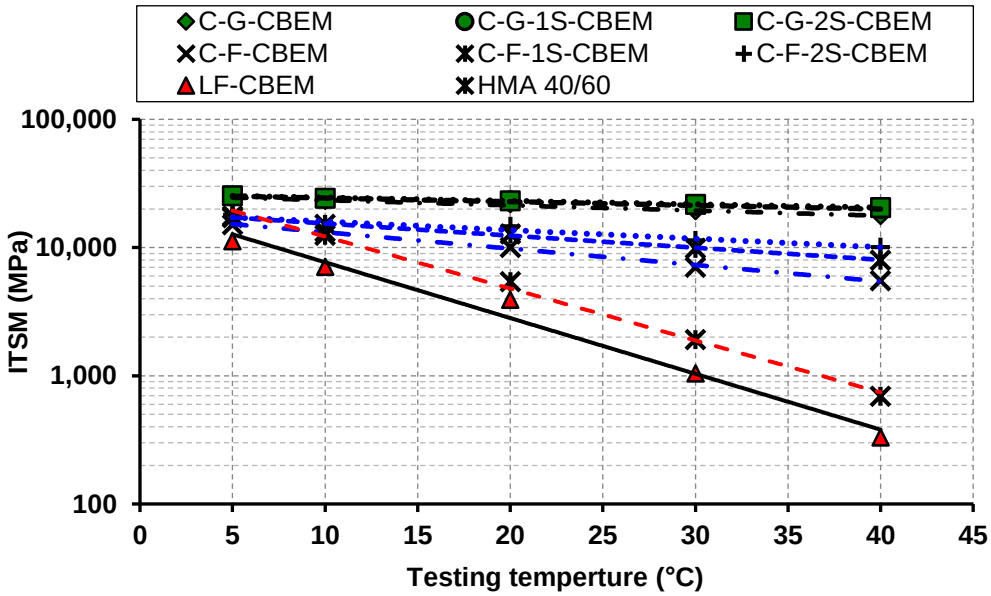


Figure 5.6 Stiffness modulus of CBEMs treated with blended fillers under different testing temperatures

Similarly, the stiffness modulus of BBF and TBF-treated mixes in Figure 5.6 is only slightly influenced by testing temperature. For example, stiffness reductions of only 28% and 43% resulted when heating C-G-CBEM and C-F-2S-CBEM respectively from 5 to 40°C. In contrast, HMA 40/60 and LF-mix lost 95-98% of their stiffness under the same conditions.

An analytical model has been used to describe the temperature sensitivity using Equation 5.2 (Bocci et al., 2011):

$$log\, S = -\alpha . T + \beta \qquad \text{Equation 5.2}$$

where:

S: Stiffness modulus at testing temperature T; α and β: are experimental parameters depending on the materials. Temperature sensitivity is expressed by α, the slope of the regression line on a semi-logarithmic plot (Figure 5.5 and Figure 5.6). Table 5.5 shows the resulting α , β and R^2 values.

Table 5.5 Temperature sensitivity of analytical model results

Treatment type	Mixture type	α	β	R^2
Reference mixes	HMA 40/60	0.0405	4.49	0.99
	LF-CBEM	0.0435	4.32	0.98
Cement-treated mixes	1C-CBEM	0.0138	4.15	0.99
	3C-CBEM	0.0051	4.42	0.99
	5C-CBEM	0.0031	4.50	0.98
BBF-treated mixes	C-G-CBEM	0.0040	4.41	0.98
	C-F-CBEM	0.0128	4.25	0.99
TBF-treated mixes	C-G-1S-CBEM	0.0029	4.42	0.96
	C-G-2S-CBEM	0.0026	4.42	0.94
	C-F-1S-CBEM	0.0094	4.28	0.99
	C-F-2S-CBEM	0.0067	4.27	0.93

The higher the α value, the more temperature sensitive the material. It is very clear that the α of LF-CBEM is three times higher than those for 1C-CBEM and C-F-

CBEM while this value becomes 14-16 times for 5C-CBEM and C-G-2S-CBEM. This decreased temperature susceptibility of CBEM treated with cement or blended fillers. This might be considered as an excellent advantage regarding pavement performance in hot weather. This could potentially make the asphalt material less prone to cracking at low temperatures and less prone to rutting at high temperatures. These results are comparable to those published by other authors (Bocci et al., 2011, Grilli et al., 2012, Pettinari et al., 2014).

5.6 Resistance to permanent deformation

Pavement layers with bituminous mixtures are subjected to continuous flexing under traffic loading which creates repeated stresses, and accordingly strains. Accumulated strains lead to permanent deformation in the pavement layers. Two major mechanisms of permanent deformation are described in the literature: (1) densification due to the repeated loading and (2) plastic shear deformation due to the repeated action of shear and tensile stress. Permanent deformation is influenced by mixture properties, i.e volumetric composition and material properties (Sunarjono, 2008). The present study aimed at evaluating the effect of different filler treatments on permanent deformation characterisation of CBEMs. This evaluation considered different stress levels and testing temperatures essential in order to understand the behaviour of CBEMs and to increase confidence in pavement design using these materials.

5.6.1 Test configuration

The repeated load axial test (RLAT) is the most widely used standard mechanical test in the UK for assessing the permanent deformation characteristics of bituminous mixtures. The test applies a repetitive pulse load to simulate the traffic and measures the permanent deformation after each repeated load. The protocol for the RLAT test is performed based on BS EN 12697-25. Table 5.6 and Figure 5.7

show the test configuration of the RLAT (European Committee for Standardization, 2005c). During this test, the repeated load is applied axially and consists of a square wave form with a frequency of 0.5 Hz, i.e. a pulse of one-second duration followed by a rest period of one-second duration. This simulates slow moving traffic, which leads to the most deformation in a real road (Kuna, 2015). During this test, the vertical strain is measured by two LVDTs mounted on the upper loading platen as shown in Figure 5.7.

Table 5.6 RLAT test configuration based on BS EN 12697-25

Item	Range
Specimen diameter	100±2 mm
Conditioning stress	10kPa
Conditioning period	600 s
Test stress	100kPa
Test Duration	3600 cycles
Test Cycle	Square wave pulses 1s on, 1s off
Specimen thickness	40-80 mm
Test temperature	40°C

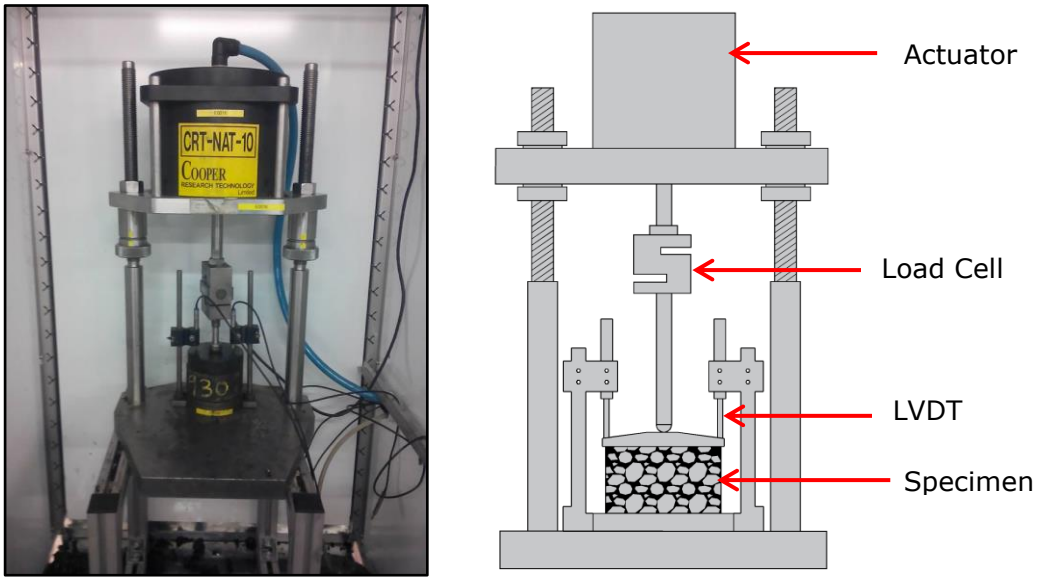


Figure 5.7 RLAT test configuration

One of the main output of RLAT is a creep rate which is calculated as the slope of the strain-cycle application during the second stage of the creep curve, between 1200 to 3600 cycles, as given by Equation 5.3.

$$\varepsilon_p = 100\left(\frac{h_o - h_n}{h_o}\right) \quad \text{Equation 5.3}$$

where

ε_p: Cumulative axial strain (%); h_o: Average height as measured by both displacement transducers after preload of the specimen (mm); h_n: Average height as measured by both displacement transducers after n load applications (mm).

5.6.2 Sample preparation

The same mixture proportions, mixing method, compaction and curing protocols were used as described previously in section 5.5.2 except that specimens were cured firstly at 20°C for 28 days, and then in a forced draft oven for a further of 7 days at 40°C. This curing protocol was selected to ensure that a fully cured condition was achieved, as recommended by Needham (1996) and Oke (2010). The two faces of the specimen were coated with a thin layer of silicone grease with graphite powder before running the test. Graphite powder is used to eliminate the influence of unevenness of the specimen face on the test results. A standard HMA were tested for comparison purposes.

5.6.3 Results and discussion

The results of the RLAT are shown in Figure 5.8 for cement-treated CBEMs while blended filler-treated CBEMs are shown in Figure 5.9. Figure 5.8 shows that the accumulated permanent strains in the cement-treated CBEMs decreased with increasing cement content. A similar trend to that of ITSM improvement can also

be found in the RLAT results, indicating the effect of using cement treatment in CBEM.

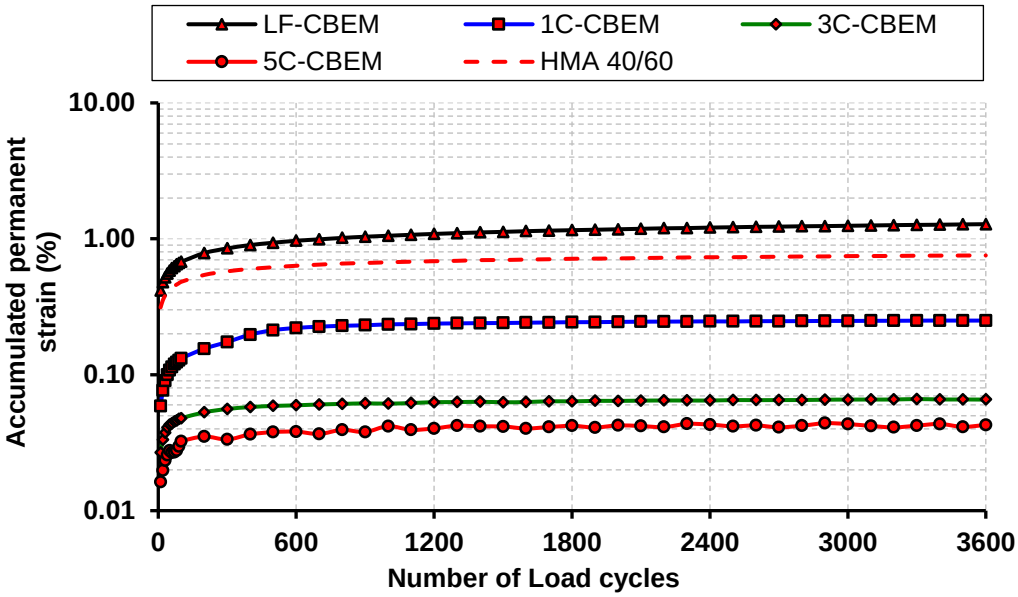


Figure 5.8 The permanent strain of CBEMs treated with cement under 100kPa stress

Moreover, the results in Figure 5.9 show that the incorporation of BBF and TBF resulted in a remarkable decrease in the permanent strains relative to the untreated LF-mix and HMA 40/60. The last two mixes exhibited much higher strain values throughout the test. In mixtures containing BBFs, the use of this type of filler combination resulted in a reduction in permanent strain of 89-93% relative to the LF-mix while the reduction was about 95-97% for mixtures containing TBFs.

In mixtures containing BBF, the replacement with GGBS exhibited better performance than the replacement with FA in CBEMs. This may be due to in the fact that GGBS mixtures maintained a higher amount of trapped water inside the mixture relative to FA replacement (see section 5.4). However, a further reason could be suggested due to the similarity of chemical oxides in GGBS relative to OPC. This is likely to enhance the hydration process considerably.

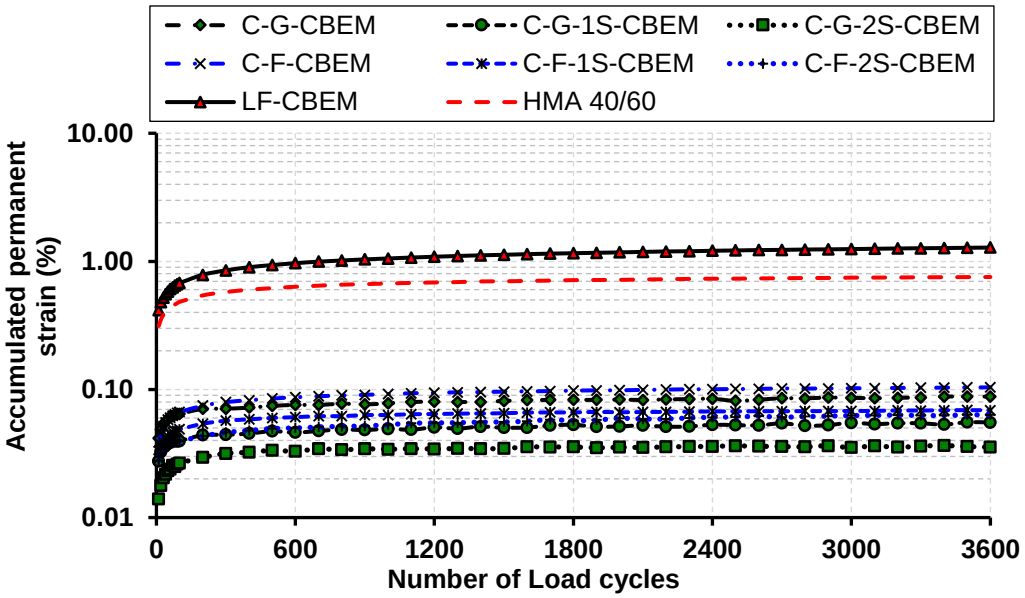


Figure 5.9 The permanent strain of CBEMs treated with blended fillers under 100kPa stress

More interestingly, the resistance to permanent deformation for the C-G-2S-CBEM is quite high compared to the 5C-CBEM. This might also be related to the role of highly densified SF in producing a dense microstructure, particularly with the GGBS combination as shown in Figure 5.8 and Figure 5.9. Moreover, it was noticed that the improvement shown in C-F-CBEM relative to 1C-CBEM is probably rather larger than would be expected based on ITSM data.

Table 5.7 presents the accumulated permanent strain (ε_p) of test specimens after 3600 load repetitions along with the creep strain curve intercept and slope. The intercept of the dynamic creep curve may represent the initial strain which could be the deformation due to mainly the densification of the mixture at early stage of test besides shear deformation (Fontes et al., 2010). For this reason, the parameters CSS slope and the intercept of the creep curve are also included in Table 5.7.

Table 5.7 Summary of RLAT test results for studied mixes

Treatment type	Mixture type	Total strain (%)	Strain rate	CSS slope	Intercept
Reference mixes	HMA 40/60	0.755	3.17E-05	0.078	0.123
	LF-CBEM	1.281	8.78E-05	0.158	-0.028
Cement treated mixes	1C-CBEM	0.250	6.01E-06	0.035	-0.024
	3C-CBEM	0.066	1.68E-06	0.006	0.019
	5C-CBEM	0.043	3.43E-07	0.004	0.010
BBF-treated mixes	C-G-CBEM	0.083	3.86E-06	0.007	0.031
	C-F-CBEM	0.104	4.50E-06	0.011	0.016
TBF-treated mixes	C-G-1S-CBEM	0.055	2.28E-06	0.004	0.021
	C-G-2S-CBEM	0.035	5.20E-07	0.003	0.010
	C-F-1S-CBEM	0.069	2.17E-06	0.006	0.018
	C-F-2S-CBEM	0.064	4.02E-06	0.006	0.012

Overall, it can be concluded that CBEMs treated with cement, BBFs and TBFs have significantly decreased susceptibility to permanent deformation, indicating the potential benefit if using this material as a surface layer. Therefore, it can be stated that, the improvement in permanent deformation resistance could be attributed to the same reason of ITSM enhancement mentioned in section 5.5.

Normally, the standard RLAT test uses a vertical stress of 100kPa at 40°C, and it is not common to test at higher pressures and more severe conditions. However, tests at 200 and 300kPa have been included in the present investigation in order to give a broad picture of what would happen if the CBEMs were used as a surface layer under a high-stress level due to direct tyre contact. Under these higher stresses, the sensitivity of the result to mixture components became particularly evident. In addition, selected mixes were tested under 300kPa pressure at 50°C, simulating a severe condition in-situ. These aspects are presented in the succeeding sections.

5.6.4 The effect of stress level on permeant deformation of CBEMs

The same mixtures were prepared and cured as described in section 5.6.2 and, as previously, specimens were pre-loaded to 10 kPa for 600 seconds. Three specimens

were tested at each stress level (100, 200 and 300kPa) unless otherwise stated. Figure 5.10 presents a comparison between the accumulated permanent strains under the different stress levels for cement treated CBEMs.

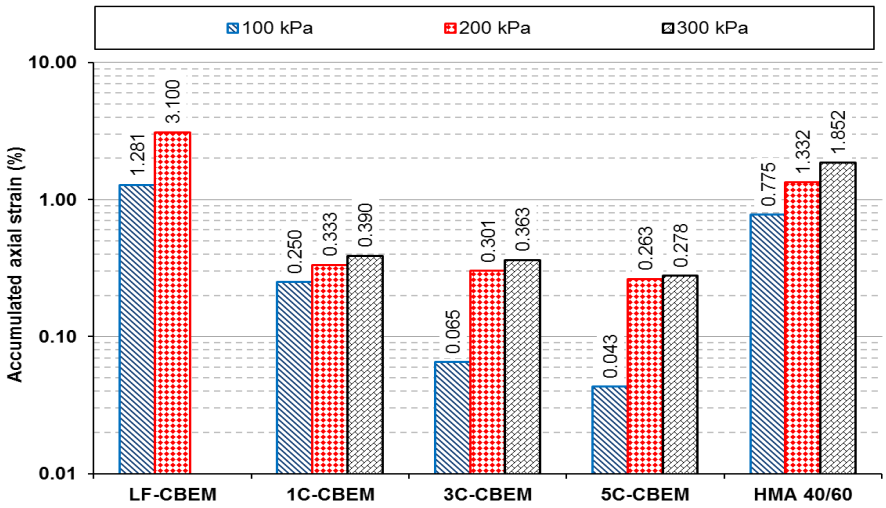


Figure 5.10 Accumulated permanent strain of cement-treated CBEMs under different stresses

It is evident from Figure 5.10 that, as expected, an increase in stress level increases the permanent deformation substantially. The untreated mixture LF-CBEM showed a relatively high permanent strain of 3.10% under 200kPa and the specimens were completely damaged under 300kPa as illustrated in Figure 5.11.

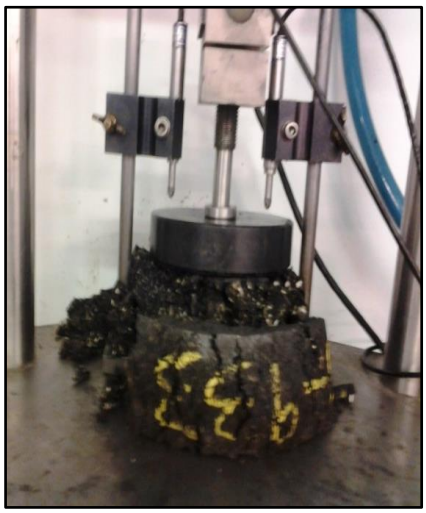


Figure 5.11 A damaged LF-CBEM under high-stress level (300kPa) in RLAT

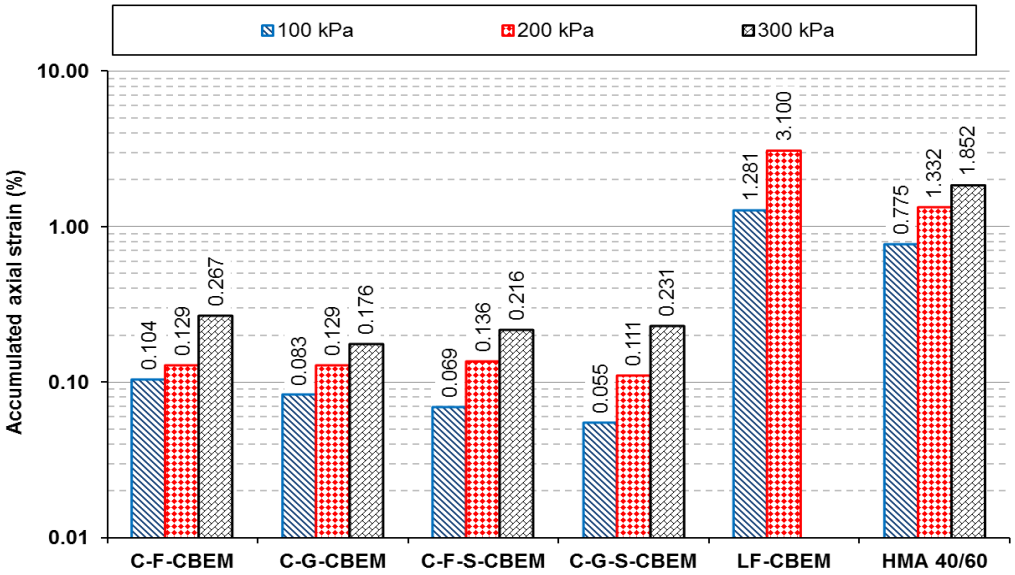


Figure 5.12 Accumulated permanent strain of blended filler-treated CBEMs under different stresses

In the mixes containing TBFs and BBFs, the permanent strain also increased with increasing the stress level, as shown in Figure 5.12. However, the TBFs and BBFs treated mixes show a comparatively better performance; e.g. at 300kPa the accumulated strain varied between 0.176 to 0.231% while the cement treated mixes had accumulated strains in the range 0.27-0.39%.

From Figure 5.10 and Figure 5.12, it can be found that both type of fillers and stress level have a significant influence on the deformation behaviour of CBEM. A two-way ANOVA statistical analysis was conducted to determine the impact of stress level and type of filler (as introduced for each mix in Table 5.1) for treated CBEMs. The analysis confirms that both the stress level and the type of filler are statistically significant at the 95% confidence level. ($P_{stress\ level}$= 0.010< 0.05 and $P_{type\ of\ fillers}$ = 0.012< 0.05).

In conclusion, the findings generally show that treated CBEMs have an excellent resistance to permanent deformation under high stresses since strain is less than 1% (Thom, 2008). Therefore, treated CBEMs are expected to have sufficient

deformation resistance for use in the construction of surface layers for medium to high traffic volume roads.

5.6.5 The effect of testing temperature

The same mixtures were prepared and cured as described in section 5.6.2. After that, they were tested under a stress of 300 kPa at two testing temperatures, namely 40 and 50°C for 3600 cycles. The results of this comparison are presented in Figure 5.13.

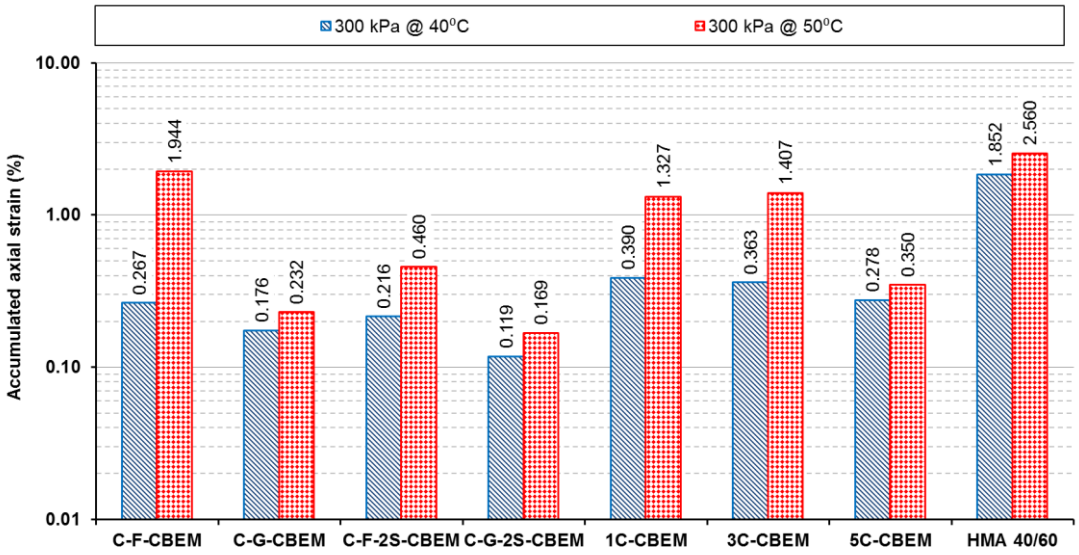


Figure 5.13 A comparison of accumulated permanent strain at 40 and 50°C under 300kPa for selected mixes

It is clear that a higher strain was shown at the higher temperature. However, 5C-CBEM and C-G-2S-CBEM were found to be least temperature susceptible. The highest accumulated strain was achieved in HMA 40/60, as can be seen from Figure 5.13. Moreover, the accumulated axial strain at 50°C was found to be 1.40 times that at 40°C. This finding consistent with the earlier findings in section 5.5.4. After the above discussion, it can be concluded that the CBEMs treated with cement or blended fillers are less susceptible to permanent deformation relative to the untreated mix LF-CBEM and traditional HMA.

5.7 Resistance to crack initiation and crack propagation

Crack initiation and propagation is one of the main failure modes of a pavement structure, resulting in degradation of the pavement materials and finally the whole pavement structure. As seen in the preceding sections, the addition of cement and blended fillers is found to resolve issues such as low early strength and improve the permanent deformation behaviour, but limited studies have focused on the effect of this kind of filler on the resistance to initiation and propagation of cracks (Kavussi and Modarres, 2010, Yan et al., 2010). For HMA, there are a number of tests that evaluate the resistance of asphalt mixtures to crack initiation. In this study, indirect tensile strength (ITS) was used for evaluating the tensile strength while for assessing the resistance of asphalt mixtures to crack initiation (fatigue behaviour), the indirect tensile fatigue test (ITFT) was carried out. Alongside the ITS and ITFT, the semi-circular bending (SCB) test was conducted to evaluate crack propagation through the evaluation of fracture toughness.

5.7.1 Indirect tensile strength (ITS)

The ITS test was applied to assess the tensile characteristics of CBEM, related to pavement cracking properties (Niazi and Jalili, 2009). The ITS test involved applying a diametric compression load with a constant deformation rate of 50 ± 2 mm/min on the samples between two uniform loading strips. This enables tensile stresses to develop along the diametric vertical plane to cause a splitting failure. The ITS was obtained for each specimen according to Equation 5.4.

$$ITS = \frac{2F}{(\pi \times d \times t)} \qquad \text{Equation 5.4}$$

where

F: Vertical load (N); d: Diameter of specimen (mm); t: Thickness of specimen (mm); v: Poisson's ratio (.35 assumed).

The test was conducted at 20°C using an INSTRON (hydraulic loading frame with a maximum load capacity of ±100 kN) test equipment in accordance with BS EN 12697-23. Figure 5.14 presents the configuration of the ITS test.

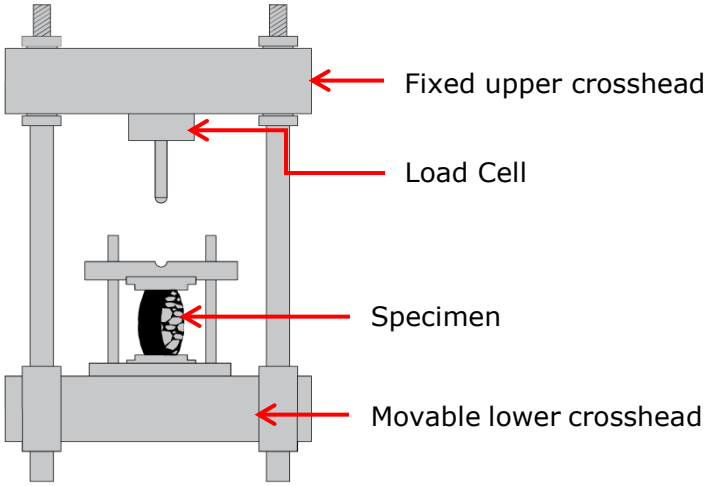


Figure 5.14 ITS test configuration

5.7.1.1 Samples preparation

After 365 days of curing at 20°C, the ITSM of CBEMs was measured as described in section 5.5.3. After that, the ITS test was carried out on the same specimens. This procedure is allowed since the ITSM test is non-destructive.

5.7.1.2 Results and discussion

The results of tensile strength for cement-treated CBEMs are shown in Figure 5.15. The results show that the tensile strength increased with the increase of cement content. The tensile strength values of 2C-CBEM were close to the value for HMA 40/60. However, the other mixes (3C-CBEM, 4C-CBEM and 5C-CBEM) were surpassed the HMA 40/60 and LF-CBEMs.

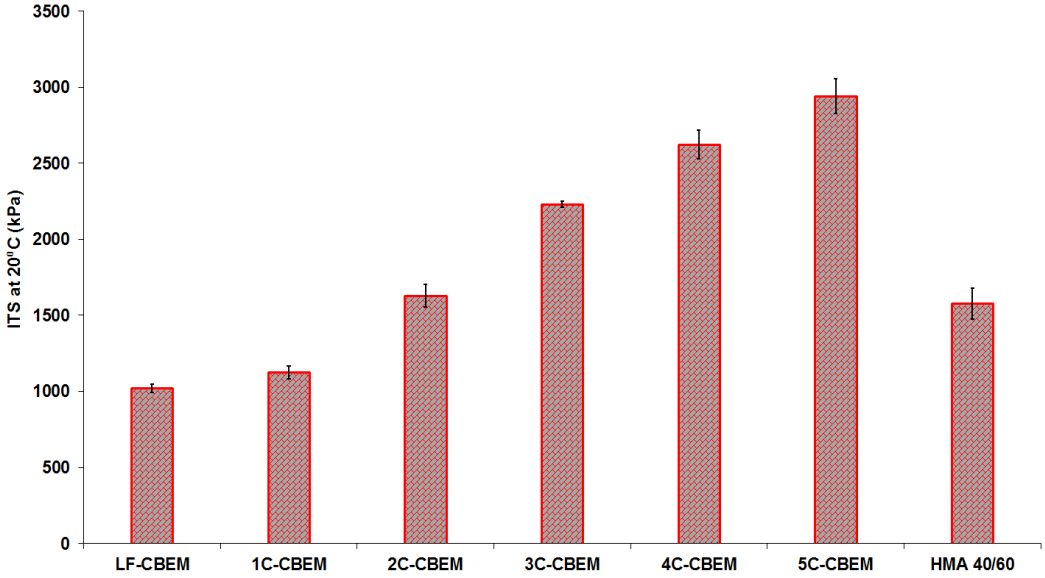


Figure 5.15 ITS of CBEMs treated with cement

The maximum tensile strength was obtained for the mixture containing 5% of OPC. This indicates that inclusion of cement to CBEMs had a positive effect on tensile strength. However, some authors (Oruc et al., 2007, Wang and Wang, 2010) have opined that replacing with high cement content (more than 3%) in the mixture could create a brittle material. Figure 5.16 shows the results of the tensile strength of CBEMs treated with BBFs and TBFs.

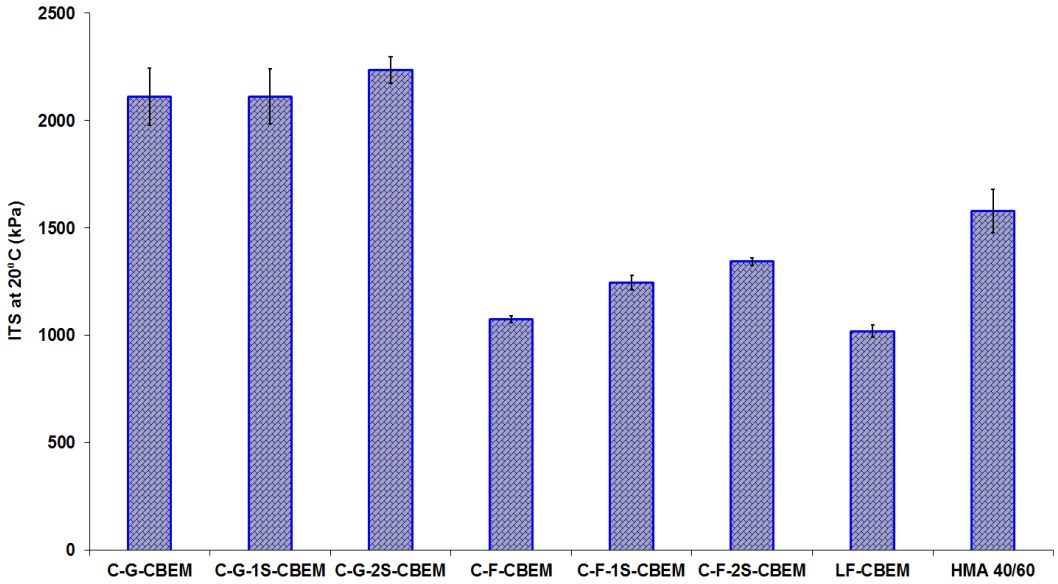


Figure 5.16 ITS of CBEMs treated with blended fillers

It is clear that a significant improvement of tensile strength is seen in those BBF and TBF-treated CBEMs treated with GGBS. Thus several modified mixtures appear to be capable of withstanding larger tensile stress prior to cracking. The maximum tensile strength value of C-G-2S-CBEM is close to the 3C-CBEM value while the tensile strength of C-F-2S-CBEM is close to 1C-CBEM. The enhancement of cement and blended filler treated CBEM tensile properties clearly relates to the occurrence of the hydration reaction either with cement or cement with SCMs.

In mixtures containing BBFs and TBFs, particularly GGBS and SF, the use of this type of filler resulted in an increase in tensile strength about 2 times relative to the LF-CBEM and 1.3 times relative to HMA 40/60. The tensile strengths of C-F-CBEM, C-F-1S-CBEM and C-F-2S-CBEM are slightly higher than LF-CBEM but lower than HMA 40/60. However, in the following sections, an evaluation will be made of the characteristics of resistance to crack initiation and propagation of the mixes.

5.7.2 Indirect tensile fatigue test (ITFT)

It has been reported in the literature that the ITFT is a simple and inexpensive test method and has the advantage of being able to test cylindrical specimens cored from in-service pavements. It has been more widely used than other fatigue tests. However, the ITFT suffers from drawbacks such as the absence of stress reversal and the accumulation of permanent deformation as stated by Cocurullo et al. (2008). In spite of these shortcomings, the ITFT is considered as a routine practical method for evaluating the fatigue life of bituminous paving mixtures (Read and Collop, 1997). However past research findings suggest that the ITFT is a conservative test for evaluating the fatigue life of CMA because of their high void content (Yan et al., 2010).

5.7.2.1 Test configuration

The ITFT test was conducted in accordance with BS EN 12697-24 (European Committee for Standardization, 2004). A compressive load is applied across the vertical diameter of a cylindrical specimen, resulting indirect tensile stress on the horizontal diameter. Consequently, this stress causes the specimen to fail by splitting along the central part of the vertical diameter. The resulting horizontal deformation of the specimen was measured and an assumed Poisson's ratio of 0.35 was used to calculate the initial tensile strain at the centre of the specimen. Equation 5.5 and Equation 5.6 were used to determine the maximum stress and maximum strain at the centre of the specimen as recommended by the standard.

$$\sigma_o = \left(\frac{2P}{\pi \times t \times \Omega}\right) \qquad \text{Equation 5.5}$$

$$\varepsilon_o = \left(\frac{2\Delta H}{\Omega}\right) \times \left(\frac{1 + 3\nu}{4 + \pi \times (\nu - \pi)}\right) \qquad \text{Equation 5.6}$$

where

σ_o: Tensile stress at specimen centre (MPa); ε_o: Tensile strain in με at the centre of the specimen; P: Maximum load (N); t: Thickness of specimen (mm); Ω: Diameter of specimen (mm); ΔH: Horizontal deformation (mm).

Fatigue life was defined as the total number of load applications before fracturing of the specimen occurred or the vertical deformation exceeded 10 mm. The specimen test setting is shown in Figure 5.17, while test conditions were as in Table 5.8.

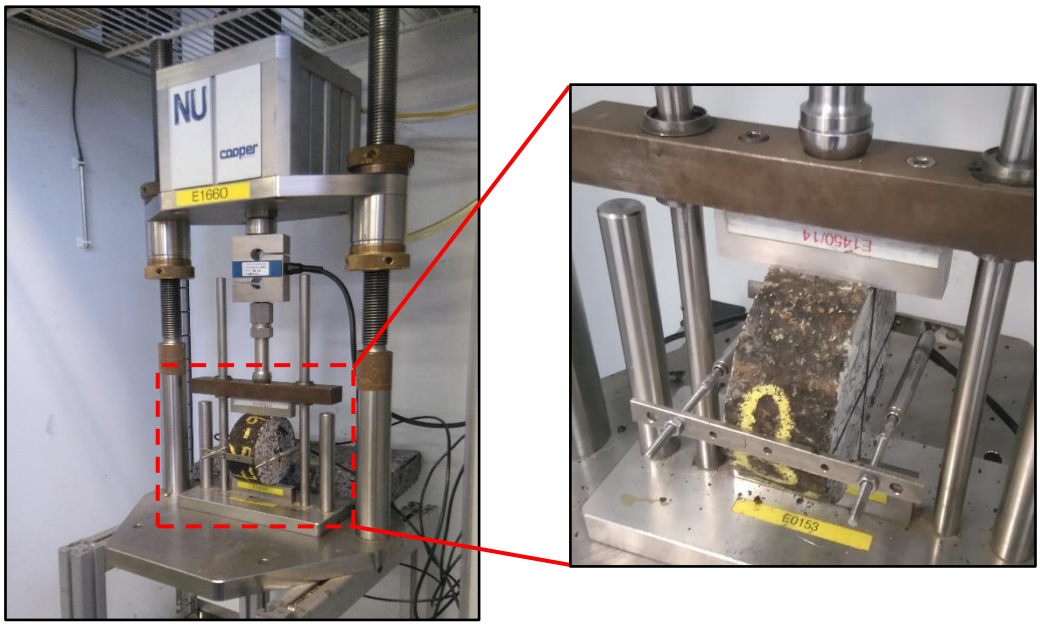


Figure 5.17 ITFT test configuration

Table 5.8 ITFT test configuration based on BS EN 12697-24

Item	Range
Specimen diameter	100±2 mm
Loading time	0.1 sec
Rest time	0.4 sec
Poisson's ratio (assumed)	0.35 for 20 °C test temperature
Specimen thickness	40 mm
Test temperature	20°C

The configuration of the test frame and specimen position in ITFT mode is similar to that in ITSM mode, but without the mounting frame and the alignment jig for LVDT instalment (Figure 5.2). The specimen is located in a central position between two loading strips (upper and lower), characterised by a concave surface and rounded edges; two deformation strips are glued on opposite sides of the horizontal diameter plane using a position rig. Also the deformation strips have a concave surface and they hold two LVDTs located horizontally in order to record the variation of the horizontal diameter, i.e. the distance between the two deformation strips (see Figure 5.17). The initial maximum tensile strain at the centre of the specimen for each respective stress level as determined for each specimen using Equation 5.6 was subsequently plotted against the corresponding number of cycles to failure

(Nf). Linear regression analysis using the least square method was then applied to the data to obtain the fatigue relation in the form of Equation 5.7.

$$N_f = C \times (\frac{1}{\varepsilon_o})^m \qquad \text{Equation 5.7}$$

where

N_f: Number of cycles to failure; C: Antilog of the intercept of the logarithmic relationship between fatigue life and tensile stress and m: Slope of the logarithmic relationship between fatigue life and tensile stress.

5.7.2.2 Samples preparation

The same mixture proportions, mixing method, compaction and curing regime were used as described previously in resistance to permanent deformation, section 5.6.2. After curing, if specimens were not tested immediately they were placed in a cold store at 5°C until they were ready for testing. Prior to test, irrespective of whether stored in the cold store or not, the specimens were placed in the conditioning cabinet at 20°C for about 8h (preferably overnight).

5.7.2.3 Results and discussion

The ITFT test results are summarized in Table 5.9. Since the strengths of the mixtures differed as found earlier in section 5.7.1, the selected ITFT stress levels were also varied accordingly. In high stiffness mixes such 3C-CBEM, 5C-CBEM, C-G-CBEM and C-G-1S-CBEM, the stress levels were higher than the stress levels recommended by BS EN 12697-24 due to the fact that the test becomes too time consuming at lower stress levels, effectively becoming non-destructive.

Table 5.9 Fatigue performance for CBEMs

Mixture type	Stress range (kPa)	Initial strain range (με)	Fatigue life (N_f)
HMA 40/60	100-600	45-355	175052-3756
LF-CBEM	100-300	55-363	13601-636
1C-CBEM	150-600	56-450	299960-146
3C-CBEM	450-1200	65-206	69071-300
5C-CBEM	650-1200	106-208	174296-500
C-G-CBEM	550-1400	66-250	213311-173
C-F-CBEM	150-550	40-270	359000-83
C-G-1S-CBEM	650-1400	68-300	200176-2113
C-F-1S-CBEM	150-650	64-287	243866-146

It has been recommended to compare the fatigue behaviours under controlled stress ratios rather than fixed stress amplitudes as in the traditional stress-controlled method (Nejad et al., 2013). For this reason, stress amplitudes applied to ITFT specimens were selected with stress ratios varying from 0.15 to 0.65 approximately. In this study, the stress level is defined as the ratio of stress amplitude to the ITS of specimen. The tabulated results in Table 5.9 represent the applied stress level (σ), initial strain (ε), fatigue life (N_f) while fatigue equations (fatigue life-strain, and fatigue life-stress ratio relations), and correlation coefficients of the fatigue equations are presented in Table 5.10.

Table 5.10 Regression coefficients for fatigue equations from ITFT tests

Mixture type	Fatigue equation for strain	Fatigue equation for stress ratio
HMA 40/60	$N_f = 6 \times 10^9 \times \varepsilon^{-2.595}$ $R^2 = 0.9391$	–
LF-CBEM	$N_f = 4 \times 10^6 \times \varepsilon^{-1.504}$ $R^2 = 0.916$	–
1C-CBEM	$N_f = 1 \times 10^{11} \times \varepsilon^{-3.424}$ $R^2 = 0.936$	$N_f = 1.7408 \times \left(\frac{\sigma}{\sigma_{max}}\right)^{-5.936}$ $R^2 = 0.9919$
3C-CBEM	$N_f = 8 \times 10^{13} \times \varepsilon^{-4.934}$ $R^2 = 0.9593$	$N_f = 8.1294 \times \left(\frac{\sigma}{\sigma_{max}}\right)^{-5.892}$ $R^2 = 0.9666$
5C-CBEM	$N_f = 2 \times 10^{15} \times \varepsilon^{-4.949}$ $R^2 = 0.9197$	$N_f = 0.1357 \times \left(\frac{\sigma}{\sigma_{max}}\right)^{-9.203}$ $R^2 = 0.9399$

Mixture type	Fatigue equation for strain	Fatigue equation for stress ratio
C-G-CBEM	$N_f = 2 \times 10^{14} \times \varepsilon^{-4.964}$ $R^2 = 0.942$	$N_f = 107.45 \times \left(\frac{\sigma}{\sigma_{max}}\right)^{-5.605}$ $R^2 = 0.801$
C-F-CBEM	$N_f = 3 \times 10^{13} \times \varepsilon^{-4.854}$ $R^2 = 0.965$	$N_f = 0.648 \times \left(\frac{\sigma}{\sigma_{max}}\right)^{-7.254}$ $R^2 = 0.933$
C-G-1S-CBEM	$N_f = 3 \times 10^{11} \times \varepsilon^{-3.289}$ $R^2 = 0.949$	$N_f = 46.481 \times \left(\frac{\sigma}{\sigma_{max}}\right)^{-6.294}$ $R^2 = 0.853$
C-F-1S-CBEM	$N_f = 2 \times 10^{14} \times \varepsilon^{-4.808}$ $R^2 = 0.959$	$N_f = 7.701 \times \left(\frac{\sigma}{\sigma_{max}}\right)^{-4.743}$ $R^2 = 0.952$

The measured initial strain (ε) values for each mixture considered in the study are plotted against the number of repeated load cycles to failure (N_f) in Figure 5.18 and Figure 5.19 for cement and blended filler-treated mixtures, respectively. Linear regression was carried out on the data points obtained for each mixture to fit the model in Equation 5.7. The corresponding coefficients obtained after fitting are tabulated in Table 5.10. R^2 values from Table 5.10 suggest that the data collected for each mixture provided a good fit with the fatigue equation (Equation 5.7); R^2 values not less than 0.9 were obtained for each mix, as recommended by BS EN 12697-24.

Referring to Table 5.9 and Figure 5.18, it can clearly be seen that the fatigue lines for cement treated CBEMs performed better than without cement (LF-CBEM). At a projected life to failure (Nf) of one million load cycles, 1C-CBEM, 3C-CBEM and 5C-CBEM can withstand 31, 48 and 85 micro-strain respectively while the LF-CBEM can take less than 10 micro-strain. A similar trend is observed when a comparison is made based on the number of cycles at a strain value of 100 micro-strain. In comparison to HMA 40/60, 3C-CBEM and 5C-CBEM have longer fatigue lives under strains less than 200 micro-strain (low stress levels) while at higher than 200 micro-strain (high stress levels) the material behaved in a brittle manner and failed

under a low number of cycles compared to HMA 40/60. This point is in agreement with previous finding by Needham (1996).

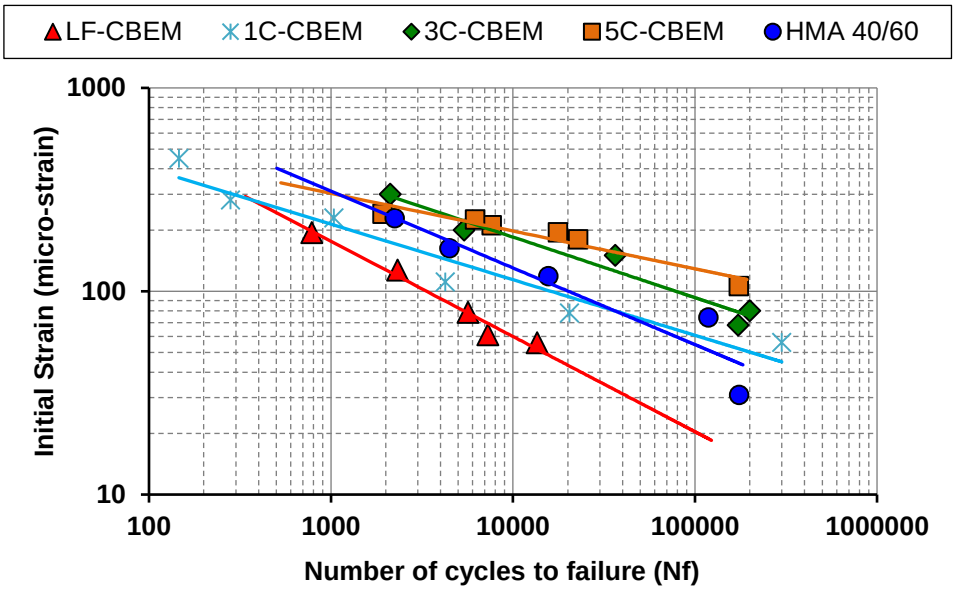


Figure 5.18 Fatigue performance of cement treated CBEMs

In summary, the results indicate a significant improvement in fatigue characteristic with increasing OPC content. However, using high OPC content produces a stiffer mixture, resulting a reduction in flexibility and consequent with behaviour.

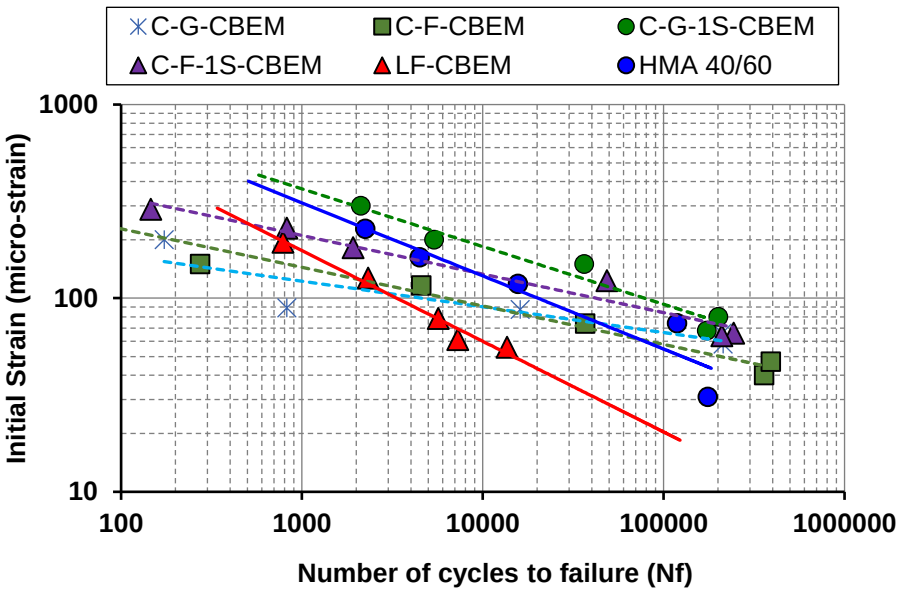


Figure 5.19 Fatigue performance of blended fillers treated CBEMs

With respect to Figure 5.19 and Table 5.9, CBEM containing BBFs and TBFs withstands more fatigue life than that of LF-CBEM at one million cycles. At a projected life to failure (Nf) of one million load cycles, C-F-CBEM, C-F-1S-CBEM, C-G-CBEM and C-G-1S-CBEM can withstand 37, 55, 50 and 50 micro-strain compared to less than 10 micro-strain for LF-CBEM. These results indicate that introducing BBFs and TBFs significantly improves the fatigue life of CBEM. This improvement could be attributed to the hydration process with these fillers. However, the fatigue characteristics of CBEM result from a combination of fatigue characteristics of bituminous and hydraulic materials inside the treated CBEM. Another important point to be mentioned is that the fatigue life of HMA at high stress level showed better fatigue characteristic than blended filler treated CBEMs; the performance was brittle as for cement treated mixes.

To fully compare the fatigue performances of these mixes with different tensile properties, the stress ratios were included to describe the fatigue life, as shown in Table 5.10. The relationships between fatigue life and stress ratio are presented in Figure 5.20 for CBEMs.

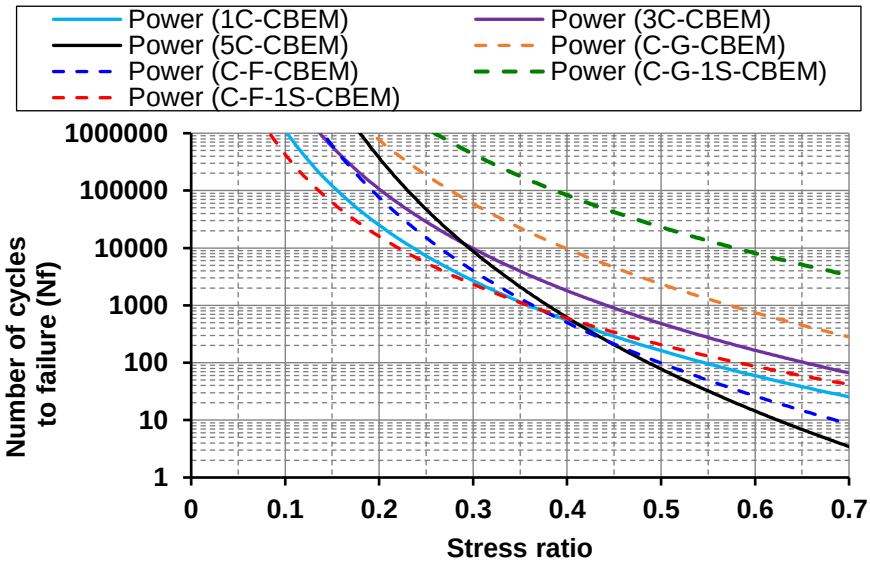


Figure 5.20 Relationship between fatigue life and stress ratio for CBEMs

It is interesting to note the ranking of mixes in resisting fatigue on the stress ratio characteristic as shown in Figure 5.20. For example, in Figure 5.19, C-F-1S-CBEM exhibited a longer fatigue life than C-G-CBEM. However, when compared in terms of stress ratios, C-G-CBEM has a longer fatigue life than C-F-1S-CBEM. Moreover, it is worth noting that the use of 5% of OPC can improve the resistance to failure by enhancing the strength of the mixture compared to the other cement treated mixes; however it has a negative impact on the fatigue performance at high stress ratio (more than 0.3). In terms of comparison by stress ratio, the BBFs and TBFs containing GGBS and SF showed a better fatigue performance than cement treated mixes. Overall, the results of fatigue characterization demonstrate the following:

- The treatment of CBEM using cement or blended fillers significantly improves the fatigue performance. However, under high stress level the material behaviour became brittle.
- The conventional CBEM exhibited inferior fatigue performance relative to HMA 40/60 and treated CBEMs.
- A mathematical power relation is valid to represent both equations of fatigue life (N_f-micro-strain and N_f- stress ratio relations).
- The enhancement of fatigue performance in treated CBEMs resulted from a combination of the fatigue characteristics of bituminous and hydraulic material inside the mixtures.

5.7.3 Semi-circular bending (SCB) test

The SCB test method was used to determine the tensile strength or fracture toughness of CBEM mixtures for the assessment of the potential for crack propagation. In the past, extensive studies have used fracture mechanics to study the cracking resistance of HMA (Mobasher et al., 1997, Roque et al., 2002, Wagoner et al., 2005, Song et al., 2006). However, in reviewing the literature, it is apparent

that relatively little experimental work has been carried out on the fracture properties of CBEM (Monney et al., 2007, Al-Hdabi et al., 2014, Dondi et al., 2014, Pettinari et al., 2014). The single edge notched beam, disk-shaped compact tension and SCB tests have all been widely used to determine fracture properties. In the current study, the SCB was selected as it has been found easy to manufacture cores for the SCB test rather than the geometries of the other tests. Also, the test setup and procedure are fairly simple and rapid. Monney et al. (2007) opined that the SCB is a suitable test due to it is applicability for testing laboratory prepared specimens and field cores, and in that its avoids the self-weight problem encountered with prismatic beam specimens. The theoretical principles, analysis and limitations of the SCB test have been reported in detail by Molenaar et al. (2002).

5.7.3.1 Test configuration

Figure 5.21 presents the SCB configuration. The test was conducted in accordance with BS EN 12697-44 (European Committee for Standardization, 2010). The specimen consists of a 150 mm diameter half cylinder containing a notch (crack) of 10 mm depth from the centre of its bottom edge as shown in Figure 5.21. A standard three-point load is applied to fracture the specimen. The maximum load that the specimen can resist before failure is recorded. During the test, the deformation increases at a constant rate of 5 mm/min. As per BS EN 12697-44 the maximum stress at failure, σ_{max} (N/mm^2) and the fracture toughness K_{Ic} (N/mm$^{3/2}$) have been calculated in accordance with Equation 5.8 and Equation 5.9, respectively.

$$\sigma_{max} = \frac{4263 \times F_{max}}{D \times t} \qquad \text{Equation 5.8}$$

where

D: Diameter of specimen (mm); t: Thickness of specimen (mm); F_{max}: Maximum force of specimen (newtons).

$$K_{Ic} = \sigma_{max} \times f\left(\frac{a}{W}\right) \qquad \text{Equation 5.9}$$

where:

W: Height of specimen (mm); a: Notch depth of specimen (mm); σ_{max}: Stress at failure of specimen (N/mm^2); $f\left(\frac{a}{W}\right)$: Geometric factor of specimen; for 9 < a < 11 mm and 70 <W< 75 mm, then $f\left(\frac{a}{W}\right)$= 5956.

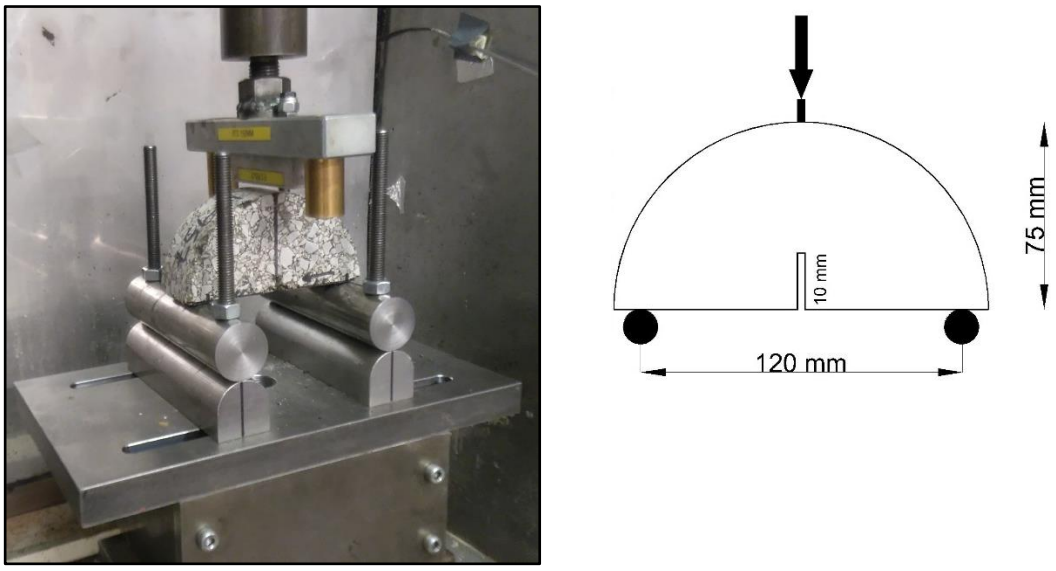


Figure 5.21 SCB configuration test

5.7.3.1 Sample preparation

Due to limitations on time and materials, the test was limited to selected mixes. The mixing proportions and processes detailed in section 5.2 were used to prepare these mixtures and they were compacted by roller compactor to achieve the desired density of 2276 kg/m^3 and air voids of 10.26%. As the slabs were produced, the volumetric properties were evaluated. It was found that the dry density of mixtures varied from 2233 to 2298 kg/cm^3 while the air voids ranged between 12.29% and

9.75%. However, the volumetric properties fluctuated to some extent around the desired average values of density and air voids. An experimental studies carried out by Gómez-Meijide et al. (2015) and Miljković and Radenberg (2016) found that the performance of CBEM had a clear dependency on the compaction method.

After compaction, the curing protocol followed was such that the specimens were left in the slab for 28 days at 20°C. After that they were cured in a forced draft oven for a further of 7 days at 40°C similar to RLAT and ITFT tests. 150 mm cores were obtained from these slabs and trimmed from the top and the bottom to give (50±3) mm thickness. Specimens were conditioned overnight in a thermostatically controlled air chamber at 0 and 20°C prior to testing.

5.7.3.2 Results and discussion

The fracture toughness K_{Ic} of six mixtures with different filler treatments is presented in Figure 5.22. The evaluation of fracture was performed at 0 and 20°C. The cracking propagation at low temperature was evaluated at 0°C as recommended by European Committee for Standardization (2010) while 20°C was selected to be similar to previous evaluation in the ITFT and ITS tests. As seen in Figure 5.22 the presence of cement or blended fillers affects the fracture resistance and reduces the fracture toughness in comparison to HMA 40/60. This point is more evident at low temperature (0°C). A 50% reduction in fracture toughness is calculated when comparing 3C-CBEM, 5C-CBEM, C-F-CBEM and C-G-CBEM with HMA 40/60 whereas this value became 25% for LF-CBEM. At 20°C, it is apparent that the fracture toughness of CBEM with 3 and 5% OPC and BBFs contain GGBS is slightly less than the HMA 40/60 value. However, in the earlier evaluation of ITS performance, the ITS of HMA 40/60 was considerably lower than that of 3C-CBEM, 5C-CBEM and C-G-CBEM, see Figure 5.15 and Figure 5.16. Moreover, the fracture toughness of treated CBEM is higher than for LF-CBEM, which reflects the benefit

from the addition of these fillers. In contrast, Al-Hdabi et al. (2014) found no difference between the fracture toughness of CBEM with 6% OPC and untreated CBEM (0%). Furthermore, the fracture toughness of cement and blended treated filler were only slightly affected by temperature between 0 and 20°C which confirms the lower degree of temperature sensitivity of these kinds of mixture, see section 5.5.4.

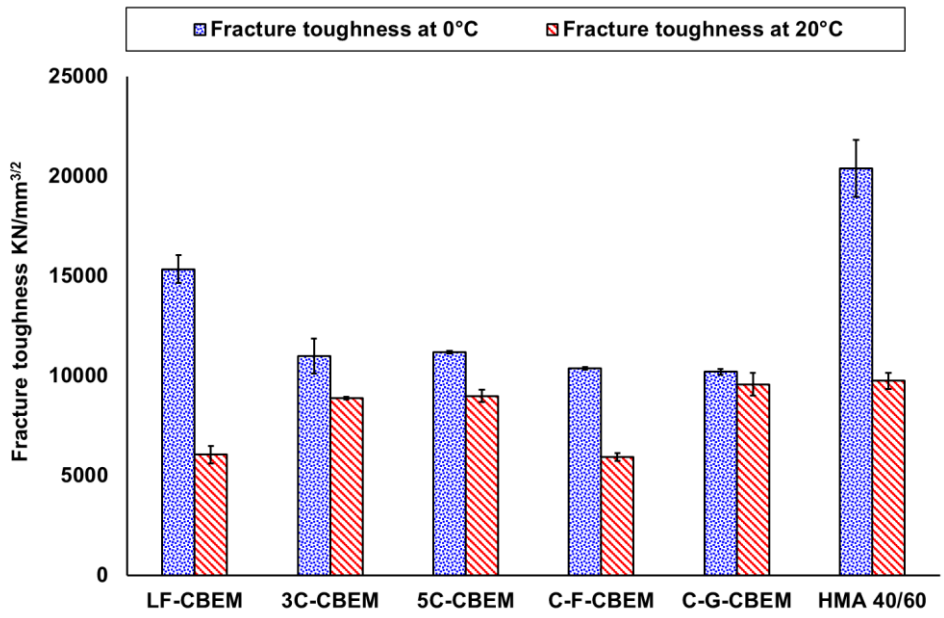


Figure 5.22 Effect of treated fillers in CBEM on fracture toughness

More interestingly, unexpected behaviour was observed in LF-CBEM at 0°C. The fracture toughness was higher than that of the other treated CBEM but less than the HMA 40/60. This behaviour could be attributed to the fact that low temperature increases the stiffness of the binder and increases the strength accordingly. At the same time, the absences of any cementitious filler increases the ductility of this material. This pattern of behaviour is in agreement to some extant with the results in section 5.5.4.

Overall, it could be concluded that the treatment of CBEMs with cement and blended filler caused a reduction in the fracture toughness and a change in the

development of fracture to become more brittle. Therefore, it is worth to suggest a future research to cover this area in order to deeply understand the fracture mechanism in CBEM.

5.8 Durability evaluation

Durability is a feature directly related to the effect of environmental condition on the performance of asphalt mixtures during the service life. The durability of CBEMs has been evaluated against both moisture and frost damage to present a broad overview regarding the performance of CBEMs in warm and cold climates. Both damage modes are potentially serious problems in a cold wet climate. They were evaluated based on BS EN 12697-12 (European Committee for Standardization, 2008) and AASHTO T283 (American Association of State Highway Transportation Officials, 2009), respectively.

5.8.1 Sample preparation and test procedures

The same mixture proportions, mixing method and compaction were used as described previously in section 5.5.2 except that specimens were cured and subjected to durability damaging protocols as follows:

- The first set of specimens (unconditioned group/dry) was tested after curing for 7 days at 20°C;
- The second set of specimens (first conditioned group/wet) was cured at 20°C for 7 days, after which the specimens were subjected to vacuum saturation for 30min (6.75kPa) before being soaked in a water bath for 3 days at 40°C and finally soaked for 2h at 20°C;
- The third set of specimens (second conditioned group/freeze-thaw) was also cured at 20°C for 7 days, after which the specimens were subjected to a vacuum for 10 to 30min (13-67kPa) until they reached saturation level between 55% and 80%. The specimens were then wrapped in plastic bags and exposed to

freeze-thaw cycles. The cycle consisted of freezing at -18°C for 16h followed by soaking in a water bath at 60°C for 24h and finally soaking for 2h at 20°C.

The durability of mixtures can be defined as the loss of strength due to the effects of the exposure condition. The evaluation of durability was measured as indirect tensile strength ratio (ITSR) as defined in Equation 5.10.

$$ITSR\ (\%) = \frac{ITS_{conditioned}}{ITS_{unconditioned}} \times 100 \qquad \text{Equation 5.10}$$

where

$ITS_{conditioned}$: Average indirect tensile strength of conditioned specimens;

$ITS_{unconditioned}$: Average indirect tensile strength of unconditioned specimens.

The ITS test involved applying diametric compression with a constant deformation rate of (50 ± 2) mm/min to the samples between two loading strips, which creates tensile stresses along the vertical diametral plane causing a splitting failure. The test was conducted at 20°C using INSTRON test equipment as described in section 5.7.1.

5.8.2 Results and discussion of moisture damage evaluation

The effect of different filler treatments on moisture the damage performance of CBEMs is shown in Figure 5.23 and Figure 5.24. The result in Figure 5.23 illustrates the effect of substituting the conventional LF with different percentages of OPC, while the effect of replacement of LF with BBFs and TBFs is presented in Figure 5.24.

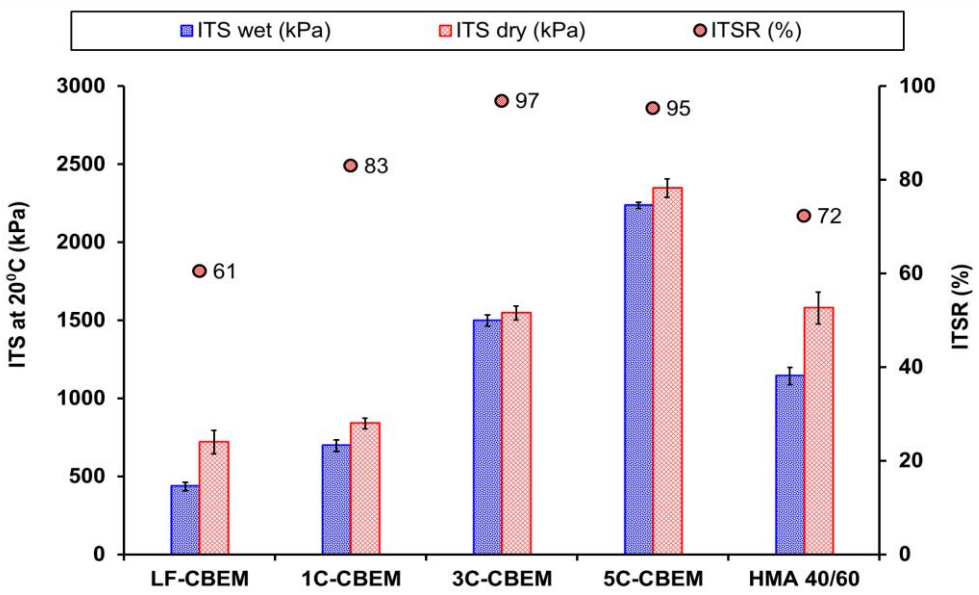


Figure 5.23 The results of moisture damage for CBEMs treated with cement

The potential benefits gained from incorporation of OPC into CBEMs can be seen in Figure 5.23. It is clearly shown that ITSR of cement-treated CBEMs was higher than that for untreated LF-CBEM and the equivalent HMA (HMA 40/60). The excellent performance of these mixes is expected due to the role played by OPC as an adhesive agent to the bitumen emulsion, according to Needham (1996)'s suggestions. Similarly, the performance of the blended treated filler mixtures is also reasonably good as shown in Figure 5.24. The ITSR values (ratios of wet to dry ITS) of treated CBEMs (with BBF and TBF) were higher than those for the untreated LF-CBEM and the equivalent HMA (HMA 40/60), and comparable with the cement-treated mixes.

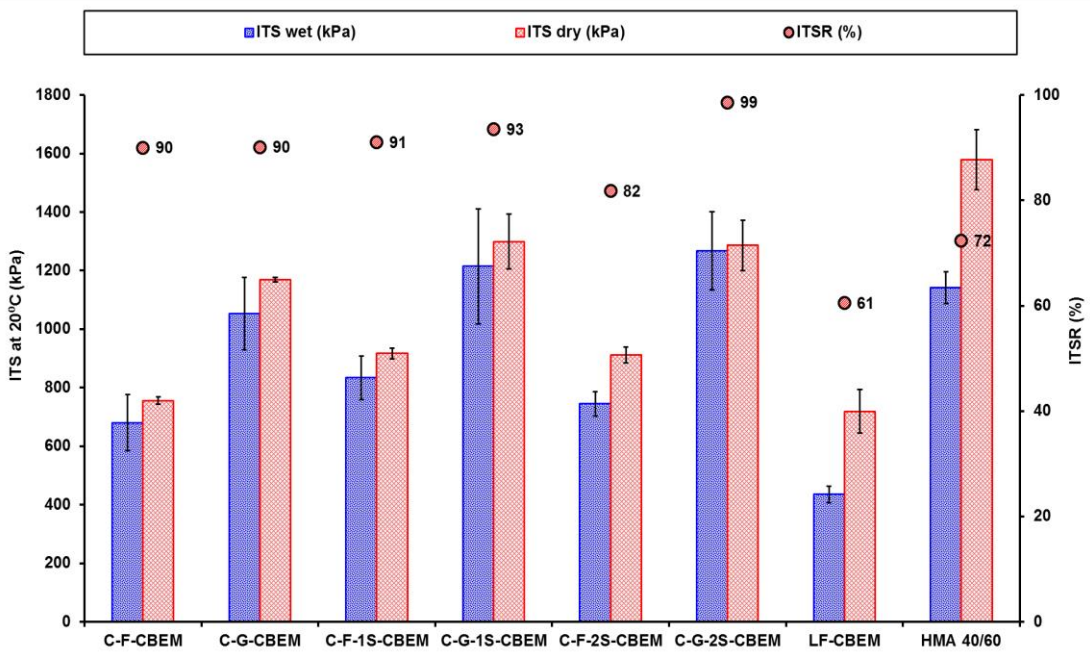


Figure 5.24 The results of moisture damage for CBEMs treated with blended fillers

These higher values of ITSR (the ability of the mix to maintain its strength after damage) may be related to the formation of new hydration products due to the incorporation of SCMs with cement. In addition, the 40°C soaking phase would have accelerated the hydration process of these active fillers. The results are consistent with trends noticed in concrete (Lothenbach et al., 2008, Mohammed, 2015). However, it is necessary to take into account the fact that the evaluation of CBEMs at an early age from 7 to 10 days was considered as a conservative test while the materials did not reach their ultimate strength. Therefore, this leads to the conclusion that CBEMs with these blended fillers are less susceptible to moisture damage compared to untreated LF-CBEM and HMA 40/60. Also, this behaviour corresponds to the results obtained for temperature susceptibility (section 5.5.4).

5.8.3 Results and discussion of frost damage evaluation

The ITS values before and after exposure to freeze-thaw cycles and corresponding ITSR values are plotted in Figure 5.25 for cement-treated CBEMs.

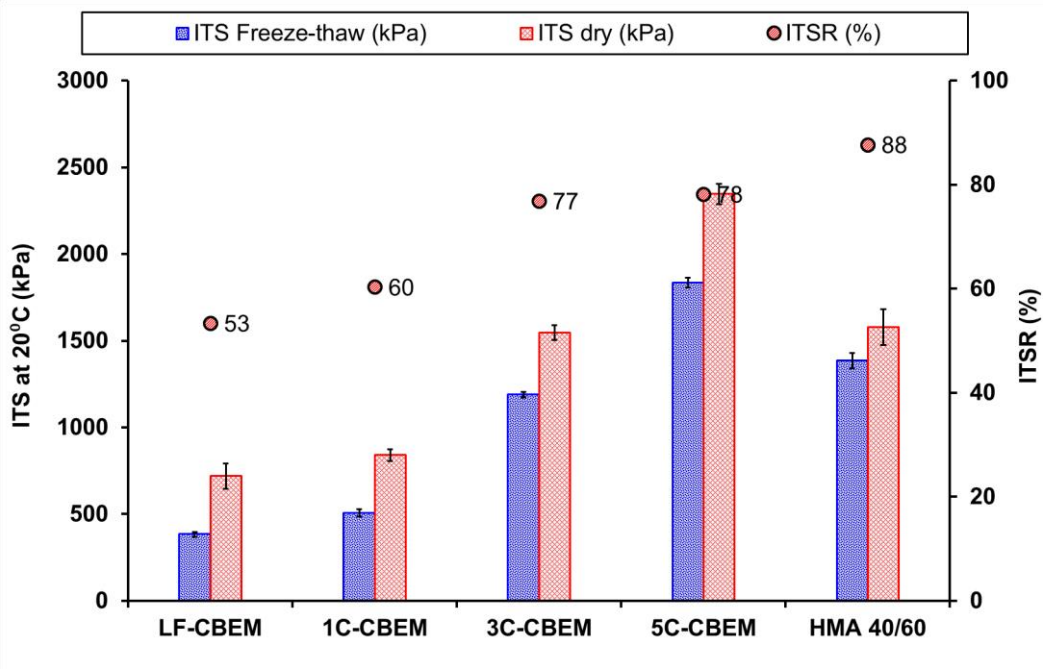


Figure 5.25 The results of frost damage for CBEMs treated with cement

It can be seen that the ITSR values of 3C-CBEM, 5C-CBEM and HMA 40/60 are in the range 77% to 88%. However, the other mixtures, LF-CBEM and 1C-CBEM, show lower values of around 50 to 60%. Therefore, it could be concluded that using relatively high cement content (more 3%) leads to an improved resistance to frost damage. However, a low cement content on its own is not sufficient to withstand frost damage.

Whilst the incorporation of low cement content with SCMs presents excellent frost damage resistance, as shown in Figure 5.26, it can be seen that the ITSR values of HMA 40/60 and CBEMs treated with BBFs, TBFs and 5% of OPC are all comparable and in the range 77% to 105%. Thus, it can be concluded that incorporating SCMs had a significant positive effect on making CBEMs less susceptible to frost damage and stripping problems. Furthermore, the C-G-2S-CBEM mix showed the highest resistance to exposure to both moisture and freeze-thaw damage, which might be attributed to the same cause suggested in the discussion relating to Figure 5.4.

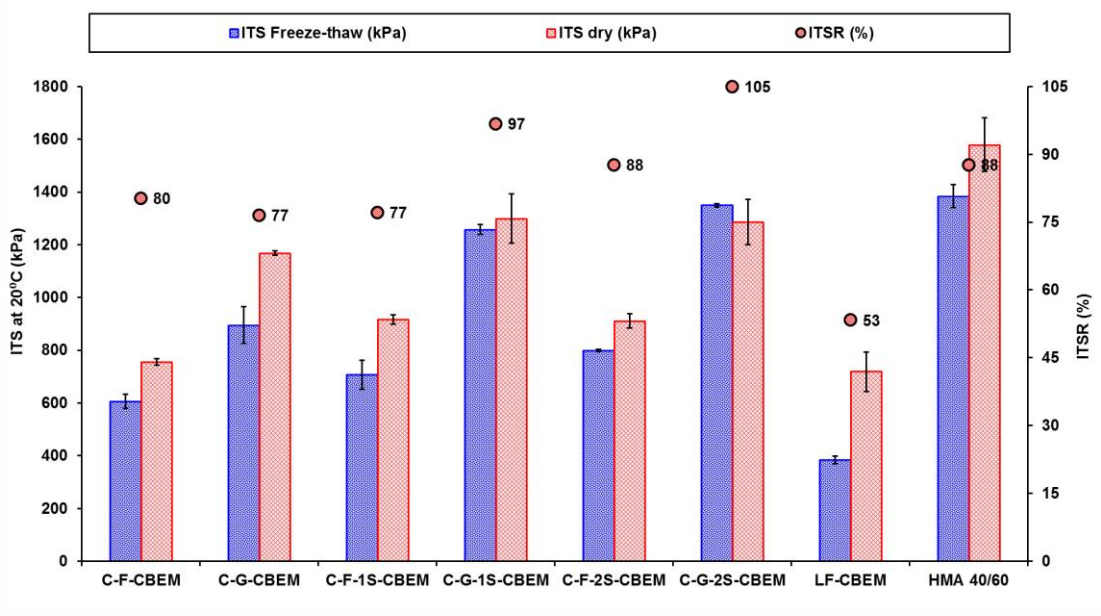


Figure 5.26 The results of frost damage for CBEMs treated with blended fillers

It should be highlighted that there is no universally accepted minimum limit to define CBEMs as durable materials for structural purposes in a pavement. However, the author would suggest that CBEMs should be considered sufficiently moisture and frost resistant for use in a surface layer if the values of ITSR for both types of damage are more than 70%. A more conservative acceptable strength ratio of 80% in CBEM was suggested by Niazi and Jalili (2009), while a similar suggestion of minimum acceptable ITSR was found in the literature for non-standard HMA (Kennedy and Anagnos, 1984, Aksoy et al., 2005). Under this proposed criterion, all the CBEMs in the present study are relatively resistant to moisture and frost damage except the untreated LF-CBEM.

It is worth mentioning that the fracture surfaces of CBEMs were influenced by the type of treated fillers. Figure 5.27 (a) and (b) show the fracture surfaces of damaged specimens after ITS testing. Differences between the CBEMs are found by visual inspection of the fracture surfaces after testing. The fracture surfaces of LF-CBEM (without active filler) occurred either in the asphalt mastic, or at the

interface between the asphalt mastic and the aggregate; no aggregate fractured (Figure 5.27 (a)).

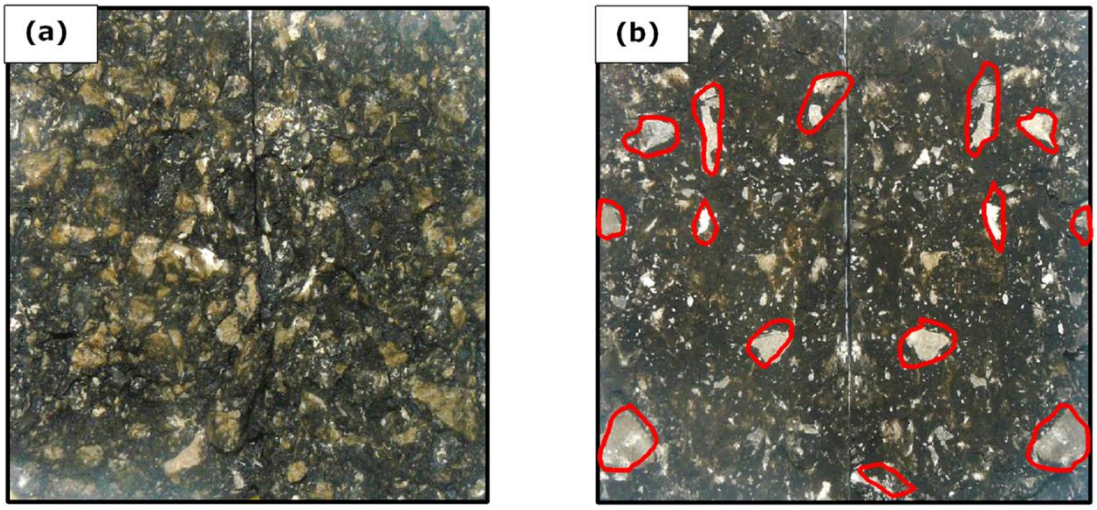


Figure 5.27 Fracture surface after moisture conditioning (a) without active filler (b) with active filler

However, for treated CBEM (with active filler) such as 5% of OPC, BBFs and TBFs, visual observations indicated that a significant portion of the fracture passed through the aggregate particles in the mixture (Figure 5.27 (b)). This is clearly related to the improved adhesion between the aggregate and bitumen due to active fillers in treated CBEMs relative to untreated CBEM.

5.9 Mineralogy and microstructure evaluation of CBEMs

It has been clearly recognized through the results presented in the previous sections that treatment with cement and blended fillers has a significant effect on volumetric, mechanical and durability properties of CBEMs. A dominant element of this improvement was attributed to the hydration process that occurred inside the mixtures. However, this raises an important question as to how these fillers (cement/active filler) interact with bitumen emulsion and affect the hydration and microstructural characteristics of CBEMs. Therefore, this section presents work designed to contribute to a deeper understanding of the microstructure and internal

composition of the mixes concerned. Two specific techniques were used to achieve the said evaluation, namely X-Ray diffraction (XRD) and scanning electron microscopy (SEM).

5.9.1 X-ray diffraction (XRD) evaluation

5.9.1.1 Test configuration

It has been established that XRD analysis is one of the most suitable techniques for examining the mineralogical patterns of materials (Rendell et al., 2002). The X-ray pattern of each material is recognised by a unique 'thumbprint'. It has been found that the solid materials can be classified into non-crystalline (amorphous) or crystalline. The atoms in the non-crystalline material are arranged in a random pattern, whereas they are arranged in a regular pattern in the crystalline material. This technique analyses the intensity and the angle of the diffracted X-ray beam after encountering a plane of atoms in a material (Alizadeh, 2009). The presence of non-crystalline material changes certain peaks in the detectable diffraction line positions and also in the magnitude of the peaks. However, each atom in the orientated structure of a crystals yields detectable diffraction lines when exposed to X-ray waves. The XRD equipment and schematic diagram for the mechanism of the test is illustrated in Figure 5.28. To simulate the detectable diffraction lines and enable identification of the crystal structure, Bragg's Law was used as described in Equation 5.11 (Rendell et al., 2002).

$$n\lambda = 2 \times d \times sin\theta \qquad \text{Equation 5.11}$$

where:

d: Distance between lattice planes in the crystal; θ: Incident/diffracted angle; n: Integer; λ: Wavelength of the scattered X-ray wave.

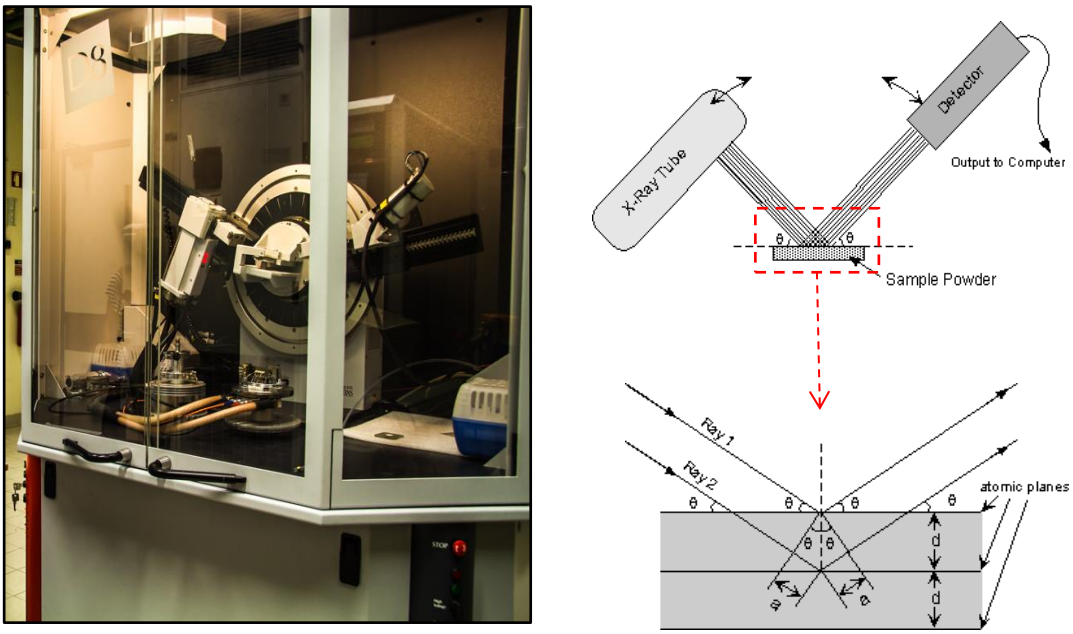


Figure 5.28 XRD equipment and schematic of X-ray diffraction, adopted from (Erdem, 2012, Nelson, 2015)

Firstly, the powder samples were positioned and flattened carefully in the sample holder of the XRD equipment. After that, these samples were illuminated with X-rays of fixed wave length by a Cu-anode x-ray tube. Then the intensity of reflected radiation was recorded using a goniometer.

The data was analysed for the reflection angle to calculate the inter-atomic spacing. The intensity was measured to distinguish the various d spacing, and the results were compared to known data to identify possible matches. A scanning speed of 2° per minute and a step of 0.02° were used in the range of 5 to 60° using a Bruker AXS D8 Advance XRD equipment.

5.9.1.2 Sample preparation

A limited study on six mixes, namely, LF-CBEM, 5C-CBEM, C-F-CBEM, C-F-2S-CBEM, C-G-CBEM and C-G-2S-CBEM was conducted. After 28 days of curing at 20°C, CBEM specimens were crushed into small parts. For XRD examination, some

of these parts (from the middle of the samples) were ground to a powder and passed through a 63μm sieve. The grinding process was continued until all parts passed through the sieve. This was to detect all the crystalline hydration phases in the XRD patterns. The powder samples were positioned and flattened carefully in the sample holder of the XRD machine. Scanning procedures as described in the previous section were carried out. Figure 5.29 summarizes the methodology to investigate the internal microstructure of CBEM using XRD and SEM investigation.

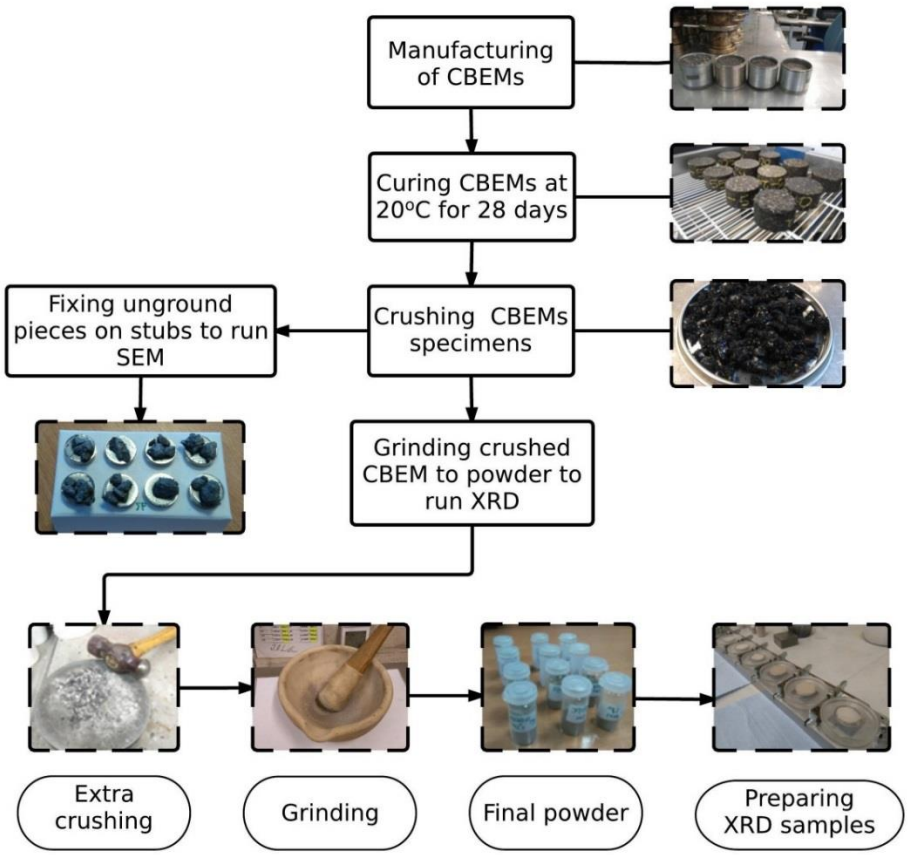


Figure 5.29 Methodology to investigate the mineralogy and microstructure of CBEMs

5.9.1.3 Results and discussion

X-ray diffraction analysis was utilised to study the hydration of blended cementitious materials and the mineralogical patterns of the crystalline solids

within the CBEMs. The X-ray diffraction pattern of selected CBEM powders is shown in Figure 5.30 (a-f).

The results demonstrate the following:

- The detected phases of LF-CBEM powder are quartz (SiO_2) and calcite ($CaCO_3$) only.
- The maximum peak of calcite in all mixes is likely to be due to the using of limestone aggregate as the test was conducted on mixture specimens.
- Different phases appeared in 5C-CBEM, namely Portlandite ($Ca(OH)_2$) and Ettringite ($Ca6Al_2(SO_4)3(OH)12.26H_2O$).
- BBF and TBF-treated mixes showed phases such as quartz (SiO_2), calcite ($CaCO_3$) and a relatively small appearance of Ettringite ($Ca6Al_2(SO_4)3(OH)12.26H_2O$), especially in C-F-CBEM.

As would be expected, LF-CBEM (Figure 5.30 (a)) does not include any phases related to hydration products; LF plays an inert filler role in the mix. However, the presence of Portlandite and Ettringite after substituting the LF with OPC in 5C-CBEM (Figure 5.30 (b)) would indicate that a change in the microstructure has occurred, accordingly. This change was as a result of the interaction between cement and bitumen emulsion/water. Also, the hydration products observed inside the mixture were supported the suggestion by Needham (1996) that OPC creates a secondary binder in cement-treated CBEMs. At the same time, the phases noticed in 5C-CBEM powder are much closer to those seen in concrete research (Lothenbach et al., 2007, Ylmén et al., 2009). Although BBF and TBF-treated mixes generally showed phases such as quartz and calcite as shown in Figure 5.30 (c-f), it is supposed that the microstructure was changed due to the hydration process of cement and other SCMs in a similar way to 5C-CBEM.

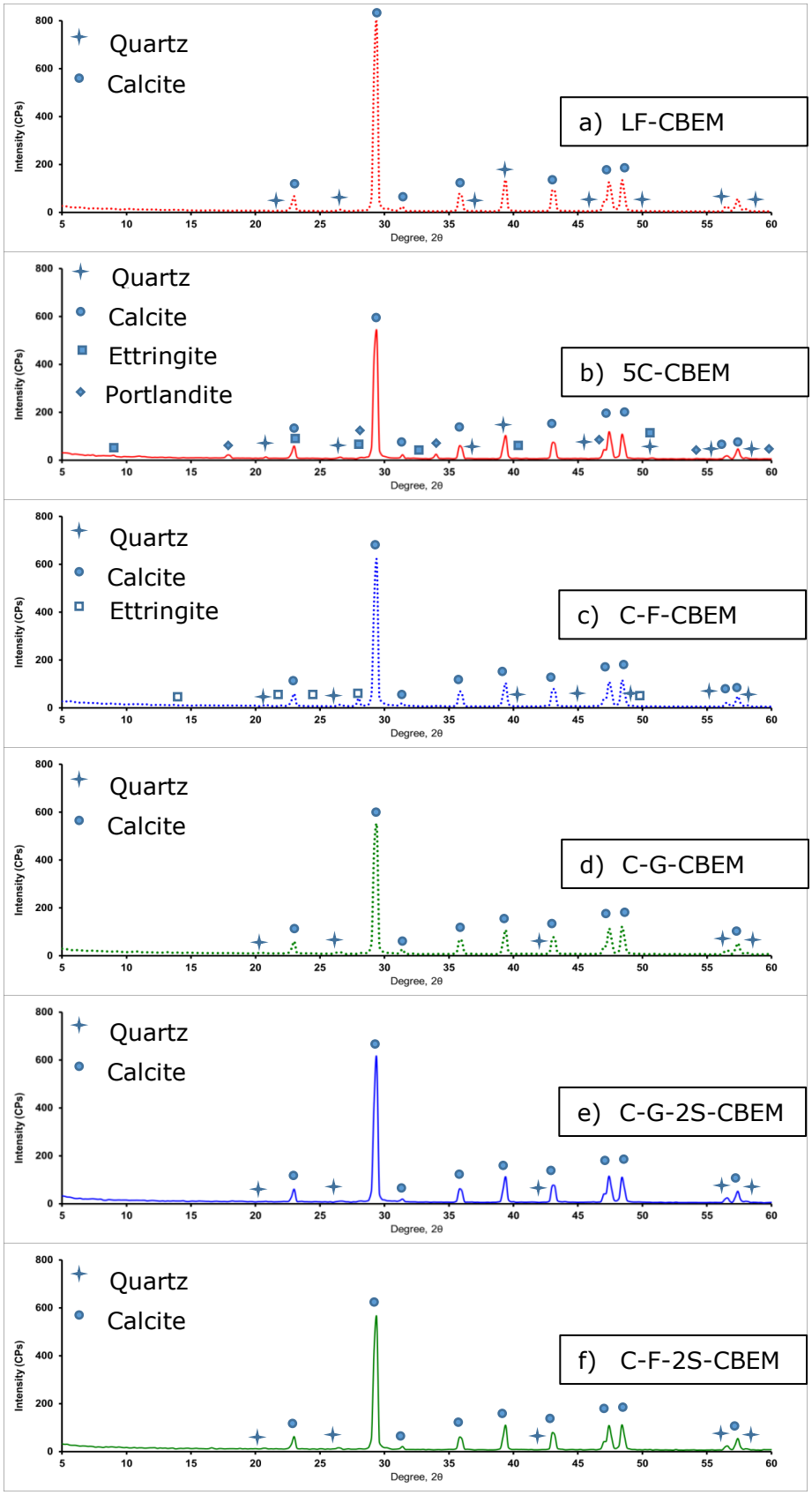


Figure 5.30 XRD results of selected CBEMs

It is also worth highlighting that the XRD analysis demonstrated a presence of Portlandite with a relatively high reference intensity peak in the 5C-CBEM indicating a lower degree of hydration compared to the other mixes. The Portlandite in all the inspected specimens was identified by a reference intensity peak at 34.1° 2-theta scale (Rizwan, 2006). The intensity values at 34.1° were reduced significantly in C-G-CBEM, C-F-CBEM, C-G-2S-CBEM and C-F-2S-CBEM compared to 5C-CBEM. This reduction might be explained by the reaction of Portlandite with pozzolanic materials. Another potential reason is that BBFs and TBFs, which contain low cement content, lead to reduced Portlandite availability.

Overall, the absence of this compound in the XRD pattern of the BBF and TBF – treated mixes might be an indicator of a higher degree of hydration by reducing the concentration of undesired hydration products such as large crystals of Portlandite. This then leads to enhancement of most engineering features of these mixes.

Another important point that must be mentioned is the presence of Ettringite particularly after 28 days of curing. This could be an indicator of a delay in the hydration process. This point will be discussed in detail in the next section. 5.9.2

5.9.2 Scanning electron microscopy (SEM) evaluation

SEM is a technique capable of revealing the details of very fine objects. It has been utilized for evaluating the microstructure of cementitious materials. Another technique is optical microscopy which has been used for the purpose of evaluating concrete and cement clinker materials. However, the use of normal light for image production in this technique gives lower resolution and depth of focus of the formed images (Hemavibool, 2007).

Fundamentally, the scanning process consists of speeding up electrons, which are originally produced from the electron gun in the microscope, by using an acceleration voltage, and then focusing them (in an electron beam) to a spot on the specimen surface. The focus can be obtained with the aid of deflection coils after the electron beam has passed through two condenser lenses for voltage acceleration purposes as shown in Figure 5.31 (Fens, 2000, Suzuki, 2002).

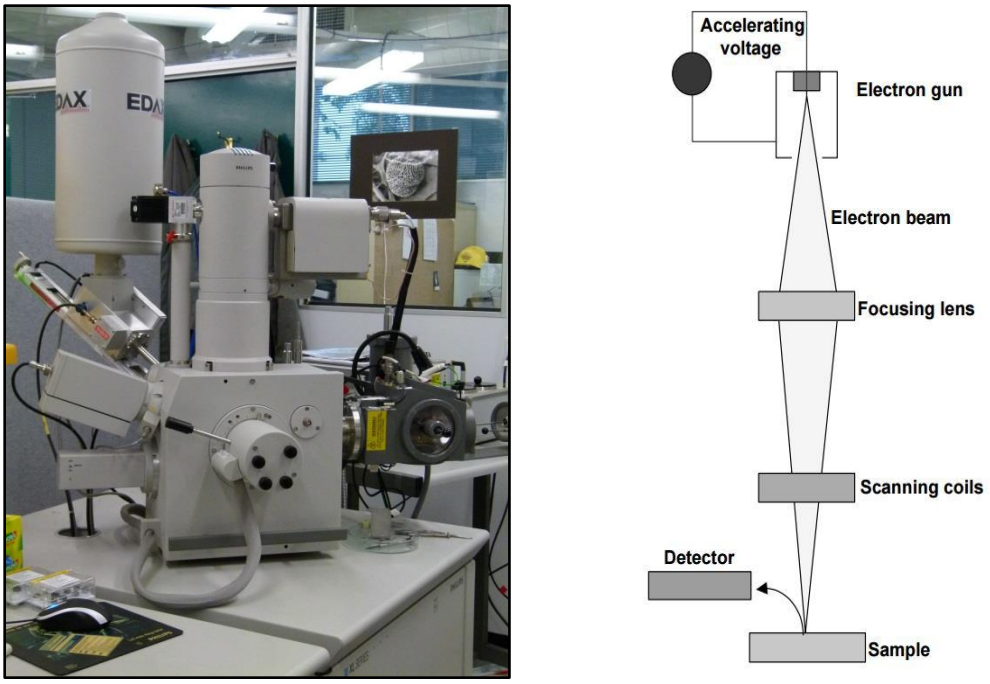


Figure 5.31 SEM equipment and schematic of SEM process (Fens, 2000)

Overall, these processes generate three major types of electrons. In fact secondary electrons, backscattered electrons, x-rays, auger electrons, and other responses are produced, as shown in Figure 5.32 (Fens, 2000). These can allow various modes of observation and/or microanalysis. SEM is the most common observation mode, which includes the capture of secondary and backscattered electrons. In this research work, SEM observations were achieved by using a Philips XL 30 SEM instrument. The SEM micrographs with different magnification were captured using a resolution of 4-5 nm under high vacuum and a test voltage 10 kV.

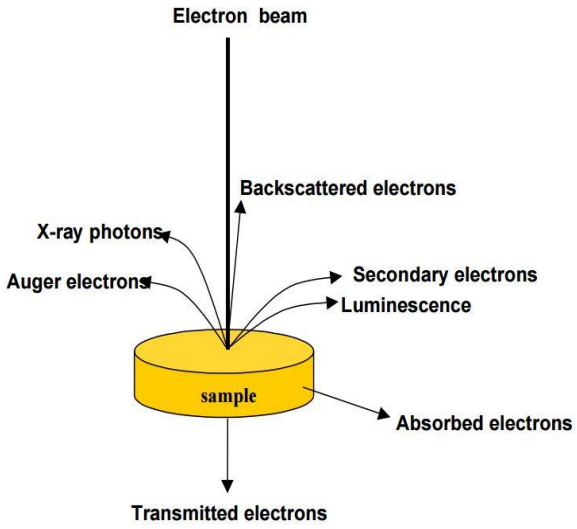


Figure 5.32 Interaction between the beam and the sample, generation of different signals (Fens, 2000)

5.9.2.1 Sample preparation

A limited study on six mixes, namely, LF-CBEM, 5C-CBEM, C-F-CBEM, C-F-2S-CBEM, C-G-CBEM and C-G-2S-CBEM was conducted. After 28 days of curing at 20°C, CBEM specimens were crushed into small parts. Thereafter, these parts were fixed on small SEM stubs and exposed to high vacuum. Then, a platinum coating was applied to the fractured specimen before capturing the SEM images (secondary electron mode) using a Philips XL 30 SEM instrument, as shown in Figure 5.31. The methodology used in this investigation is presented in Figure 5.29.

5.9.3 Results and discussion

SEM observations for the selected mixes are shown in Figure 5.33 to Figure 5.36. Figure 5.33 and Figure 5.34 present the morphology of microstructure for LF-CBEM and 5C-CBEM, respectively. While the morphology of microstructure for (C-G-CBEM and C-G-2S-CBEM) and (C-F-CBEM and C-F-2S-CBEM) are illustrated in Figure 5.35 and Figure 5.36, respectively.

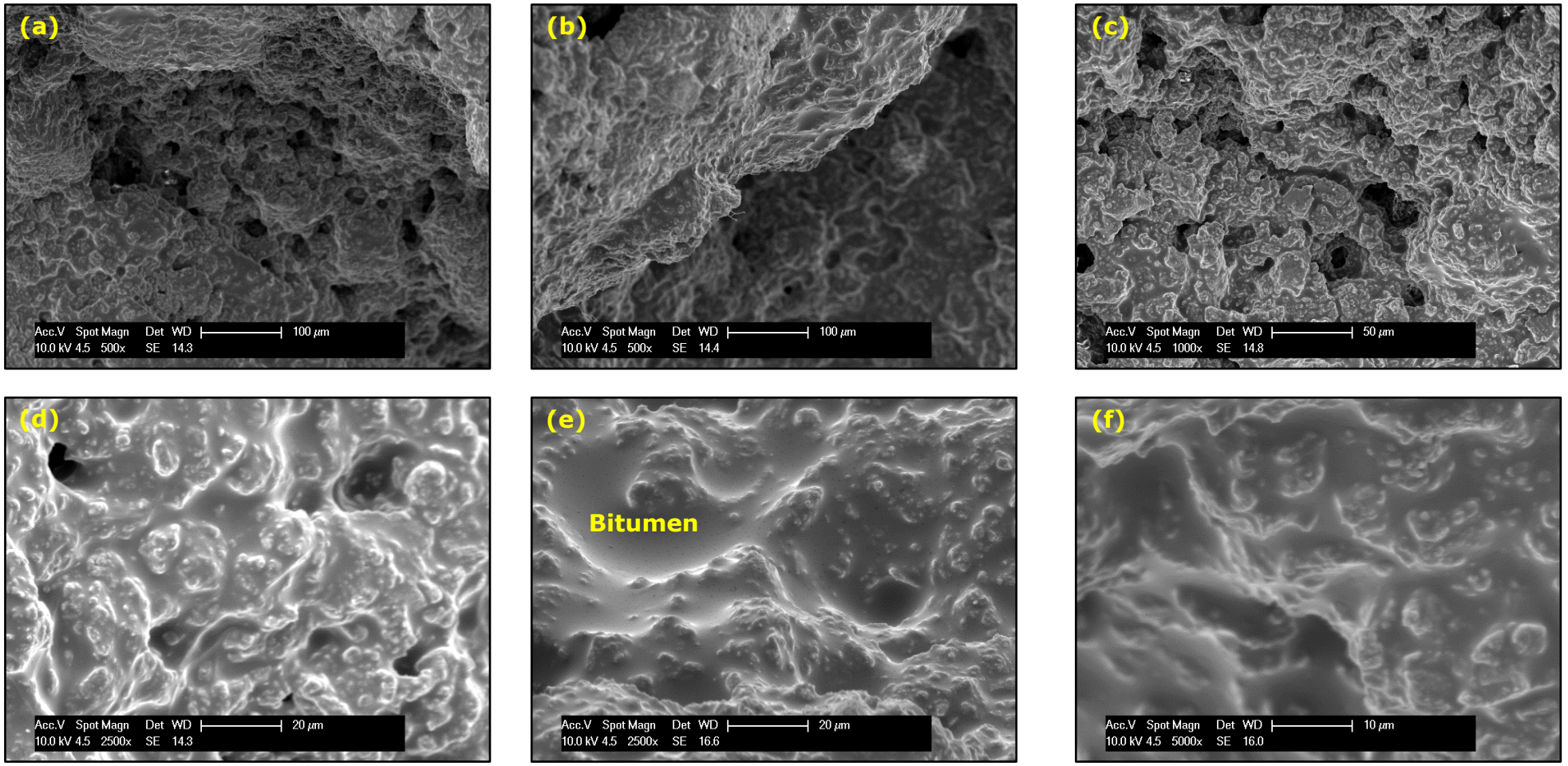


Figure 5.33 Morphology details of the microstructure of LF-CBEM

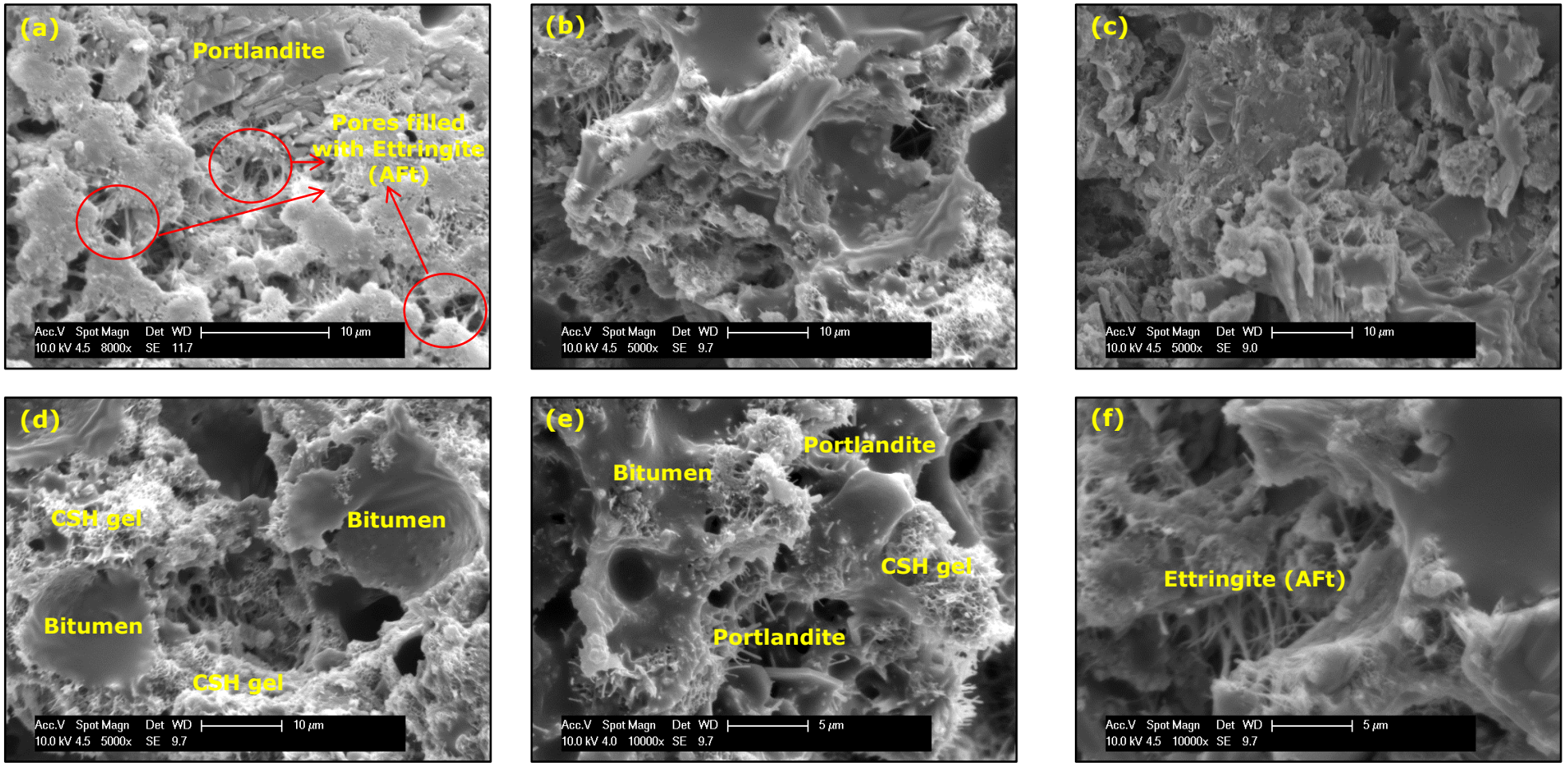


Figure 5.34 Morphology details of the microstructure of 5C-CBEM

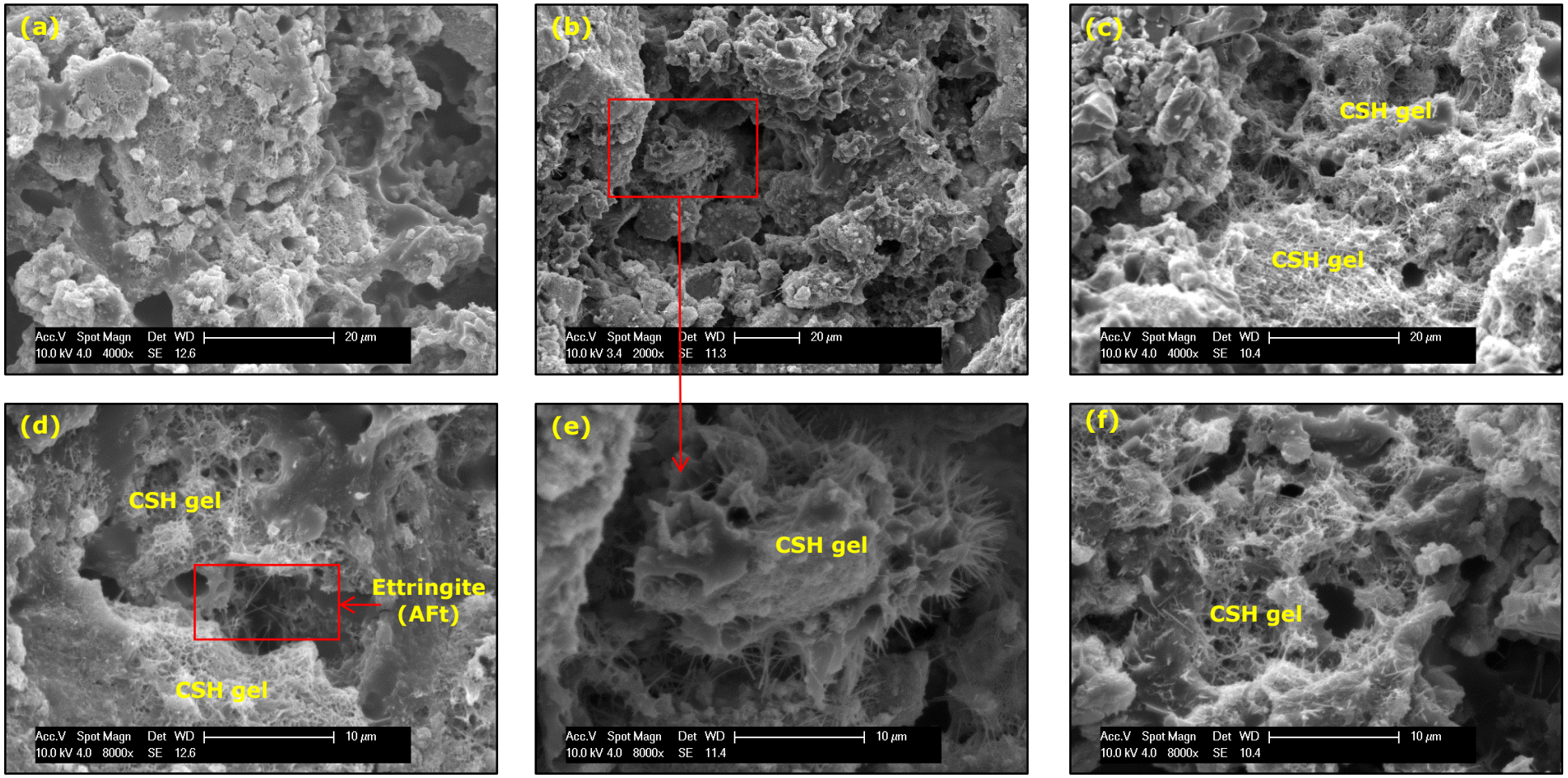


Figure 5.35 Morphology details of the microstructure of C-G-CBEM (a, b, d and e) and C-G-2S-CBEM (c and f)

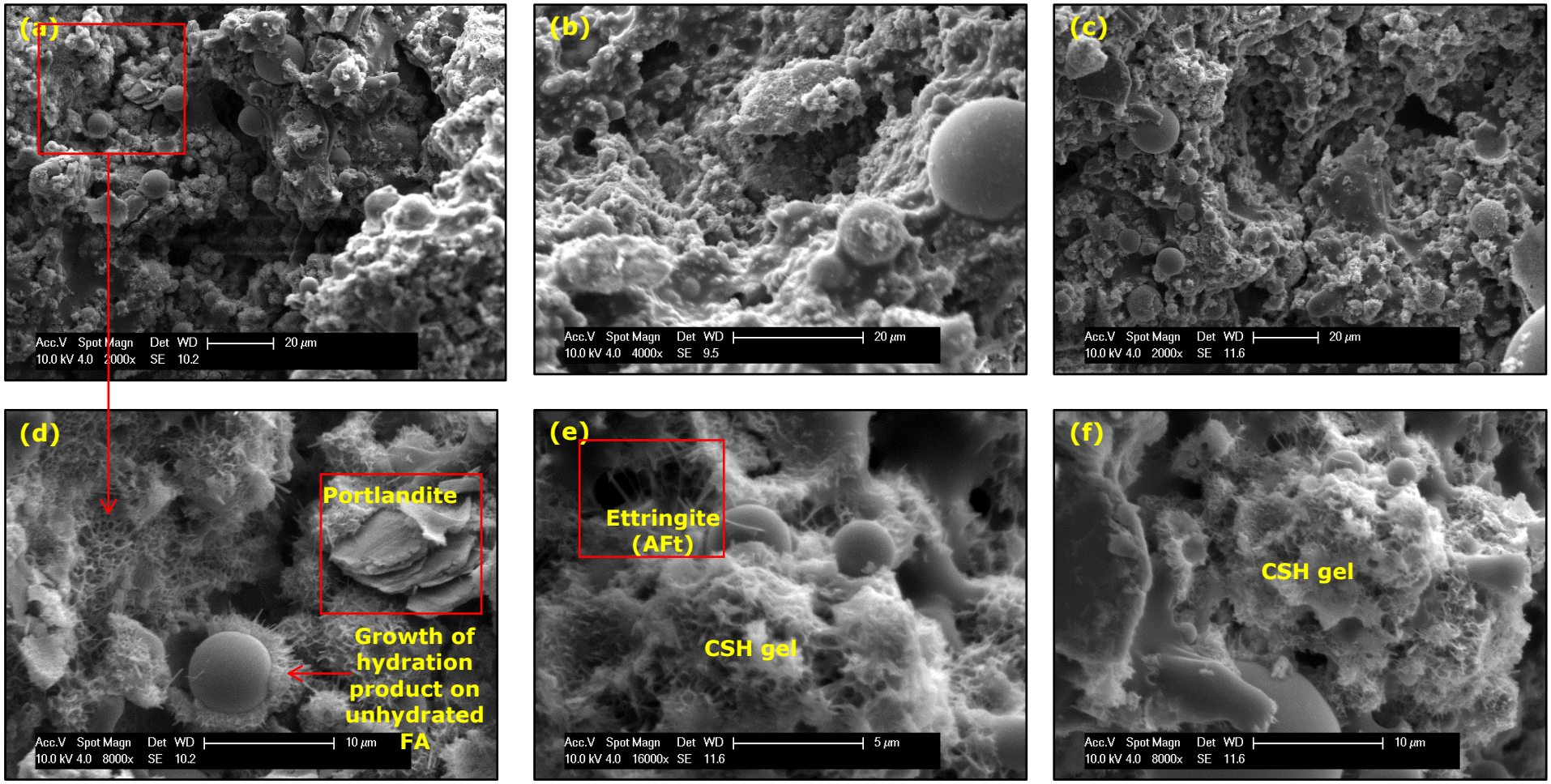


Figure 5.36 Morphology details of the microstructure of C-F-CBEM (a, b, c, d and e) and C-F-2S-CBEM (f)

The following points can be noticed from these figures:

- In LF-CBEM, the SEM observation presents a smooth surface texture while the other mixes are much rougher in texture, having a pock-marked surface.
- A CSH gel was observed in all mixes except LF-CBEM. This gel is considered as one of the main hydration products able to change the microstructure of CBEM. However, this is an amorphous phase which is not detected by XRD. The shape of this gel type is flaky aspect-like shape, and rounded and compact globule-like shape.
- Also the same crystalline hydrated phases detected by XRD (Portlandite and Ettringite) are also observed in Figure 5.34. The shape of Portlandite is tiny hexagonal plate-like shape and Ettringite takes the form of needle-like shapes.
- SEM confirmed the finding of Ettringite in the XRD results of C-F-CBEM, Figure 5.36. Moreover, the SEM also proved the presence of tiny hexagonal crystals of Portlandite in the C-F-CBEM, which was not detected by XRD.
- The SEM observation of TBFs, particularly GGBS+SF, shows the CSH gel as the dominant hydration product in the mixture.

Based on the XRD results and SEM observation for LF-CBEM, there is no evidence that a change in the composition of LF occurred after mixing with water and emulsion. This indicates the non-reactivity of this filler and its inability to enhance the internal microstructure and chemical composition, as the microstructural observation revealed.

A particular issue that should be highlighted is the growth and development of the hydration products in CBEMs, due to the presence of bitumen emulsion. In fact, different studies (Pouliot et al., 2003, Du, 2014, Wang et al., 2015) suggest the

presence of bitumen emulsion with cement in the mixture has a delaying effect on the cement hydration. In contrast, a recent experimental study carried out by Fang et al. (2014) revealed that the behaviour of bitumen emulsion in the presence of cement and filler is still unclear and it may slightly retard or accelerate cement hydration, but has no significant effect on the overall degree of cement hydration. Thus, it would be interesting to identify the changes in the formation of the hydration products in CBEMs as well as those due to the addition of active fillers in these mixtures.

The SEM examination in Figure 5.34 suggested that the presence of the bitumen might not affect the hydration of the silicates in cement. The formation of additional CSH gel was observed due to the replacement of conventional LF by cement and active fillers. However, it seems that it can cause a delay in the formation of other hydration products (Ettringite) resulting from the hydration of aluminates in cement (as shown in Figure 5.34 (a) and (f)). Nevertheless, the SEM examination (Figure 5.35 (d) and Figure 5.36 (f)) reveals that, even after 28 days of curing, the presence of Ettringite with needle shape (AFt) was clearly observed in many places in the BBF-treated mixes. This is especially the case in the capillary voids of the C-F-CBEM and C-G-CBEM. The presence of the AFt phase at later ages indicates a delayed reaction, similar to the observation for 5C-CBEM. However, the resulting AFt phase is not an expansive hydration phase at ambient temperature (Stark and Bollmann, 1999). Thus, it can improve the volumetric properties (less porosity) of the CBEM by minimising both the pore sizes and their continuity, see section 5.5. This consequently inhibits the movement of water and other types of aggressive fluid into the mixture and can thus effectively improve the durability of CBEMs.

However, when exposed to heat due to hot/warm weather in the presence of water, AFt transforms into the second expansive form which is monosulfate with prismatic shape (AFm). This form comes with an increase of 2.3 times in volume (Stark and

Bollmann, 1999). The formation of internal stresses inside the capillary pores of the bitumen-cement matrix due to this volume increase and the susceptibility of AFt to dissolve in the presence of water might be a potential reason for less durable mixtures.

The SEM observations indicated that the deposition of AFt phase inside the capillary pores was more pronounced in the FA binary mixture in comparison with GGBS. However, it completely disappeared in the presence of SF addition for the TBF mixtures (both FA and GGBS). Instead, internal CSH gel formation was deduced as shown in Figure 5.35 (c) and (f) and Figure 5.36 (e), indicating the potential benefit of adding SF. From these results, it was concluded that a higher degree of hydration in the BBF and TBF mixtures had been obtained. This observation may lead to enhancement of most engineering features. This might be as a result of the pozzolanic activity of the FA, GGBS and the very high reactivity of SF. Active fillers and mineral admixtures can efficiently consume the Portlandite phase in the cement matrix and produce a higher degree of hydration and dense internal microstructure with less porosity. This might be achieved by producing an additional CSH (cement gel) in the presence of water. Both Ca/Si ratio and the available water molecules in the new CSH products might give different features compared to the original CSH hydration product (Mohammed, 2015).

5.10 Summary

The primary aim of this chapter was to investigate the enhancement of CBEMs using cement, binary and ternary blended fillers (BBFs and TBFs), including an in-depth assessment of the microstructure. The mechanical performance was evaluated in terms of stiffness modulus over one year and resistance to permanent deformation and resistance to crack initiation and crack propagation while durability evaluation was carried out in terms of resistance to moisture and frost damage.

Furthermore, the mineralogy and microstructure of CBEMs were evaluated using X-ray diffraction analysis and scanning electron microscopy.

The conclusions of the study can be summarized as follows:

- A considerable amount of water is maintained inside CBEM treated with cement and blended fillers which may be used for enhancing the hydration process with time and producing new hydration products due to the filler reactivity.
- A significant improvement was achieved in stiffness modulus of CBEMs due to incorporation of cement and blended fillers. This improvement might be attributed to a complex mechanism occurring inside treated CBEMs, which could be described as follows:
    - The cement and active filler create another binder in the mixture through the hydration process of cement and SCMs.
    - The presence of this kind of filler would increase the breaking of bitumen emulsion as reported in the literature.
    - Cement and SCMs could absorb the trapped water and enhance the hydration process.
    - The presence of cement and SCMs may lead to an improvement in the volumetric properties

- All treated CBEMs were also found to reduce temperature susceptibility as the slopes of stiffness modulus variation were less than the equivalent for HMA 40/60 and untreated CBEM (LF-CBEM). This might be considered as an excellent advantage regarding pavement performance in hot weather. It could potentially make the asphalt material less prone to cracking at low temperatures and less prone to rutting at high temperatures.
- Excellent performance was found in the resistance of CBEM treated with cement and blended fillers to permanent deformation, as follows:
    - The accumulated permanent strains in the CBEMs treated with cement or blended fillers was found to be less than 1% under high

stresses. A decrease in stress level decreased the permanent deformation substantially.

- The treated CBEMs were also found to be less temperature susceptible than HMA and untreated CBEM in terms of permanent deformation.

- A significant improvement in tensile strength was found in CBEM treated with cement and blended fillers, particularly those treated with GGBS. This would further imply that modified mixtures appear to be capable of withstanding large tensile stress prior to cracking.
- The treatment of CBEMs using cement or blended fillers significantly improves the fatigue performance. They have a longer fatigue life at strains of less than 200 micro-strain (low stress levels) while at higher than 200 micro-strain (high stress levels) the material behaved in a brittle manner and failed under a low number of cycles compared with HMA 40/60. However, the untreated CBEM (LF-CBEM) exhibited inferior fatigue performance relative to both HMA 40/60 and treated CBEMs.

- A reduction in the fracture toughness and an increased tendency for the fracture to become brittle were also confirmed with CBEM treated using cement and blended fillers.
- For durability evaluation, the treated CBEMs showed less susceptibility to severe environmental conditions such as moisture and frost damage.
- Mineralogical and microstructural assessments suggested that the presence of bitumen emulsion might not affect the hydration of the silicates in treated CBEMs. The formation of additional CSH was observed due to the replacement of conventional LF by cement and blended fillers. However, it seems that this can cause a delay in the formation of other hydration products (Ettringite) resulting from the hydration of aluminates in cement.

- Moreover, the mechanical properties and the mineralogical and microstructural assessments suggest that the SF addition to BBF-CBEMs can eliminate any delay in hydration product formation (aluminates in cement) caused by bitumen emulsion in the CBEMs. However, the effect on the other hydration products (silicates in cement) might be closer to that for a pure cement matrix without bitumen emulsion.

Chapter 6

Parametric Curing Study and Maturity Relationship Application of CBEMs

6.1 Introduction

It has been reported in the literature that the performance of CBEM is directly related to the properties and proportions of materials that are used in the mixture and to the curing condition (Needham, 1996, Jenkins, 2000, Thanaya, 2003, Oruc et al., 2007, Niazi and Jalili, 2009, Bocci et al., 2011). The CBEM requires a certain curing time to build up the required ultimate mechanical properties such as strength and stiffness. This process involves emulsion breaking, moisture loss and/or hydration of cementitious compounds in the case of CBEMs treated with cement/active fillers (Serfass et al., 2004, García et al., 2013, Cardone et al., 2014).

A wide range of studies has been undertaken to investigate the effect of accelerated curing of cold recycled asphalt mixtures cured at elevated temperature (more than 40°C). Furthermore, it is worth noting that most researchers have considered the curing temperature as a major factor that affects the curing process of CBEMs (Serfass et al., 2004, Tebaldi et al., 2014, Kuna, 2015, Ojum, 2015). Jenkins and Moloto (2008) listed several parameters affecting the curing process, categorized

into (1) climatic parameters like temperature, humidity and wind, and (2) other parameters such as aggregate gradation and properties, layer thickness, initial water content, binder content, active filler content, layers applied on top, drainage condition and, finally, traffic load.

From the literature review, it was understood that there is a lack of clarity regarding the influence of the curing process under different climatic conditions on the performance of CBEMs treated with cement/active fillers. This is because of the complex combination of three phenomena acting together during the curing process: emulsion breaking, moisture loss and hydration of cementitious compounds (Serfass et al., 2004, García et al., 2013, Cardone et al., 2014). It is important that the bitumen emulsion breaking process is achieved as soon as possible after emulsion application. However, it must not occur until after the completion of the mixing and compaction phases. Furthermore, the presence of water after emulsion breaking can negatively affect early strength gain. Increasing the curing temperature leads to an increase in the rate of water evaporation, resulting in an acceleration in the strength gain process. Furthermore, the presence of cement further accelerates the emulsion breaking process, increases the rate of bitumen coalescence and reduces the amount of evaporable water (Needham, 1996). Hydration of cementitious compounds is also linked to moisture loss; the chemical reactions that take place during the hydration of cementitious fillers require the presence of water or at least humid environment and do not require any moisture loss.

Thus, the main objective of this chapter is to investigate the level of impact of climatic parameters such as curing temperature and relative humidity (RH) in addition to the impact of curing time and the presence of active filler (cement/ blended fillers) on the curing process in CBEMs. The effect of such factors on the curing process has been evaluated in the laboratory in terms of moisture loss

monitoring, stiffness modulus and resistance to permanent deformation, and binder characterization before and after curing. Also, the study aimed at developing a prediction model to assess in-situ CBEM performance using maturity relationships, which is a normalised expression of the degree of in-situ curing of CBEM. The maturity is a method that has been extensively used to predict the in-situ strength gain of concrete, using the principle that concrete strength is directly related to both age and curing temperature history.

6.2 Methodology adopted

In order to achieve the above-mentioned objectives, the present study was conducted in two phases. In the first phase a comprehensive experimental curing design program was carried out to deduce the level of impact that factors such as temperature, humidity, time, presence of cement/active fillers have on the curing of CBEMs. Therefore, the curing procedure was selected in such a way as to evaluate a wide range of contributory factors on the curing process. Table 6.1 summarizes the experimental program for the first phase. Meanwhile the second phase treats the applicability of the maturity method as a tool to predict the in-situ characteristics of CBEMs.

Table 6.1 Summary of experimental program for the first phase

Test	Curing Time (days)	Curing Temperature (°C)	Relative Humidity
Moisture loss monitoring	2, 3, 5, 7, 10, 14, 28, 54, 84	5, 20, 40	Low level, less than 50%
ITSM	3, 7, 10, 14, 28, 54, 84	5, 20, 40	Low level, less than 50%
ITSM	7, 28	5, 20, 40	High level, more than 85%
RLAT	28	5, 20, 40	Low level, less than 50%
Frequency sweep, softening point	28	5, 20, 40	Low level, less than 50%

Due to shortness of time and materials, the test was limited to CBEMs treated with cement and BBFs. A series of mixtures including LF-CBEM, 1C-CBEM, 3C-CBEM, 5C-CBEM, C-F-CBEM and C-G-CBEM, cured at constant temperature (5, 20, 40°C), have been evaluated. Moreover, two RH levels (less than 50% and higher than 85%) were adopted in this study. All specimens were cured unwrapped in order to guarantee free water evaporation.

The curing temperatures were selected to represent different conditions that may apply during CBEM curing. The severe condition at 5°C was selected to simulate cold climatic conditions (Bocci et al., 2011) while the curing at 20°C was chosen to simulate a more usual site condition while avoiding any early ageing of the binder (Serfass et al., 2004). Finally, curing at 40°C was used to represent typical summer temperature in some European countries (Bocci et al., 2011) and also to represent the accelerated curing suggested by literature (Jenkins, 2000, Thanaya, 2003, Cardone et al., 2014, Graziani et al., 2016). Noteworthy, several authors suggest to keep the curing temperature below the softening point of the bitumen in order to avoid the ageing of bitumen (Khalid and Monney, 2009, Cardone et al., 2014, Kuna, 2015); hence 40°C is reasonable. A plastic box with dimensions 605×370×355 mm was used as a simple humidity chamber to cure the CBEMs under high level of humidity. A schematic diagram and photograph of the chamber are shown in Figure 6.1.

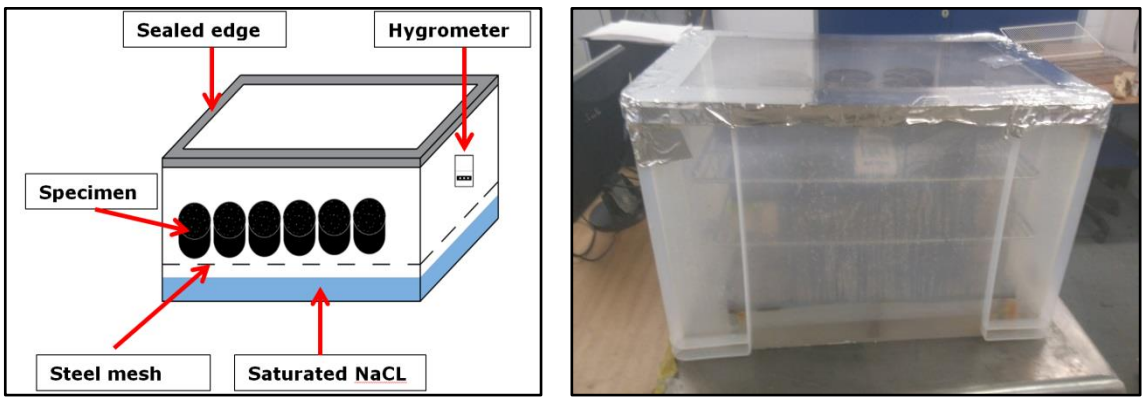


Figure 6.1 Schematic diagram and photograph of the RH chamber

A saturated NaCl solution was used to maintain a high level of humidity as recommended by Kubo (2007). The actual recorded humidity varied between 85% and 95% through the curing period (28 days) with a temperature of between 19 and 23°C. The specimens were stored over a steel mesh to avoid any contact with the saturated NaCl solution and the chamber sealed to keep the moisture inside.

6.2.1 Sample preperation and curing procedures

The same mixture proportions as in the control mix (LF-CBEM) were used to prepare the selected mixes as discussed Chapter 5. Marshall specimens were prepared for all CBEMs. The same mixture proportions, mixing method and compaction were used as described previously in section 5.5.2. After that, impact compaction (Marshall Hammer) was utilized to compact the specimens; 75 blows were applied to each face. After compaction, the curing protocol followed was divided into two stages as recommended by Jenkins (2000). In the first stage, the specimens were left in their moulds (in a sealed condition) after compaction for 24h. This was due to the fragile nature of the specimens in early life. In the second stage, the specimens were extruded and divided into two groups. The first group was conditioned in a thermostatically controlled air chamber at 5, 20 or 40°C with low RH, i.e. less than 50%. In order to keep a low level of humidity, Silica gel was placed inside the conditioning cabinet as a desiccant dehumidifier, as shown in Figure 6.2. The second group was cured in the humidity chamber. In both groups, specimens were left unsealed during the second stage of curing to guarantee free water evaporation. Table 6.2 summarizes the curing procedure for CBEMs.

Table 6.2 CBEM curing protocols used in first phase

Curing Temperatures	First stage	Second stage
5°C	24h at 20°C (sealed)	84 days at 5°C (unsealed, low RH)
20°C	24h at 20°C (sealed)	84 days at 20°C (unsealed, low RH)
40°C	24h at 20°C (sealed)	84 days at 40°C (unsealed, low RH)
20°C	24h at 20°C (sealed)	28 days at 20°C (unsealed, high RH)

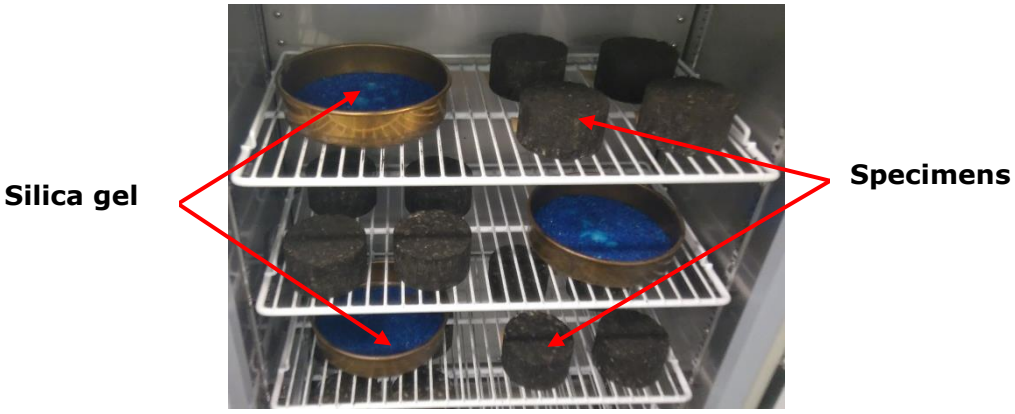


Figure 6.2 Curing CBEM at different curing temperature with lower RH

6.2.2 Experimental programme

6.2.2.1 Moisture loss monitoring

The moisture in the CBEM comprises of the water added during mixing (pre-wetting water) and the water in the bitumen emulsion. Moisture loss by evaporation is defined as the difference between the initial weight of the specimen and the weight at a given time divided by the initial weight of the specimen. During the curing period, weight measurements were made at 2, 3, 5, 7, 10, 14, 28, 54 and 84 days.

6.2.2.2 Indirect tensile stiffness modulus (ITSM) evaluation

The stiffness gain (curing trend) of CBEMs was monitored over a period of time. The non-destructive stiffness test, ITSM, was selected for assessing the stiffness modulus over a period of approximately 3 months. Three specimens per mix were conditioned before the test for 4h at 20°C then tested at 20°C. The test was carried out according to BS EN 12697-26 (European Committee for Standardization, 2012). Details of this test were given in the previous chapter, see section 5.5.1. The ITSM was chosen to allow the test to be carried out repeatedly on the same set of specimens to nullify variability in the mixtures and to derive reliable trends for stiffness evolution.

6.2.2.3 Repeated load axial test (RLAT)

The repeated load axial test (RLAT) is the most widely used standard mechanical test in the UK for assessing the permanent deformation characteristics of bituminous mixtures. The test applies a repeated pulse load to simulate the traffic and measures the permanent deformation after each repeated load. The protocol for the RLAT test was performed based on BS EN 12697-25 (European Committee for Standardization, 2005c). Details of this test were given in the previous chapter, see section 5.6.1. The specimens were cured for 28 days as mentioned in Table 6.1; thereafter they were cured at 40°C for 4h then tested at 40°C.

6.2.2.4 Bitumen binder characterization before and after the curing

After 28 days curing at 5, 20 or 40°C, the bitumen was extracted based on European Committee for Standardization (2005a) from the LF-CBEM specimens. Also, the bitumen was extracted from the bitumen emulsion by the distillation method. The extracted bitumen was characterised using frequency sweep and softening point tests.

- **Softening point test**

The softening point of extracted bitumen was obtained using the ring and ball test. The test was carried out based on the BS EN 1427 (European Committee for Standardization, 2015).

- **Frequency sweep test**

A frequency sweep test was performed on extracted bitumen using the dynamic shear rheometer (Gemini). The tests were performed under controlled strain, and the strain amplitude was limited within the linear viscoelastic response of the samples. Data were obtained from a frequency range between 0.01 rad/s and 10 rad/s, conducted between 0°C and 80°C. The 8 mm measurement system with

2 mm gap was adopted below 40°C and the 25 mm plate with 1 mm gap at temperatures higher than 40°C. The complex shear modulus G* was obtained and presented in the form of master curves with 20°C as the reference temperature.

6.3 Results and discussion of parametric curing study

6.3.1 Moisture loss monitoring

The moisture loss by evaporation during the curing process of CBEM is one of the major phenomena occurring. Monitoring the moisture loss by evaporation was carried out over 3 months of curing to explore the rate and sequence of loss of water as shown in Figure 6.3 to Figure 6.5. The initial water content in the mixture was 4.427% of total mixture weight. It was assumed that the compaction does not influence the moisture content inside the mixture through getting out the excess water.

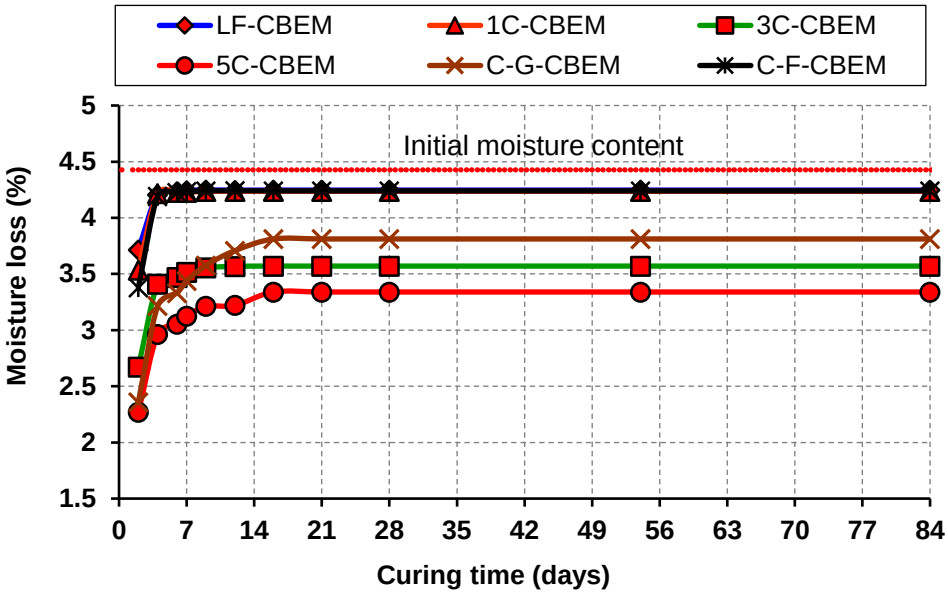


Figure 6.3 Moisture loss by evaporation for CBEMs cured at 40°C

It can be observed that the rate of evaporation during the first month is significantly influenced by the curing temperature. The higher the curing temperature the faster

was the moisture loss. In Figure 6.3, the moisture loss for mixes cured at 40°C hardly increased after 14 days, having reached an equilibrium condition. In contrast, the equilibrium condition was achieved after 28-35 days for mixes cured at 5°C and 20°C, see Figure 6.4 and Figure 6.5. The trend suggests the rate of moisture loss decreased with time at a given curing temperature. After the CBEMs had reached their equilibrium condition, there was very little moisture loss over the rest of curing period.

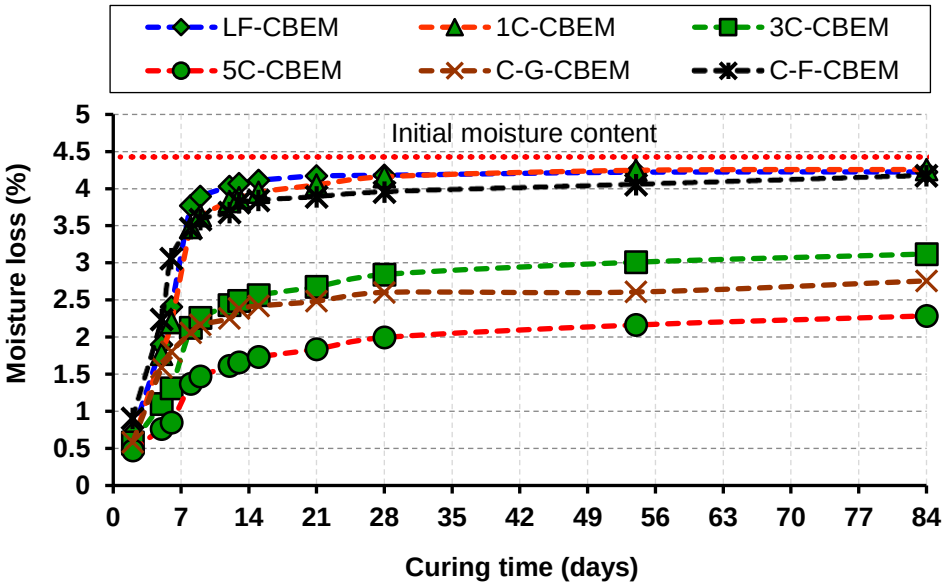


Figure 6.4 Moisture loss by evaporation for CBEMs cured at 20°C

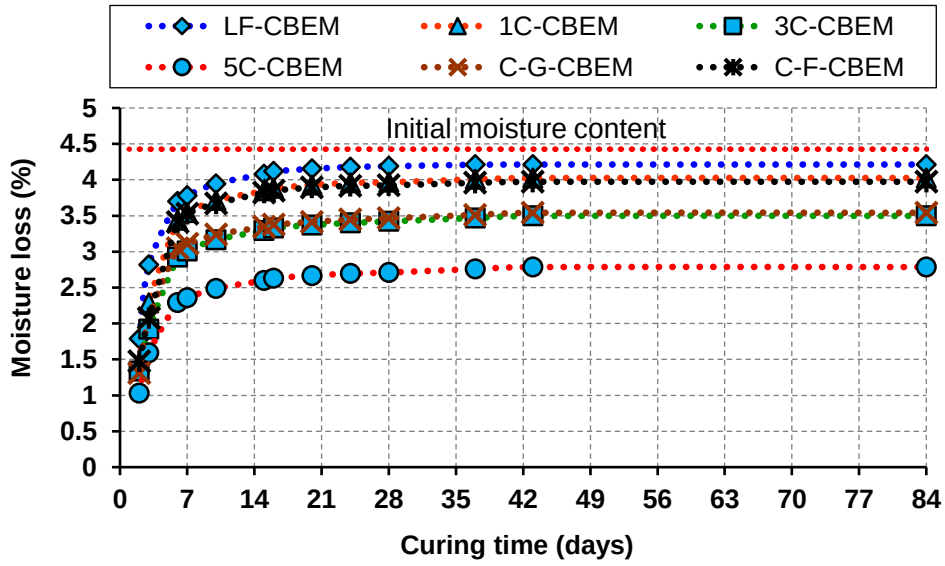


Figure 6.5 Moisture loss by evaporation for CBEMs cured at 5°C

With respect to filler treatments, the results suggest that cement/BBFs have significant influence on the amount of moisture loss in CBEM. The moisture loss decreased with increasing cement content and was similarly influenced by BBFs. This is because the water had been absorbed by the hydration process; this point will be discussed in detail in subsequent sections. The results are very close to the findings of Needham (1996) and Oruc et al. (2007).

6.3.2 Indirect tensile stiffness modulus (ITSM) evaluation

6.3.2.1 Influence of curing time and temperatures

The stiffness modulus measured at 20°C at different curing times and temperatures, is reported in Figure 6.6 to Figure 6.11. It is clear from Figure 6.6 that the stiffness modulus of LF-CBEM increased with increasing curing temperature and time. This gain was rapid for specimens cured at higher temperatures (40°C). This could be attributed to rapid water loss at higher temperature as shown in section 6.3.1. Also, in cement treated mixes (1C-CBEM, 3C-CBEM, 5C-CBEM), the stiffness modulus increased with increasing curing time. However, this gain was significantly influenced by both moisture loss and cement hydration. This leads to the interesting observation that improvement in the stiffness modulus did not continue after 28 days for 5°C and 40°C cured mixes while the 20°C cured specimens showed slight further development, as shown in Figure 6.7 to Figure 6.9. A similar observation can be noted in Figure 6.10 and Figure 6.11 for BBF treated mixes. However, the increasing of stiffness modulus after 28 days was more evident in C-F-CBEM than in to C-G-CBEM.

6.3.2.2 Influence of active filler content and curing temperatures

Figure 6.6 to Figure 6.9 show that the stiffness modulus of cement treated CBEM increased with increasing cement content at a given curing temperature. This

increase might be partly due to the removal of water from the system and partly due to the formation of cementitious bonds. However, it is noticeable that 20°C cured mixes showed the highest stiffness moduli over the curing period in comparison to 5°C and 40°C cured mixes. For example, the 5C-CBEM specimens achieved stiffness modulus of 15600, 27000 and 22500 MPa after 28 days cured at 5, 20 and 40°C, respectively. It is believed that the low curing temperature (5°C) limited the stiffness modulus gain since a low hydration reaction temperature tends to prevent hydration development (Puertas et al., 2000), although this effect has been little studied in cement treated CBEM under different curing temperatures. Moreover, the low rate of moisture evaporation also contributes in this case. More surprisingly, the results in Figure 6.6 to Figure 6.9 illustrate that the stiffness modulus for 1C-CBEM-20°C, 3C-CBEM-20°C and 5C-CBEM-20°C specimens was higher than for those cured at 40°C.

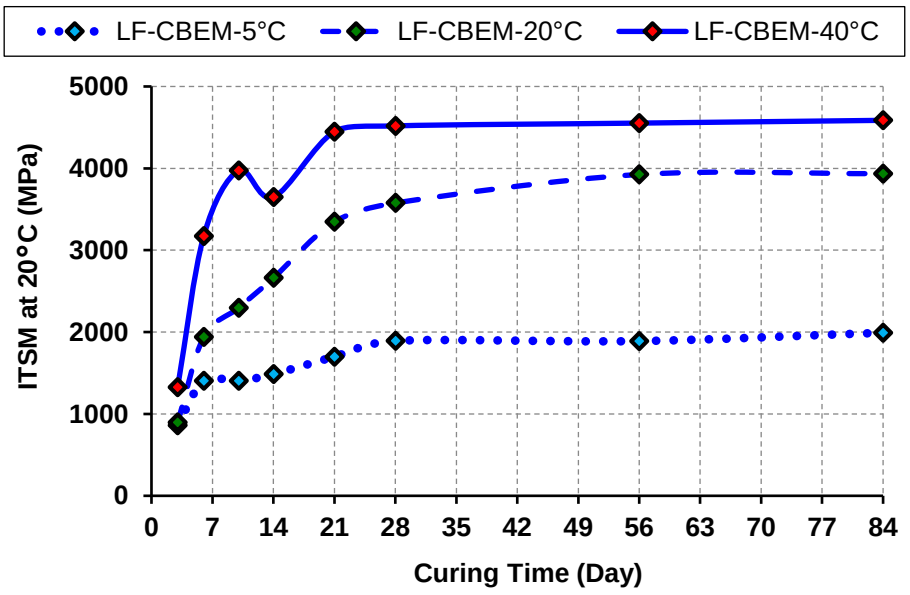


Figure 6.6 Evolution of ITSM at different curing temperatures for LF-CBEM

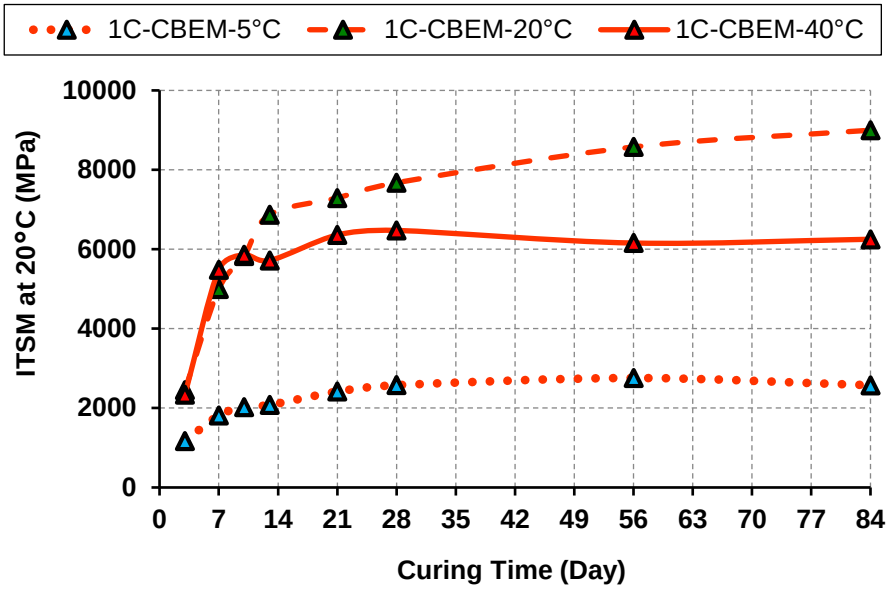


Figure 6.7 Evolution of ITSM at different curing temperatures for 1C-CBEM

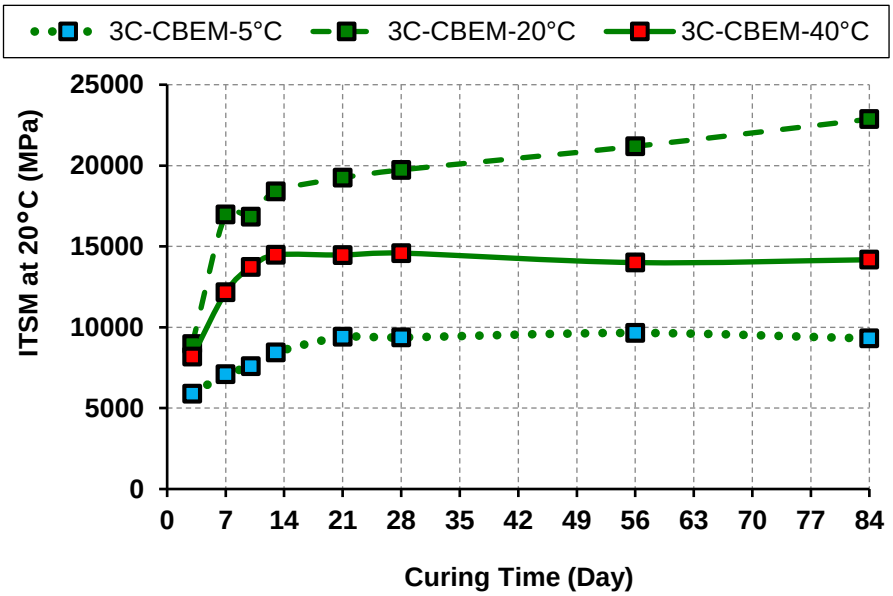


Figure 6.8 Evolution of ITSM at different curing temperatures for 3C-CBEM

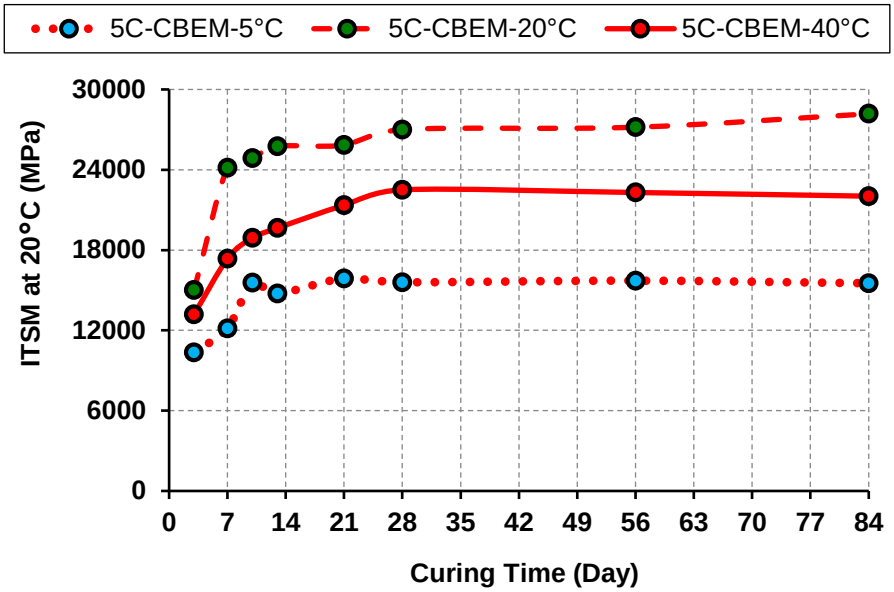


Figure 6.9 Evolution of ITSM at different curing temperatures for 5C-CBEM

A similar observation was made by Cardone et al. (2014). This could be because the rate of moisture loss is greater at higher curing temperature (40°C), particularly at early age. This may lead to insufficient water which may hinder the hydration process as suggested in the next section. Furthermore, it is interesting to mention that the density of hardened cement tends to be less uniform at higher curing temperature, which can lead to weaker spots in the microstructure (Rovnaník, 2010). Thus, further research is needed to study the effect of curing temperature on the microstructure of cement treated CBEM.

A similar observation regarding stiffness modulus can be made in the case of C-F-CBEM cured at 20°C in comparison to the other temperatures, see Figure 6.10. However, the performance of C-G-CBEM, in Figure 6.11, showed that higher curing temperature has no significant detrimental influence on stiffness modulus. The stiffness modulus for C-G-CBEM cured at 40°C is only slightly less than cured at 20°C. This may be related to the ability of GGBS treated mixtures to retain a higher amount of trapped water, which could improve the hydration process accordingly, as proved in earlier finding in chapter 5. Therefore this point might add a further

potential benefit of using BBF treated CBEMs, particularly with GGBS. However, both mixes (C-F-CBEM and C-G-CBEM) showed their lowest stiffness modulus at 5°C which may also be attributed to the same reason mentioned with respect to cement-treated CBEMs.

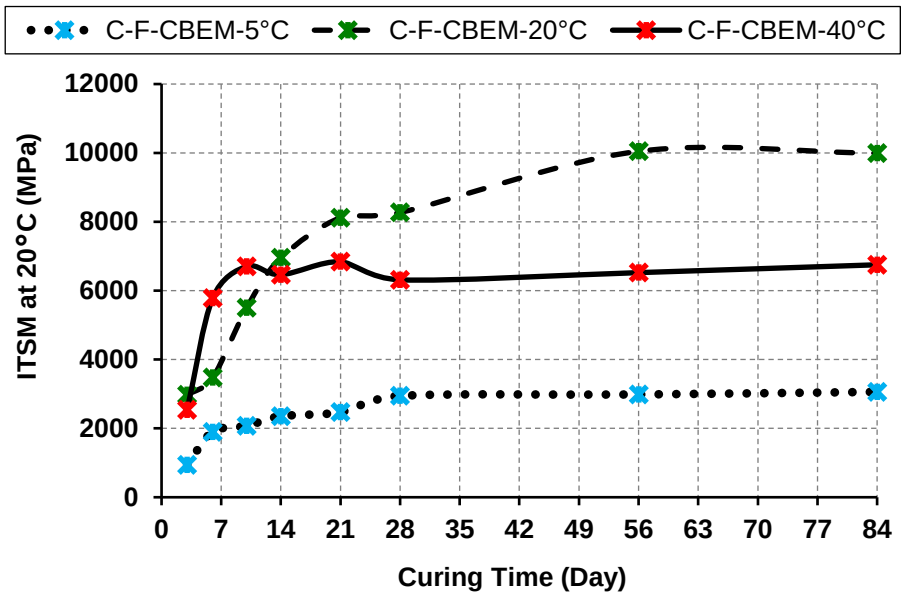


Figure 6.10 Evolution of ITSM at different curing temperatures for C-F-CBEM

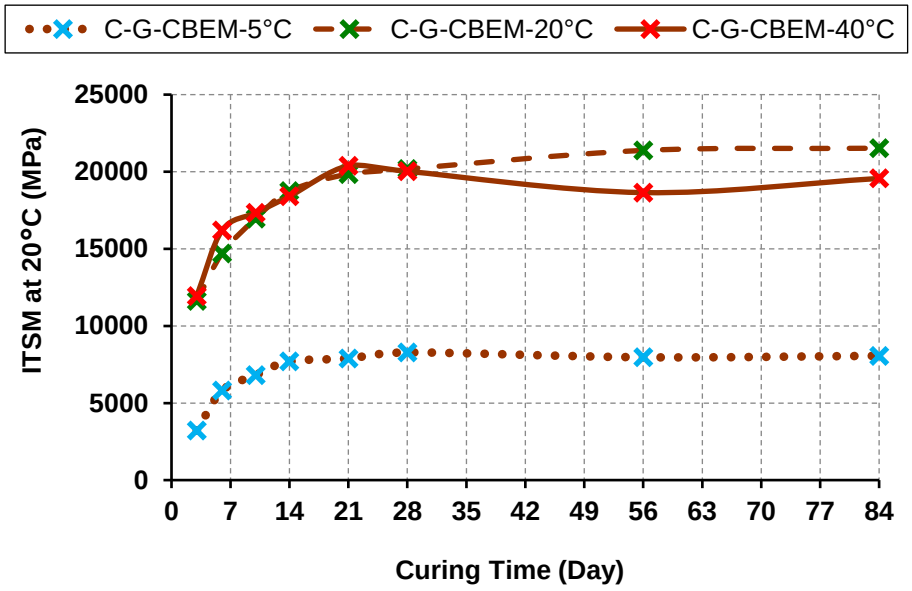


Figure 6.11 Evolution of ITSM at different curing temperatures for C-G-CBEM

Overall as a general trend, with increase in moisture loss the stiffness increased regardless of the filler treatment in the CBEM. Further discussion of the effect of moisture loss on stiffness modulus and the moisture content of CBEMs will be presented in the next section.

6.3.2.3 Influence of moisture loss on stiffness modulus

In the previous section the evaluation of stiffness modulus was presented as a function of curing time. However, some researches have suggested that in laboratory curing, the shape and dimension of the specimens may affect the curing trend of a CBEM. They suggest that a smaller specimen will cure faster than larger specimens (Serfass et al., 2004, Graziani et al., 2016, Miljković and Radenberg, 2016). Thus, a possible way to overcome this point is to look for a direct correlation between moisture loss and stiffness modulus.

For this purposes a further analysis of the relationship between the moisture loss by evaporation and stiffness modulus was carried out, as shown in Table 6.3 and Figure 6.12 to Figure 6.17. It is worth noting that the slopes of the exponential equations for LF-CBEM, 1C-CBEM and C-F-CBEM cured at 40°C are higher than for the same mixture cured at 5 and 20°C by 2.5 to 5 times, as shown in Table 6.3. This may suggest that the mechanism of stiffness modulus gain based on moisture loss is more dominant in these mixes. Meanwhile, the slopes of the exponential equations for 3C-CBEM, 5C-CBEM and C-G-CBEM are not significantly influenced by curing temperature from a mathematical point of view. However, these mixes presented high initial moisture loss at 40°C compared to other curing temperatures.

Table 6.3 The relationship between moisture loss and stiffness modulus for CBEMs

Mixture type	Curing at 5°C	Curing at 20°C	Curing at 40°C
LF-CBEM	$S = 176.1\, e^{0.55 M_{Evap}}$ $R^2 = 0.92$	$S = 645.26\, e^{0.39 M_{Evap}}$ $R^2 = 0.84$	$S = 0.481\, e^{2.131 M_{Evap}}$ $R^2 = 0.91$
1C-CBEM	$S = 388.9\, e^{0.46 M_{Evap}}$ $R^2 = 0.93$	$S = 1929.8\, e^{0.328 M_{Evap}}$ $R^2 = 0.93$	$S = 19.34\, e^{1.36 M_{Evap}}$ $R^2 = 0.98$
3C-CBEM	$S = 3074.6\, e^{0.313 M_{Evap}}$ $R^2 = 0.86$	$S = 7437.5\, e^{0.36 M_{Evap}}$ $R^2 = 0.99$	$S = 1611\, e^{0.61 M_{Evap}}$ $R^2 = 0.91$
5C-CBEM	$S = 4625.5\, e^{0.452 M_{Evap}}$ $R^2 = 0.90$	$S = 13962\, e^{0.333 M_{Evap}}$ $R^2 = 0.84$	$S = 5656.7\, e^{0.371 M_{Evap}}$ $R^2 = 0.91$
C-G-CBEM	$S = 1812.7\, e^{0.42 M_{Evap}}$ $R^2 = 0.96$	$S = 9342\, e^{0.291 M_{Evap}}$ $R^2 = 0.90$	$S = 5229.5\, e^{0.342 M_{Evap}}$ $R^2 = 0.96$
C-F-CBEM	$S = 468.8\, e^{0.44 M_{Evap}}$ $R^2 = 0.92$	$S = 1884.2\, e^{0.36 M_{Evap}}$ $R^2 = 0.88$	$S = 63.56\, e^{1.1 M_{Evap}}$ $R^2 = 0.98$

S= Stiffness modulus (MPa), M_{Evap}= Moisture loss by evaporation (%)

It is clear from Figure 6.12 to Figure 6.17, that for all curing temperatures the stiffness increased with increasing moisture loss. Also, it may be observed that when a certain moisture loss is considered the curing temperatures have different impacts on the stiffness modulus for the same mixtures. For instance, LF-CBEM cured at 40°C exhibited far better stiffness than LF-CBEM cured at 5 and 20°C with the same moisture loss at the end of the curing period, as shown in Figure 6.12. This can be explained by the fact that specimens cured at 40°C are subject to ageing over the curing period, a point that will be investigated by binder characterisation before and after the curing, see section 6.3.4.

On the other hand, the stiffness modulus of mixes 1C-CBEM, 3C-CBEM, 5C-CBEM, C-F-CBEM and C-G-CBEM showed a marked influence of moisture loss under different curing temperatures. At the same cement/BBF content, the stiffness modulus of specimens cured at 20°C was higher than those cured at 5°C or 40°C. In this case, contrary to the previous research which presents that higher curing temperature yields to high stiffness values with the time (Oke, 2010, Kuna, 2015, Ojum, 2015, Godenzoni et al., 2016, Graziani et al., 2016). Therefore, a further

study to evaluate the moisture content is need in order to explain this unexpected behaviour.

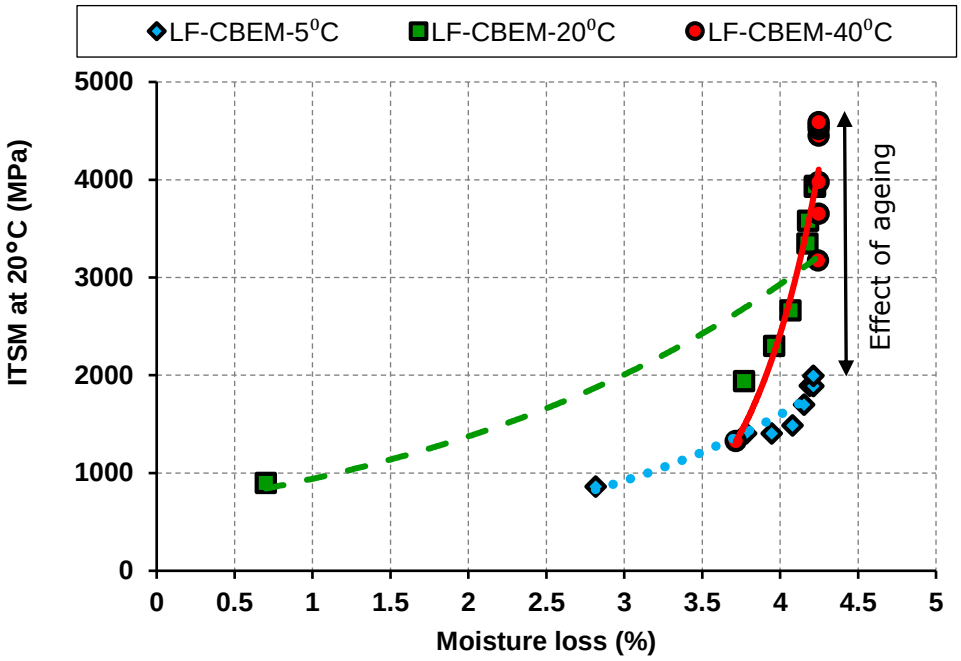


Figure 6.12 The relationship between moisture loss and stiffness modulus under different curing temperatures for LF-CBEM

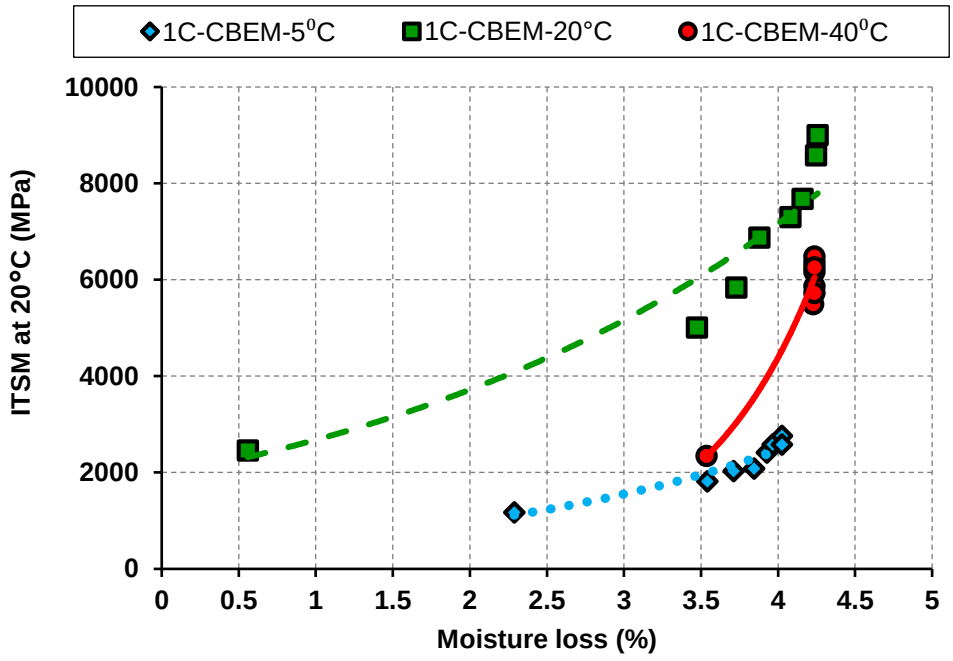


Figure 6.13 The relationship between moisture loss and stiffness modulus under different curing temperatures for 1C-CBEM

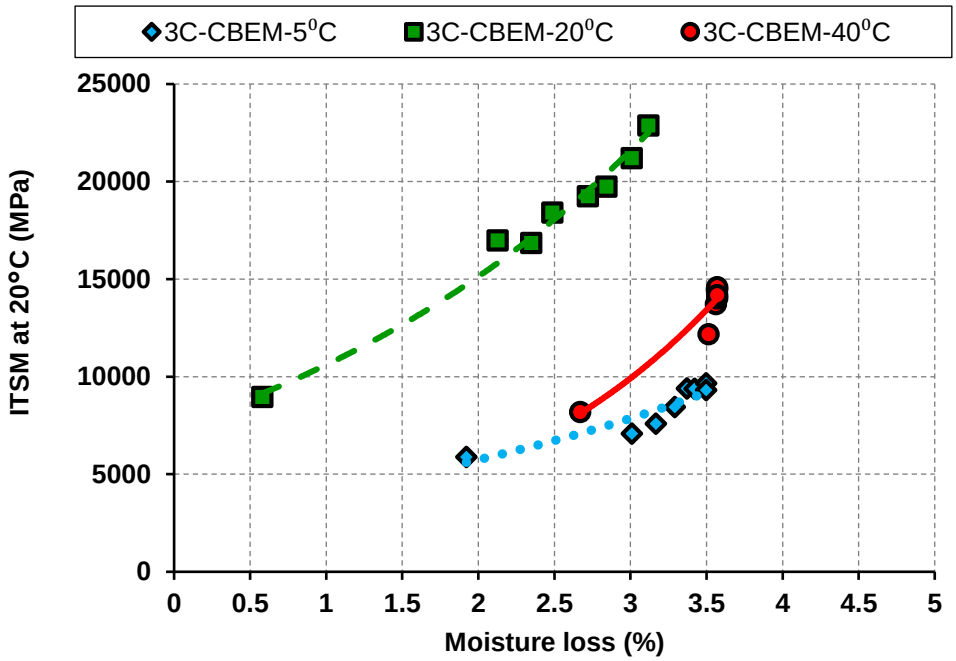


Figure 6.14 The relationship between moisture loss and stiffness modulus under different curing temperatures for 3C-CBEM

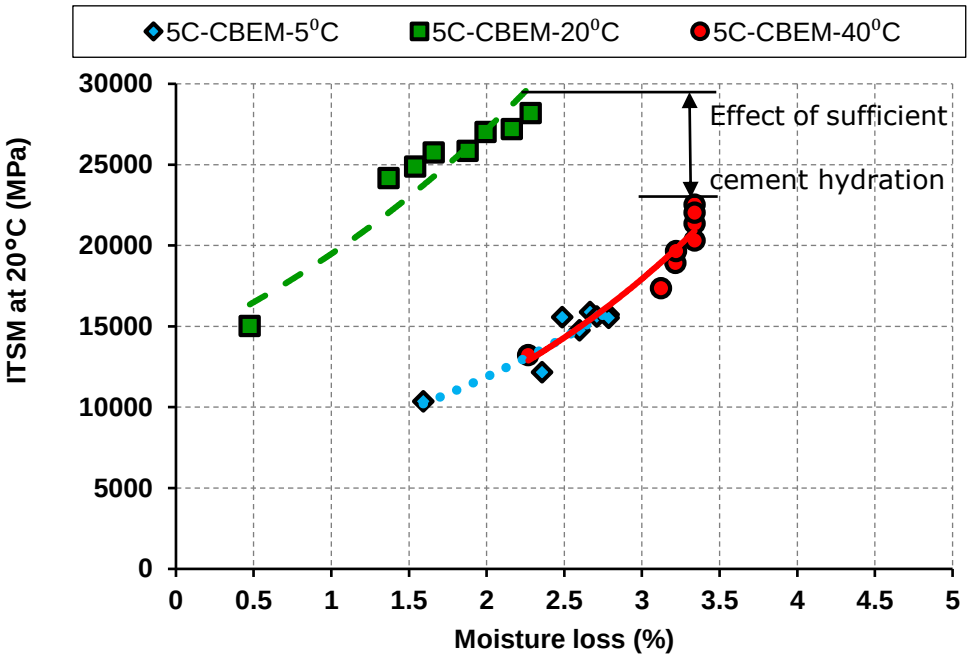


Figure 6.15 The relationship between moisture loss and stiffness modulus under different curing temperatures for 5C-CBEM

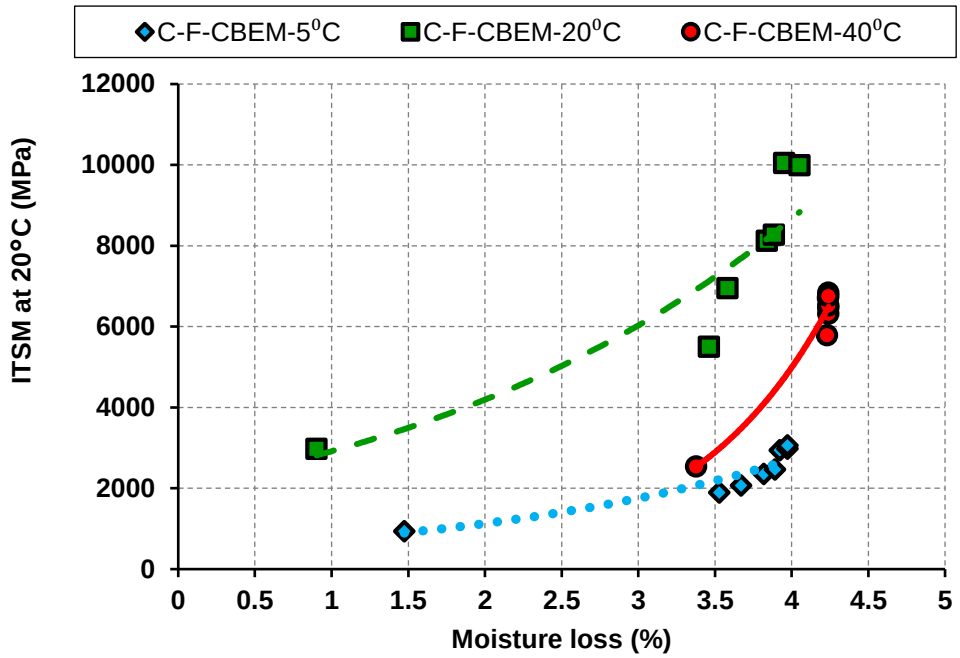


Figure 6.16 The relationship between moisture loss and stiffness modulus under different curing temperatures for C-F-CBEM

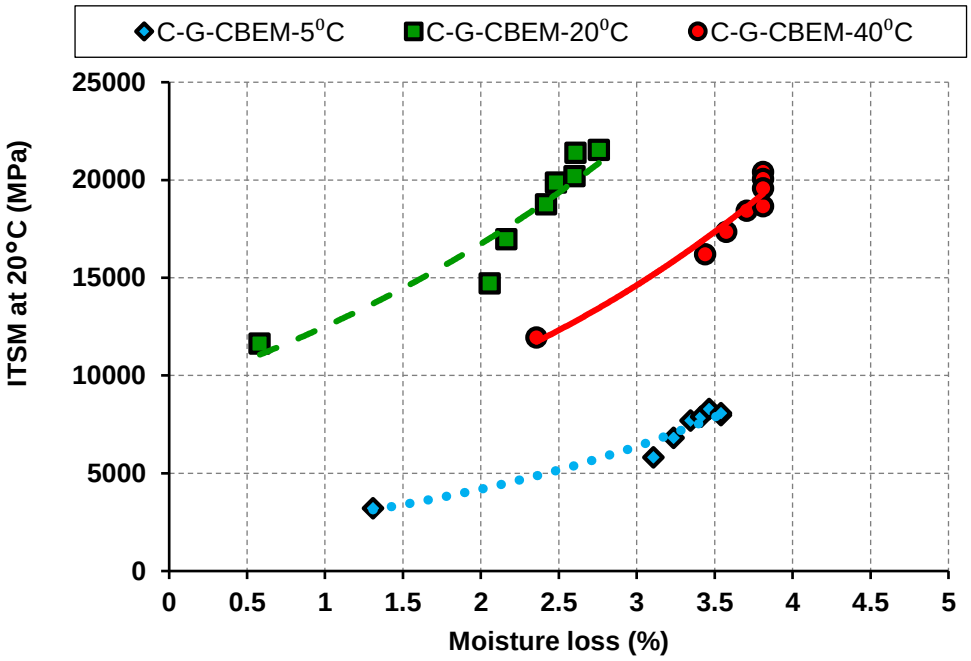


Figure 6.17 The relationship between moisture loss and stiffness modulus under different curing temperatures for C-G-CBEM

6.3.2.4 Influence of moisture loss on the moisture content of CBEMs

In order to understand more deeply the effect of moisture loss by evaporation on the moisture content of CBEM, the moisture content has been divided into two types to simplify the calculation. This calculation was limited to cement treated CBEM. The first type is the evaporated moisture (M_{Evap}) which is calculated based on the difference between the initial weight and the weight after the end of the curing period. The second type is the trapped moisture (M_{Trap}) inside the mix due to (1) the water physically adsorbed on the surface of aggregate/filler, (2) the water trapped in the closed pores within the bitumen and (3) the water used during cement hydration. The M_{Trap} was calculated by subtracting the evaporated water from the initial water content present in the CBEM specimens. The amount of moisture required for the hydration of cement (M_{Hyd}) was calculated based on Equation 6.1 as recommended by Mehta and Monteiro (1995):

$$M_{Hyd} = (0.23 + 0.19) \times \alpha \times k \times C \qquad \text{Equation 6.1}$$

where

α: Degree of hydration of the cement paste; C: Cement content within the mixture;

k: Fraction of Portland cement clinker in the cement.

The moisture types are summarized in Table 6.4, where it is assumed that k = 0.87 (average of the clinker content range) and α = 0.95 at 100 days of curing. It was found that the amount of M_{Trap} inside the CBEM cured at 5°C and 20°C is more than M_{Hyd} whereas the M_{Trap} inside the CBEM cured at 40°C is less than M_{Hyd}. It is therefore evident that the moisture loss by evaporation affects the hydration of cement, particularly at high curing temperature (40°C). This will hinder the hydration process. This result is in agreement with the finding of Cardone et al.

(2014). Moreover, the calculation in Table 6.4 indicates that most CBEMs still maintained some residual water (M_{Trap} - M_{Hyd}). This moisture may be trapped inside the surface pores of the aggregate or inside the bituminous mortar (García et al., 2013).

Table 6.4 Summary of moisture content calculations

Mixture code	M_{Evap}			M_{Trap}			M_{Hyd}
	40°C	20°C	5°C	40°C	20°C	5°C	
LF-CBEM	4.25%	4.22%	4.19%	0.18%	0.21%	0.24%	0.00%
1C-CBEM	4.24%	4.08%	3.96%	0.19%	0.35%	0.46%	0.32%
3C-CBEM	3.57%	3.12%	3.42%	0.86%	1.31%	1.01%	0.96%
5C-CBEM	3.34%	2.29%	2.71%	1.09%	2.14%	1.72%	1.59%

A statistical analysis was conducted using three-way analysis of variance (ANOVA) in order to determine the effect of cement content (0, 1, 3, 5%), curing temperature (5, 20, 40°C) and curing time (3, 7, 10, 14, 28, 54, 84 days) on the stiffness modulus of CBEMs. The result showed that these factors are all statistically significant at the 99% confidence level. The p-values obtained for these factors are less than 0.001. Also, the result of the ANOVA analysis shows that the cement content presented the largest F-value of 314.078, followed by curing temperature at 72.234 and curing time at 9.357. This means that the cement content and curing temperature had a more significant effect on stiffness modulus of CBEM, compared to curing time.

6.3.2.5 Influence of relative humidity (RH)

As mentioned earlier, air humidity was considered as one of the main climatic parameters affect the curing process. However, Fu et al. (2010) found that it is very hard to investigate the effect of air humidity at different curing temperatures. At a temperature of 40°C, the relative natural humidity of the air is typically about 2.5 times lower than that at 23°C (Hugener et al., 2014). For this reason and the limitation of laboratory equipment the comparison between two levels of RH was

carried out at 20°C only. Figure 6.18 presents stiffness modulus results of specimens cured at 20°C and conditioned at two different levels of RH (low=less than 50%, high= more than 85%).

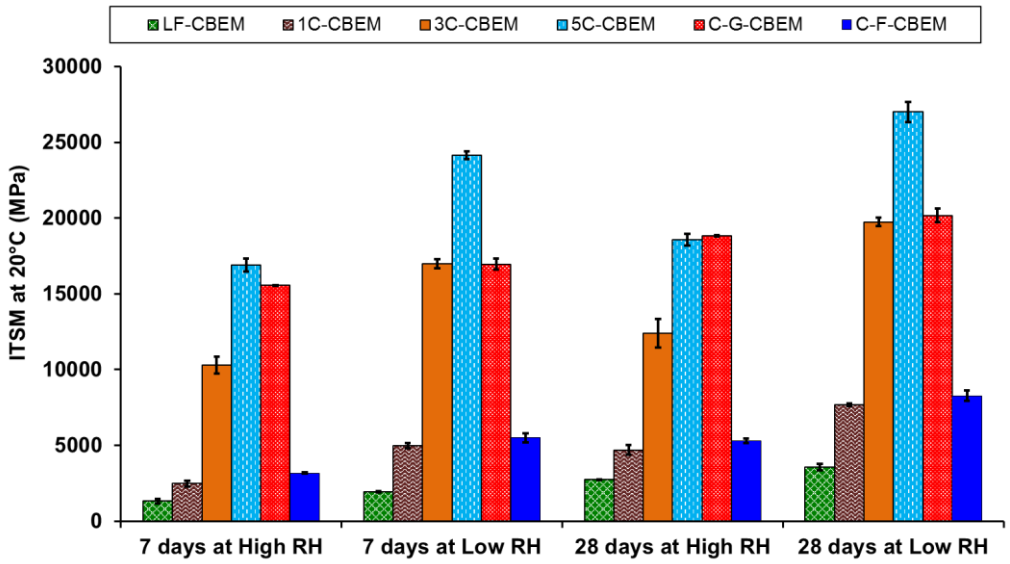


Figure 6.18 The effect of RH on the stiffness modulus of CBEM.

The results in Figure 6.18 show that higher humidity decreases the stiffness development rate of CBEM. Thus, longer curing time would be needed to achieve full strength. This behaviour implies that a high level of humidity decreases the rate of water evaporation from the mixture which influences the stiffness negatively. The amount of evaporated water after 7 days from the mixes cured at high RH (more than 85%) reduced by half in some cases when compared to the same mixes cured at low RH (less than 50%). For instance, at low RH after 7 days, LF-CBEM, 1C-CBEM and C-G-CBEM had lost about 3.57%, 3.46% and 1.9% moisture content, whereas these values became 3.04%, 2.77% and 1.39% at high RH level, respectively. However, high humidity is often desirable for curing mixes with cement, as the hydration process takes place in the presence of water. But, if the moisture content inside the mixture is enough for the hydration process, then exposure to a humid environment would be unnecessary or even detrimental. This result is consistent with the findings of Fu et al. (2010), García et al. (2013) and

Lin et al. (2015). For example, García et al. (2013) have found that CBEMs harden faster when cured at 35% and 70% RH compared to those cured at 90% RH.

A two-way ANOVA analysis was conducted to determine the impact of humidity level and cement content on CBEM modulus. The analysis confirms that both the humidity level and cement content are statistically significant at the 95% confidence level ($P_{Humidity\ level}$= 0.005 < 0.05, $P_{Cement\ content}$<0.001).

6.3.3 Resistance to permanent deformation

The effect of curing process in terms of resistance to permanent deformation is evaluated in this section. After 28 days of curing at different temperatures (5, 20 and 40°C), the resistance to permanent deformation was investigated through RLAT using a stress of 100kPa at 40°C. More information about RLAT is presented in previous chapter, see section 5.6.1. Figure 6.19 presents accumulated axial strain (%) of CBEMs at different curing temperatures.

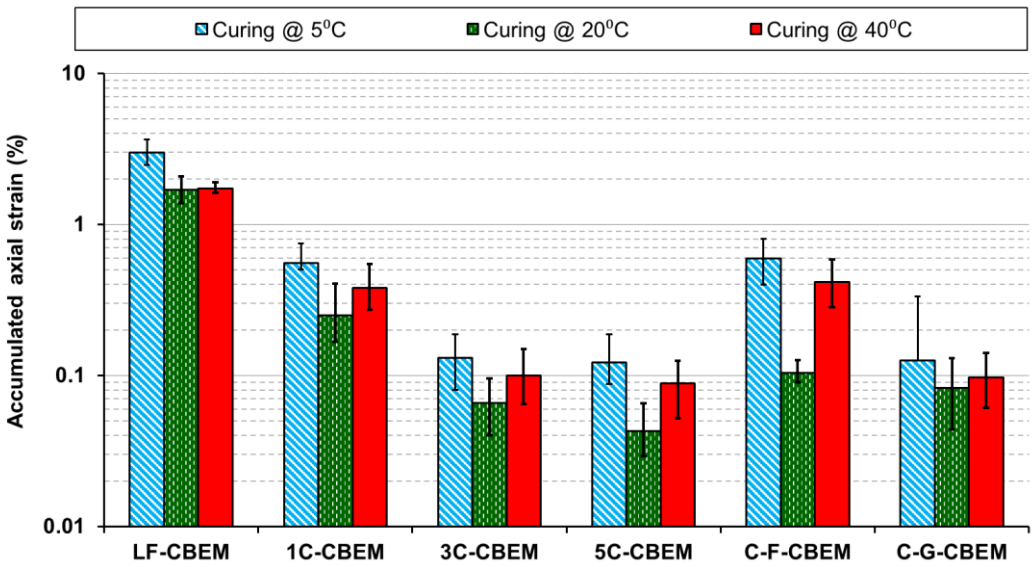


Figure 6.19 A comparison of accumulated permanent strain for CBEMs cured at 5, 20, 40°C

Similar to the ITSM results, the curing condition has a significant effect on the performance of CBEMs in terms of permanent deformation resistance. As can be seen from Figure 6.19, the lower curing temperature (5°C) resulted in relatively low permanent strains in 3C-CBEM, 5C-CBEM and C-G-CBEM, representing the potential benefit of this treatment. Moreover, the results replicate the trends observed from ITSM analysis in that the permanent strain for mixes cured at 20°C is lower than for those cured at 40 and 5°C. This is could be attributed to the same reason put forward in the previous discussion on ITSM results, see section 6.3.2.

6.3.4 Bitumen characterization before and after curing

To study the effect of curing temperature on bitumen properties, bitumen was extracted from LF-CBEM samples cured for 28 days at 5, 20 and 40°C. Softening point and frequency sweep tests were carried out. Figure 6.20 illustrates the complex modulus (G*) master curves at a reference temperature of 20°C. It can be noticed from Figure 6.20 that the differences in complex modulus of the recovered bitumen are significant, particularly at low frequency, which indicates that the bitumen ageing effect differs considerably between different curing temperatures.

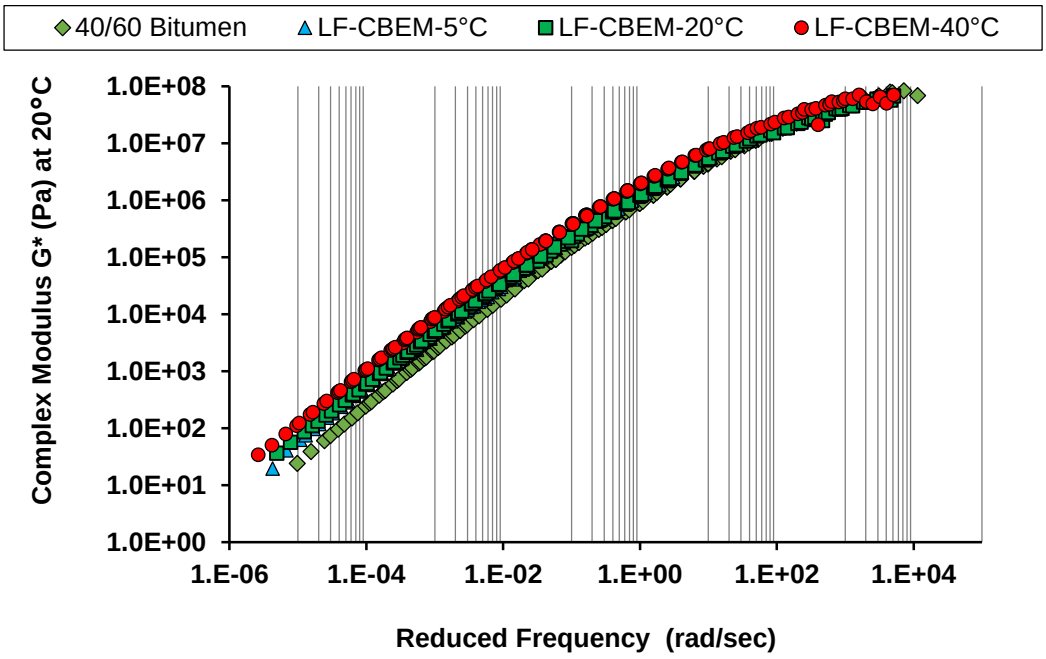


Figure 6.20 The effect of curing temperatures on bitumen properties

Moreover, the effect of curing temperature on the softening point of the binder was also evaluated. Before mixing and applying the curing protocols, the softening point of the original base binder was 52.8°C. After applying the curing protocols the softening points of extracted binder were 55.6, 56.2, and 59.2°C for LF-CBEM-5°C, LF-CBEM-20°C and LF-CBEM-40°C, respectively. Overall, based on softening point and frequency sweep test results, it may be concluded that the binder properties changed appreciably during the curing process. Hence, it is evident that water loss and cement hydration are not the only mechanisms involved during curing of CBEMs. High curing temperature is also responsible for additional stiffness gain due to ageing. This finding is in agreement with a previous work in foamed bitumen mixtures (Kuna, 2015).

6.4 Laboratory simulation of field curing

6.4.1 Introduction

It has been recognized in the literature that simulating the field curing conditions is one of the hardest tasks in selecting a CBEM the curing procedure (Leech, 1994, Serfass et al., 2004, Tebaldi et al., 2014). This is because there are many inter-related factors affecting the curing process in the field which are extremely difficult to standardise. Different factors can contribute to the complexity of the curing process which may be related to the composition of the mixture, construction issues and environmental factors as stated by Tebaldi et al. (2014). A lot of researchers have tried to accelerate the achievement of ultimate properties (accelerated curing) by increasing the conditioning time and temperature since curing time and temperature are influential parameters in the CBEMs curing process (Jenkins and Moloto, 2008). Therefore, this point directed the current study towards utilizing the maturity method, which is an approach that accounts for the combined effect of curing time and temperature on the development of concrete strength. The maturity method has increased in popularity in recent decades due to its ability to estimate in-situ compressive strength of concrete (Wilde, 2013). Since the central theme of this study focused on evaluation of the effect of contributory factors on the CBEM curing process using stiffness modulus (ITSM), this data was used to create maturity–stiffness relationships as a tool to evaluate the effect of climatic variations on in-situ curing of CBEM performance

6.4.2 The maturity approach

The concept of maturity is used to describe the combined effect of temperature and age on concrete strength development. This method requires that the temperature history of the curing concrete be measured and recorded against time. An extensive literature review and description of the theory and applicability of the maturity

method is available in Carino (2001). There are two primary techniques for applying the concepts of maturity, namely the Nurse-Saul method and the Arrhenius method. The maturity developed through the use of these techniques can be correlated with the strength gain of a concrete at a particular time, as presented in the following subsections.

6.4.2.1 Nurse-Saul method

The Nurse-Saul method is the most commonly used method for computing maturity. The widespread use of this method is attributable to its ease of calculation. This method is often known as the temperature time factor (TTF) through converting time and temperature history of in-situ concrete to a factor which is related to its strength using an equation called the Nurse-Saul equation as shown in Equation 6.2:

$$M = \sum_{0}^{t} (T - T_0) \times \Delta t \qquad \text{Equation 6.2}$$

where

M: Maturity at age t; T: Average temperature of the concrete during the time interval Δt; T_0: Datum temperature

The Nurse-Saul function can be used to convert a given temperature and time curing history to an equivalent age of curing at a reference temperature as follows in Equation 6.3:

$$t_e = \frac{\sum(T - T_o)}{\sum(T_r - T_o)} \times \Delta t \qquad \text{Equation 6.3}$$

where

t_e: Equivalent age at the reference temperature, T_r: Reference temperature

In this case equivalent age represents the duration of the curing period at the reference temperature that would result in the same maturity as the curing period at the actual temperature. The above equation can be written as presented in Equation 6.4:

$$t_e = \sum_0^t \propto \times \Delta t \qquad \text{Equation 6.4}$$

where

$\propto$: Age conversion factor.

One limitation to this equation is that this TTF approach is a linear one. Carino (2001) opined that this is might be acceptable as long as the curing temperature does not fluctuate widely through the period of concrete strength gain. This is because errors in the computations begin to become more evident with larger temperature differences. Therefore, later in 1977, Hansen and Pedersen suggested a new TTF based on the Arrhenius method (Carino, 2001).

6.4.2.2 Arrhenius method

The Arrhenius method was developed as an alternative to Nurse-Saul to produce a more precise maturity model. It is also known as the equivalent age method. The Arrhenius function allows the computation of an equivalent age of concrete as shown in Equation 6.5:

$$t_e = \sum \left[e^{-Q\left(\frac{1}{T} - \frac{1}{T_r}\right)} \right] \times \Delta t \qquad \text{Equation 6.5}$$

where

t_e: Equivalent age at a specific reference temperature (h); Q: Activation energy of the mix divided by the universal gas constant; T: Average temperature at the given interval (Kelvin); T_r: Reference temperature (Kelvin), and Δt: Time interval.

Carino (2001) suggested that this approach yielded to a complex equation that is much more difficult to implement than the Nurse-Saul approach to maturity rather than obtaining accurate values for activation energy is not practical approach. In an attempt to simplify this method, Carino (2001) proposed a variation of this approach that is referred to as the exponential approach. This variation transforms to Equation 6.6.

$$t_e = \sum_0^t e^{B(T-T_r)} \times \Delta t \qquad \text{Equation 6.6}$$

The expression for the age conversion factor then becomes as shown in Equation 6.7:

$$\propto = e^{B(T-T_r)} \qquad \text{Equation 6.7}$$

B: Temperature sensitivity factor (1/°C)

In previous work focused on applying the maturity concept to foamed bitumen mixtures, Kuna (2015) explained the meaning of equivalent age and the summation considered in Equation 6.6 as shown in Figure 6.21. For instance, when the curing condition changed from 5°C to 20°C on the 40th day, the stiffness gain rate was given by a horizontally transferred 20°C curve rather than the rate of the actual 20°C curing curve on the 40th day.

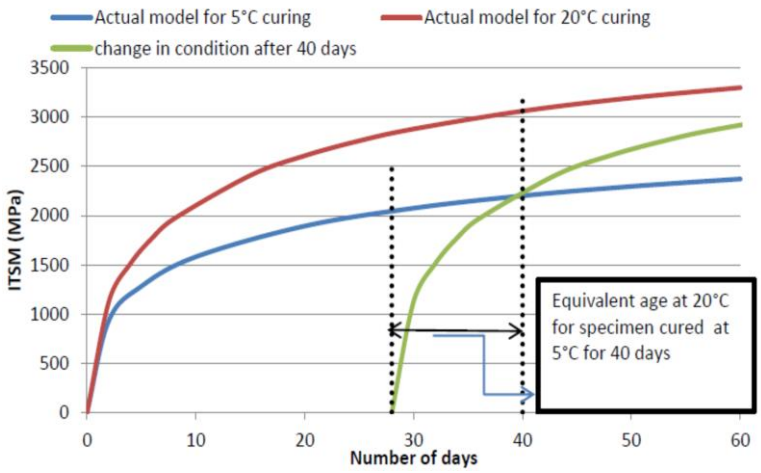


Figure 6.21 Illustrating equivalent age (curing temperature was changed from 5°C to 20°C at 40 days) adopted (Kuna, 2015)

Based on the discussion in the previous sections, and the relative advantages and disadvantages of the two methods, the remainder of this study uses the Arrhenius method for computing CBEM maturity. As the rate of strength or stiffness gain is dependent on the curing temperature it is important to formulate temperature dependency in maturity–strength models. Carino (2001) suggested that the following exponential equation (Equation 6.8) can represent the temperature dependence of the rate constant (K) for strength gain:

$$K = A_0 e^{BT} \qquad \text{Equation 6.8}$$

where

A_0: The value of the rate constant at 0°C; B: Temperature sensitivity factor (1/°C); and T: Curing temperature (°C).

6.4.3 Maturity–strength relationships

This section introduces the three mathematical models that are used to characterize the maturity–strength relationships for concrete. The three mathematical models are the logarithmic, hyperbolic, and exponential forms

(Carino, 2001, Wilde, 2013). For determining the values of the coefficients in the models, the least square curve fitting technique is conducted to find the best fit for the actual data collected in the field or in the laboratory.

6.4.3.1 Logarithmic model

The logarithmic model for the maturity–strength relationship is presented in Equation 6.9:

$$S = \frac{a}{S_0} + \frac{b}{S_0} \log M \qquad \text{Equation 6.9}$$

where

S_0: Strength when strength development is assumed to begin; a and b: Constants related to the water–cement ratio of the concrete and the type of cement.

6.4.3.2 Exponential model

The exponential model, sometimes called the sigmoidal model, is given in Equation 6.10:

$$S = S_e \times e^{-\left[\frac{\tau}{M}\right]^{\beta}} \qquad \text{Equation 6.10}$$

where

S: Compressive strength (MPa); Su: Limiting compressive strength (MPa); M: Maturity index (hours); τ: Characteristic time constant (hours), and β: Shape parameter.

6.4.3.3 Hyperbolic model

The hyperbolic model is introduced in two forms namely, linear-hyperbolic (Equation 6.11) and parabolic-hyperbolic (Equation 6.12). This categorization was suggested based on the hydration kinetics of cement particles as stated by Carino (2001). This means that the degree of hydration of an individual cement particle is a linear function of the product of time and the rate constant in Equation 6.11 and a parabolic function in Equation 6.12.

- **Linear-hyperbolic model**

$$S = S_u \times \left[\frac{k \times (M - M_0)}{1 + k \times (M - M_0)}\right] \qquad \text{Equation 6.11}$$

- **Parabolic-hyperbolic model**

$$S = S_u \times \left[\frac{\sqrt{k \times (M - M_0)}}{1 + \sqrt{k \times (M - M_0)}}\right] \qquad \text{Equation 6.12}$$

where

M_o: Maturity when strength development is assumed to begin (°C·hours or hours) and k: Rate constant (1/[°C·hours] or 1/hours).

6.4.4 Application of maturity methods to CBEM

The above mentioned discussion presents maturity as a powerful tool that has the potential to account for the combined effects of curing time and temperature on strength gain. Since the first part of this study demonstrated the effect of curing time and temperature on the stiffness development of CBEMs, the application of the maturity method to CBEMs is a logical steps. Moreover, the importance of curing temperature at early ages on the stiffness gain in CBEMs was noted from earlier findings. Besides, it has been recognized that estimating the in-situ properties of

CBEM is not straightforward based on data obtained under laboratory conditions (Cardone et al., 2014, Tebaldi et al., 2014, Graziani et al., 2016). Therefore the applicability of the maturity method to CBEM stiffness gain will be investigated with some modification in order to predict stiffness modulus as accurately as possible. The said modification is introduced due to the different curing mechanism compared to concrete. In the concrete industry, the curing process relies on preventing moisture loss in order to enhance the hydration process of cement. In contrast, in CBEMs the curing process is a complex one and depends on a combination of three phenomena acting together: emulsion breaking, moisture loss and hydration of cementitious compounds (Serfass et al., 2004, García et al., 2013, Cardone et al., 2014). Therefore, in the present study, maturity refers to a function of temperature and equivalent age computed using a TTF which is similar to the definition given by Carino (2001). Carino (2001) suggested that maturity of concrete could be attributed to either a TTF computed using the Nurse-Saul function (Equation 6.2) or an equivalent age calculated using any of the maturity functions (Equation 6.3 and Equation 6.6). Figure 6.22 summarizes the methodology adopted to apply a maturity–stiffness relationship. Application will be limited to four mixes (LF-CBEM, 1C-CBEM, C-F-CBEM and C-G-CBEM) and explained with reference to LF-CBEM. This limitation is because the stiffness development of the other CBEMs (3C-CBEM and 5C-CBEM) was interrupted at an early age for mixes cured at high temperature due insufficient hydration as discussed in section 6.3.2. Yang et al. (2015) reported that the early strength gain of concrete at a higher curing temperature was critical, because a significant amount of strength development occurred very early. Therefore, early strength evaluation was required for accurate maturity–strength model establishment.

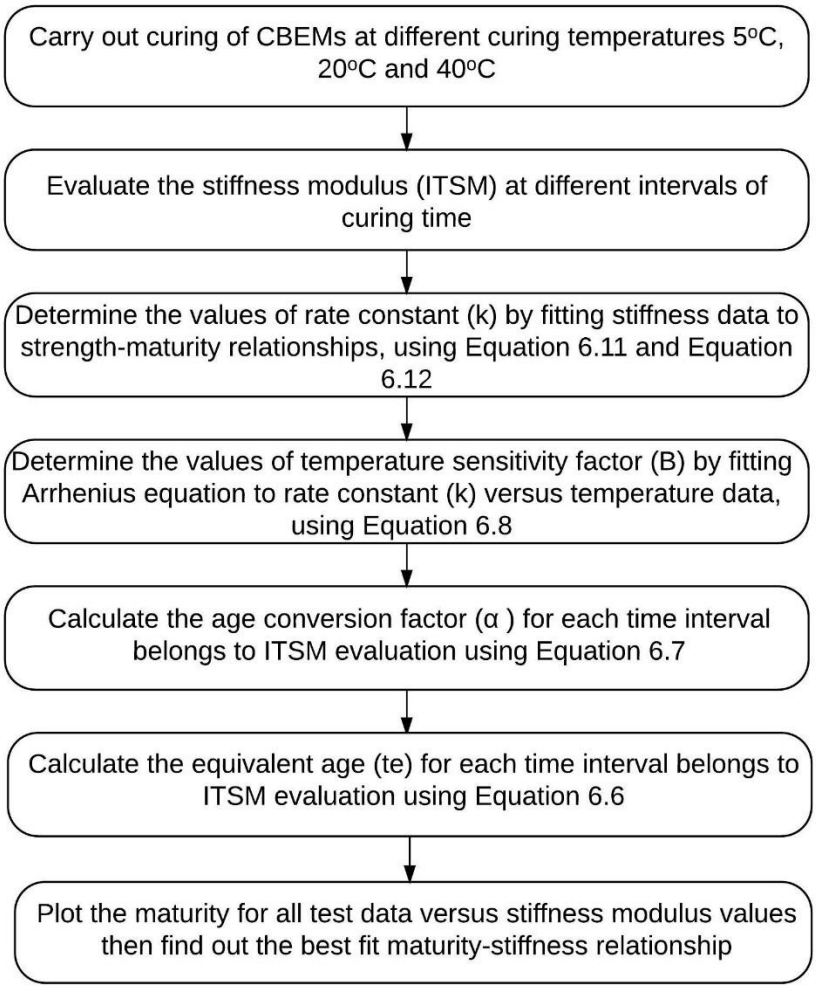


Figure 6.22 The methodology adopted to apply a maturity–stiffness relationship

6.4.4.1 Stiffness–age relationships

It has been acknowledged in previous works that a logarithmic fit best describes the stiffness increase of CMA over time (Doyle et al., 2013, Kuna, 2015, Graziani et al., 2016), since the logarithmic function simulates the high initial rate of stiffness gain well. However, Kuna (2015) noticed an overestimation of predicted stiffness values over a long period of time when using the logarithmic function; and a similar effect can be noticed in Figure 6.23 to Figure 6.25. These figures present the stiffness modulus for LF-CBEM cured at different temperatures and monitored over one year. Due to the over estimation by the logarithmic function in the long term, a hyperbolic equation is used to fit the stiffness data over time as described

in the previous section. But the maturity term M was replaced with the time term (t) from Equation 6.11 and Equation 6.12. Also, as the material property considered is stiffness (ITSM), strength (S) is replaced by ITSM. The adopted equations are presented in Equation 6.13 and Equation 6.14.

- **Linear-hyperbolic model**

$$ITSM = ITSM_u \times \left[\frac{k \times (t - t_0)}{1 + k \times (t - t_0)}\right] \quad \text{Equation 6.13}$$

- **Parabolic-hyperbolic model**

$$ITSM = ITSM_u \times \left[\frac{\sqrt{k \times (t - t_0)}}{1 + \sqrt{k \times (t - t_0)}}\right] \quad \text{Equation 6.14}$$

where

ITSM: Stiffness modulus at age t; $ITSM_u$: Asymptotic value of the stiffness modulus for the hyperbolic function that fits the data; k: Rate constant which is related to the rate of stiffness gain at a constant temperature; t_0: Age at the start of stiffness development which was assumed to start immediately after compaction ($t_0 = 0$).

The stiffness–time data for the three curing temperatures (5°C, 20°C and 40°C) was fitted by the hyperbolic relationships given Equation 6.13 and Equation 6.14 as shown in Figure 6.23 to Figure 6.25. The least square curve fitting technique was used to determine the equation parameters. The determination coefficient R^2 are tabulated in Table 6.5. Referring to Figure 6.23 to Figure 6.25 and Table 6.5, the results demonstrate that the linear-hyperbolic model is the best fit to ITSM values over the long term. At the same time, Carino (2001) suggested that the linear-hyperbolic model is suitable up to a degree of hydration of 85%. The suitability of the linear-hyperbolic model was also verified in the different studies on the applicability of the maturity method to mortar mixtures with low water-

cementitious material ratios (Knudsen, 1984, Carino and Tank, 1992, Zelić et al., 2004).

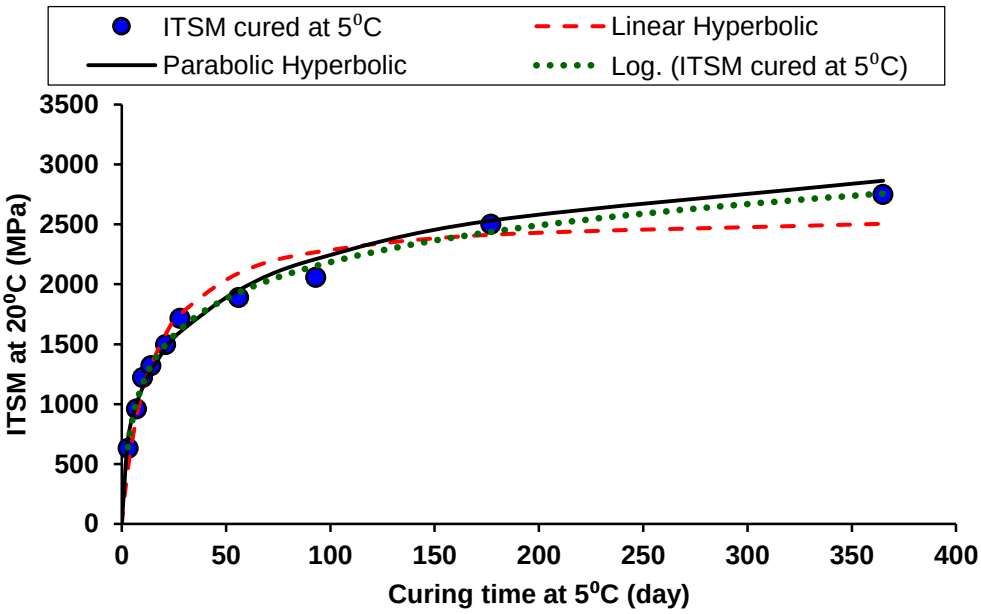


Figure 6.23 Stiffness development relationships for LF-CBEM cured at 5°C

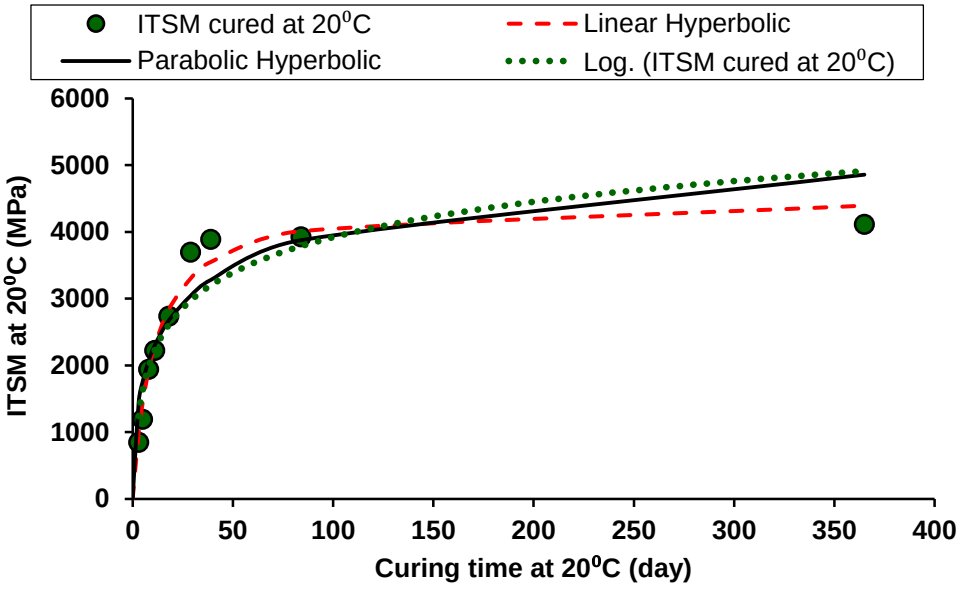


Figure 6.24 Stiffness development relationships for LF-CBEM cured at 20°C

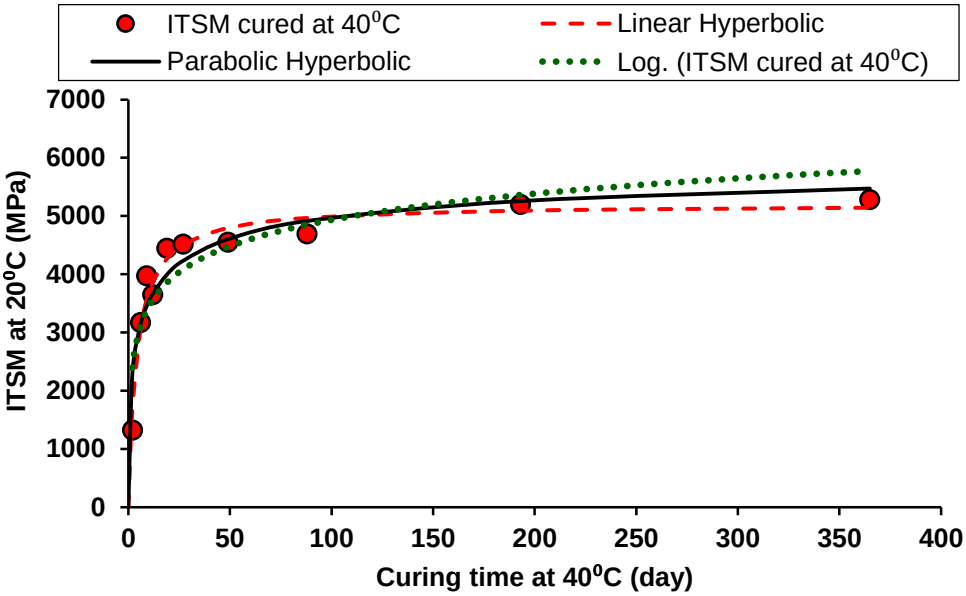


Figure 6.25 Stiffness development relationships for LF-CBEM cured at 40°C

Table 6.5 Determination coefficient R^2 of curing models

Model type	Linear-hyperbolic			Parabolic-hyperbolic			Logarithmic		
Curing temp.	**5°C**	**20°C**	**40°C**	**5°C**	**20°C**	**40°C**	**5°C**	**20°C**	**40°C**
LF-CBEM	0.94	0.95	0.94	0.97	0.80	0.88	0.99	0.87	0.84
1C-CBEM	0.99	0.94	0.89	0.96	0.81	0.85	0.95	0.76	0.60
FA-CBEM	0.97	0.97	0.89	0.94	0.88	0.86	0.94	0.87	0.61
GGBS-CBEM	0.96	0.97	0.98	0.90	0.98	0.95	0.78	0.76	0.66

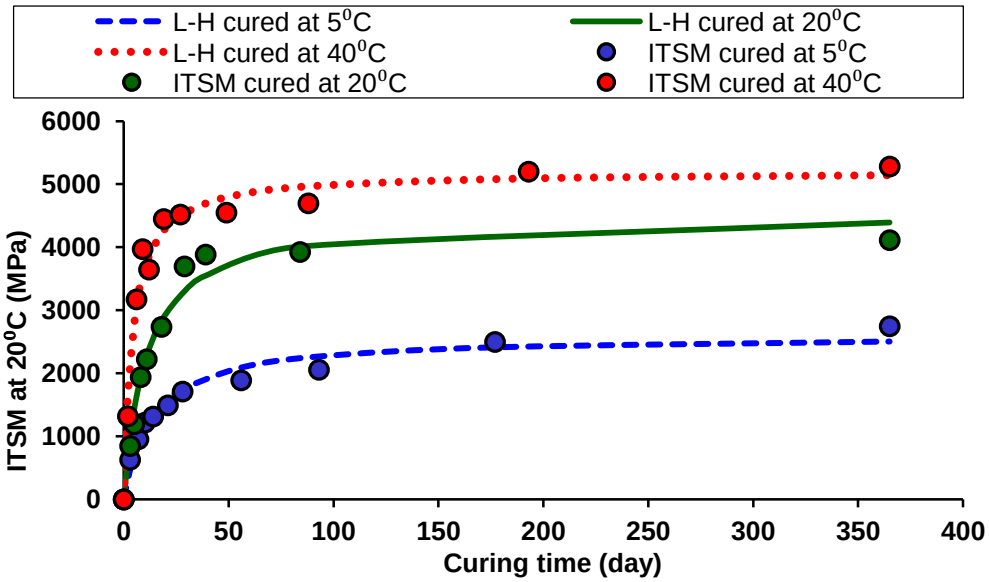


Figure 6.26 Stiffness development relationships for LF-CBEM cured at 5, 20, 40°C with best fit linear-hyperbolic model

The other model parameters, $ITSM_u$ and the rate constant (k), resulting from regression analysis, were presented in Table 6.6.

Table 6.6 Summary of parameters resulted by regression analysis

Curing temp.	5°C		20°C		40°C	
Model parameters	**k (1/day)**	**$ITSM_u$ (MPa)**	**k (1/day)**	**$ITSM_u$ (MPa)**	**k (1/day)**	**$ITSM_u$ (MPa)**
LF-CBEM	0.079	2528	0.085	4705	0.212	5388
1C-CBEM	0.11	3438	0.137	9256	0.31	7512
FA-CBEM	0.13	3666	0.14	10513	0.37	7386
GGBS-CBEM	0.25	9028	0.37	22018	0.53	21702

6.4.4.2 Temperature sensitivity factor

The next step in building the maturity–stiffness model is to investigate the temperature sensitivity factor (B). Figure 6.27 presents the rate constant (k) against the curing temperature for CBEMs.

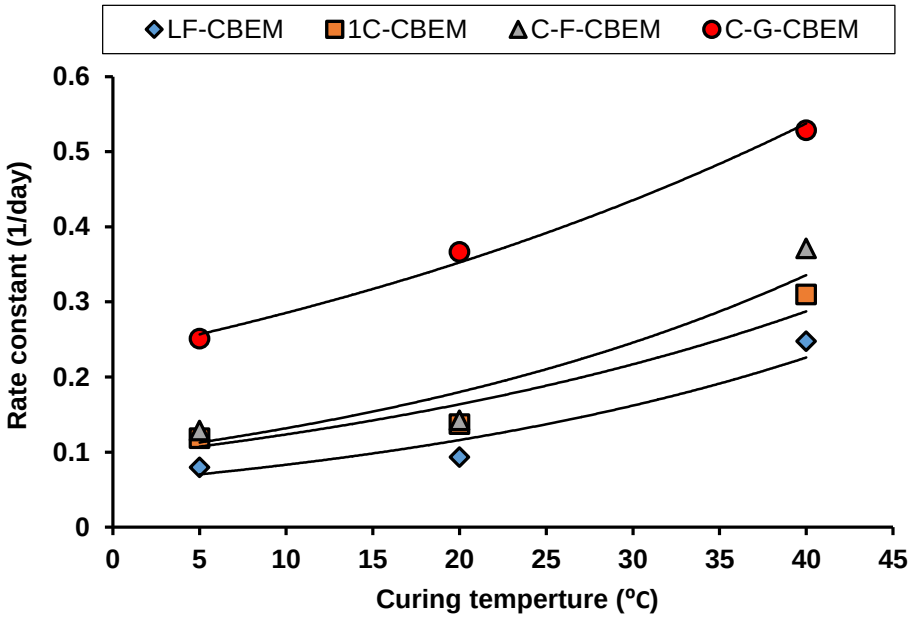


Figure 6.27 Variation of rate constant with curing temperature for linear-hyperbolic model

The rate constant (k) value exhibits the rate of stiffness modulus development at a certain curing temperature. Therefore, the variation in the k values demonstrates

the effect of different curing temperature on the rate of stiffness development. The best fit for the Arrhenius equation was carried out in order to find out (A) and (B) values which represent the values of the rate constant at 0°C and the temperature sensitivity factor, respectively. The results of regression analysis are summarized in Table 6.7.

Table 6.7 Summary of temperature sensitivity factors (B) based on linear-hyperbolic model

Mixture type	A	B (1/°C)	R^2
LF-CBEM	0.0596	0.0333	0.91
1C-CBEM	0.0932	0.0282	0.91
FA-CBEM	0.0964	0.0312	0.89
GGBS-CBEM	0.2311	0.0211	0.99

6.4.4.3 Age conversion factor and equivalent age

After the temperature sensitivity factor had been obtained for each mix, the age conversion factor was calculated based on Equation 6.7. Figure 6.28 shows the age conversion factor based on 20°C as a reference temperature.

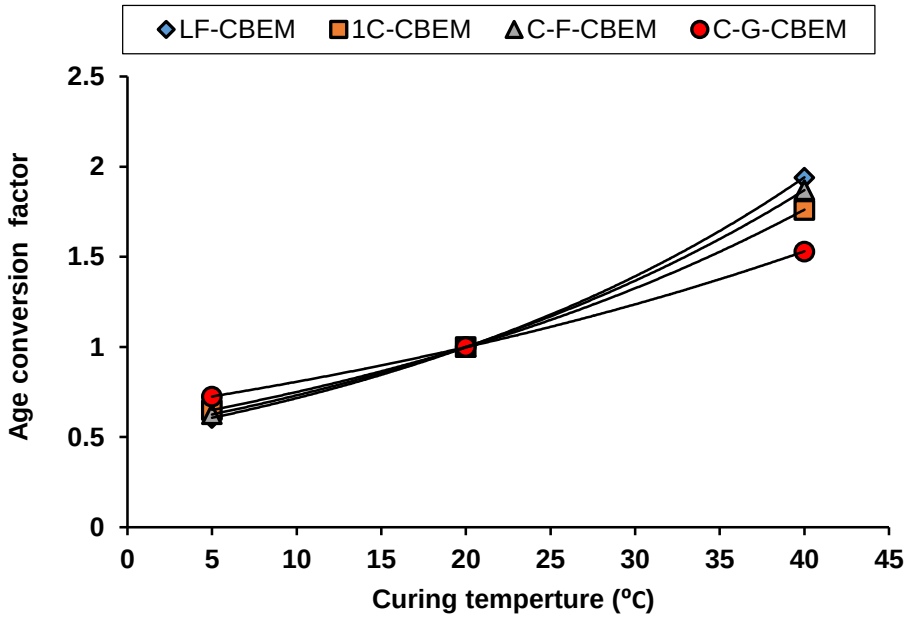


Figure 6.28 Age conversion factor for reference temperature of 20°C

The equivalent age is the duration of time that a specimen would need to be cured at a specified reference temperature (in the present case 20°C) to equal the maturity of the specimen cured at other temperatures. The age conversion factor for mixes cured at 20°C is 1 as the reference temperature is 20°C. The equivalent age obtained from Equation 6.7 based on the reference temperature of 20°C is plotted against the stiffness values in Figure 6.29.

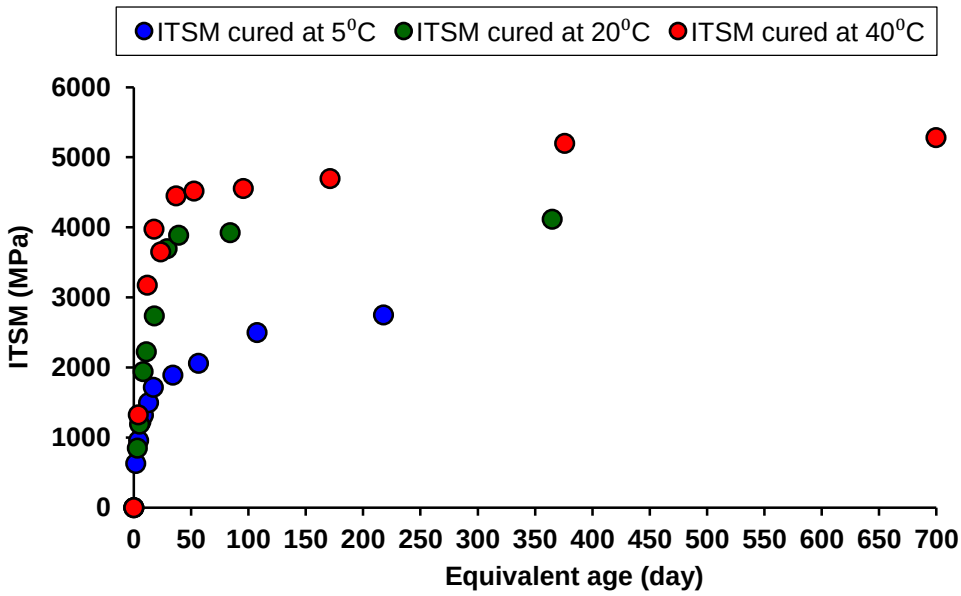


Figure 6.29 Equivalent age referenced to 20°C for LF-CBEM

As can be seen from Figure 6.29, the equivalent age–stiffness data for mixes cured at 20°C remains the same since 20°C is the reference temperature. Also, it is evident that there is no unique relationship between mixes with the same equivalent age and their stiffness modulus independent of curing history. This observation therefore reveals a shortcoming of the traditional maturity concept which assumes that the limiting stiffness or strength of the mixture subjected to continuous curing is not affected by early age temperature history. In other words, the curing temperature affects the initial rate of stiffness development as well as the limiting stiffness value.

Similarly, Kuna (2015) noticed the same problem and suggested a modification to the maturity equation. A temperature term is introduced into the equivalent age function, Equation 6.6. The resulting function is Equation 6.15. This equation is analogous to the Nurse-Saul maturity function (Equation 6.2) in which the time term is replaced by equivalent time (t_e) and the datum temperature is 0°C.

$$M_{mod} = t_e \times \mathrm{T} = \sum_0^t e^{B(T-T_r)} \times \Delta t \times T \qquad \text{Equation 6.15}$$

Maturity values calculated based on Equation 6.15 is plotted against stiffness in Figure 6.30. The datum temperature (T_0) was assumed as 0°C as there is direct influence of water evaporation on the mixture stiffness gain and this was recommended in previous works (Doyle et al., 2013, Kuna, 2015).

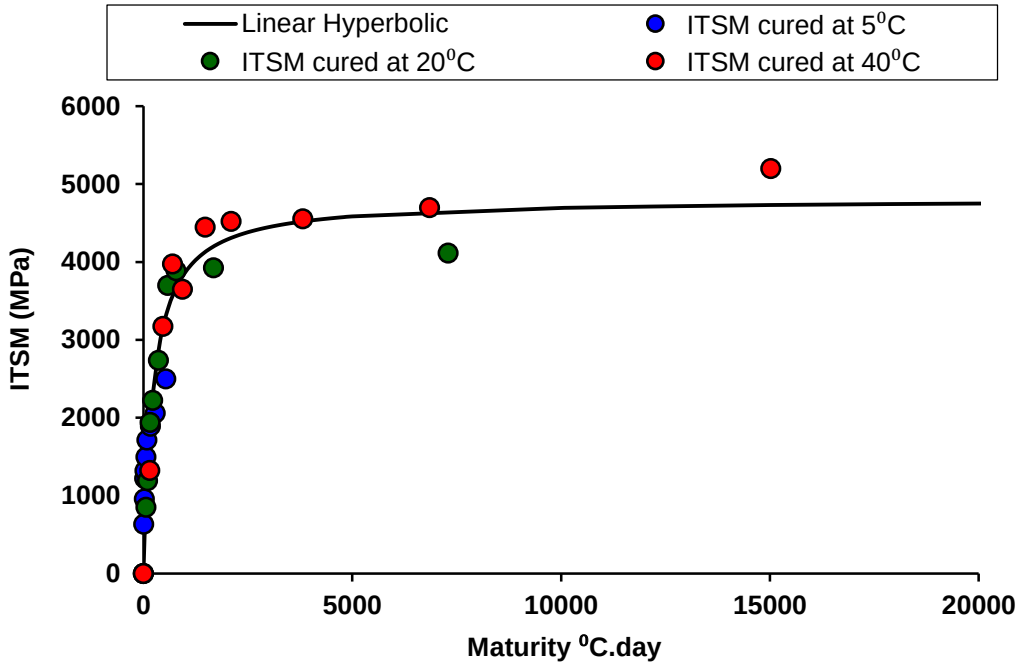


Figure 6.30 Maturity–stiffness relationship for LF-CBEM

As can be seen in Figure 6.30, the data points very much group around a single curve and therefore it can be interpreted that there exists a relationship between relative strength and equivalent age. The stiffness values were fitted to maturity

values with Equation 6.16 using the least square curve fitting technique and the parameters $ITSM_u$ and k were obtained. The parameters obtained are presented in Table 6.8.

$$ITSM = ITSM_u \times \left[\frac{k \times \mathrm{M}_{mod}}{1 + k \times \mathrm{M}_{mod}}\right] \quad \text{Equation 6.16}$$

Table 6.8 Summary of maturity–stiffness model parameters

Mixture type	$ITSM_u$ (MPa)	K (1/day)	R^2
LF-CBEM	4808	0.00411	0.98
1C-CBEM	7722	0.00712	0.90
C-F-CBEM	7812	0.00741	0.87
C-G-CBEM	20646	0.01153	0.88

6.4.5 Validation of developed maturity models

This section discusses the validation of the maturity–stiffness models using a different set of data which was not included when developing the model. The validation data was generated to cover two curing regimes. The first was isothermal curing at 30°C for 28 days, as shown in Figure 6.31. The second was a variable curing regime, with the temperature at 10°C for 21 days and then 30°C for 7 days, as shown in Figure 6.32.

With respect to Figure 6.31, the ITSM-test data was obtained for CBEMs cured at 30°C for 28 days and tested at 20°C. The ITSM-predicted data was calculated based on the maturity–stiffness model developed in previous section. The results demonstrate that the models of maturity–stiffness were able to predict the stiffness modulus reasonably closely for all mixes.

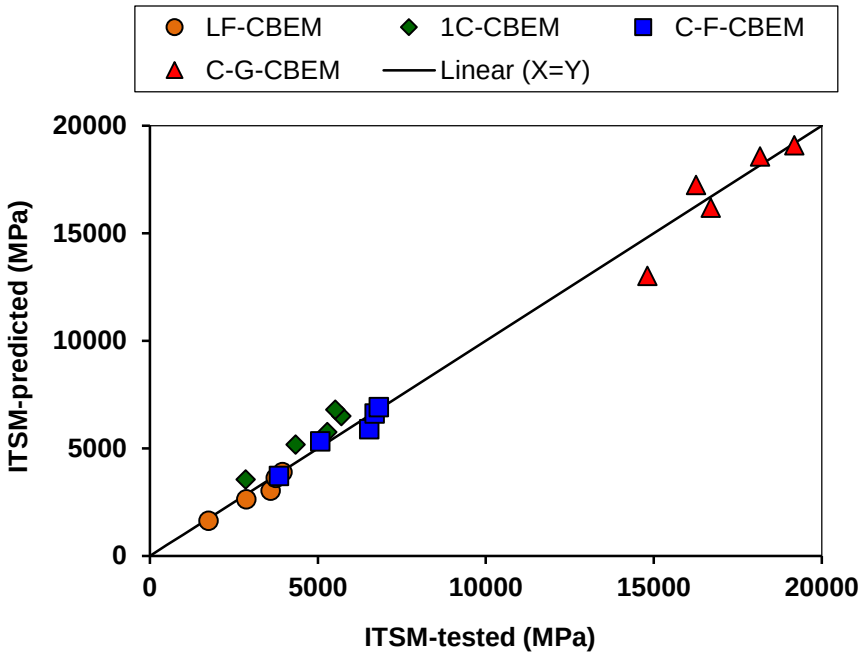


Figure 6.31 Validation of the maturity–stiffness model for CBEMs cured at 30°C for 28 days

In Figure 6.32, the maturity–stiffness model was applied to verify performance under variable curing temperature (10°C for 21 days, 30°C for 7 days). As can be seen in this figure, the model predicted the stiffness modulus adequately for LF-CBEM, 1C-CBEM and C-F-CBEM. However, the predicted stiffness values for C-G-CBEM were marginally higher than the actual values. The reason for this may relate to the effect of curing temperature reducing when the mix strength is close to its ultimate value. A very close observation was noticed in previous work (Kuna, 2015). He also noted that the mix failed to gain stiffness at the rate the model estimated after changing the conditioning temperature. Nevertheless, although the predicted stiffness modulus varies slightly compared to the test results, the model is able to simulate the stiffness gain reasonably well for varying temperature conditions. Overall, the maturity approach provides a powerful tool for predicting the in-situ stiffness modulus of CBEMs in a satisfactory manner.

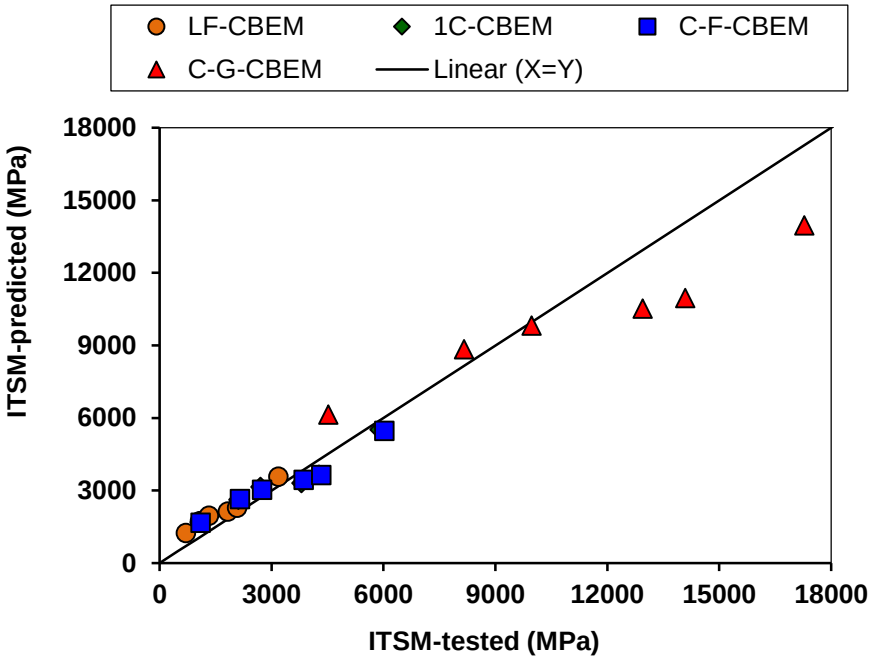


Figure 6.32 Validation of the maturity–stiffness model for CBEMs cured at 10°C for 21 days + 30°C for 7 days

6.4.6 Practical implications

The use of the maturity approach to describe CBEM properties presents a good opportunity to better understand the performance of CBEM. Moreover, in order to present the applicability of the maturity relationship to estimate in-situ stiffness modulus, three hypothetical locations were selected to represent different temperatures conditions. These locations are Nottingham (UK), Rome (Italy) and Doha (Qatar), representing cold, moderate and warm weather, respectively. The temperature history record for the various locations was available from the accuweather website which is a well-known weather forecasting agency (http://www.accuweather.com). The profiles of the mean daily temperature fluctuation for May, 2015 are presented in Figure 6.33.

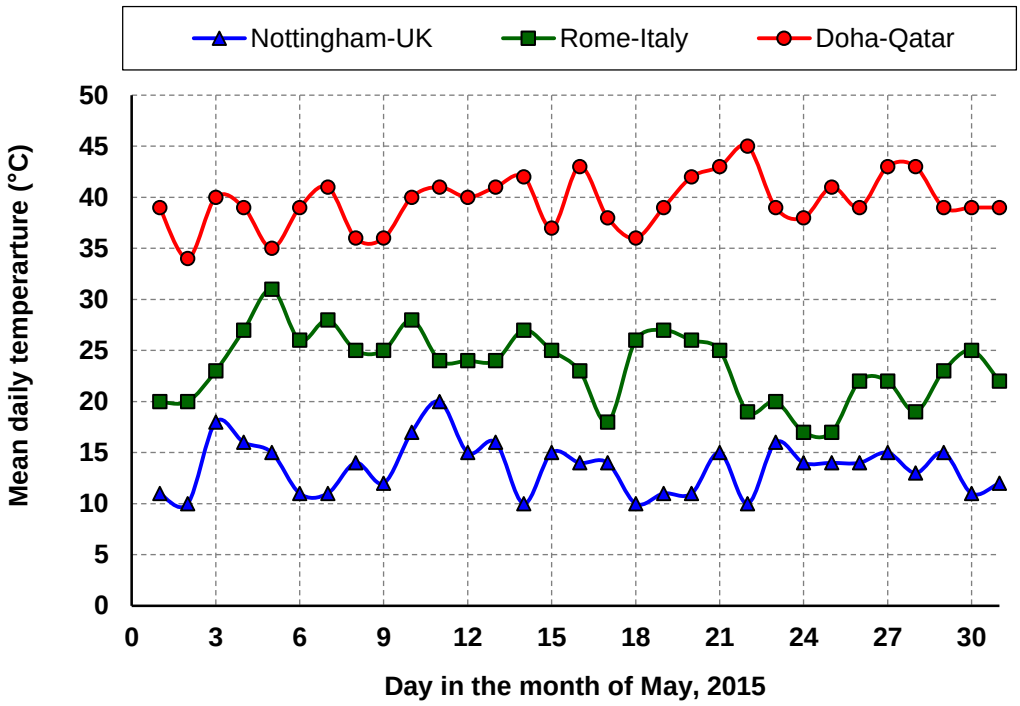


Figure 6.33 Mean daily temperatures for month of May, 2015 in locations selected in the study

Figure 6.33 illustrates a significant difference in ambient temperature for the selected locations; Nottingham is the coldest whereas Doha is the warmest. It was assumed that construction was carried out on 1st of May and the mixture started gaining stiffness from the first day. The stiffness values for each day were calculated using the cumulative maturity approach, as presented in Figure 6.34 and Figure 6.35.

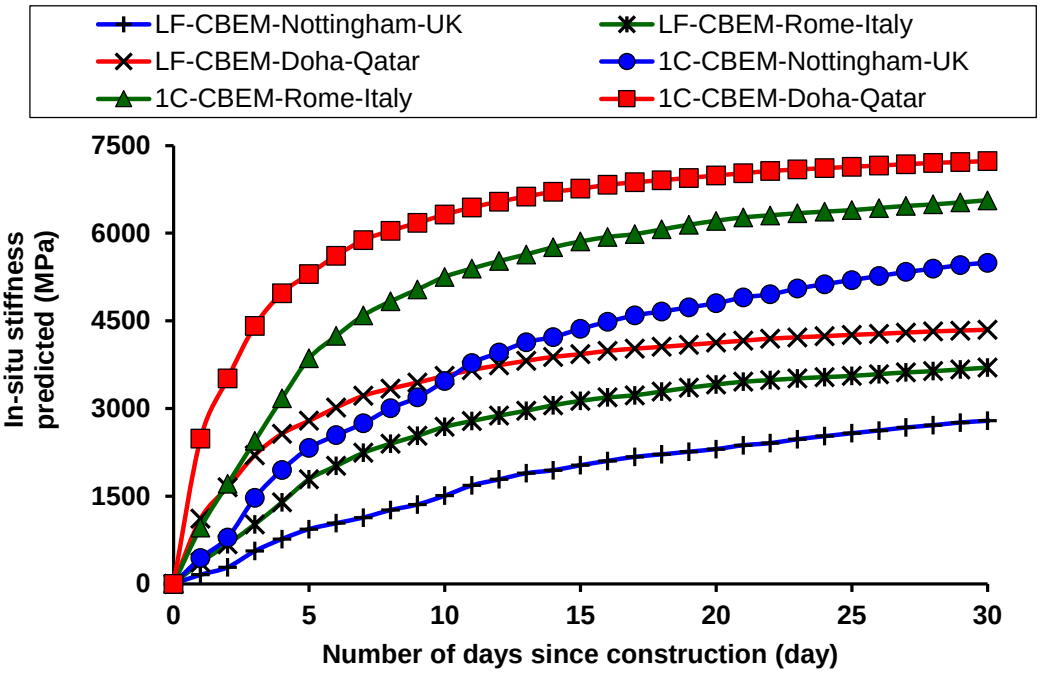


Figure 6.34 Prediction of the stiffness modulus in hypothetical sections using maturity–stiffness relationships for LF-CBEM and 1C-CBEM

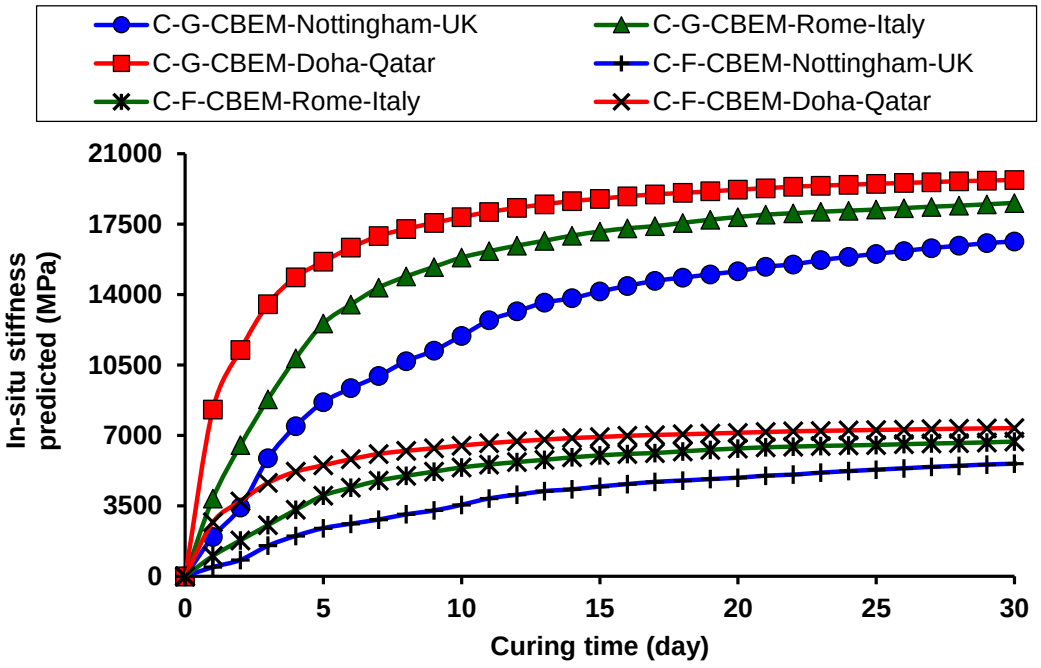


Figure 6.35 Prediction of the stiffness modulus in hypothetical sections using maturity–stiffness relationships for C-G-CBEM and C-F-CBEM

As can be seen from Figure 6.34 and Figure 6.35, both location and presence of cement/BBFs significantly influence the stiffness gain trend. It is clear that the

relatively cold weather (Nottingham) results in the lowest stiffness modulus values whereas in Doha (Qatar) the mixes show the highest values of stiffness modulus. Therefore, generally, the higher curing temperatures resulted in higher stiffness values. For instance, the stiffness modulus of C-F-CBEM after 28 days in Nottingham (5500 MPa) can be achieved after 5 days in Doha and 11 days in Rome. Moreover, the results clearly showed that in-situ curing affects the strength development compared with laboratory curing.

Table 6.9 presents a comparison of the stiffness modulus values obtained under laboratory conditions (curing at 20°C) and the predicted in-situ stiffness modulus after 7 and 28 days.

Table 6.9 Comparison the obtained laboratory stiffness modulus of CBEM to in-situ predicted modulus

Mixture type	Laboratory curing at 20°C		Stiffness modulus in-situ (MPa)					
	ITSM (MPa) at 20°C		Nottingham		Rome		Doha	
Curing time (day)	7	28	7	28	7	28	7	28
LF-CBEM	1900	3500	1100	2700	2250	3600	3200	4300
1C-CBEM	5000	7600	2750	5400	4600	6500	5900	7200
C-F-CBEM	3500	8300	2850	5500	4750	6600	6000	7350
C-G-CBEM	14700	20000	10000	16500	14000	18500	17000	19650

A considerable difference was found between the laboratory and in-situ properties of CBEMs. This difference depends on the construction location. Therefore, it is suggested that protocols for CBEMs curing need to be more related to time and location of CBEM construction. Another possible reason for this difference could be related to the difference between physical conditions in the laboratory and in-situ condition i.e. in the lab the specimens are unwrapped while in-situ they are quit confined. Therefore, it is also suggested to consider the effect of curing conditioning such as wrapped, unwrapped and partly wrapped on selecting the laboratory curing regime.

6.5 Summary

In the present chapter, the effects of several contributory factors on the curing process of CBEM have been evaluated with reference to stiffness modulus gain, resistance to permanent deformation and moisture loss of specimens. These factors were the curing time, curing temperature, cement/BBF content and relative humidity. In addition, the application of a maturity relationship to estimate the in-situ characteristic of CBEMs was investigated.

On the basis of the laboratory test results in the parametric study, the following conclusions were derived:

- An increase in curing temperature facilitated the evaporation of moisture in the CBEMs leading to improved mechanical and performance properties.
- The results also showed the role of cement/BBFs and their usefulness in positively improving the stiffness modulus, especially during the early life of CBEMs.
- High curing temperature was responsible for additional stiffness gain by increasing the binder stiffness due to ageing and by increasing the moisture loss by evaporation during the curing process. However, at high curing temperature the moisture loss by evaporation may hinder the hydration of cementitious materials.
- The results confirm that moisture loss by evaporation can be used to estimate ITSM due to curing. It seems a promising approach to estimate the mechanical properties to reduce the effect of size and shape of specimens on the curing condition.
- The treatment of CBEMs using cement/BBFs improves the resistance to permanent deformation even at lower curing temperature.

- Increasing the level of humidity may negatively influence the mechanical properties by reducing the moisture loss by evaporation. Therefore, it is important to consider the humidity level in any suggestion for curing protocol for CBEMs.

Regarding application of the maturity relationship, the following could be concluded:

- The results indicate that it was possible to establish reasonable correlations between maturity and stiffness modulus of CBEM using the equivalent age time instead of the time term in the maturity function.
- The maturity approach provides a powerful tool for predicting the stiffness modulus of CBEMs in a satisfactory manner. Therefore the maturity relationship could be implemented for estimating in-situ characteristics.
- Application of the maturity model in the hypothetical locations shows the effect of ambient temperature, curing age and filler treatments on the in-situ stiffness modulus.

Chapter 7

Pavement Analysis and Design Incorporating CBEMs

7.1 Introduction

From a road engineering perspective, pavement design should accommodate the effect of traffic, material characteristics and environmental conditions (Otte, 2013). These parameters are the main design inputs needed for pavement design. Meanwhile, it has been recognized in the literature that there is never a unique design solution for any combination of design inputs (Thom, 2008). In recent decades, the mechanistic–empirical approach has been found to be a useful tool incorporating the relation between laboratory and field performance of materials used in the pavement (Huang, 2004).

In the light of the findings in the previous chapters, an important question arises: how do the different filler treatments affect the final pavement performance. Therefore, the objective of this chapter is to investigate the effect of incorporating treated CBEMs on pavement performance. In the present study, CBEMs are suggested to be used in two scenarios: the first is as a surface course and the second is as a base course. Also, the scope of the study is limited here to design based on the fatigue criterion only.

7.2 Pavement arrangements and properties

CBEMs are normally used in highways as base courses particularly with recycled asphalt pavement involvement (Niazi and Jalili, 2009, Oke, 2010, Tebaldi et al., 2014, Ojum, 2015). Since the previous findings in Chapter 5 indicated the potential benefit of using treated CBEMs as a surface course due to their excellent performance, an attempt is made in this chapter to investigate this suggestion. However, it is believed that treated CBEMs still need more characterization tests to validate these suggestion fully. On the other hand, the use of treated CBEMs as base course is very common practice in the field. Table 7.1 summarizes the selected treated CBEMs involved in this study.

Table 7.1 The properties of the treated CBEMs involved in the pavement analysis

Mixture type	Stiffness modulus (MPa)	Poisson's ratio (assumed)	Fatigue life equation
1C-CBEM	7800	0.35	$N_f = 1 \times 10^{11} \times \varepsilon^{-3.424}$
3C-CBEM	19700	0.35	$N_f = 8 \times 10^{13} \times \varepsilon^{-4.934}$
C-G-CBEM	20200	0.35	$N_f = 2 \times 10^{14} \times \varepsilon^{-4.964}$
C-F-CBEM	8300	0.35	$N_f = 3 \times 10^{13} \times \varepsilon^{-4.854}$
C-G-1S-CBEM	21800	0.35	$N_f = 3 \times 10^{11} \times \varepsilon^{-3.289}$
C-F-1S-CBEM	11400	0.35	$N_f = 2 \times 10^{14} \times \varepsilon^{-4.808}$

7.2.1 The first scenario: study the effect of incorporating treated CBEMs as a surface course

In the first scenario, the pavement section consists of treated CBEMs as surface courses (60 mm), asphalt concrete (AC 50) as base course (150mm), a granular subbase (200 mm) and soft soil subgrade. Also, two alternative surface courses were included for comparison purposes which are hot rolled asphalt (HRA) and grouted macadam (GM). Figure 7.1 presents the pavement section arrangement for the first scenario. Table 7.2 summarizes the other conventional mixtures used to complete the pavement structure or used for comparison purposes.

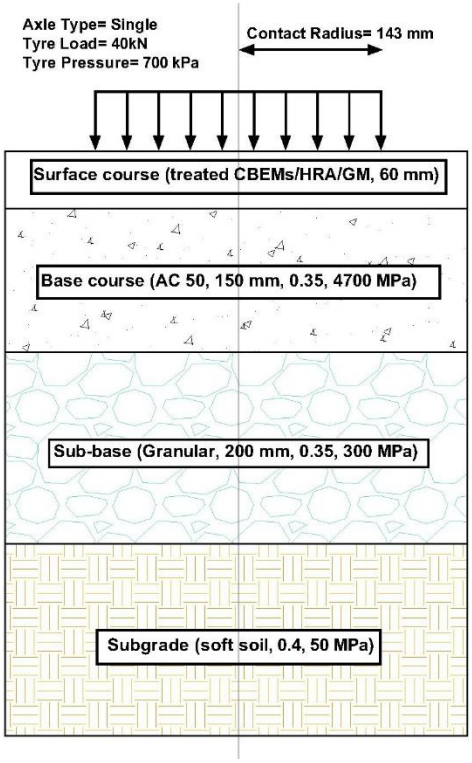


Figure 7.1 Pavement structure considered for analysis of the first scenario

Table 7.2 The properties of the other mixes involved the in the pavement analysis

Mixture type	Stiffness modulus (MPa)	Poisson's ratio	References
HRA	3100	0.35	(Read, 1996)
GM	12000	0.25	(Oliveira, 2006)
AC 50	5400	0.35	(Oliveira, 2006)
Granular sub-base	300	0.35	(Oke, 2010)
Unbound subgrade	50	0.4	(Huang, 2004)

7.2.2 The second scenario: study the effect of incorporating treated CBEMs as a base course

In the second scenario, the pavement section consists of HRA as surface course (60 mm), treated CBEM base course (150 mm), a granular subbase (200 mm) and soft soil subgrade, as shown in Figure 7.2. Also, a conventional bituminous base course (AC 50) was included for comparison purposes, see Table 7.2.

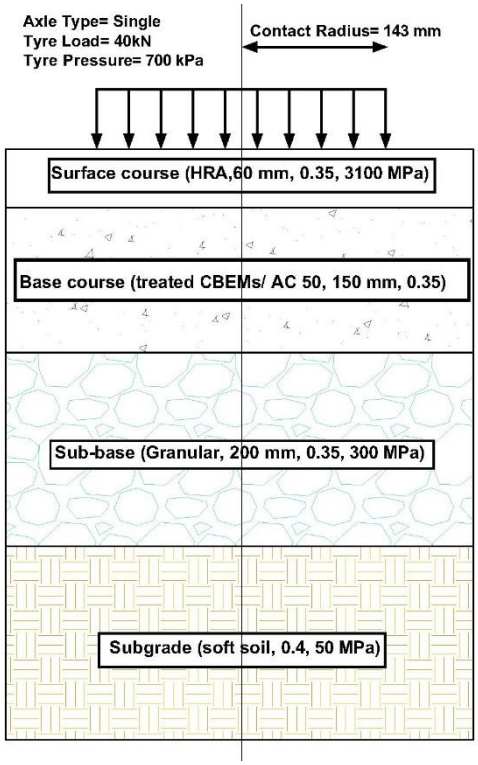


Figure 7.2 Pavement structure considered for analysis of the second scenario

For designing the pavements, a single 40kN tyre load, 700kPa tyre pressure and tyre contact area radius of 143mm were used for load application as recommended by Ebels (2008). The single wheel loading means that the critical horizontal position lies directly under the wheel load. More importantly, Twagira (2010) observed that the use of a single wheel also leads to a slightly more conservative estimate, because the stresses under single wheel loading are generally slightly higher than under dual wheel loading.

The analysis of the pavement structure was conducted using the software called KENLAYER which was developed by Huang (2004) at Kentucky University. KENLAYER is a multilayer elastic solution system under different wheel loads. Each layer can be considered as linear elastic, nonlinear elastic or viscoelastic material. More details and a description of the capabilities of the program are documented by Huang (2004). For simplicity, in the present study all layers have been

considered as linear elastic materials in order to show the relative change in pavement performance due to different filler treatments.

7.3 Pavement design methodology

In this work, the mechanistic-empirical pavement design approach was applied due to its ability to design using any new materials as stated by Lav et al. (2006). This is due to the fact that this approach deals with the mechanics of pavement materials and the pavement response, such as strain or stress. The response values are subsequently used to predict distress based on laboratory tests and field performance data. This aspect makes this method suitable since many laboratory tests have been conducted in the present work.

Following the mechanistic-empirical approach, two steps are necessary to design a flexible pavement. In the first step, the stress and strain responses of the pavement layers due to the wheel loads are calculated using analytical tools which enables the identification of critical points within the pavement structure. In the second step, these critical stress and strain responses are compared to the allowable stresses and strains identified from laboratory tests (Brown, 2013).

In conventional pavements, two principal modes of failure occur, cracking of bound layers and rutting in the wheel tracks. For successful structural design these two modes of failure should be included to ensure that the pavement resists both (Brown, 2013). Since this study was limited to design based on the fatigue criterion only, the tensile stress/strain should be checked at the bottom of each bound layer. Therefore, for design purposes, two locations in the pavement structure are considered for critical stresses and strains. These are the bottom of the surface and base courses where the tensile stress/strain may cause fatigue cracking. The tensile strain is then generally used to characterise the fatigue life of a bituminous material

using equations such as those in Table 7.1. This is because fatigue cracking of a bituminous layer under repeated wheel loads is controlled by the magnitude of tensile strain rather than the stress (Kuna, 2015).

7.4 Pavement stress and strain distribution results

7.4.1 Vertical stress and strain distributions for the first scenario

The vertical stress and strain were plotted against the depth of pavement, as shown in Figure 7.3 and Figure 7.4 respectively.

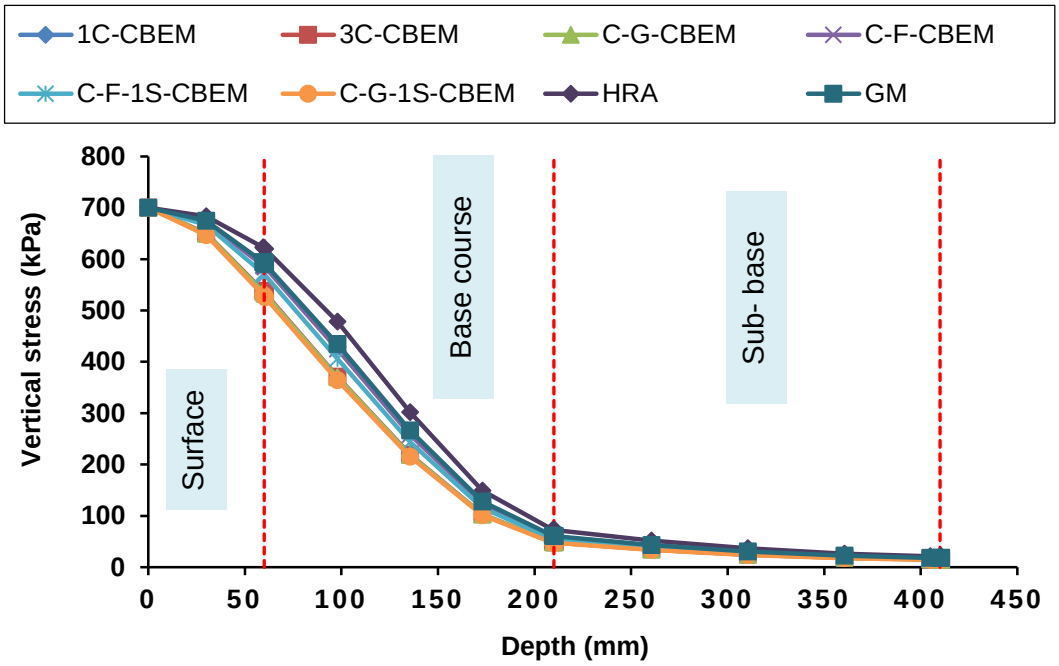


Figure 7.3 Vertical stress distribution through pavement structure for first scenario

Figure 7.3 illustrates the reduction in the vertical stress as the depth of pavement increases. The results of the analyses indicate that vertical stress in BBF and TBF surface pavements, particularly with GGBS, is considerably decreased relative to HRA and GM mixes.

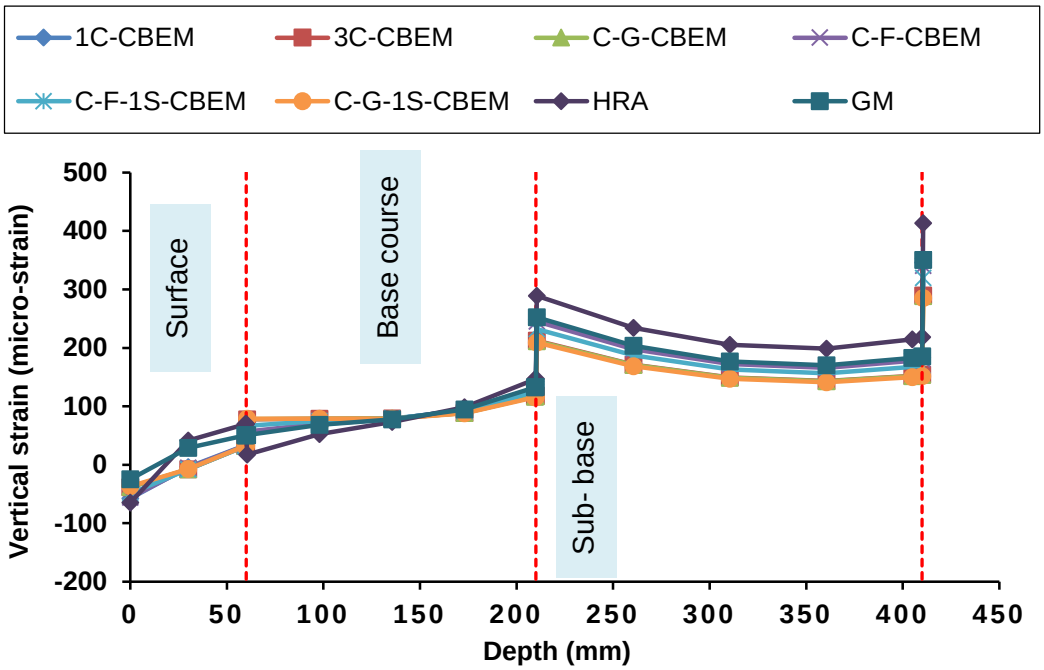


Figure 7.4 Vertical strain distribution through pavement structure for the first scenario

Furthermore, Figure 7.4 shows the vertical strain distribution in the pavements. It can be seen from that figure that, as a result of the high stiffness modulus of treated CBEMs, the vertical strain at depth is decreased in comparison to HRA.

7.4.2 Horizontal stress and strain distributions for the first scenario

Figure 7.5 presents the horizontal stress distribution in the pavement structure. The results show that the horizontal stress gradually changes with depth from a relatively high compressive stress at the top of the surfacing layer. For tensile strain, it can be seen in Figure 7.6, the strain changes gradually through the surface layer from a relatively high compressive strain (positive value) at the top of the surfacing layer to a tensile strain (negative value) at the bottom; similar performance was noticed in HRA and GM mixes.

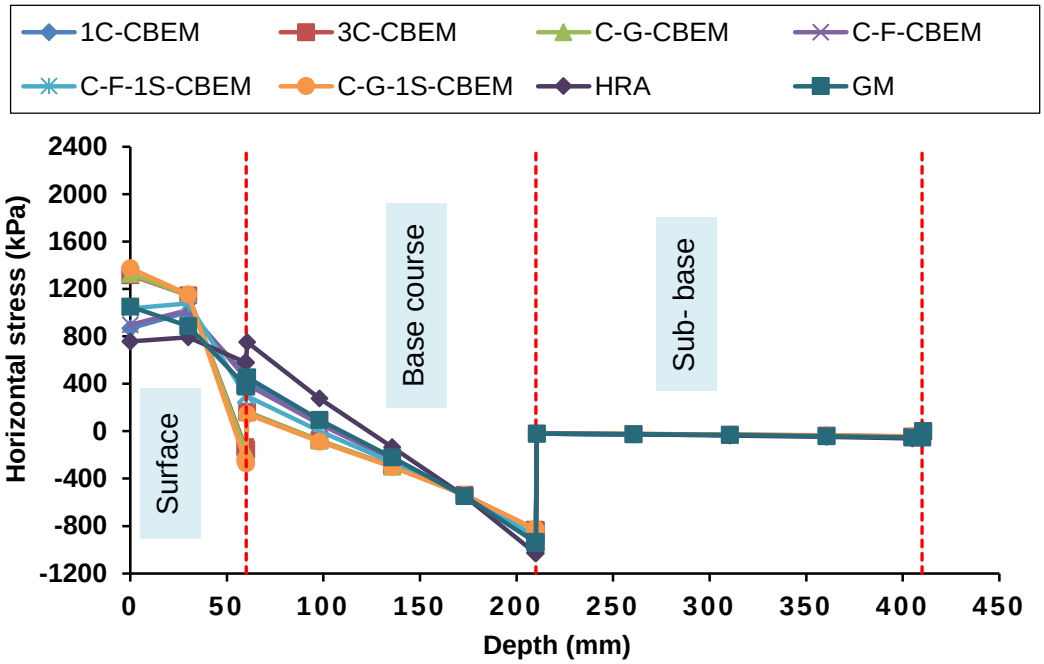


Figure 7.5 Horizontal stress distribution through pavement structure for the first scenario

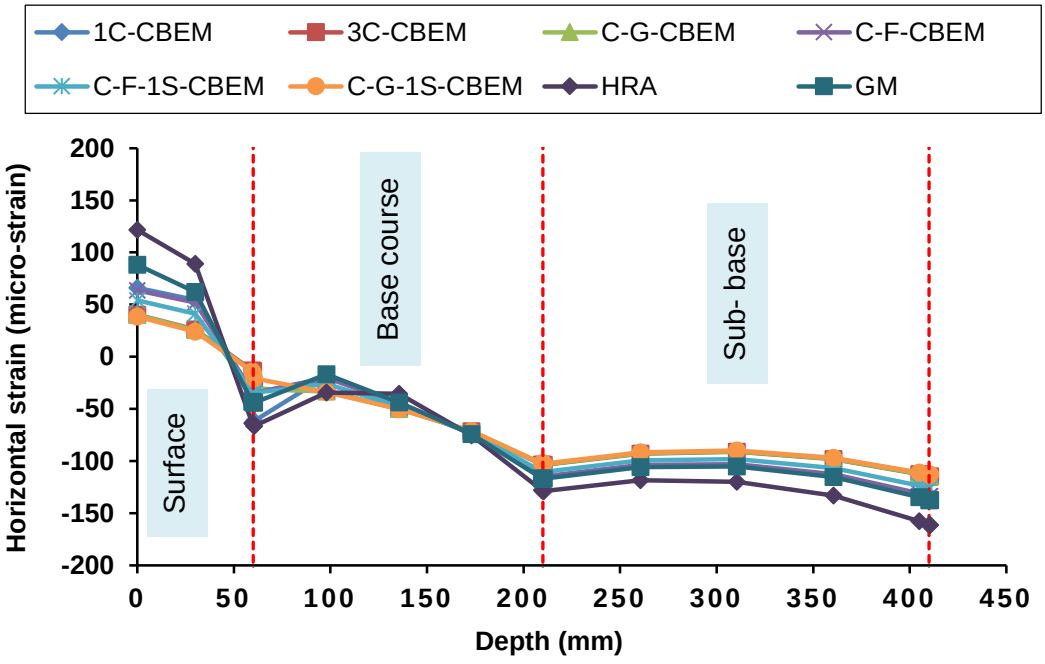


Figure 7.6 Horizontal strain distribution through pavement structure for the first scenario

7.4.3 Vertical stress and strain distributions for the second scenario

In the second scenario, as seen in Figure 7.7, the vertical stress reduces with the pavement depth again. Also, it was found that there is a relative decrease in the vertical stress on the top of the sub-base layer when using different filler treatments for CBEM base in comparison to the traditional bituminous mixture (AC 50). Figure 7.8 shows the vertical strain distribution in the pavements. This figure indicates significant differences in the vertical strain at the bottom of the base course. Figure 7.8 also shows that the treated CBEMs generally have lower strain values compared to AC 50.

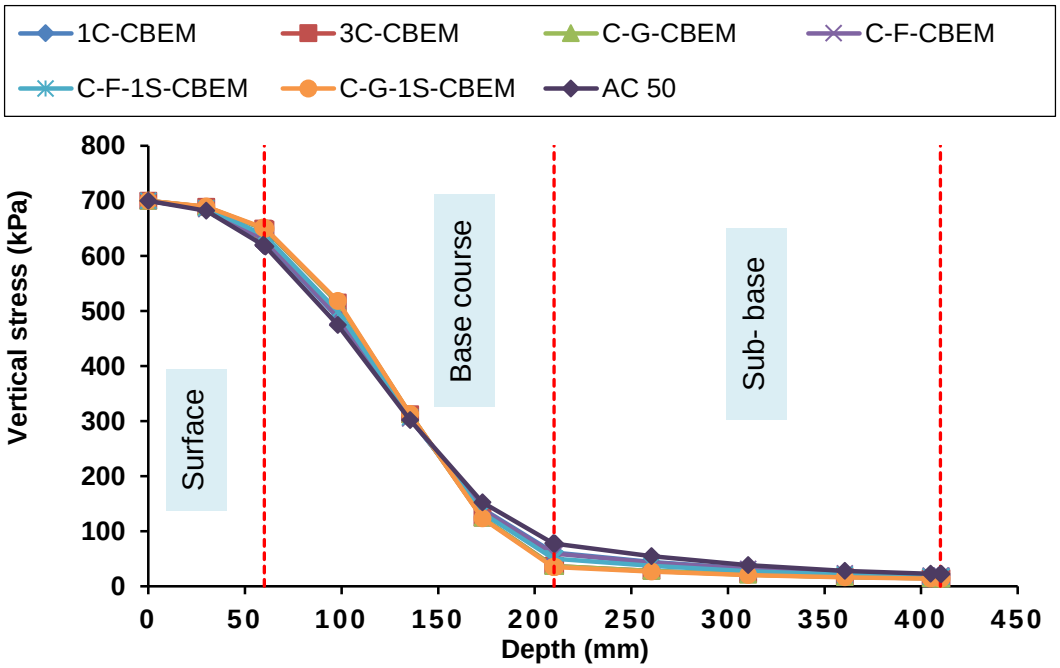


Figure 7.7 Vertical stress distribution through pavement structure for the second scenario

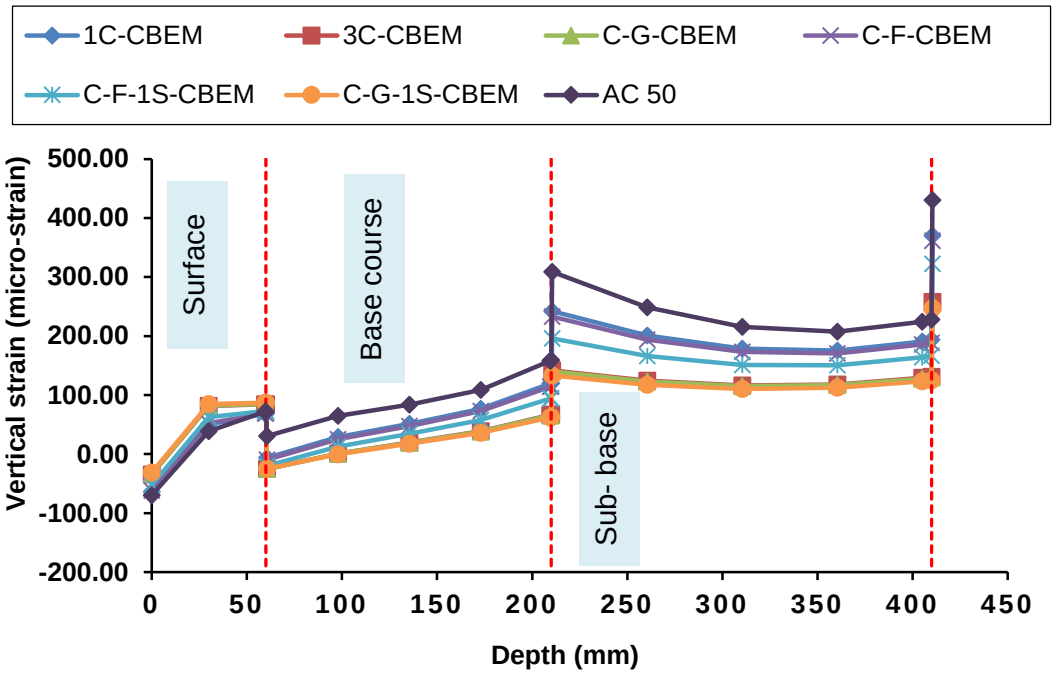


Figure 7.8 Vertical strain distribution through pavement structure for the second scenario

7.4.4 Horizontal stress and strain distributions for the second scenario

Figure 7.9 and Figure 7.10 show the horizontal stress and strain in the pavement structure for the second scenario. Figure 7.9 shows that the horizontal stress gradually changes with depth from a relatively high compressive stress (positive value) at the top of the base course layer to a tensile stress (negative value) on top of the subbase. At the bottom of the base course, greater applied stress was found as consequence of the high stiffness modulus of treated CBEMs in comparison to AC 50. Figure 7.10 also indicates significant differences in strains for the base course and the maximum horizontal tensile strain was found at the bottom of the base layer. In contrast, Oke (2010) and Ojum (2015) found the maximum horizontal and vertical strains to be located at the middle of base layers; which may results due to using non-linear approach.

By way of comparison, the treated CBEMs had lower tensile strain at the bottom of the base layer relative to AC 50. Another point that should be noted is that the high stiffness of treated CBEMs causes a decrease in the horizontal strain applied at the bottom of the surface layer (HRA). The absence of tensile strain at the bottom of the surface layer can be attributed to the full contact/friction assumed between layers and the high stiffness modulus mixes used as base course. A similar observation was noted in a recent work focussing on incorporating rubberized cement-stabilized mixture as base course material (Farhan, 2016). The lowest tensile strain at the bottom of the base course was noted for 3C-CBEM, C-G-CBEM and C-G-1S-CBEM.

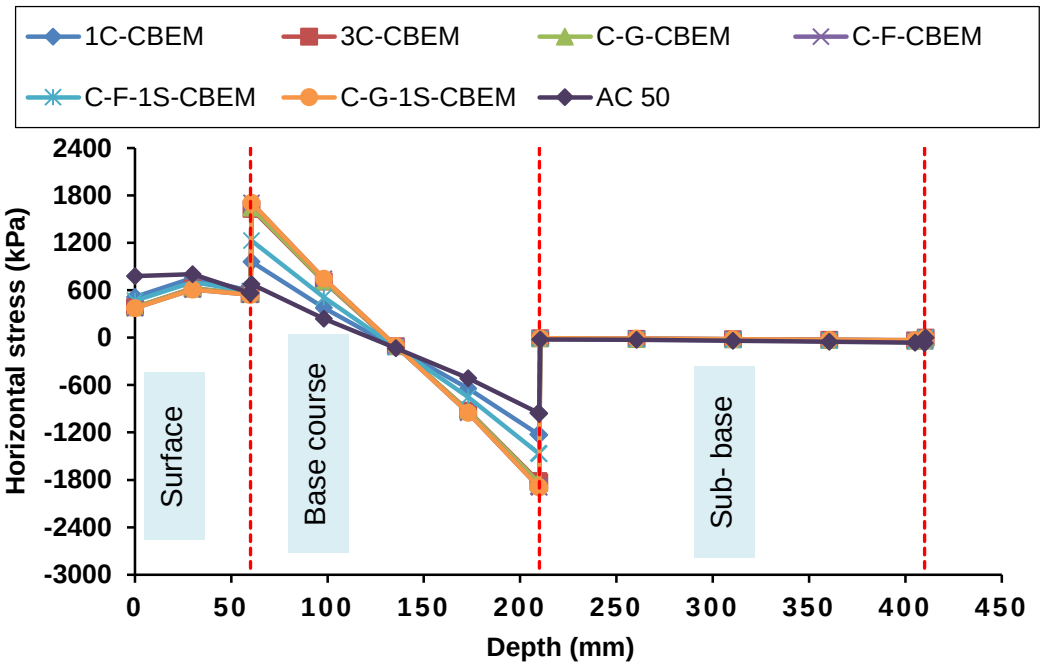


Figure 7.9 Horizontal stress distribution through pavement structure for the second scenario

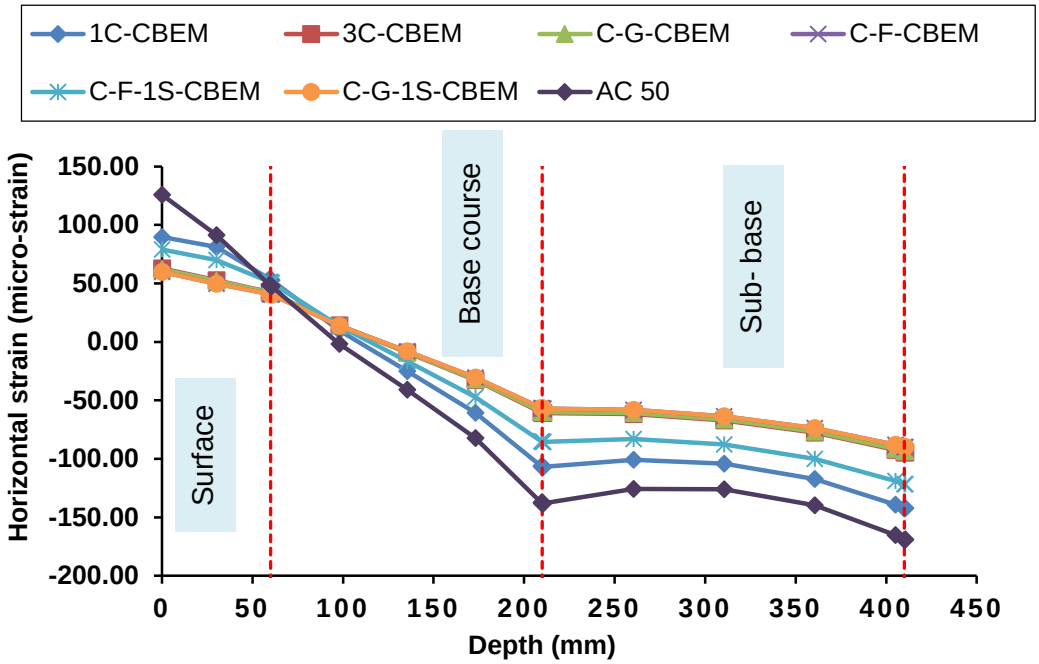


Figure 7.10 Horizontal strain distribution through pavement structure for the second scenario

7.5 Pavement design sensitivity analysis

7.5.1 Introduction

The evaluation of different pavement structures including treated CBEMs was carried out in terms of fatigue life according to the tensile strains obtained. A major difficulty with fatigue testing is developing a relevant relationship between the results of laboratory tests and field performance. Therefore, to overcome this issue in structural analysis and design of pavements multipliers known as shift factors (or transfer functions) should be applied. However, it is believed that to apply such a factor will reduce the integrity of this research as long as determination of these shift factors is not in the scope of the study and as the objective of this study is to present the relative difference caused using different filler treatments in CBEMs. Therefore, using shift factors will be ignored and the result will be presented in terms of allowable values taken directly from laboratory testing.

The fatigue life calculations for the treated CBEM layers were made according to the laboratory results obtained during the present project, see Table 7.1. The fatigue life of other bituminous mixtures involved in the pavement structures (AC 50) was calculated according to the fatigue criteria given by Read (1996), as given by Equation 7.1. The stress and strain distribution in previous sections showed that the maximum horizontal strains occurred at the bottom of the base course, which resulted in these strains being appropriate for design purposes.

$$N_f = 2.45 \times 10^{13} \times \varepsilon^{-3.923} \qquad \text{Equation 7.1}$$

7.5.2 Incorporating CBEMs as surface course

60 mm layers of treated CBEM, HRA or GM were assumed as surface courses with different AC 50 base course thicknesses. The thickness of base course layer was varied from 100 to 300 mm in 50 mm increments. The reason for this was to evaluate the effect of including the treated CBEMs as a surface layer on the base layer performance, the latter layer having a large thickness in comparison to the surface layer. Figure 7.11 presents the fatigue life based on the tensile strain at the bottom of the AC 50 layer as a result of incorporating the selected surface layers. The fatigue life calculations were based on Equation 7.1, the fatigue life being expressed as the number of load application till failure in terms of millions of standard axles (MSA).

It can be seen from Figure 7.11, that a significant improvement in the fatigue life of the base course is noted as a result of reduction in the horizontal tensile strain at the bottom of the base layer (AC 50) due to incorporating treated CBEMs. The GM mix also showed a very similar behaviour to CBEMs while the HRA showed lower fatigue life relative to both CBEMs and GM. It can be concluded that the benefits of

using the treated CBEMs as a surface course are evident and a longer fatigue life could be expected from such pavement structures.

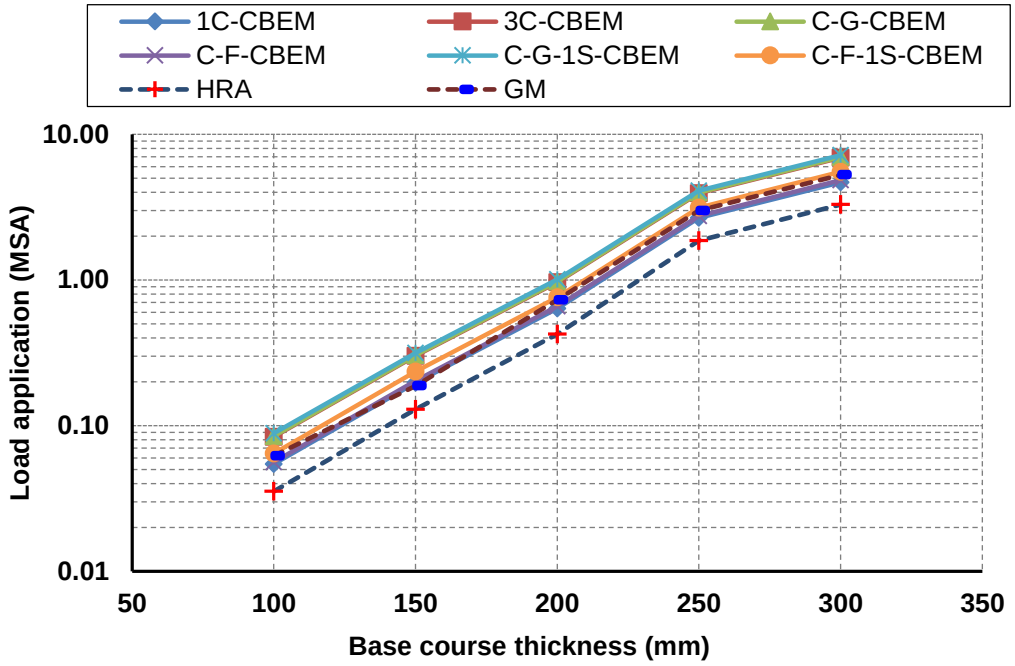


Figure 7.11 Allowable load applications for variable AC 50 base course thicknesses under 60 mm of treated CBEM as a surface

7.5.3 Incorporating CBEMs as base course

A similar methodology to that described in section 7.5.2 was used to study the design of pavements incorporating CBEM base courses. In this case, the material used in the surface course was a traditional HRA mixture with 60 mm thickness. The treated CBEMs and AC 50 were assumed to be used as a base course with different thicknesses from 100 to 300 mm in 50 mm increments. The tensile strains at the bottom of base course were used for fatigue life calculations based on the fatigue equations obtained from the laboratory results as shown Table 7.1 for CBEMs and based on Equation 7.1 for AC 50. The results are shown in Figure 7.12.

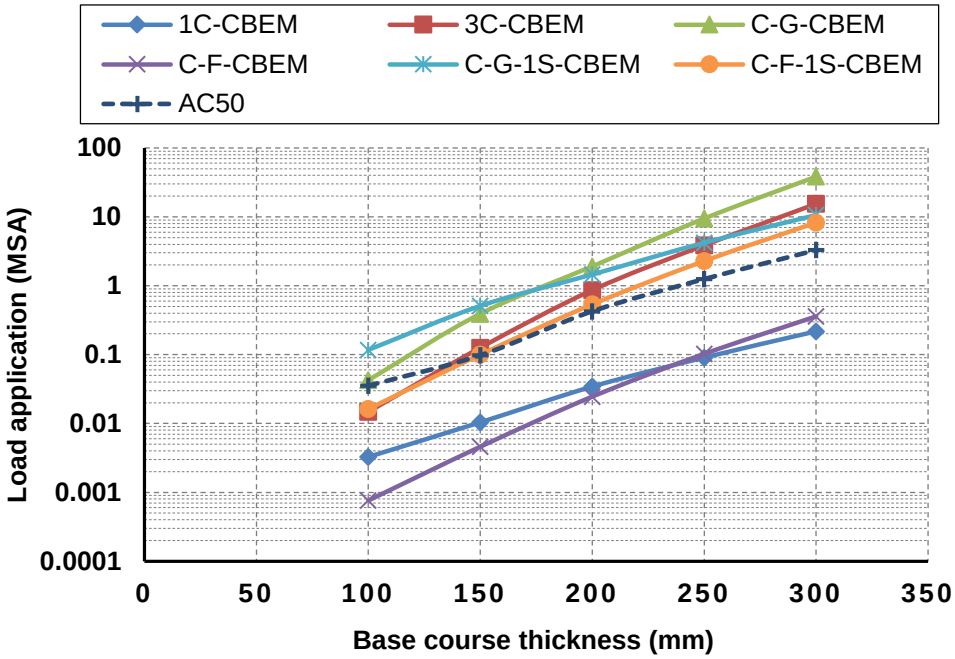


Figure 7.12 Allowable load applications for variable treated CBEM base course thicknesses under 60 mm HRA as a surface

As can be seen in Figure 7.12, a considerably longer fatigue life was found by increasing the base course thickness and this is most evident for stiffer treated CBEM bases which cause a reduction in the tensile strain at the bottom of the layer. The AC 50 mix presents lower fatigue life compared to CBEMs except 1C-CBEM and C-F-CBEM. The latter two mixes show lower fatigue life in comparison to other mixes as a result of their low tensile strength, as found in Chapter 5.

7.6 Summary

This chapter has investigated the structural design and modelling of flexible pavements incorporating treated CBEMs. Two scenarios of CBEM incorporation were applied: as a surface course compared with HRA and GM; or as a base course compared to AC 50. A pavement design sensitivity analysis to study the effect of treated CBEMs in the pavement structure was carried out in terms of fatigue life. As a result of this study, the following conclusions can be put forward:

- A longer fatigue life of the pavement structure was found due to incorporating both CBEMs and GM as a surface course compared to traditional HRA.
- The incorporation of CBEMs as a base course, except 1C-CBEM and C-F-CBEM, give longer fatigue life compared to AC 50.

Chapter 8

Conclusions and Recommendations

8.1 Introduction

In this thesis, an investigation into enhancing the performance of cold bitumen emulsion mixture (CBEM) using supplementary cementitious materials (SCMs) has been performed. With this purpose, the design and optimization of CBEM was studied in Chapter 4 to develop a performance-based mix design due to the absence of any widely accepted mix design method. Characterization of the mechanical and durability properties of CBEMs treated with cement and SCMs was carried out with attention paid to the microstructure of these mixes, as presented in Chapter 5. Furthermore, the effect of curing on the performance of CBEMs was evaluated and extended to apply the maturity model in Chapter 6, enabling prediction of the performance of CBEM based on its curing condition. Finally, a brief study was carried out in Chapter 7 to evaluate the effect of incorporating the CBEMs into the pavement structure in terms of surface and base courses.

This chapter summarizes the main issues discussed in each of the previous chapters. The main conclusions are presented in section 8.2. Some recommendations for future research are also suggested in section 8.3.

8.2 Conclusions

8.2.1 The main conclusions related to design and optimization of CBEM

The optimization of CBEM was investigated in Chapter 4, to determine optimum proportions to gain suitable mechanical and volumetric properties. A statistical tool, response surface methodology (RSM), was applied to optimize the mix design parameters, namely bitumen emulsion content (BEC), pre-wetting water content (PWC) and curing temperature (CT). The indirect tensile stiffness modulus test and indirect tensile strength test in both dry and wet conditions were performed to obtain the mechanical response while air voids and dry density were measured to obtain volumetric responses. Based on the laboratory experiments and analyses, the following conclusions can be drawn:

- The experimental results for the optimum mix design corresponded well with model predictions. It was concluded that optimization using RSM is an effective approach for mix design of CBEMs.
- The RSM approach offers a more comprehensive view of the effect of the variation of each mix design parameter on the mechanical and volumetric responses of CBEMs than would otherwise be the case. It has the advantage that all parameters are investigated at one time.
- The individual effects of BEC and PWC are important, rather than simply the total fluid content which is used in conventional mix design methods.
- The results indicate that the interaction of BEC, PWC and CT influences the mechanical properties of CBEM. However, the PWC tended to influence the volumetric properties more significantly than BEC.

- The evaluation of stiffness modulus of CBEM after 10 days is likely to give the designer appropriate information to optimize the mix design in a relatively short time.
- Based on the optimization by RSM, it can be concluded that the optimum mix design proportions (BEC and PWC) tend to be only slightly influenced by CT.

8.2.2 The main conclusions related to performance characterization of CBEMs

An extensive performance characterization of CBEMs treated with cement and blended fillers was carried out in Chapter 5. The CBEMs were treated using Ordinary Portland cement (OPC), binary and ternary blended fillers (BBF and TBF). OPC, fly ash (FA) and ground granulated blast furnace slag (GGBS) were used for the BBF while silica fume (SF) was added to the BBF to obtain TBF. The mechanical performance was evaluated in terms of stiffness modulus over one year and resistance to permanent deformation and resistance to crack initiation and crack propagation, while durability evaluation was carried out in terms of resistance to moisture and frost damage. Furthermore, the mineralogy and microstructure of CBEMs were evaluated using X-ray diffraction analysis and scanning electron microscopy. The conclusions of the study can be summarized as follows:

- A considerable amount of water is maintained inside CBEM treated with cement and blended fillers which may be used for enhancing the hydration process with time and producing new hydration products due to filler reactivity.
- The study also found that a significant improvement was achieved in stiffness modulus of CBEMs due to incorporation of cement and blended fillers. This improvement might be attributed to a complex mechanism

occurring inside treated CBEMs, which could be related to the hydration process of cement and SCMs through absorbing the trapped water and enhancing the process.

- The presence of cement and SCMs may lead to an improvement in the volumetric properties.
- All treated CBEMs were also found to reduce temperature susceptibility relative to HMA 40/60 and untreated CBEM (LF-CBEM).
- Excellent performance was found in the resistance of CBEM treated with cement and blended fillers to permanent deformation. The findings show that the accumulated permanent strain in CBEMs treated with cement or blended fillers was found to be less than 1% under high stresses.
- A significant improvement in tensile strength was found in CBEM treated with cement and blended fillers, particularly those treated with GGBS. This would further imply that modified mixtures appear to be capable of withstanding large tensile stress prior to cracking.
- The treatment of CBEMs using cement or blended fillers significantly improves the fatigue performance. They have a longer fatigue life at strains of less than 200 micro-strain (low stress levels) while at higher than 200 micro-strain (high stress levels) the material behaved in a brittle manner and failed under a low number of cycles compared with HMA 40/60.
- A reduction in the fracture toughness and an increased tendency for the fracture to become brittle were also confirmed for CBEM treated using cement and blended fillers.
- In the durability evaluation, the treated CBEMs showed less susceptibility to severe environmental conditions such as moisture and frost damage.
- Mineralogical and microstructural assessments suggested that the presence of bitumen emulsion might not affect the hydration of the silicates (formation of CSH gel) in treated CBEMs.

- A delay in the formation of other hydration products (Ettringite) was noticed; this product results from the hydration of aluminates in cement.
- Moreover, the mechanical properties and the mineralogical and microstructural assessments suggest that SF addition to BBF-CBEMs can eliminate any delay in hydration product formation (aluminates in cement) caused by bitumen emulsion in the CBEMs.
- This finding suggests that the use of BBF-CBEMs might be appropriate for pavements in cold climates whereas TBF-CBEMs would be effective in road pavements exposed to severe conditions both in hot and cold climates.

8.2.3 The main conclusions related to parametric curing study and maturity relationship application of CBEMs

In chapter 6, the effects of several contributory factors on the curing process of CBEM have been evaluated with reference to stiffness modulus gain, resistance to permanent deformation and moisture loss of specimens. These factors were the curing time, curing temperature, cement/BBF content and relative humidity. In addition, the application of a maturity relationship to estimate the in-situ characteristic of CBEMs was investigated. The following conclusions were derived:

- An increase in curing temperature facilitated the evaporation of moisture in the CBEMs leading to improved mechanical and performance properties.
- High curing temperature was responsible for additional stiffness gain by increasing the binder stiffness due to ageing and by increasing the moisture loss by evaporation during the curing process.
- A high curing temperature may hinder the hydration of cementitious materials through increasing the early moisture loss by evaporation.

- The correlation between moisture loss by evaporation and ITSM could be a promising approach to estimate the mechanical properties regardless of the size and shape of specimens used on the curing process.
- Increasing the level of humidity may negatively influence the mechanical properties by reducing the moisture loss by evaporation.
- A reasonable correlation has been established between maturity and stiffness modulus of CBEM using the equivalent age time instead of the time term in the maturity function.
- The maturity approach provides a powerful tool for predicting the stiffness modulus of CBEMs in a satisfactory manner. Therefore the maturity relationship could be implemented for estimating in-situ characteristics.
- Application of the maturity model in hypothetical locations demonstrates the effect of ambient temperature, curing age and filler treatment on the in-situ stiffness modulus.

8.2.4 The main conclusions related to pavement analysis and design incorporating CBEMs

Chapter 7 has investigated the structural design and modelling of flexible pavements incorporating treated CBEMs. Two scenarios of CBEM incorporation were applied: as a surface course compared with HRA and GM; or as a base course compared to AC 50. A pavement design sensitivity analysis to study the effect of treated CBEMs in the pavement structure was carried out in terms of fatigue life. As a result of this study, the following conclusions can be put forward:

- A longer fatigue life of the pavement structure was found due to incorporating both CBEMs and GM as a surface course compared to traditional HRA.
- The incorporation of CBEMs as a base course, except 1C-CBEM and C-F-CBEM, give longer fatigue life compared to AC 50.

8.3 Recommendations for further research

This investigation has revealed areas where further research could be undertaken to support and validate the findings of the present study. Therefore, some recommendations for future studies areas are made as the follows:

- Although this project has contributed to developing a performance-based mix design using a statistical tool as an alternative mix design approach, the scope of the present study was limited to consider three mix design parameters. Therefore, it is recommended to carry out a further investigation with the same statistical tools but involving more parameters such as active filler content, aggregate type, aggregate gradation and different bitumen emulsion type.
- In the present study, the philosophy of incorporating the cement/blended fillers assumed that the replacement of these fillers does not influence either the optimum bitumen emulsion content or pre-wetting water content optimization. It is worth verifying whether the presence of cement/blended fillers in CBEMs affects this optimization.
- Since the present study was carried out by mixing the SCMs with 1% of cement, it is recommended to investigate other types of activation, e.g. using hydrated lime and other alkali-activated materials as an alternative to ordinary Portland cement.
- One of the major assumptions in the present study is the amount of cement (1%) needed to activate the SCMs. It is recommended to investigate and optimize both cement and SCMs proportions.
- It is highly recommended to make a field trial incorporating treated CBEM in order to gain practical information on such mixes where, to date, there is no broad experience available. Also, it could be a useful opportunity to correlate between laboratory and field performance and monitor the deterioration phenomenon. This is expected to be more evident in the field.

- An economic study should be performed to determine the actual costs effectiveness of incorporating SCMs as filler treatment in CBEMs instead of conventional treatment such as ordinary Portland cement and hydrated lime.
- In the present study, it was suggested to use the treated CBEMs as a surface course based on limited laboratory tests due to time and material constraints. It is recommended to extend the laboratory tests to evaluate different properties such as resistance to ravelling, and ageing damage and skid resistance. These evaluations could validate this suggestion.
- In Chapter 5, the findings showed that the treatment of CBEMs with cement and blended filler caused a reduction in the fracture toughness and a change in the development of fracture to become more brittle. Therefore, it is worth carrying out research to establish the stress-strain relationships for treated CBEMs in order to understand the fracture mechanism in CBEM more deeply.
- The microstructure investigation of treated CBEMs revealed that the presence of bitumen emulsion might not affect the hydration of the silicates. However, it seems that this can cause a delay in the formation of other hydration products (Ettringite) resulting from the hydration of aluminates in cement. It is recommended to investigate the interaction mechanism between the bitumen emulsion and cement/blended fillers. This study needs to examine the hydration products at nano-scale to understand the effect of the presence bitumen emulsion on the structure of hydration products. Such a study will add further understanding to the mechanism of strength gain in CBEMs.
- As seen in Chapter 6, curing CBEMs at 20°C at a high humidity level resulted in lower stiffness modulus relative to a low humidity level. Acknowledging that limited research has covered this point, it is recommended to study the impact of different levels of humidity and curing temperatures together on the performance characteristics. Moreover, the maturity functions that were

applied in the present study do not consider the effect of relative humidity on stiffness evolution. Therefore, it is recommended to incorporate relative humidity in such functions in a future study.

- Chapter 6 shows the effect of high curing temperature on moisture loss, which may affect the hydration process of active filler. Therefore, it is recommended to study the effect of curing temperature on the hydration process in CBEMs. This should be extended to investigate also the microstructure of CBEMs at different curing temperatures.
- The central theme of performance evaluation in the parametric curing study, Chapter 6, relates to mechanical properties. Therefore, it is suggested to investigate the influence of physical properties of CBEMs under different curing conditions. Also, it would be beneficial for this study to include the effect of different compaction methods and specimen sizes on the curing mechanism of CBEMs.
- During the present study, the traditional curing method of heating the cured specimens to different curing temperatures was used. Future work could usefully investigate the applicability of other curing methods such as using microwaves, induction heating and vacuuming treatment.
- In Chapter 7 the structural design and was carried based on fatigue criteria only. However, it is important to consider other type of pavement distress. Therefore, it is very essential to perform a details investigation related to structural design of pavement incorporating CBEMs (after collecting sufficient data regarding the effect of different pavement stress such as fatigue, permanent deformation, ravelling, ….etc.) to validate the results and suggestion to use CBEMs as surface and base courses.
- One of the shortcomings in laboratory performance evaluation is the gap between laboratory fatigue tests and field conditions. For this reason in structural analysis and design a multipliers known as shift factors (or transfer functions) were applied. These shift factors were sensibly ignored

in the present study as determination of these shift factors is not in the scope of the study and the point is to see the sensitivity of pavement structure due to using different filler treatments. Therefore, future research is needed to identify appropriate shift factors (or transfer functions) that could be applied for CBEMs to effectively fill the gap between laboratory fatigue tests and field conditions.

References

AIREY, G. D., HUNTER, A. E. & COLLOP, A. C. 2008. The effect of asphalt mixture gradation and compaction energy on aggregate degradation. *Construction and Building Materials,* 22**,** 972-980.

AKEROYD, F. & HICKS, B. 1988. Foamed bitumen road recycling. *Highways,* 56.

AKSOY, A., ŞAMLIOGLU, K., TAYFUR, S. & ÖZEN, H. 2005. Effects of various additives on the moisture damage sensitivity of asphalt mixtures. *Construction and Building Materials,* 19**,** 11-18.

AKZONOBEL 2009. Bitumen Emulsion, Technical Bulletin. Stenungsund,Sweden: Akzo Nobel Surface Chemistry.

AL-BUSALTAN, S., AL NAGEIM, H., ATHERTON, W. & SHARPLES, G. 2012. Mechanical Properties of an Upgrading Cold-Mix Asphalt Using Waste Materials. *Journal of Materials in Civil Engineering,* 24**,** 1484-1491.

AL-HDABI, A., AL NAGEIM, H., RUDDOCK, F. & SETON, L. 2013a. Development of Sustainable Cold Rolled Surface Course Asphalt Mixtures Using Waste Fly Ash and Silica Fume. *Journal of Materials in Civil Engineering,* 26**,** 536-543.

AL-HDABI, A., AL NAGEIM, H., RUDDOCK, F. & SETON, L. 2013b. A novel Cold Rolled Asphalt mixtures for heavy trafficked surface course. *Construction and Building Materials,* 49**,** 598-603.

AL-HDABI, A., AL NAGEIM, H. & SETON, L. 2014. Performance of gap graded cold asphalt containing cement treated filler. *Construction and Building Materials,* 69**,** 362-369.

ALDAHDOOH, M., MUHAMAD BUNNORI, N. & MEGAT JOHARI, M. 2013. Evaluation of ultra-high-performance-fiber reinforced concrete binder content using the response surface method. *Materials & Design,* 52**,** 957-965.

ALIZADEH, R. A. 2009. *Nanostructure and engineering properties of basic and modified calcium-silicate-hydrate systems.* PhD Thesis, University of Ottawa ,Canada.

AMERI, M., SANIJ, H. K., TOOLABI, S. & HOSSEINI, S. H. 2012. Optimization of The Cold In-Place Recycling Mix Design by Nonlinear Simplex Method. *Transportation Research,* 2**,** 1.

AMERICAN ASSOCIATION OF STATE HIGHWAY TRANSPORTATION OFFICIALS 2009. AASHTO T283: Resistance of compacted bituminous mixture to moisture induced damage standard specifications for transportation materials and methods of sampling and testing. *Part II tests.* Washington, DC.

ARIMILLI, S., JAIN, P. K. & NAGABHUSHANA, M. 2015. Optimization of Recycled Asphalt Pavement in Cold Emulsified Mixtures by Mechanistic Characterization. *Journal of Materials in Civil Engineering,* 28**,** 04015132.

ASI, I. M. 2006. Laboratory comparison study for the use of stone matrix asphalt in hot weather climates. *Construction and Building Materials,* 20**,** 982-989.

ASPHALT ACADEMY 2009. A Guideline for the Design and Construction of Bitumen Emulsion and Foamed Bitumen Stabilised Materials. *Technical guideline*

(TG2): Bitumen Stabilized Materials Second ed. CSIR Built Environment, South Africa, Pretoria.

ASPHALT INSTITUTE 1989. Asphalt Cold Mix Manual. *Series No. 14.* Maryland, USA.

BATISTA, F. & ANTUNES, M. Pavement rehabilitation using asphalt cold mixtures. Maintenance and Rehabilitation of Pavements and Technological Control, 7-10th July 2003 Guimaraes, Portugal

BAYRAMOV, F., TAŞDEMIR, C. & TAŞDEMIR, M. A. 2004. Optimisation of steel fibre reinforced concretes by means of statistical response surface method. *Cement and Concrete Composites,* 26**,** 665-675.

BEHNOOD, A. & ZIARI, H. 2008. Effects of silica fume addition and water to cement ratio on the properties of high-strength concrete after exposure to high temperatures. *Cement and Concrete Composites,* 30**,** 106-112.

BEKTAS, F. & BEKTAS, B. A. 2014. Analyzing mix parameters in ASR concrete using response surface methodology. *Construction and Building Materials,* 66**,** 299-305.

BENTZ, D. P. & PELTZ, M. A. 2008. Reducing thermal and autogenous shrinkage contributions to early-age cracking. *ACI Materials Journal,* 105**,** 414.

BETTI, G., AIREY, G., JENKINS, K., MARRADI, A. & TEBALDI, G. Active Filler's Effect on In Situ Performances of Bitumen Emulsion Recycled Mixtures. 8th RILEM International Symposium on Testing and Characterization of Sustainable and Innovative Bituminous Materials, 2016. Springer, 799-810.

BOCCI, M., GRILLI, A., CARDONE, F. & GRAZIANI, A. 2011. A study on the mechanical behaviour of cement–bitumen treated materials. *Construction and Building Materials,* 25**,** 773-778.

BONAVETTI, V., DONZA, H., MENENDEZ, G., CABRERA, O. & IRASSAR, E. 2003. Limestone filler cement in low w/c concrete: a rational use of energy. *Cement and Concrete Research,* 33**,** 865-871.

BRAYTON, T. E., LEE, K., GRESS, D. & HARRINGTON, J. Development of performance-based mix design for Cold in-Place Recycling of asphalt mixtures. 80th Annual Meeting of the Transportation Research Board, 2000 Washington, D.C.,USA

BROUWERS, H. 2006. Particle-size distribution and packing fraction of geometric random packings. *Physical Review E.* American Physical Society.

BROWN, S. F. An introduction to asphalt pavement design in the UK. Proceedings of the Institution of Civil Engineers-Transport, 2013. Thomas Telford Ltd, 189-202.

BUENO, B., DA SILVA, W., DE LIMA, D. & MINETE, E. 2003. Engineering Properties of Fiber Reinforced Cold Asphalt Mixes. *Journal of Environmental Engineering,* 129**,** 952-955.

BUTTON, J. W., ESTAKHRI, C. & WIMSATT, A. 2007. A synthesis of warm mix asphalt. Texas Transportation Institute, Texas A & M University System College Station, TX.

CARDONE, F., GRILLI, A., BOCCI, M. & GRAZIANI, A. 2014. Curing and temperature sensitivity of cement–bitumen treated materials. *International Journal of Pavement Engineering***,** 1-13.

CARINO, N. J. The maturity method: From theory to application. Structures Congress & Exposition, May 21-23, 2001 Washington, D.C, USA. American Society of Civil Engineering, Reston, Virginia, Peter C. Chang, Edit., 2001.

CARINO, N. J. & TANK, R. C. 1992. Maturity function for concretes made with various cements and admixtures. *Materials Journal,* 89**,** 188-196.

CEDR 2014. Report on available test and mix design procedures for cold-recycled bitumen stabilised materials. *Conference of European Directors of Roads Call2012: Transnational Road Research Programme.* Prague, The Czech Republic.

CHAPPATI, M. & BILAL, J. 2003. The environmental road of the future: energy consumption and greenhouse gas emission. France.

CHÁVEZ-VALENCIA, L., ALONSO, E., MANZANO, A., PEREZ, J., CONTRERAS, M. & SIGNORET, C. 2007. Improving the compressive strengths of cold-mix asphalt using asphalt emulsion modified by polyvinyl acetate. *Construction and Building Materials,* 21**,** 583-589.

CHÁVEZ-VALENCIA, L., MANZANO-RAMÍREZ, A., LUNA-BARCENAS, G. & ALONSO-GUZMÁN, E. 2005. Modelling of the performance of asphalt pavement using response surface methodology. *Building and Environment,* 40**,** 1140-1149.

CHEHOVITS, J. & GALEHOUSE, L. Energy usage and greenhouse gas emissions of pavement preservation processes for asphalt concrete pavements. Compendium of papers from the first international conference on pavement preservation, 2010. 27-41.

COCURULLO, A., AIREY, G., COLLOP, A. & SANGIORGI, C. Indirect tensile versus two-point bending fatigue testing. Proceedings of the Institution of Civil Engineers-Transport, 2008. Thomas Telford Ltd, 207-220.

COSTA, N. R., LOURENÇO, J. & PEREIRA, Z. L. 2011. Desirability function approach: A review and performance evaluation in adverse conditions. *Chemometrics and Intelligent Laboratory Systems,* 107**,** 234-244.

CSANYI, L. H. 1957. Foamed asphalt in bituminous paving mixtures. *Highway Research Board Bulletin*.

D'ANGELO, J. A., HARM, E. E., BARTOSZEK, J. C., BAUMGARDNER, G. L., CORRIGAN, M. R., COWSERT, J. E., HARMAN, T. P., JAMSHIDI, M., JONES, H. W. & NEWCOMB, D. E. 2008. Warm-mix asphalt: European practice.

DAMTOFT, J., LUKASIK, J., HERFORT, D., SORRENTINO, D. & GARTNER, E. 2008. Sustainable development and climate change initiatives. *Cement and Concrete Research,* 38**,** 115-127.

DE SCHUTTER, G., BARTOS, P. J., DOMONE, P. & GIBBS, J. 2011. Self-compacting concrete. *International Review of Chemical Engineering,* Vol. 3, N. 1 296.

DONDI, G., TATARANNI, P., PETTINARI, M., SANGIORGI, C., SIMONE, A. & VIGNALI, V. 2014. Crumb Rubber in cold recycled bituminous mixes: Comparison between Traditional Crumb Rubber and Cryogenic Crumb Rubber. *Construction and Building Materials,* 68**,** 370-375.

DOYLE, T., GIBNEY, A., MCNALLY, C. & TABAKOVIC, A. 2013. Developing maturity methods for the assessment of cold-mix bituminous materials. *Construction and Building Materials,* 38**,** 524-529.

DU, S. 2014. Interaction mechanism of cement and asphalt emulsion in asphalt emulsion mixtures. *Materials and Structures,* 47**,** 1149-1159.

DU, S. 2015. Performance Characteristic of Cold Recycled Mixture with Asphalt Emulsion and Chemical Additives. *Advances in Materials Science and Engineering,* Volume 2015.

EAPA. 2014a. *Asphalt in Figures* [Online]. The Netherlands, Breukelen: European Asphalt Pavement Association. Available: http://www.asefma.es/wp-content/uploads/2015/12/AIF_eapa_2014.pdf [Accessed 25th May 2014].

EAPA 2014b. The use of Warm Mix Asphalt. Belgium: European Asphalt Pavement Association.

EBELS, L.-J. 2008. *Characterisation of material properties and behaviour of cold bituminous mixtures for road pavements.* PhD Thesis, Stellenbosch University, South Africa.

ELLIS, C., ZHAO, B., BARNES, J. & JONES, N. 2004. Properties of GGBS-bitumen emulsion systems with recycled aggregates. *Road Materials and Pavement Design,* 5**,** 373-383.

ENVIRONMENTAL AGENCY 2010. Pulverised Fuel Ash (PFA). Banbury, Oxon, UK,: North Iraland Enviromental Agency.

EPPS, J., LITTLE, D., HOLMGREEN, R. & TERREL, R. 1980. Guidelines for recycling pavement materials. *NCHRP Report*.

ERDEM, S. 2012. *Impact load-induced microstructural damage of concrete made with unconventional aggregates.* PhD Thesis, University of Nottingham, United Kingdom.

EUROPEAN COMMITTEE FOR STANDARDIZATION 2003. BS EN 12697-23:Test methods for hot mix asphalt. *Part 23: Determination of the indirect tensile strength of bituminous specimens.* London, United Kingdom: British Standards Institution.

EUROPEAN COMMITTEE FOR STANDARDIZATION 2004. BS EN 12697-24:Test methods for hot mix asphalt. *Part 24: Resistance to fatigue.* London, United Kingdom: British Standards Institution.

EUROPEAN COMMITTEE FOR STANDARDIZATION 2005a. BS EN 12697-4 Bituminous mixtures —Test methods for hot mix asphalt. *Part 4: Bitumen recovery: Fractionating column.* London, United Kingdom: British Standards Institution.

EUROPEAN COMMITTEE FOR STANDARDIZATION 2005b. BS EN 12697-12: Bituminous mixtures. Test methods for hot mix asphalt. *Part 12: Determination of the water sensitivity of bituminous specimens.* London, United Kingdom: British Standards Institution.

EUROPEAN COMMITTEE FOR STANDARDIZATION 2005c. BS EN 12697-25 Bituminous mixtures. Test methods for hot mix asphalt. *Part 25: Cyclic compression test.* London, United Kingdom: British Standards Institution.

EUROPEAN COMMITTEE FOR STANDARDIZATION 2006. BS EN 13108-1 Bituminous Mixtures- Material Specifications. *Part 1: Asphalt Concrete* London, United Kingdom: British Standards Institution.

EUROPEAN COMMITTEE FOR STANDARDIZATION 2008. BS EN 12697-12: Bituminous mixtures. Test methods for hot mix asphalt. *Part 12: Determination of the water sensitivity of bituminous specimens.* London, United Kingdom: British Standards Institution.

EUROPEAN COMMITTEE FOR STANDARDIZATION 2009. BS EN 13263-1: Silica fume for concrete. . *Part 1: Definitions, requirements and conformity criteria.* London, United Kingdom: British Standards Institution.

EUROPEAN COMMITTEE FOR STANDARDIZATION 2010. BS EN 12697-44:Test methods for hot mix asphalt. *Part 44: Crack propagation by semi-circular bending test.* London, United Kingdom: British Standards Institution.

EUROPEAN COMMITTEE FOR STANDARDIZATION 2012. BS EN 12697-26: Bituminous mixtures: Test methods for hot mix asphalt. *Part 26: Stiffness.* London, United Kingdom: British Standards Institution.

EUROPEAN COMMITTEE FOR STANDARDIZATION 2015. BS EN 1427: Bitumen and bituminous binders. Determination of the softening point. *Ring and Ball method.* London, United Kingdom: British Standards Institution.

FANG, X., GARCIA, A., WINNEFELD, F., PARTL, M. N. & LURA, P. 2014. Impact of rapid-hardening cements on mechanical properties of Cement Bitumen Emulsion Asphalt. *Materials and Structures***,** 1-12.

FANG, X., GARCIA, A., WINNEFELD, F., PARTL, M. N. & LURA, P. 2016. Impact of rapid-hardening cements on mechanical properties of cement bitumen emulsion asphalt. *Materials and Structures,* 49**,** 487-498.

FARHAN, A. H. 2016. *Characterization of Rubberized Cement-Stabilized Roadbase Mixtures.* PhD Thesis, University of Nottingham, United Kingdom.

FASEEULLA KHAN, M. D., DWIVEDI, D. K. & SHARMA, S. 2012. Development of response surface model for tensile shear strength of weld-bonds of aluminium alloy 6061 T651. *Materials & Design,* 34**,** 673-678.

FELEKOĞLU, B., TOSUN, K., BARADAN, B., ALTUN, A. & UYULGAN, B. 2006. The effect of fly ash and limestone fillers on the viscosity and compressive strength of self-compacting repair mortars. *Cement and Concrete Research,* 36**,** 1719-1726.

FENS, T. W. 2000. *Petrophysical properties from small rock samples using image analysis techniques.* PhD Thesis, Delft University of Technology, The Netherlands.

FERROTTI, G., PASQUINI, E. & CANESTRARI, F. 2014. Experimental characterization of high-performance fiber-reinforced cold mix asphalt mixtures. *Construction and Building Materials,* 57**,** 117-125.

FEUERBORN, H.-J. Coal ash utilisation over the world and in Europe. Workshop on environmental and health aspects of coal ash utilization, 23rd–24th November 2005 Tel-Aviv, Israel.

FONTES, L. P. T. L., TRICHÊS, G., PAIS, J. C. & PEREIRA, P. A. A. 2010. Evaluating permanent deformation in asphalt rubber mixtures. *Construction and Building Materials,* 24**,** 1193-1200.

FORTH, J., ZOOROB, S. & THANAYA, I. Development of bitumen-bound waste aggregate building blocks. Proceedings of the Institution of Civil Engineers-Construction Materials, 2006 London, UK 23-32.

FU, P., JONES, D., HARVEY, J. T. & HALLES, F. A. 2010. Investigation of the curing mechanism of foamed asphalt mixes based on micromechanics principles. *Journal of Materials in Civil Engineering,* 22**,** 29-38.

GARCÍA, A., LURA, P., PARTL, M. N. & JERJEN, I. 2013. Influence of cement content and environmental humidity on asphalt emulsion and cement composites performance. *Materials and Structures,* 46**,** 1275-1289.

GEDAFA, D. S. 2006. Comparison of flexible pavement performance using KENLAYER and HDM-4. *Fall Student Conference Midwest Transportation Consortium.* Ames, Iowa.

GIBB, J. M. 1996. *Evaluation of resistance to permanent deformation in the design of bituminous paving mixtures.* PhD Thesis.

GINGRAS, J.-P., TANGUY, P. A., MARIOTTI, S. & CHAVEROT, P. 2005. Effect of process parameters on bitumen emulsions. *Chemical Engineering and Processing: Process Intensification,* 44**,** 979-986.

GIULIANI, F. X-ray diffraction method for studying cement-modified bitumen-emulsion mixtures in asphalt pavement cold recycling. International Symposium on Subgrade Stabilisation and In Situ Pavement Recycling Using Cement 1-4 October 2001 Salamanca, Spain.

GODENZONI, C., CARDONE, F., GRAZIANI, A. & BOCCI, M. The Effect of Curing on the Mechanical Behavior of Cement-Bitumen Treated Materials. 8th RILEM International Symposium on Testing and Characterization of Sustainable and Innovative Bituminous Materials, 2016. Springer, 879-890.

GÓMEZ-MEIJIDE, B. & PÉREZ, I. 2014a. Effects of the use of construction and demolition waste aggregates in cold asphalt mixtures. *Construction and Building Materials,* 51**,** 267-277.

GÓMEZ-MEIJIDE, B. & PÉREZ, I. 2014b. A proposed methodology for the global study of the mechanical properties of cold asphalt mixtures. *Materials & Design,* 57**,** 520-527.

GÓMEZ-MEIJIDE, B., PÉREZ, I., AIREY, G. & THOM, N. 2015. Stiffness of cold asphalt mixtures with recycled aggregates from construction and demolition waste *Construction and Building Materials,* 77**,** 168-178.

GRAZIANI, A., GODENZONI, C., CARDONE, F. & BOCCI, M. 2016. Effect of curing on the physical and mechanical properties of cold-recycled bituminous mixtures. *Materials & Design,* 95**,** 358-369.

GRILLI, A., GRAZIANI, A. & BOCCI, M. 2012. Compactability and thermal sensitivity of cement–bitumen-treated materials. *Road Materials and Pavement Design,* 13**,** 599-617.

HAGHSHENAS, H., KHODAII, A., MEHRARA, A., DEHNAD, M. & AHARI, A. 2013. Frequency and temperature interactive effects on hot mix permanent deformation using response surface methodology. *Journal of Materials in Civil Engineering,* 26.

HAMZAH, M. O., GOLCHIN, B. & TYE, C. T. 2013. Determination of the optimum binder content of warm mix asphalt incorporating Rediset using response surface method. *Construction and Building Materials,* 47**,** 1328-1336.

HAMZAH, M. O., OMRANIAN, S. R., GOLCHIN, B. & HAININ, M. R. H. 2015. Evaluation of Effects of Extended Short-Term Aging on the Rheological Properties of Asphalt Binders at Intermediate Temperatures Using Respond Surface Method. *Jurnal Teknologi,* 73.

HEAD, R. W. 1974. An informal report of cold mix research using emulsified asphalt as a binder. *Association of Asphalt Paving Technologists* 43**,** 110-131.

HEMAVIBOOL, S. 2007. *The microstructure of synthetic aggregate produced from waste materials and its influence on the properties of concrete.* PhD Thesis, University of Leeds, United Kingdom.

HUANG, Y. H. 2004. *Pavement analysis and design,* USA, Pearson Prentice Hall.

HUGENER, M., PARTL, M. N. & MORANT, M. 2014. Cold asphalt recycling with 100% reclaimed asphalt pavement and vegetable oil-based rejuvenators. *Road Materials and Pavement Design,* 15**,** 239-258.

HUNTER, A. E., MCGREAVY, L. & AIREY, G. D. 2009. Effect of compaction mode on the mechanical performance and variability of asphalt mixtures. *Journal of Transportation Engineering,* 135**,** 839-851.

HURLEY, G. C. & PROWELL, B. D. 2005. Evaluation of Sasobit for use in warm mix asphalt. *NCAT report,* 5.

IBRAHIM, H. E.-S. M. 1998. *Assessment and design of emulsion-aggregate mixtures for use in pavements.* PhD Thesis, University of Nottingham, United Kingdom.

IVANOV, I. B., DANOV, K. D. & KRALCHEVSKY, P. A. 1999. Flocculation and coalescence of micron-size emulsion droplets. *Colloids and Surfaces A: Physicochemical and Engineering Aspects,* 152**,** 161-182.

JACOBSON, T. Cold recycling of asphalt pavement-mix in plant. Seminar on Road Pavement Recycling, 2002 Swedish National Road and Transport Research Institute, Sweden.

JENKINS, K. & MOLOTO, P. 2008. Updating bituminous stabilized materials guidelines: mix design report. Phase II–Curing protocol: improvement. Technical memorandum task 7.

JENKINS, K., VAN DE VEN, M. & DE GROOT, J. Characterisation of foamed bitumen. 7th Conference on asphalt pavements for Southern Africa, 1999. 1-18.

JENKINS, K. J. 2000. *Mix design considerations for cold and half-warm bituminous mixes with emphasis of foamed bitumen.* PhD Thesis, Stellenbosch University, South Africa.

JITAREEKUL, P. 2009. *An Investigation into Cold In-Place Recycling of Asphalt Pavements.* PhD Thesis, University of Nottingham, United Kingdom.

KAVUSSI, A. & MODARRES, A. 2010. Laboratory fatigue models for recycled mixes with bitumen emulsion and cement. *Construction and Building Materials,* 24**,** 1920-1927.

KAVUSSI, A., QORBANI, M., KHODAII, A. & HAGHSHENAS, H. 2014. Moisture susceptibility of warm mix asphalt: A statistical analysis of the laboratory testing results. *Construction and Building Materials,* 52**,** 511-517.

KENNEDY, T. W. & ANAGNOS, J. N. 1984. Wet-dry indirect tensile test for evaluating moisture susceptibility of asphalt mixtures.

KHALID, H. & ETA, K. Laboratory and field performance of dense emulsified bitumen macadam used for highway reinstatement Eurasphalt & Eurobitume Congress, 7-10 May 1996 Strasbourg, France.

KHALID, H. A. & MONNEY, O. K. 2009. Moisture damage potential of cold asphalt. *International Journal of Pavement Engineering,* 10**,** 311-318.

KHAN, M. & LYNSDALE, C. 2002. Strength, permeability, and carbonation of high-performance concrete. *Cement and Concrete Research,* 32**,** 123-131.

KHODAII, A., HAGHSHENAS, H. & KAZEMI TEHRANI, H. 2012. Effect of grading and lime content on HMA stripping using statistical methodology. *Construction and Building Materials,* 34**,** 131-135.

KHODAII, A., MOUSAVI, E., KHEDMATI, M. & IRANITALAB, A. 2015. Identification of dominant parameters for stripping potential in warm mix asphalt using response surface methodology. *Materials and Structures***,** 1-13.

KHURI, A. I. & CORNELL, J. A. 1996. *Response surfaces: designs and analyses*, CRC press.

KHWEIR, K., FORDYCE, D., STRICKLAND, D. & READ, J. Effect of curing time on the performance of cold asphalt mixtures 3rd Eurasphalt & Eurobitume Congress, 12-14th May 2004 Vienna, Austria 460.

KIM, Y.-R., LITTLE, D. & SONG, I. 2003. Effect of mineral fillers on fatigue resistance and fundamental material characteristics: mechanistic evaluation. *Transportation Research Record: Journal of the Transportation Research Board***,** 1-8.

KIM, Y.-R., LUTIF, J. S., BHASIN, A. & LITTLE, D. N. 2008. Evaluation of moisture damage mechanisms and effects of hydrated lime in asphalt mixtures through measurements of mixture component properties and performance testing. *Journal of Materials in Civil Engineering,* 20**,** 659-667.

KIM, Y., IM, S. & LEE, H. D. 2010. Impacts of curing time and moisture content on engineering properties of cold in-place recycling mixtures using foamed or emulsified asphalt. *Journal of Materials in Civil Engineering,* 23**,** 542-553.

KIM, Y. & LEE, H. D. 2006. Development of mix design procedure for cold in-place recycling with foamed asphalt. *Journal of Materials in Civil Engineering,* 18**,** 116-124.

KIM, Y., LEE, H. D. & HEITZMAN, M. 2007. Validation of new mix design procedure for cold in-place recycling with foamed asphalt. *Journal of Materials in Civil Engineering,* 19**,** 1000-1010.

KNUDSEN, T. 1984. The dispersion model for hydration of Portland cement I. General concepts. *Cement and Concrete Research,* 14**,** 622-630.

KONRAD, J.-M. & WALTER, J. 2001. Influence of curing on the mechanical properties of a dense graded emulsion mix. *Road Materials and Pavement Design,* 2**,** 181-194.

KRISTJANSDOTTIR, O. 2006. *Warm mix asphalt for cold weather paving.* MSc Thesis, University of Washington, USA.

KUBO, J. 2007. *Methods of remedial treatment for carbonation-induced corrosion of reinforced concrete.* PhD Thesis, University of Leeds, United Kingdom.

KUNA, K. 2015. *Mix design considerations and performance characteristics of foamed bitumen mixtures (FBMs).* PhD Thesis, University of Nottingham, United Kingdom.

LAV, A. H., LAV, M. A. & GOKTEPE, A. B. 2006. Analysis and design of a stabilized fly ash as pavement base material. *Fuel,* 85**,** 2359-2370.

LE BOUTEILLER, É. Asphalt Emulsions for Sustainable Pavements. First International Conference on Pavement Preservation, 2010.

LE COROLLER , A. 2002. *The Use Of Bitumen Emulsion In Europe* [Online]. European Asphalt Pavement Association. Available: http://www.eapa.org/publications.php?c=73 [Accessed 08 August 2016].

LEECH, D. 1994. Cold bituminous materials for use in the structural layers of roads. *Transport Research Laboratory, Project Report,* 75.

LESUEUR, D. & POTTI, J. J. 2004. Cold mix design: a rational approach based on the current understanding of the breaking of bituminous emulsions. *Road Materials and Pavement Design,* 5**,** 65-87.

LI, G., ZHAO, Y., PANG, S.-S. & HUANG, W. 1998. Experimental study of cement-asphalt emulsion composite. *Cement and Concrete Research,* 28**,** 635-641.

LIEBENBERG, J. & VISSER, A. 2004. Towards a mechanistic structural design procedure for emulsion-treated base layers: technical paper. *Journal of the South African Institution of Civil Engineering,* 46**,** p. 2-9.

LIN, J., WEI, T., HONG, J., ZHAO, Y. & LIU, J. 2015. Research on development mechanism of early-stage strength for cold recycled asphalt mixture using emulsion asphalt. *Construction and Building Materials,* 99**,** 137-142.

LOIZOS, A. 2007. In-situ characterization of foamed bitumen treated layer mixes for heavy-duty pavements. *International Journal of Pavement Engineering,* 8**,** 123-135.

LOTHENBACH, B., MATSCHEI, T., MÖSCHNER, G. & GLASSER, F. P. 2008. Thermodynamic modelling of the effect of temperature on the hydration and porosity of Portland cement. *Cement and Concrete Research,* 38**,** 1-18.

LOTHENBACH, B., WINNEFELD, F., ALDER, C., WIELAND, E. & LUNK, P. 2007. Effect of temperature on the pore solution, microstructure and hydration products of Portland cement pastes. *Cement and Concrete Research,* 37**,** 483-491.

LU, C.-T., KUO, M.-F. & SHEN, D.-H. 2009. Composition and reaction mechanism of cement–asphalt mastic. *Construction and Building Materials,* 23**,** 2580-2585.

MAZLOOM, M., RAMEZANIANPOUR, A. & BROOKS, J. 2004. Effect of silica fume on mechanical properties of high-strength concrete. *Cement and Concrete Composites,* 26**,** 347-357.

MEHTA, P. K. High-performance, high-volume fly ash concrete for sustainable development. Proceedings of the international workshop on sustainable development and concrete technology, 2004 Iowa State University Ames, IA, USA. 3-14.

MEHTA, P. K. & MONTEIRO, P. J. 1995. *Concrete: Structure, Properties, and Materials,* New York, USA, 2nd Edition. McGraw-Hill.

MILJKOVIĆ, M. 2014. *Influence of Bitumen Emulsion and Reclaimed Asphalt on Mechanical and Pavement Design-related Performance of Asphalt Mixtures.* PhD Thesis, Universität Bochum, Germany.

MILJKOVIĆ, M. & RADENBERG, M. 2014. Fracture behaviour of bitumen emulsion mortar mixtures. *Construction and Building Materials,* 62**,** 126-134.

MILJKOVIĆ, M. & RADENBERG, M. 2016. Effect of compaction energy on physical and mechanical performance of bitumen emulsion mortar. *Materials and Structures,* 49**,** 193-205.

MILTON, L. & EARLAND, M. 1999. Design guide and specification for structural maintenance of highway pavements by cold in-situ recycling. *TRL REPORT 386*.

MOBASHER, B., MAMLOUK, M. S. & LIN, H.-M. 1997. Evaluation of crack propagation properties of asphalt mixtures. *Journal of Transportation Engineering,* 123**,** 405-413.

MODARRES, A. & AYAR, P. 2014. Comparing the mechanical properties of cold recycled mixture containing coal waste additive and ordinary Portland cement. *International Journal of Pavement Engineering***,** 1-14.

MODARRES, A. & AYAR, P. 2016. Comparing the mechanical properties of cold recycled mixture containing coal waste additive and ordinary Portland cement. *International Journal of Pavement Engineering,* 17**,** 211-224.

MOGHADDAM, T. B., SOLTANI, M., KARIM, M. R. & BAAJ, H. 2015. Optimization of asphalt and modifier contents for polyethylene terephthalate modified asphalt mixtures using response surface methodology. *Measurement,* 74**,** 159-169.

MOHAMMED, M. K. 2015. *Multi-scale Response of Sustainable Self-Compacting Concrete (SCC) to Carbonation and Chloride Penetration.* PhD Thesis, University of Nottingham, United Kingdom.

MOHAMMED, M. K., DAWSON, A. R. & THOM, N. H. 2013. Production, microstructure and hydration of sustainable self-compacting concrete with different types of filler. *Construction and Building Materials,* 49**,** 84-92.

MOLENAAR, A., SCARPAS, A., LIU, X. & ERKENS, S. 2002. Semi-circular bending test; simple but useful? *Journal of the Association of Asphalt Paving Technologists,* 71.

MONNEY, O. K., KHALID, H. A. & ARTAMENDI, I. 2007. Assessment of fracture properties of emulsified asphalt mixtures. *Road Materials and Pavement Design,* 8**,** 87-102.

MONTEPARA, A. & GIULIANI, F. A Study on Design and performance of Recycled Pavement Cold Stabilized with Cement and Bituminous Emulsion. Proceeding of 4th European Symposium on Performance of Bituminous and Hydraulic Materials in Pavement, 11-12th April 2002 Nottingham, United Kingdom 213-217.

MONTGOMERY, D. C. 2008. *Design and analysis of experiments,* New York, USA, John Wiley & Sons, Inc.

MURALIDHAR, R., CHIRUMAMILA, R., MARCHANT, R. & NIGAM, P. 2001. A response surface approach for the comparison of lipase production by Candida cylindracea using two different carbon sources. *Biochemical Engineering Journal,* 9**,** 17-23.

NEEDHAM, D. 1996. *Developments in bitumen emulsion mixtures for roads.* PhD Thesis, University of Nottingham, United Kingdom.

NEJAD, F. M., AZARHOOSH, A. R. & HAMEDI, G. H. 2013. The effects of using recycled concrete on fatigue behavior of hot mix asphalt. *Journal of Civil Engineering and Management,* 19**,** S61-S68.

NEKAHI, A. & DEHGHANI, K. 2010. Modeling the thermomechanical effects on baking behavior of low carbon steels using response surface methodology. *Materials & Design,* 31**,** 3845-3851.

NELSON, S. A. 2015. *X-Ray Crystallography* [Online]. Tulane University Available: http://www.tulane.edu/~sanelson/eens211/x-ray.htm [Accessed 10/04/2016].

NIAZI, Y. & JALILI, M. 2009. Effect of Portland cement and lime additives on properties of cold in-place recycled mixtures with asphalt emulsion. *Construction and Building Materials,* 23**,** 1338-1343.

NICHOLLS, C. 1998. *Asphalt Surfacings : A guid to asphalt surfacing and treatments used for the surface course of road pavements* London and NewYork, E & FN Spon.

NIKOLAIDES, A. A New Design Method for Dense Cold Mixtures. The First European Symposium on Performance and Durability of Bituminous Materials, 1994 University of Leeds, United Kingdom. 259.

NIKOLAIDES, A. F. 1983. *Design of dense graded cold bituminous emulsion mixtures and evaluation of their engineering properties.* PhD Thesis, University of Leeds, United Kingdom.

NKINAMUBANZI, P., BAALBAKI, M., BICKLEY, J. & AITCIN, P. The use of slag for making high performance concrete. Sixth NCB international seminar on cement and building materials (New Delhi: NCB), 1998. 13-39.

NOORDIN, M. Y., VENKATESH, V. C., SHARIF, S., ELTING, S. & ABDULLAH, A. 2004. Application of response surface methodology in describing the performance of coated carbide tools when turning AISI 1045 steel. *Journal of Materials Processing Technology,* 145**,** 46-58.

OJUM, C., KUNA, K., THOM, N. H. & AIREY, G. 2014. An investigation into the effects of accelerated curing on Cold Recycled Bituminous Mixes. *International Conference on Asphalt Pavements, ISAP.* North Carolina, USA

OJUM, C. K. 2015. *The design and optimisation of cold asphalt emulsion mixtures.* PhD Thesis, University of Nottingham, United Kingdom.

OKE, O. L. 2010. *A study on the development of guidelines for the production of bitumen emulsion stabilised RAPs for roads in the tropics.* PhD Thesis, University of Nottingham, United Kingdom.

OLIVEIRA, J. 2006. *Grouted macadam: material characterisation for pavement design.* PhD Thesis, University of Nottingham, United Kingdom.

ONER, A. & AKYUZ, S. 2007. An experimental study on optimum usage of GGBS for the compressive strength of concrete. *Cement and Concrete Composites,* 29**,** 505-514.

ORUC, S., CELIK, F. & AKPINAR, M. V. 2007. Effect of cement on emulsified asphalt mixtures. *Journal of Materials Engineering and Performance,* 16**,** 578-583.

OTTE, E. 2013. *A structural design procedure for cement-treated layers in pavements.* PhD Thesis, University of Pretoria, South Africa.

ÖZBAY, E., ERDEMIR, M. & DURMUŞ, H. İ. 2016. Utilization and efficiency of ground granulated blast furnace slag on concrete properties – A review. *Construction and Building Materials,* 105**,** 423-434.

PAL, S., MUKHERJEE, A. & PATHAK, S. 2003. Investigation of hydraulic activity of ground granulated blast furnace slag in concrete. *Cement and Concrete Research,* 33**,** 1481-1486.

PARTL, M. N., FLISCH, A. & JÖNSSON, M. 2007. Comparison of laboratory compaction methods using x-ray computer tomography. *Road Materials and Pavement Design,* 8**,** 139-164.

PASETTO, M. & BALDO, N. 2010. Experimental evaluation of high performance base course and road base asphalt concrete with electric arc furnace steel slags. *Journal of Hazardous Materials,* 181**,** 938-948.

PEDERSEN, K. H., JENSEN, A. D., BERG, M., OLSEN, L. H. & DAM-JOHANSEN, K. 2009. The effect of combustion conditions in a full-scale low-NOx coal fired unit on fly ash properties for its application in concrete mixtures. *Fuel Processing Technology,* 90**,** 180-185.

PEREZ, F., MIRO, R., MARTINEZ, C., FERNANDEZ, M. & SOTO, J. Mix Design and Performance of Cold Pavement Recycling with Emulsion in the Paramix-Project. 3rd Eurasphalt & Eurobitume Congress, 12-14th May 2004 Vienna, Austria 576.

PÉREZ, I., MEDINA, L. & DEL VAL, M. Á. 2013. Mechanical properties and behaviour of in situ materials which are stabilised with bitumen emulsion. *Road Materials and Pavement Design,* 14**,** 221-238.

PETTINARI, M., DONDI, G., SANGIORGI, C. & HEDEDAL, O. 2014. The effect of Cryogenic Crumb Rubber in cold recycled mixes for road pavements. *Construction and Building Materials,* 63**,** 249-256.

PETTINARI, M. & SIMONE, A. 2015. Effect of crumb rubber gradation on a rubberized cold recycled mixture for road pavements. *Materials & Design,* 85**,** 598-606.

POULIOT, N., MARCHAND, J. & PIGEON, M. 2003. Hydration mechanisms, microstructure, and mechanical properties of mortars prepared with mixed

binder cement slurry-asphalt emulsion. *Journal of Materials in Civil Engineering,* 15**,** 54-59.

PROWELL, B. D., HURLEY, G. C. & FRANK, B. 2011. *Warm-mix asphalt: Best practices*, National Asphalt Pavement Association Lanham, Md, USA.

PUERTAS, F., MARTíNEZ-RAMíREZ, S., ALONSO, S. & VÁZQUEZ, T. 2000. Alkali-activated fly ash/slag cements: Strength behaviour and hydration products. *Cement and Concrete Research,* 30**,** 1625-1632.

READ, J. & WHITEOAK, D. 2003. *The shell bitumen handbook,* London, UK, Thomas Telford.

READ, J. M. 1996. *Fatigue cracking of bituminous paving mixtures.* PhD Thesis, University of Nottingham, United Kingdom.

READ, J. M. & COLLOP, A. C. 1997. Practical Fatigue Characterization of Bituminous Paving Mixture. *Journal of the Association of Asphalt Paving Technologists,* 66.

RENDELL, F., JAUBERTHIE, R. & GRANTHAM, M. 2002. *Deteriorated concrete: Inspection and physicochemical analysis,* London, Thomas Telford.

RIZWAN, S. A. 2006. *High-performance mortars and concrete using secondary raw materials.* PhD Thesis, Technischen Universitat Bergakademic Freiberg, Germany.

ROBERTS, F. L., ENGELBRECHT, J. C. & KENNEDY, T. W. 1984. *Evaluation of recycled mixtures using foamed asphalt*.

ROBINSON, R. & THAGESEN, B. 2004. *Road engineering for development,* London and NewYork, Spon Press.

ROJAS, M. F. A. & CABRERA, J. 2002. The effect of temperature on the hydration rate and stability of the hydration phases of metakaolin–lime–water systems. *Cement and Concrete Research,* 32**,** 133-138.

ROQUE, R., BIRGISSON, B., SANGPETNGAM, B. & ZHANG, Z. 2002. Hot mix asphalt fracture mechanics: a fundamental crack growth law for asphalt mixtures. *Journal of the Association of Asphalt Paving Technologists,* 71.

ROVNANÍK, P. 2010. Effect of curing temperature on the development of hard structure of metakaolin-based geopolymer. *Construction and Building Materials,* 24**,** 1176-1183.

RUBIO, M. C., MARTÍNEZ, G., BAENA, L. & MORENO, F. 2012. Warm mix asphalt: an overview. *Journal of Cleaner Production,* 24**,** 76-84.

RUCKEL, P., ACOTT, S. & BOWERING, R. 1983. Foamed-asphalt paving mixtures: preparation of design mixes and treatment of test specimens. *Transportation Research Record,* 911**,** 88-95.

SALEH, M. 2006. Effect of aggregate gradation, mineral fillers, bitumen grade, and source on mechanical properties of foamed bitumen-stabilized mixes. *Transportation Research Record: Journal of the Transportation Research Board***,** 90-100.

SALOMON, A. & NEWCOMB, D. E. 2000. Cold in-place recycling literature review and preliminary mixture design procedure. Minnesota Department of Transportation, Office of Research Services, Minnesota, USA.

SALOMON, D. R. 2006. *Asphalt emulsion technology,* Washington, D.C., Transportation Research Board.

SALOU, M., SIFFERT, B. & JADA, A. 1998. Study of the stability of bitumen emulsions by application of DLVO theory. *Colloids and Surfaces A: Physicochemical and Engineering Aspects,* 142**,** 9-16.

SANTAGATA, E. & CHIAPPINELLI, G. 2004. Improvements in the mix design of cold recycled bituminous mixtures. *3rd Eurasphalt and Eurobitume Congress.* Vienna, Austria

SANTERO, N. 2010. Life cycle assessment of pavements: A critical review of existing literature and research. *Lawrence Berkeley National Laboratory*.

SARıDEMIR, M., TOPÇU, İ. B., ÖZCAN, F. & SEVERCAN, M. H. 2009. Prediction of long-term effects of GGBFS on compressive strength of concrete by artificial neural networks and fuzzy logic. *Construction and Building Materials,* 23**,** 1279-1286.

SCHMIDT, R., SANTUCCI, L. & COYNE, L. 1973. Performance characteristics of cement-modified asphalt emulsion mixes. *Association of Asphalt Paving Technologists* 42**,** 300-319.

SEBAALY, P. E., BAZI, G., HITTI, E., WEITZEL, D. & BEMANIAN, S. Performance of cold in-place recycling in Nevada. 83th Annual Meeting of the Transportation Research Board, 2004 Washington DC, USA 162-169.

SEGUI, P., AUBERT, J., HUSSON, B. & MEASSON, M. 2012. Characterization of wastepaper sludge ash for its valorization as a component of hydraulic binders. *Applied Clay Science,* 57**,** 79-85.

SERFASS, J.-P., POIRIER, J.-E., HENRAT, J.-P. & CARBONNEAU, X. 2004. Influence of curing on cold mix mechanical performance. *Materials and Structures,* 37**,** 365-368.

SHA, W. & PEREIRA, G. 2001. Differential scanning calorimetry study of hydrated ground granulated blast-furnace slag. *Cement and Concrete Research,* 31**,** 327-329.

SHANNAG, M. 2000. High strength concrete containing natural pozzolan and silica fume. *Cement and Concrete Composites,* 22**,** 399-406.

SIDDIQUE, R. 2011. Utilization of silica fume in concrete: Review of hardened properties. *Resources, Conservation and Recycling,* 55**,** 923-932.

SOLÀ, N. Q. 2013. *Highly concentrated bitumen emulsions "A state of the art, review of experimental results".* MSc Thesis, University in Lleida, Spain.

SONG, S. H., PAULINO, G. H. & BUTTLAR, W. G. 2006. Simulation of crack propagation in asphalt concrete using an intrinsic cohesive zone model. *Journal of Engineering Mechanics,* 132**,** 1215-1223.

SOUTH AFRICAN BITUMEN ASSOCIATION 1999. ETB–The design and use of emulsion-treated bases. *SABITA Manual 21.* Cape Town, South Africa

STAPLES, P. Cold emulsion macadam performance trials for footway surfacing in Leicestershire. Proceedings of the Institution of Civil Engineers. Transport, 1997. Institution of Civil Engineers, 174-177.

STARK, J. & BOLLMANN, K. Delayed ettringite formation in concrete. Nordic Concrete Research Meeting, 1999 Oslo 4-28.

SULLIVAN, E. J. & MOSS, A. 2014. Paving Cost Comparisons: Warm-Mix Asphalt Versus Concrete. *PCA Market Intelligence* America's Cement Maunfacturers.

SUNARJONO, S. 2008. *The influence of foamed bitumen characteristics on cold-mix asphalt properties.* PhD Thesis, University of Nottingham, United Kingdom.

SUZUKI, E. 2002. High-resolution scanning electron microscopy of immunogold-labelled cells by the use of thin plasma coating of osmium. *Journal of Microscopy,* 208**,** 153-157.

SWIERTZ, D., JOHANNES, P., TASHMAN, L. & BAHIA, H. 2012. Evaluation of laboratory coating and compaction procedures for cold mix asphalt. *Asphalt Paving Technology-Proceedings Association of Asphalt Technologists,* 81**,** 81.

TEBALDI, G., DAVE, E. V., MARSAC, P., MURAYA, P., HUGENER, M., PASETTO, M., GRAZIANI, A., GRILLI, A., BOCCI, M. & MARRADI, A. 2014. Synthesis of standards and procedures for specimen preparation and in-field evaluation of cold-recycled asphalt mixtures. *Road Materials and Pavement Design,* 15**,** 272-299.

TERRELL, R. & WANG, C. 1971. Early curing behavior of cement modified asphalt emulsion mixtures. *Association of Asphalt Paving Technologists* 40**,** 108-125.

THANAYA, I. N. A. 2003. *Improving the performance of cold bituminous emulsion mixtures (CBEMs): incorporating waste.* PhD Thesis, University of Leeds, United Kingdom.

THANAYA, I. N. A., ZOOROB, S. & FORTH, J. 2009. A laboratory study on cold-mix, cold-lay emulsion mixtures. *Proceedings of the ICE-Transport,* 162**,** 47-55.

THOM, N. 2008. *Principles of pavement engineering,* London, United Kingdom Thomas Telford Publishing Ltd.

THOMAS, T. & KADRMAS, T. Performance-related tests and specifications for cold in-place recycling: lab and field experience. CD-ROM of TRB 82th Annual Meeting, Washington, DC, 2003.

TWAGIRA, E. M. 2010. *Influence of durability properties on performance of bitumen stabilised materials.* PhD Thesis, University of Stellenbosch, South Africa.

VAN JAARSVELD, J. G. S., VAN DEVENTER, J. S. J. & LUKEY, G. C. 2002. The effect of composition and temperature on the properties of fly ash- and kaolinite-based geopolymers. *Chemical Engineering Journal,* 89**,** 63-73.

WAGONER, M., BUTTLAR, W., PAULINO, G. & BLANKENSHIP, P. 2005. Investigation of the fracture resistance of hot-mix asphalt concrete using a disk-shaped compact tension test. *Transportation Research Record: Journal of the Transportation Research Board***,** 183-192.

WANG, F., LIU, Y. & HU, S. 2013. Effect of early cement hydration on the chemical stability of asphalt emulsion. *Construction and Building Materials,* 42**,** 146-151.

WANG, J.-P., CHEN, Y.-Z., WANG, Y., YUAN, S.-J. & YU, H.-Q. 2011. Optimization of the coagulation-flocculation process for pulp mill wastewater treatment using a combination of uniform design and response surface methodology. *Water Research,* 45**,** 5633-5640.

WANG, Z. & SHA, A. 2010. Micro hardness of interface between cement asphalt emulsion mastics and aggregates. *Materials and Structures,* 43**,** 453-461.

WANG, Z., SHU, X., RUTHERFORD, T., HUANG, B. & CLARKE, D. 2015. Effects of asphalt emulsion on properties of fresh cement emulsified asphalt mortar. *Construction and Building Materials,* 75**,** 25-30.

WANG, Z., WANG, Q. & AI, T. 2014. Comparative study on effects of binders and curing ages on properties of cement emulsified asphalt mixture using gray correlation entropy analysis. *Construction and Building Materials,* 54**,** 615-622.

WANG, Z. J. & WANG, R. Influences and mechanisms of ordinary Portland cement on properties of asphalt emulsion composites. Advanced Materials Research, 2010. Trans Tech Publ, 235-240.

WENDLING, L., GAUDEFROY, V., GASCHET, J., OLLIER, S. & GALLIER, S. 2016. Evaluation of the compactability of bituminous emulsion mixes: experimental device and methodology. *International Journal of Pavement Engineering,* 17**,** 71-80.

WILDE, W. J. 2013. Development of a Concrete Maturity Test Protocol. Minnesota State University, Mankato, USA: Center for Transportation Research and Implementation

WIRTGEN 2005. Cold Recycling Rehabilitation of a Heavily Trafficked Road. Windhagen: Wirtgen Group.

YAN, J., NI, F., YANG, M. & LI, J. 2010. An experimental study on fatigue properties of emulsion and foam cold recycled mixes. *Construction and Building Materials,* 24**,** 2151-2156.

YANG, E.-H., YANG, Y. & LI, V. C. 2007. Use of high volumes of fly ash to improve ECC mechanical properties and material greenness. *ACI Materials Journal,* 104**,** 620-628.

YANG, K.-H., MUN, J.-S. & CHO, M.-S. 2015. Effect of Curing Temperature Histories on the Compressive Strength Development of High-Strength Concrete. *Advances in Materials Science and Engineering,* 2015.

YLMÉN, R., JÄGLID, U., STEENARI, B.-M. & PANAS, I. 2009. Early hydration and setting of Portland cement monitored by IR, SEM and Vicat techniques. *Cement and Concrete Research,* 39**,** 433-439.

YOUNESI, M. & BAHROLOLOOM, M. E. 2010. Formulating the effects of applied temperature and pressure of hot pressing process on the mechanical properties of polypropylene–hydroxyapatite bio-composites by response surface methodology. *Materials & Design,* 31**,** 4621-4630.

YOUNIS, S. A., EL-AZAB, W. I., EL-GENDY, N. S., AZIZ, S. Q., MOUSTAFA, Y. M., AZIZ, H. A. & AMR, S. S. A. 2014. Application of Response Surface Methodology to Enhance Phenol Removal from Refinery Wastewater by Microwave Process. *International Journal of Microwave Science and Technology,* Vol. 2014**,** 12.

ZAPATA, P. & GAMBATESE, J. A. 2005. Energy consumption of asphalt and reinforced concrete pavement materials and construction. *Journal of Infrastructure Systems,* 11**,** 9-20.

ZELIĆ, J., RUŠIĆ, D. & KRSTULOVIĆ, R. 2004. A mathematical model for prediction of compressive strength in cement–silica fume blends. *Cement and Concrete Research,* 34**,** 2319-2328.

ZHANG, Q., FAN, W., WANG, T. & NAN, G. Studies on the temperature performance of SBR modified asphalt emulsion. Electric Technology and Civil Engineering (ICETCE), 2011 International Conference on, 2011. IEEE, 730-733.

ZHAO, B. 2007. *Bounding Recycled Aggregate Pavement Mixtures Using Hydraulic Binders and Cold Bitumen Emulsion.* PhD Thesis, Sheffield Hallam University, United Kingdom.